DEVELOPMENT OF NON-AQUEOUS ETHYLCELLULOSE GEL FOR TOPICAL DRUG DELIVERY

CHOW KEAT THENG
(B.Sc. (Pharm.)(Hons.), NUS)

A THESIS SUBMITTED

FOR THE DEGREE OF DOCTOR OF PHILOSOPHY

DEPARTMENT OF PHARMACY

NATIONAL UNIVERSITY OF SINGAPORE

2006

ACKNOWLEDGEMENTS

I wish to express my heartfelt gratitude to my supervisors, Associate Professor Paul Heng Wan Sia and Associate Professor Chan Lai Wah for their advice and guidance throughout my candidature as a graduate student.

I am indebted to A*STAR for providing a graduate scholarship, and GEA-NUS Pharmaceutical Processing Research Laboratory, Department of Pharmacy for providing various research facilities.

My warm thanks to all laboratory officers and administrative staff of Department of Pharmacy for their technical and logistical assistance, especially Teresa, Mei Yin and Peter.

Last but not least, I wish to thank all my friends in GEA-NUS and fellow graduate students for their various help, words of encouragement and most importantly, for making my life as a graduate student memorable.

TABLE OF CONTENTS

SUMMARY

This study reports the development of a non-aqueous gel system intended for topical delivery of moisture-sensitive drugs. Both the non-aqueous hydrophilic and lipophilic gel systems were formulated. The hydrophilic gels were formulated using a solvent system consisting of propylene glycol, glycerin and the stabilizing agent, magnesium chloride, and the gelling agent, poly N-vinylacetamide (PNVA), methyl vinyl ether/maleic acid copolymer (Gantrez S-97) or vinyl pyrrolidone/vinyl acetate copolymer (Plasdone S-630). The lipophilic gel systems, consisting of the gelling agent, ethylcellulose (EC) and the solvent, propylene glycol dicaprylate/dicaprate were found to be superior to the hydrophilic gel systems for the purpose of formulating moisture-sensitive drugs. This was attributed to the ability of the lipophilic gel systems to stabilize minocycline hydrochloride (MH), the model moisture-sensitive drug and the existence of structured gel network suitable for topical application.

The non-aqueous gels, formulated using three fine particle grades of EC that corresponded to different polymeric chain lengths, were characterized in terms of rheological and mechanical properties, wetting behavior, spreadability and gel performance characteristics, namely the stability, *in vitro* release and antibacterial efficacy of MH incorporated in the gel. Continuous and oscillatory shear rheometry was performed using a cone-and-plate rheometer and mechanical characterization was performed using a universal tensile tester. Wetting behavior was characterized using dynamic contact angle measurements of sessile drops of water and isopropylmyristate on EC gel matrices. Spreadability was measured using dynamic contact angles of sessile drops of EC samples on silicone elastomer. The *in vitro* drug release and antibacterial

testing were performed using the vertical Franz diffusion cell and the agar diffusion method, respectively.

The gel matrices exhibited prominent viscoelastic behavior, yield stress and thixotropy. Rheological and mechanical parameters increased with increased polymeric chain length and polymer concentration, and decreased polymer polydispersity. The solvent molecular conformation was found to affect gel network formation via intermolecular hydrogen bonding between EC polymer chains.

The feasibility of employing dynamic contact angle as an alternative technique to measure gel wettability and spreadability was demonstrated. The gel matrices were wetted by both water and isopropylmyristate, with much higher wettability by the isopropylmyristate indicating a predominance of lipophilic property. Increased EC concentration and polymeric chain length decreased the extent and rate of wetting. Gel wetting parameters were linearly correlated to rheological and mechanical properties.

EC gel spreadability was dependent on EC concentration, polymeric chain length and polydispersity. These factors affected the extent of gel-substrate interaction through conformation changes. The silicone elastomer substrate exhibited similar hydrophilic/lipophilic properties as the human skin. Linear correlation observed between spreading parameter and EC gel compressibility verified the applicability of dynamic contact angle to characterize gel spreadability.

EC gels containing MH demonstrated sustained release behavior that followed the Higuchi kinetics. MH release was dependent on EC chain length and concentration. Gel matrix hydration was identified as a prerequisite for release. The release phenomenon was governed by the interplay among gel matrix hydration, drug-polymer interaction and

polymeric chain coiling. High antibacterial efficacy was demonstrated by the MH-loaded gels against two opportunistic pathogens commonly found on human skin. Antibacterial activity was dependent on the factors that governed MH release and the bacteria sensitivity to MH.

All the EC gel samples tested showed desirable rheological and mechanical properties, wettability and spreadability for the ease of topical application, and to serve as moisture barrier and bioadhesive. The MH-loaded gels demonstrated sustained drug delivery and antibacterial efficacy. The physical properties and performance characteristics of EC gel was potentially useful for its application as a topical drug delivery system for moisture-sensitive drugs. The EC gel to be selected for topical application would be dependent on the relative importance of the physical properties and performance characteristics with respect to that particular application.

LIST OF TABLES

LIST OF FIGURES

LIST OF SYMBOLS

M_w = weight average molecular weight

M_n = number average molecular weight

τ_1 = longest relaxation time of a polymeric chain

f = oscillatory frequency (Hz)

ω = oscillatory frequency (rad s^{-1})

ν_0 = shear strain

ν_m = maximum strain

ν = shear rate

σ = shear stress

σ_y = yield stress

σ^* = complex stress

k = consistency index

H = hysteresis area

c = EC concentration

n = flow behavior index

η = shear viscosity (creep viscosity)

η_o = steady state viscosity

η^* = complex dynamic viscosity

G' = shear storage (elastic) modulus

G'' = shear loss (viscous) modulus

G^* = complex shear modulus

δ = loss angle

s = slope of the double logarithmic plot of shear storage modulus versus radial frequency

Bo = Bond number

We = Weber number

Ca = capillary number

L = sessile drop radius

U = velocity of the macroscopic three-phase line = dL/dt

ρ = liquid density

η = liquid viscosity

g = gravitational acceleration

ΔP = pressure difference across a curved interface to the surface tension and the curvature of the interface

R_1, R_2 = the principal radii of curvature

γ = interfacial tension

γ_{LV} = surface tension of a liquid

γ_{SV} = surface tension of a solid

γ_{SL} = interfacial tension between a solid and a liquid

θ = equilibrium contact angle

θ_w = contact angle of sessile water drop on gel surface

$\theta_{w/0}$ = initial contact angle of sessile water drop on gel surface

$\theta_{w/e}$ = equilibrium contact angle of sessile water drop on gel surface

$\Delta\theta_w$ = % change of contact angle of sessile water drop on gel surface

θ_i = contact angle of sessile IPM drop on gel surface

$\theta_{i/0}$ = initial contact angle of sessile IPM drop on gel surface

$\theta_{i/h}$ = initial contact angle of sessile IPM drop on human skin

θ_s = contact angle of sessile liquid drop on silicone elastomer

θ_e = extrapolated equilibrium contact angle for EC gels from the plot of equilibrium contact angle of EC solution on silicone elastomer versus EC concentration

V_w = standing volume of sessile water drop on gel surface

$V_{w/0}$ = initial standing volume of sessile water drop on gel surface

$V_{w/e}$ = equilibrium standing volume of sessile water drop on gel surface

ΔV_w = % change of standing volume of sessile water drop on gel surface

V_i = standing volume of sessile IPM drop on gel surface

$V_{i/0}$ = initial standing volume of sessile IPM drop on gel surface

A_w = base area of sessile water drop on gel surface

$A_{w/0}$ = initial base area of sessile water drop on gel surface

$A_{w/e}$ = equilibrium base area of sessile water drop on gel surface

ΔA_w = % change of base area of sessile water drop on gel surface

A_i = base area of sessile IPM drop on gel surface

$K_{\theta w}$ = first-order rate constant for gel wetting by water

$K_{\theta i}$ = first-order rate constant for gel wetting by IPM

t_a = time taken for complete absorption of sessile IPM drop

Wa = work of adhesion

At = adhesion tension

Sc = spreading coefficient

S = slope of the linear plots of logarithm of apparent viscosity versus EC concentration

Ra = arithmetic mean roughness of a surface

A_0 = % MH remaining at time, t = 0

A = % MH remaining at time, t

A_e = % MH remaining at steady state

k_1 = forward reaction rate constant

k_{-1} = backward reaction rate constant

M_t / M_∞ = fractional drug release

n = diffusional exponent characteristic of the drug release mechanism

Q = amount of drug release per unit area

D = diffusivity of a drug in a matrix

C_o = original concentration of a drug in a semisolid matrix

C_s = solubility of a drug in a matrix

$M_T[n]$ = cumulative mass of drug transported across a membrane at time, t

C[*n*] = concentration of drug in the receptor release medium

V_r = volume of the receptor release medium

V_s = volume of the receptor release medium removed for analysis at each sampling point

M_G = amount of drug remaining in a gel matrix at time, t

M_0 = amount of drug remaining in a gel matrix at t = 0

K_0 = zero order release constant

Q = amount of drug release per unit area

K_H = Higuchi rate constant

W_0 = weight of gel or Miglyol at t = 0

W_t = weight of gel or Miglyol at time, t

r_{gel} = radius of the zone of inhibition produced by EC gels containing MH

$r_{standard}$ = radius of the zone of inhibition produced by MH standard solutions

$R_{g/s} = r_{gel} / r_{standard}$

cfu = colony-forming units

r = correlation coefficient

r^2 = coefficient of determination

C.V. = coefficient of variation

GMEC = Global Minimum Energy Conformation

LMEC = Local Minimum Energy Conformations

HPLC = high performance liquid chromatography

AFM = atomic force microscope

EC = ethylcellulose

MH = minocycline hydrochloride

PNVA = poly N-vinylacetamide

NMP = N-methylpyrrolidone

PG = propylene glycol

IPM = isopropylmyristate

LIST OF EQUATIONS

$G^* = \sigma^* / \nu_m = (G'^2 + G''^2)^{1/2}$ Equation 1

$\sigma(t) = \nu_0 [G'(\omega) \sin(\omega t) + G''(\omega) \cos(\omega t)]$ Equation 2

$\eta^* = G^* / \omega$ Equation 3

$\eta(\nu) = |\eta^*(\omega)|$ where $\nu = \omega$ Equation 4

$\gamma_{LV} \cos\theta = \gamma_{SV} - \gamma_{SL}$ Equation 5

$Bo = \rho g L^2 / \gamma$ Equation 6

$We = \rho U^2 L / \gamma$ Equation 7

$Ca = \eta U / \gamma$ Equation 8

$\gamma (1/R_1 + 1/R_2) = \Delta P$ Equation 9

$M_t / M_\infty = Kt^n$ Equation 10

$Q = [DC_s(2C_o - C_s)\, t]^{1/2}$ Equation 11

$\sigma = k\nu^n$ Equation 12

$\sigma^{1/2} = \sigma_y^{1/2} + (\eta\nu)^{1/2}$ for $\sigma > \sigma_y$ Equation 13

Gel Density = (Weight of Gel / Weight of Water) × 0.998 g/ml Equation 14

$$M_T[n] = V_r \cdot C[n] + V_s \cdot \sum_{i=1}^{i=n-1} \{C[n-1]\}$$ Equation 15

$M_G = M_0 - K_0 t$ Equation 16

$Q = K_H t^{1/2}$ Equation 17

% Moisture uptake = $(W_t - W_0) \times 100 / W_0$ Equation 18

$\ln (A/A_0) = -k_1 t$ Equation 19

$\ln (A_o - A_e)/(A - A_e) = (k_1 + k_{-1})\, t$ Equation 20

$(100 - A_e) / A_e = k_1 / k_{-1}$ Equation 21

$Wa = \gamma_{LV} (\cos\theta + 1)$ Equation 22

$At = \gamma_{LV} \cos\theta$ Equation 23

$Sc = \gamma_{LV} (\cos\theta - 1)$ Equation 24

$[\text{unionized}] / [\text{ionized}] = 10^{(pH-pKa)}$ Equation 25

I. INTRODUCTION

I-A. The human skin

The skin is the largest organ of the body. Its large surface area in direct contact with the environment presents tremendous opportunities for drug delivery (Menon, 2002). The human skin is organized into two distinct layers, namely the epidermis and dermis directly beneath (Figure 1). The highly vascular dermis is made up of a connective tissue matrix containing the nerves, hair follicles, pilosebaceous units and sweat glands. The epidermis is avascular and its outermost layer, the stratum corneum, consists of keratin-rich, dead epidermal cells called corneocytes embedded within a lipid-rich matrix. The stratum corneum forms the primary barrier for drug permeation especially to water-soluble compounds. Consequently, drug delivery across the stratum corneum has become the essence in the design of many dermal delivery systems (Shah, 2003).

I-B. Transdermal and topical drug delivery

Transdermal drug delivery involves transport of drug through the skin into the systemic circulation for treatment of disorders remote from the site of application. As the drug needs to traverse multiple skin layers in sufficient amount to attain and maintain the therapeutic drug concentration, only highly potent drugs can serve as appropriate candidate for transdermal drug delivery. The most common form of transdermal drug delivery system comes in an adhesive patch containing the drug within a polymeric matrix.

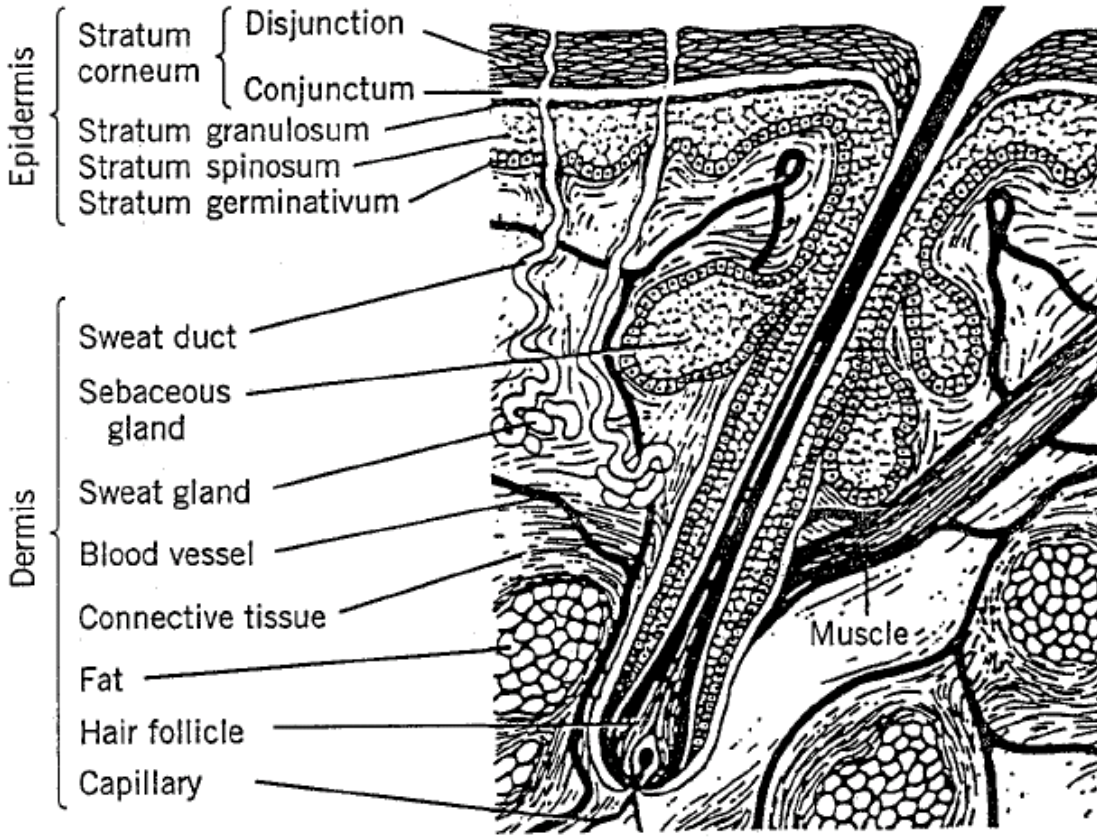

Figure 1: Structure of human skin.
(Adapted from Cohen and Rice, 2001)

Topical drug delivery is often intended for the local treatment of disorder by direct application of a formulation containing the appropriate drug. The disorder can be of cutaneous origin such as bacterial skin infections and dermatitis, as well as diseases associated with mucosal surfaces such as candidiasis and periodontitis. The drug should ideally be confined to the surface or within the site of application to effectively treat the disorder without appreciable systemic drug absorption. Thus, the site of application forms the target of topical drug delivery systems. The most commonly employed vehicles to achieve topical drug delivery are semisolids such as ointments, creams and gels. Subsequent discussions will revolve around topical drug delivery as this is the main focus of the present study.

I-B1. Advantages and limitations of topical drug delivery

The principal advantage of topical drug delivery lies in targeting the drug action directly to the site of disorder by allowing accumulation of high local drug concentration within the tissue and around its vicinity for enhanced drug action. Such targeted drug action is unlikely to be attainable if drug is conveyed via systemic pathway from oral drug administration. The potential systemic and gastrointestinal side effects as well as variable drug bioavailability associated with first-pass metabolism for drugs administered systemically can be avoided. Topical drug delivery has the capacity to achieve controlled and sustained drug delivery to provide predictable and extended duration of drug activity that many conventional modes of drug administration fail to achieve. Other advantages include ease of administration which will improve patient compliance and reversibility of

drug delivery by prompt removal of the applied formulation in the case of any adverse event.

Although topical drug delivery offers certain advantages over systemic delivery for selected drugs and conditions, the human skin natural barrier to drug permeation remains a major challenge to efficient drug delivery by this route. There is also potential of skin irritation or contact dermatitis arising from one or more components in the topical formulation. Exposure of a formulation to the environment upon application subjects it to the likelihood of solvent evaporation, thus rendering inconsistencies in the formulation composition. Solvent evaporation is particularly prevalent in formulations containing high proportion of water such as hydrogels or formulations containing volatile liquid such as ethanol. Water and ethanol are some of the most commonly used vehicles in topical formulations.

I-B2. Factors affecting topical drug delivery

The success of topical drug delivery is dependent on the interplay among various factors; physiological factors, physicochemical properties of the drug, formulation components and their interactions, are among those of fundamental importance.

Physiological factors concern mainly the properties of the skin such as thickness, hydration level and hair follicle density. These properties can demonstrate high individual variability depending on the age, gender, race, anatomical site, general health and environment condition such as temperature and humidity (Flynn *et al*., 1987). Although the role of these factors towards drug permeability may not be significant in some situation, they may contribute to sufficient variability to compromise topical drug

delivery in some instances. In order to minimize the effects of such physiological variability, the rate-limiting step for topical drug delivery should reside in the formulation instead of the biological barrier (Ranade *et al.*, 2004).

The drug physicochemical properties almost invariably influence its ease of diffusion through the topical vehicle as well as permeation through the skin or mucosal surfaces. Properties of great significance include the molecular size as reflected by the molecular weight, partition coefficient between the vehicle and skin, melting point, stability, and chemical functionality which influence ionization potential, binding affinity and drug solubility in the vehicle (Ranade *et al.*, 2004; Kydonieus, 1987).

The plethora of work associated with formulation optimization for topical drug delivery over the past few decades underlines the essential role of the drug delivery vehicle. The role of vehicle formulation is evident through its effect on the drug as well as the site of application. The effect on the drug encompasses drug diffusion, thermodynamic activity, stability and degree of ionization of weakly acidic or basic drugs. The effect on site of application is associated with modification of barrier property via chemical changes imparted by simultaneous uptake of formulation components and physical occlusion. These processes promote skin hydration or changes that increase drug penetration. The formulation factor also has an impact on vehicle consistency and viscosity which in turn, determine the adhesion and retention properties of the vehicle. These properties were important to ensure vehicle retention in its site of application for effective drug delivery. Topical vehicles can be broadly classified as liquids, semisolids and solids (Table 1). The semisolids are by far the most widely used form of topical vehicles (Behl *et al*., 1993).

Table 1: Simple classification system for dermatological vehicles [a].

System	Monophasic	Diphasic	Multiphasic
Liquid	Non-polar solution	Emulsion (o/w, w/o)	Emulsion (o/w/o, w/o/w)
	Polar solution	Suspension	Suspension
Semisolid	Anhydrous ointment, non-polar ointment, polar ointment	Emulsion (o/w, w/o)	Emulsion (o/w, w/o) with powder
	Hydrogel, non-polar gel, polar gel	Suspension	
Solid	Powder	Transdermal patch	Transdermal patch

[a] Modified from Smith *et al.,* 1999.

I-C. Gel

A gel is a two-component, crosslinked three-dimensional network consisting of structural materials interspersed by an adequate but proportionally large amount of liquid to form an infinite rigid network structure which immobilizes the liquid continuous phase within. A gel is an intermediate state of matter possessing property of a solid and a liquid, termed as viscoelasticity (Larson, 1999). The structural materials that form the gel network can be composed of inorganic particles or organic macromolecules, primarily polymers (Alvarez-Lorenzo and Concheiro, 2001). Polymer gel is the main focus of the current study. Crosslinks can be formed via chemical or physical interactions. This leads to gel classification into chemical and physical gel systems, respectively. Chemical gels are associated with permanent covalent bonding while physical gels result from relatively weaker and reversible secondary intermolecular forces such as hydrogen bonding,

electrostatic interactions, dipole-dipole interactions, van der Waals forces and hydrophobic interactions (Larson, 1999).

The prerequisite for gelation is branching or multifunctionality of a large molecule capable of forming intermolecular interactions consecutively between polymeric chains (Larson, 1999; Kavanagh and Ross-Murphy, 1998). This leads to the formation of a greater inter-connected branched structure which grows with progressive increase in weight average molecular weight (M_w) until it becomes infinite, M. At this point, the inter-connected structure spans the entire space limiting the system, hence forming a gel. Accordingly, the longest relaxation time, τ_1 also becomes infinite, where $\tau_1 \alpha M^3$ based on the reptation theory (Kajiwara, 2001). Relaxation time is the time required for a segment of a perturbed polymer chain to respond to an external stress by thermal motion. Polymer chain relaxation has been modeled using the reptation theory to describe the limited snake-like motion of the polymer chains within the network constraint. Non-reptative relaxation mechanisms such as the primitive-path fluctuation and constraint release have also been proposed. The details on the theories and the applicability of these relaxation mechanisms have been described in greater depth by Larson (1999).

Attempts have been made to explain the gelation process by theoretical models, of which the Flory-Stockmayer and percolation models, as detailed elsewhere (Larson, 1999; Kajiwara, 2001; Kavanagh and Ross-Murphy, 1998), are among the most commonly employed. The Flory-Stockmayer model is based on a covalent-bonded gel structure (Kajiwara, 2001). According to this model, a gel network is formed from monomers reacting randomly and growing in a tree-like manner until the entire limiting

space of the system is occupied. The percolation model describes gelation as a process involving random filling of monomers on a square lattice, eventually forming a cluster that spans the lattice and this state corresponds to the gel point. The Flory-Stockmayer model is widely regarded as the classical model and despite its simplicity, it is able to provide a precise estimate of the gel point, thus strategically captures the essence of gelation.

I-C1. Types of gel

There are many methods to classify gels as depicted by Table 2 and a more detailed account of each class can be found in the literature (Yamauchi, 2001). For the purpose of this current study, a classification of gels into chemical and physical polymer gels bears more direct relevance.

I-C1.1. Chemical gel

Chemical gel can be created by condensation polymerization of multifunctional precursors or crosslinking high molecular weight linear polymer chains by free radical polymerization with or without the presence of crosslinking agent and initiator (Osada, 2001). Condensation polymerization reaction produces a completely disordered network microstructure as the polymer chains grow in a random manner (Klech, 1992). Chemical gels are true macromolecules, covalently bonded and irreversible gels that do not dissolve easily in solvents due to their high crosslinking density.

Table 2: Classification of gels.

Method of classification	Type
Crosslinking system [a] (semi-crosslinking)	Covalent bonding
	Coulombic force
	Hydrogen bonding
	Coordination bonding
	Entanglement
Structural polymers [a]	Natural gels
	Hybrid gels
	Synthetic gels
Configuration size [a]	Microgels
	Macrogels
Solvent [a]	Air (aerogel, xerogel)
	Water (hydrogel)
	Oil (lyopic gel or organo gel)
Gel structure	Chemical gel
	Physical gel

[a] Adapted from Yamauchi, 2001.

I-C1.2. Physical gel

Physical gel is a result of polymer chain interaction by secondary forces that form physical crosslinks throughout the entire gel network as typified by organic polymers of biological and synthetic origin such as gelatin and the semisynthetic cellulose derivatives, respectively. In contrast to covalent crosslinks, physical crosslinks are reversible with small, finite energy or finite lifetime. Thus, such gels are able to exhibit reversible sol-gel transitions in response to external environmental factors such as temperature, pH and ionic additives (Kavanagh and Ross-Murphy, 1998; Klech, 1992). The basic interaction forces, namely hydrogen bonding, electrostatic interactions, dipole-dipole interactions, van der Waals forces and hydrophobic interactions can lead the organization of the interacting polymer chains into higher order structures called junction zones consisting of local helical structures, microcrystallites or nodular domains (Larson, 1999). Each respective type of junction zone can be illustrated by the egg-box junctions of alginate gels, microcrystalline domains of the semisynthetic cellulose gels or micelle junction zones of methylcellulose-poloxamer gels (Klech, 1992).

The entanglement network can also be classified as a physical gel formed by simple topological interaction of polymer chains and consists of a highly disordered microstructure as opposed to the well organized junction zones (Klech, 1992). Entanglement takes place when the product of polymer concentration and molecular weight exceeds the critical entanglement molecular weight (Kavanagh and Ross-Murphy, 1998). The inability of polymer chains to pass through each other imparts topological restrictions on molecular motion (Larson, 1999).

I-C2. Rheological properties

Rheology is the study of flow and deformation of matter. Rheological properties of a gel can be described by continuous shear rheology and oscillatory rheology which is conveniently represented by a flow curve or rheogram, and the storage and loss moduli, respectively. Continuous shear rheology can demonstrate the degree of structural changes within the gel system in response to continuous deformation, thus reflects the ease of gel to flow as required during manufacturing, processing and application. Oscillatory rheology serves as an indicator of the viscoelastic character of the gel and reveals the gel mechanical properties at rest. Rheological assessment is undoubtedly one of the most useful means of gel characterization as it is able to provide indirect structural information especially those pertaining to the rigidity and deformability of the gel system (Craig *et al.,* 1994) and, in turn, can reflect the practical usefulness of the gel to fulfill the requirements of its intended purpose such as adhesion, retention and drug release.

I-C2.1. Continuous shear rheology

A rheogram depicts the relationship between shear rate and shear stress of a material (Figure 2). It allows classification of the material into one of the various types of flow patterns such as Newtonian, plastic, pseudoplastic, thixotropic, dilatant or rheopectic.

Simple materials as typified by many pure liquids and dilute polymer solutions exhibit Newtonian behavior. The steady shear viscosity, which represents the resistance of the material to flow, is constant regardless of the magnitude of the applied shear. On the contrary, materials exhibiting non-Newtonian flow behavior do not show a constant

shear viscosity, hence rheological measurements need to be performed over a range of shear rate and shear viscosity is more appropriately represented by the apparent viscosity at any particular shear rate.

Plastic material exhibits a yield stress, defined by a minimum shear stress required to initiate flow. At a shear stress below the yield stress, the material will deform reversibly, hence returns to its original shape upon removal of shear. Further shearing beyond the yield stress will eventually result in a flow with constant shear viscosity, similar to Newtonian systems. Pseudoplastic material is regarded as a plastic material with an extremely low yield stress or non-existent yield stress. The apparent viscosity decreases continuously with applied stress until constant shear viscosity is achieved. Both plastic and pseudoplastic materials demonstrate reversible shear-thinning behavior due to progressive structural break down with increased shear.

A dilatant material demonstrates shear-thickening behavior with higher apparent viscosity as the stress increased. Such material usually consists of closely packed and deflocculated particles with only sufficient liquid to fill the interparticulate voids. Shearing results in particles rearranging, bringing about interparticulate void expansion causing the original amount of liquid available to be insufficient to fill the voids, thus imparting higher resistance for the system to flow.

Thixotropy and rheopexy are time-dependent analogues of shear-thinning and shear-thickening behavior, respectively. The internal structure of thixotropic material that is broken down by shear forces will only reform slowly but not completely with time, hence resulting in a reverse rheogram that does not overlap with the initial curve, forming a hysteresis loop. The area of hysteresis quantifies the extent of structural break down

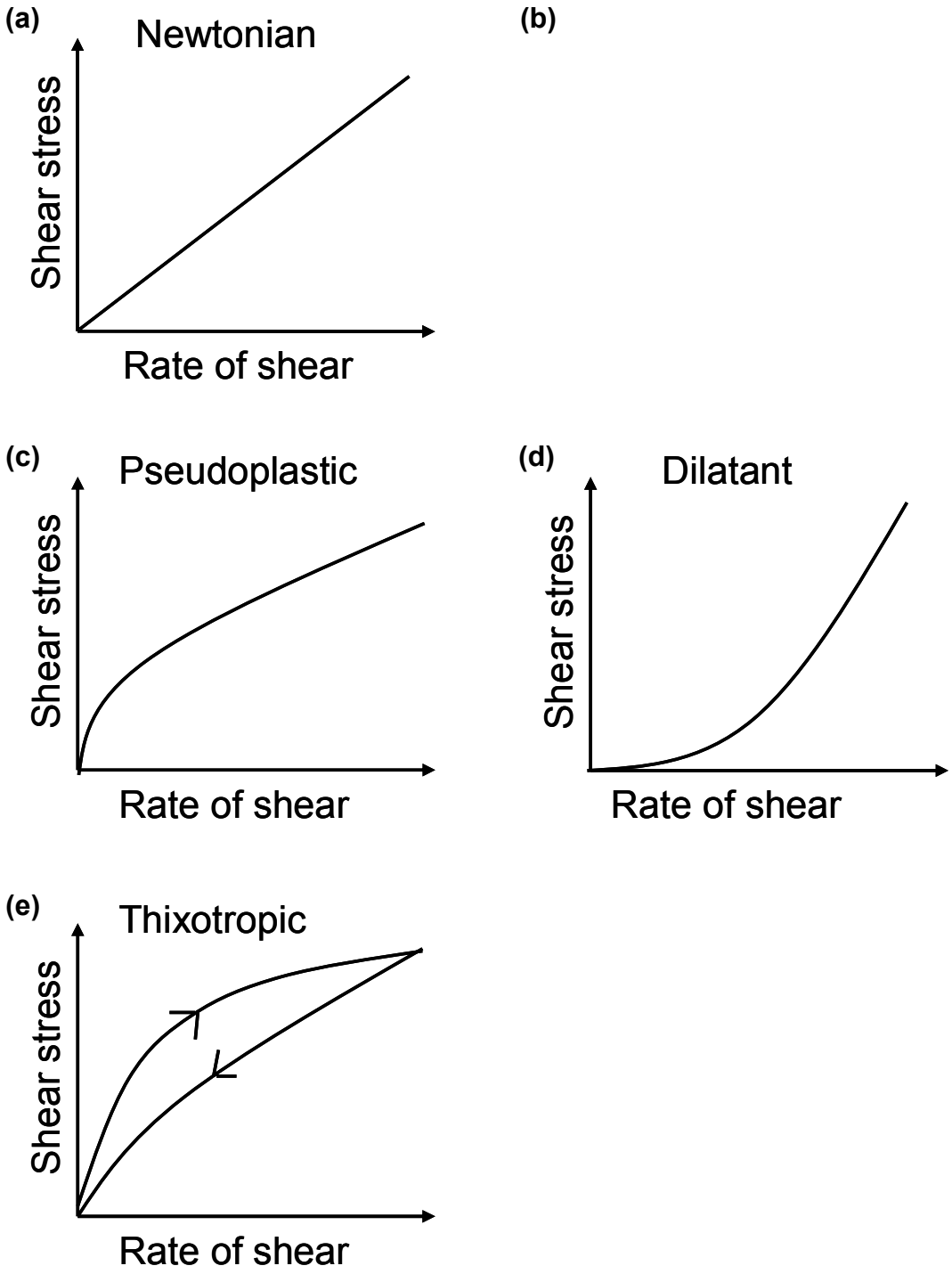

Figure 2: Rheograms to illustrate different types of liquid flow.

induced by shear forces. Rheopexy is described as a phenomenon where the time of solidification after disruption by a relatively high shear rate is shortened by applying low shear forces, hence rheopexy can be viewed as an accelerated thixotropic recovery. Rheopectic materials show increased viscosity with time as it is sheared at a constant rate.

The flow behaviors of greater relevance to polymer gel systems are those associated with shear-thinning. As polymer gel is composed of a network of closely bonded asymmetric macromolecules, shear forces will break down the intermolecular interactions holding the polymer network together and align the polymer chains along the direction of flow, thus causing a decrease in apparent viscosity. The degree of thixotropic break down corresponds to the density of crosslinks between the polymer chains. Hence, a more extensively crosslinked gel network will exhibit a greater area of hysteresis. An exception to the abovementioned general gel rheological behavior may be demonstrated by certain polymeric systems comprising multifunctional polymer chains with a high tendency for intramolecular interactions. Shearing will break down the intramolecular interactions and extend the polymer chains. This, in turn, facilitates interpolymeric chain interactions via the newly exposed functional groups, leading to increase in apparent viscosity or shear-thickening. This mechanism was proposed to explain shear-induced gel formation but it should be noted that such gel system is likely to be unstable due to the high propensity of phase separation (Larson, 1999).

I-C2.2. Oscillatory rheology

I-C2.2.1. Theoretical models

The behavior of semisolid materials under oscillation stresses can be represented by the generalized Maxwell model. This is a mechanical model made up of a combination of springs representing the elastic elements typical of solids, and dashpots representing the viscous elements typical of liquids (Figure 3). Each spring is associated with the Hookean tensile modulus while the dashpot is associated with Newtonian viscosity. According to the model, at a high frequency of oscillation, the springs are capable of responding instantaneously, elongate and contract correspondingly whereas the dashpots, with slower responses, do not have sufficient time to move. Hence, the system behaves essentially as an elastic solid with full structural recovery upon removal of shear. As the oscillation frequency is decreased, there is more time available for the continuous movement of dashpots which eventually become greater than the extension of the springs. This results in viscous fluid behavior without any structural recovery. At a frequency intermediate between the extremes which corresponds to the viscoelastic region, the behavior of the model is dependent on contributions from both the springs and dashpots. Hence, the system exhibits properties characteristic of both solids and liquids. Such property is termed viscoelasticity and is exhibited by most semisolids, for example, polymeric gels.

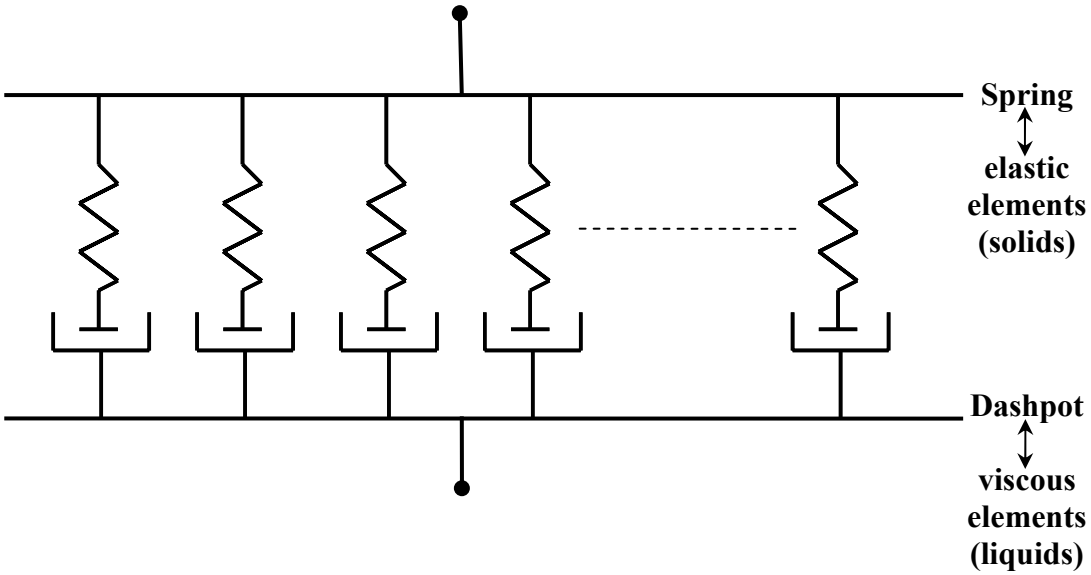

Figure 3: Generalized Maxwell model.

I-C2.2.2. Oscillatory rheometry

Oscillation tests are dynamic rheological measurements for determining the viscoelastic properties of a test material in its rheological ground state (Eccleston *et al*. 1973). Oscillatory techniques are non-destructive, in that they do not disrupt static structures of the test materials owing to the small amplitude oscillatory shear forces involved as opposed to the continuous shear techniques. As many pharmaceutical semisolids exhibit complex rheological behavior, continuous shear rheology alone is inadequate to fully characterize their rheological behavior (Davis, 1969). Furthermore, oscillation tests have the capability to characterize the elastic and viscous contributions to the entire response of the material (Tamburic and Craig, 1995) whereas continuous shear techniques only lead to an integrated characterization. In oscillatory measurement, when the strain amplitude is sufficiently small, the shear stress measured is governed by the rate of spontaneous rearrangements or relaxations within the material in its equilibrium state. Thus, this technique can be used to examine structural rearrangement within a complex material (Larson, 1999).

In dynamic rheological testing, a material is subjected to a small amplitude sinusoidal shear strain, ν_0 and the resultant shear stress, σ is measured. If the material is perfectly elastic, the resultant shear stress wave is also sinusoidal and will be exactly in phase (0°) with the strain wave. In contrast, the shear stress wave will be exactly out-of-phase (90°) with the imposed deformation for viscous materials. For viscoelastic materials, the stress wave will have a phase difference, δ ($0° < \delta < 90°$). Thus, δ or $\tan \delta$, the loss tangent, will be a measure of the viscous/elastic ratio for the material at

frequency, f (Hz) or ω (rad s^{-1}). The in-phase, shear storage (elastic) modulus, G′ and out-of-phase, shear loss (viscous) modulus, G″ are defined by

$$G^* = \sigma^* / \nu_m = (G'^2 + G''^2)^{1/2} \qquad \text{(Equation 1)}$$

where G* = complex shear modulus, σ* = complex stress, and ν_m = maximum strain. G′, the energy stored and recovered per cycle of deformation is a measure of the elastic response of the material, whereas G″, the energy dissipated or lost as heat per cycle is a measure of the viscous response. The tan δ is the ratio G″/G′, which serves as a measure of the ratio of energy lost to energy stored in a cyclic deformation. It provides a comparative parameter that combines both the elastic and the viscous contributions. The linear viscoelastic region corresponds to the region where the sinusoidal shear stress can be represented by

$$\sigma(t) = \nu_0 [G'(\omega) \sin(\omega t) + G''(\omega) \cos(\omega t)] \qquad \text{(Equation 2)}$$

The complex dynamic viscosity of the material, η* is given by

$$\eta^* = G^* / \omega \qquad \text{(Equation 3)}$$

Oscillation measurements are performed in the linear viscoelastic region of the gel systems, so that the existing gel structures are not damaged and the characteristics of the gel may be observed. An oscillatory stress sweep at constant frequency is employed to determine the appropriate range of shear stress where the linear viscoelastic behavior of the gel systems is maintained. This linear viscoelastic region is identified as the region where the responses of the material in terms of G′, G″, G* and δ are independent of the applied stress or strain. The limit of the viscoelastic region is attained at a critical stress or strain value. Beyond this critical value, a progressive decrease of the shear modulus and increase in δ is observed. An oscillatory frequency sweep test measures the response

of a material in terms of G′, G″ and η* as a function of frequency at a constant stress amplitude within the linear viscoelastic region of the material. This test provides information about the viscous and elastic behaviors of a semisolid system and the network structure formed by interactions between molecular chains.

I-C2.2.3. Oscillatory rheological properties of polymer gels

Oscillatory rheometry probes the dynamic structure of a polymer gel. It is able to provide information to discern the type of polymer gels under examination by quantifying their characteristic frequency sweep profiles and determining the contribution level of the viscoelastic parameters.

I-C2.2.3.1. Oscillatory rheological profile of chemical gels

As chemical gel is composed of a network of infinite molecular weight with infinite relaxation time, the viscoelastic parameters are relatively insensitive to small oscillatory shear as reflected by a frequency sweep profile where $G' \alpha \omega^0$, $G'' \alpha \omega^0$, $G' >> G''$ and $\tan \delta << 1$ (Figure 4a). Tangent $\delta << 1$ indicates that the solid-like elastic character of the gel is much more prominent than the liquid-like viscous character owing to the strongly crosslinked and irreversible gel network.

I-C2.2.3.2. Oscillatory rheological profile of physical gels

Physical gels can be further subdivided as entanglement network, weak gel or strong gel on the basis of their rheological profiles. The entanglement networks, also known as pseudogels, demonstrate a more dominant viscous behavior with $G'' > G'$ and

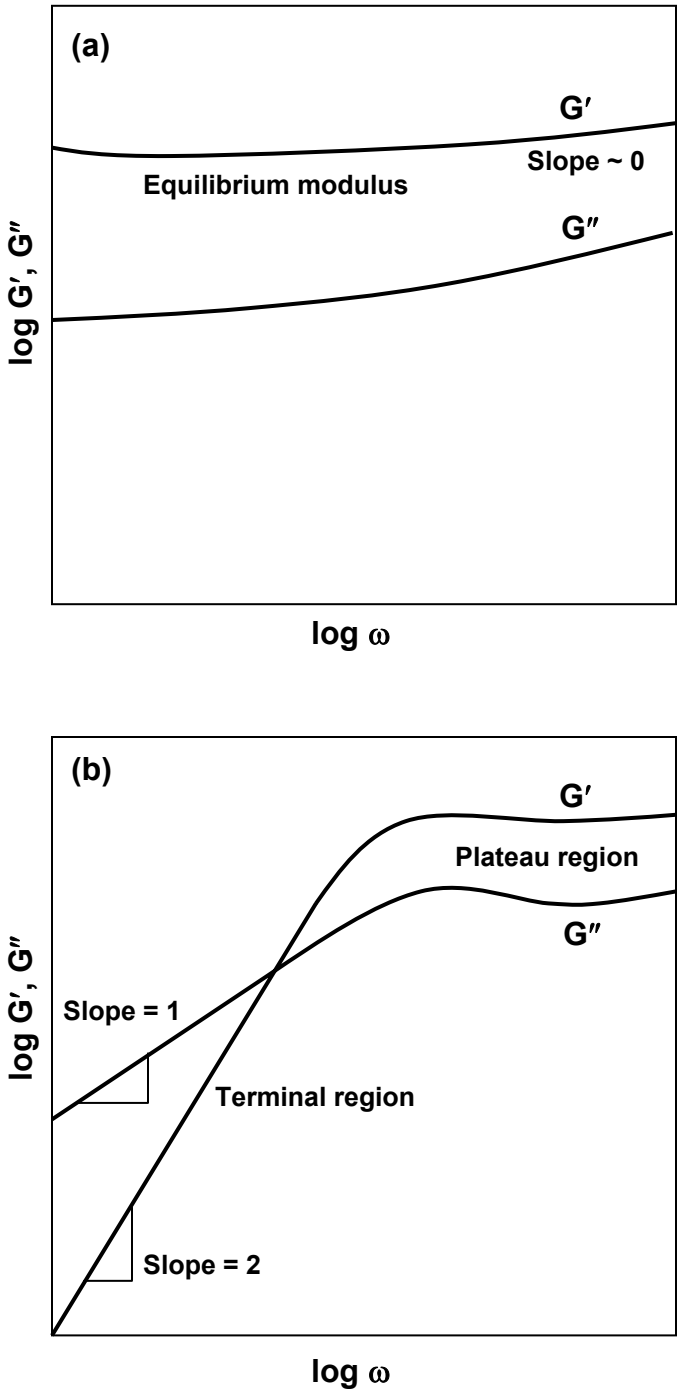

Figure 4: Dynamic rheological profiles of (a) covalently crosslinked networks and (b) entanglement networks.

tan $\delta > 1$ especially at low frequency range, known as the terminal region where $G' \alpha \omega^2$ and $G'' \alpha \omega^1$ (Figure 4b). Viscous polymer solutions are an examples of entanglement network. For weak gels, both G' and G'' show monotonous increase with frequency (Kohyama and Nishinari, 1993) and such gels tend to exhibit a more liquid-like behavior at higher frequency. Strong gels are relatively less frequency dependent and able to maintain their solid-like state, hence $G' > G''$ and tan $\delta < 1$.

I-C2.2.3.3. Cox-Merz superposition principle

The Cox-Merz superposition principle provides another useful method to distinguish between a polymer gel and a simple polymeric solution. This empirical principle states that the steady-shear viscosity, $\eta(\nu)$ and the complex dynamic viscosity, $\eta^*(\omega)$ obtained from continuous shear rheometry and oscillatory rheometry, respectively will be almost identical for simple polymeric solutions (Larson, 1999) such that $\eta(\nu)$ and $\eta^*(\omega)$ profiles are superimposible (Macosko, 1994).

$$\eta(\nu) = |\eta^*(\omega)| \text{ where } \nu = \omega \qquad \text{(Equation 4)}$$

As a consequence, $\eta(\nu)$ and $\eta^*(\omega)$ profiles of polymer gels will be expected to deviate from the Cox-Merz rule.

I-C2.2.4. Creep analysis

Creep analysis, a transient measurement, is another non-destructive method of investigating the viscoelastic behavior of polymer gels. In creep testing, a constant shear stress is applied to the sample and held constant. The resulting strain is monitored over a period of time. The recovery curve is obtained by setting the shear stress to zero so that

the recoverable elastic portion of the deformation can be determined. The creep curve, which is a plot of creep compliance (strain divided by stress) versus time, is dependent on the viscoelastic nature of the material (Kavanagh and Ross-Murphy, 1998; Barry, 1983). The creep curve (Figure 5) can be divided into separate regions that represent the gel response to an applied stress. The reversible elastic and viscoelastic components, and the irreversible viscous flow are illustrated by A-B, B-C and C-D, respectively. Energy dissipation due to viscous flow resulted in the inability of the creep curve to return to original upon removal of stress as shown by D-E. The elastic deformation, steady state compliance, and steady state viscosity, η_o can be obtained from creep testing. The η_o in creep testing corresponds to the η^* at very low frequency in oscillatory frequency sweep.

Both creep (transient) and oscillatory (dynamic) measurements can be conducted at a frequency range of $4\times10^{-3} < \omega < 10^{-1}$ rad s^{-1}. However, rheological properties at frequencies of $\omega > 10^{-1}$ and $\omega < 4\times10^{-3}$ rad s^{-1} can only be determined by oscillatory measurement and creep measurement, respectively. Thus, creep analysis is useful for determining rheological properties at very low oscillation frequency, and complementary information on gel viscoelasticity can be obtained from creep and oscillatory measurements (Barry and Meyer, 1979a).

I-C3. Mechanical properties

Mechanical parameters have been shown as important predictors of textural properties and bioadhesion of semisolids. The close correlation of textural properties to *in vivo* sensory parameters perceived by the end user has led to the use of mechanical parameters in complement to rheological properties as a basis for screening of semisolid

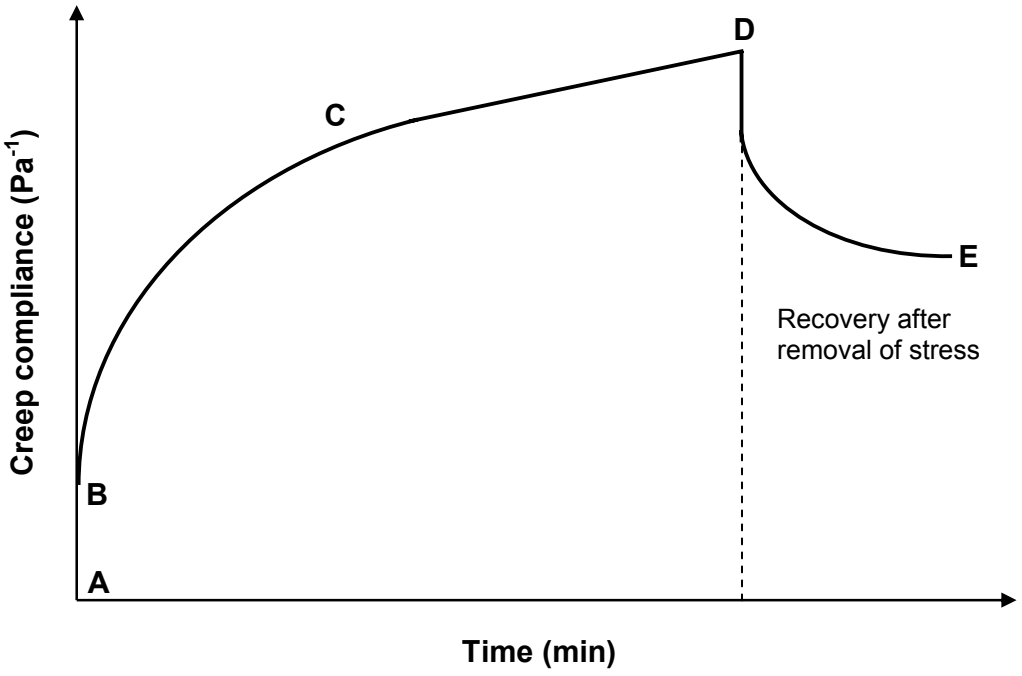

Figure 5: Typical creep curve for a viscoelastic material.

formulations for potential clinical application (Szczesniak *et al.,* 1963; Jones *et al.,* 1996a and 1997a). Mechanical characterization methods also collectively known as texture analysis, albeit extensively employed for characterization of food materials, is relatively new with regard to characterization of pharmaceutical semisolid formulations as this technique started to be increasingly used only from the early 1990's. A clear distinction between mechanical and rheological characterizations was not apparent before the emergence of texture analysis because rheometry was previously the sole method employed for both types of characterizations. Texture analysis enabled a quantifiable set of mechanical parameters relevant to pharmaceutical semisolids to be used as an objective description of textural properties of such systems.

The most widely employed method for texture analysis is provided by the texture profile analyzer or other similar techniques. The measurement is based on the principle of penetrometry that measures the resultant force and deformation upon application of a constant deformation rate on a material using a flat-faced compression probe (Tamburic and Craig, 1997; Telis *et al.,* 2005). The most basic sensory parameters derived from the force-distance or force-time curves of texture analysis include hardness, compressibility, cohesion or cohesiveness and adhesiveness. These parameters can represent the ease of product removal from its container, product spreadability, application characteristics, bioadhesion and retention (Tamburic and Craig, 1997; Jones *et al.,* 1996a and 1997b).

Unlike rheological measurement which is regarded as the fundamental technique to evaluate a semisolid for information on its microstructure and related molecular mechanisms, texture analysis is an empirical technique as data obtained cannot be fitted directly into basic theories of elasticity and viscoelasticity. Texture analysis has the

advantage of fast measurements, well-suited for a wide range of materials and deemed to provide a better predictor of texture (Telis *et al.,* 2005) although rheological parameters such as viscosity had also been shown to offer good correlation to skin feel of cosmetic emulsions (Brummer and Godersky, 1999). However, texture analysis results are difficult to compare among different testing systems as the measurements are governed by test conditions such as dimensions of test probe, sample as well as sample holder. In contrast, rheological measurement is relatively independent of these factors (Telis *et al.,* 2005).

Despite the apparent differences highlighted between textural and rheological parameters, the relationship between certain key aspects associated with these techniques have recently been demonstrated using dimensional analysis in an attempt to apply texture profile analysis for quantification of rheological properties of pharmaceutical gels. The probe deformation as given by the probe speed and distance in the gel was found to be a component of shear rate whereas the resultant hardness parameter as a component of shear stress (Jones *et al.,* 2002). The complementary nature of both the rheological and mechanical properties with respect to gel behavior is evident as the structural information derived from rheological testing often serves as the basis to account for the observed mechanical character of a gel system (McTaggart and Halbert, 1993; Ferrari *et al.,* 1994; Jones *et al.,* 2002; Bromberg *et al.,* 2004). Thus, it will be worthwhile to characterize a gel in terms of rheological as well as mechanical property in order to gain a complete understanding of the individual and combined influence of each property on the overall gel behavior pertaining to the application of the gel system as a topical vehicle.

I-C3.1. Role of rheological and mechanical characterization in semisolid gel systems

Rheological characterization of topical gels provides crucial information on the gel structure and behavior under different shear and stress conditions. Viscoelastic materials were associated with the ability to withstand mechanical strain (Davis, 1969). These properties were found to have a significant influence on drug release from many topical gel systems. Difference in rheological behavior between xanthan gum and hydroxypropylmethylcellulose gel matrices had been quoted as the reason for the difference in drug retarding capacity between these matrices (Talukdar *et al.,* 1996). Jones *et al.* (1996a) attributed product viscosity as the basis for the observed drug release behavior of different topical gel formulations containing hydroxyethylcellulose, polyvinylpyrrolidone and polycarbophil. Rheological behavior of poly(acrylic acid) gels had been found to be a highly influential factor affecting mucoadhesion as it served as an integral part of the detachment process (Tamburic and Craig, 1997). A gel structure in semisolid formulations was shown to be favorable for bioadhesion (Tamburic and Craig, 1997; Needleman *et al.,* 1998), an important prerequisite for effective delivery of drug from any topical dosage form. Rheological and mechanical properties were also found to be good predictors of the final product performance such as spreading and retention of the gel on its substrate (Chang *et al.,* 2002).

I-C4. Wetting behavior

Wetting is defined as displacement of one fluid by another from a surface. The fluid must make up at least two phases consisting either of a liquid and a gas or two immiscible liquids. The surface, also known as the substrate can be assumed either by a

solid or another liquid. Thus, the wetting process always involves three phases (Rosen, 1989). Spontaneous wetting occurs when the intermolecular adhesive force between the wetting liquid and the substrate is stronger than the cohesive force within the wetting liquid and the adhesive force between the substrate and its surrounding fluid. Adhesive forces may comprise primary bonds that are ionic, covalent and metallic in nature, donor-acceptor bonds as seen in acid-base interactions, and secondary bonds namely hydrogen bonds and van der Waals forces (Lazghab *et al.,* 2005).

I-C4.1. Role of wettability

Wetting behavior is one of the more important physical properties that can potentially affect the performance of polymer-based solid and semisolid dosage forms especially with regard to bioadhesion and drug release. Wettability was cited as one of the most crucial aspects in adhesion (Toledano *et al.,* 1999) as it would eventually lead to polymer hydration. Wettability was shown to be an important predictor of compatibility and bioadhesion to skin and soft tissue substrates such as mucosal membranes. A significantly better correlation was found between the work of adhesion obtained by surface thermodynamic approach, and the tensile adhesive strength between a mucin suspension and several polymers when the presence of a water layer at the polymer-mucin interface was considered in the mathematical model (Esposito *et al.,* 1994). This highlights the importance of wettability on bioadhesion because aqueous wetting led to interfacial hydration. A study by Lehr *et al.* (1992) concluded that mucoadhesion involved two steps. It began with an adsorptive contact which was facilitated by polymer hydration followed by interpenetration between the polymer chains of mucoadhesive gel

and the mucosal glycoproteins. The important role of polymer hydration in mucoadhesion was also supported by previous study that reported a higher rate of interpenetration in a more swollen or hydrated polymer system (Peppas and Buri, 1985). In the evaluation of the bioadhesive performance of a buccal formulation, the dry surface of the formulation had to be wetted with water in order to initiate bioadhesion with its substrate (Miyazaki *et al.,* 2000).

The role of wettability as a prerequisite for drug release is well established. This has been observed for drug release from hydrophobic tablet matrices, films, coated beads and microspheres as well as for the release of hydrophobic drugs from their formulated matrices (Ferrero *et al.,* 2003; Rosilio *et al.,* 1998; Wan *et al.,* 1991; Bodmeier and Paeratakul, 1991; Buckton, 1990). The pronounced influence of wettability on drug release had resulted in numerous attempts to improve drug release by incorporation of surfactants into hydrophobic formulations or dissolution medium in view of the ability of surfactants to improve wettability (Efentakis *et al.,* 1991; Buckton *et al.,* 1991; Luner *et al.,* 1996). Difference in wetting process was cited as the main reason for the altered release of urea or potassium nitrate from a gel-based controlled release device (Shavit *et al.,* 2003). Water vapor penetration into deeper region of the device encouraged higher rate and extent of wetting of gel matrix by the dissolution medium, hence resulting in faster release. The release of guaifenesin, a highly water soluble drug encapsulated within hydrophobic wax matrices was reported to increase due to increased wetting of microspheres with smaller particle size and microspheres containing poloxamer owing to surface active property of the additive (Mani *et al.,* 2005). The enhanced release of hydrophobic steroids from the liquisolid tablets was partly attributed to improved wetting

of the liquisolid matrices as compared to tablets obtained by direct compression (Spireas and Sadu, 1998; Spireas *et al.,* 1998). Liquisolid matrices were made of drug solutions or suspensions blended with powder excipients. The drugs were held in its original solubilized or suspended state by the excipient particles hence contributing to enhanced wetting in such formulation.

I-C4.2. Measurement of wettability

Polymer wetting and hydration processes are commonly quantified by hydration study, liquid penetration and contact angle measurement. Liquid penetration study measures volume of liquid uptake over time and the liquid contact angle on its substrate is derived using the Washburn equation (Rosilio *et al.,* 1998). However, this method is only appropriate for solid formulations such as powders, granules and tablets, and these formulations must possess adequate affinity for the penetrating liquid in order to demonstrate observable amount of liquid penetration.

Hydration studies or swelling experiments can be performed on both solid and semisolid formulations. These studies involve immersion of the sample into an aqueous medium and the rate of liquid uptake or swelling is an indicator of wetting or hydration (Needleman *et al.,* 1998; Mohan *et al.,* 2005). However, these methods necessitate sufficient sample consistency in order to allow accurate determination of weight change or a well-defined sample shape for determination of dimension change of the semisolid sample. Topical gels are applied on relatively “dry” substrates, for instance skin or buccal mucosa, and such applications by no means entail the enormous amount of fluid media as needed by hydration studies. Hence, a more appropriate method is necessary for the

investigation of water uptake ability by topical gels. The dynamic contact angle measurement of small sessile water drops on topical gel matrices is a more appropriate method as the small drop size ensures the absence of drop deformation due to the influence of gravity, hence giving accurate contact angle values by axisymmetric drop shape analysis-profile (Kwok *et al.,* 1997). The slight deformation of a large drop could also be easily detected using this technique. In addition, the small amount of liquid involved in the measurement mimics more closely the *in use* conditions for a topical gel.

I-C4.2.1. The contact angle

A liquid drop in contact with a surface, known as a sessile drop will form a hemispherical section that exhibits a contact angle at the three-phase contact line. The contact angle formed at a stationary liquid front is known as the static contact angle while the contact angle formed with a moving liquid front is known as the dynamic contact angle. The wetting of a drop of liquid at equilibrium on an ideal solid substrate which is smooth, homogeneous, planar and non-deformable is described by the Young's equation (Wu, 1982):

$$\gamma_{LV} \cos \theta = \gamma_{SV} - \gamma_{SL} \qquad \text{(Equation 5)}$$

where θ is the equilibrium contact angle, γ_{LV} and γ_{SV} are the surface tensions of the liquid and solid, respectively, and γ_{SL} is the interfacial tension between the solid and the liquid (Figure 6). The equilibrium contact angle is formed when the cohesive forces within the liquid is balanced by the liquid-substrate adhesive forces. The former tends to maintain the hemispherical drop shape while the latter encourages liquid spreading (Lazghab *et al.,* 2005).

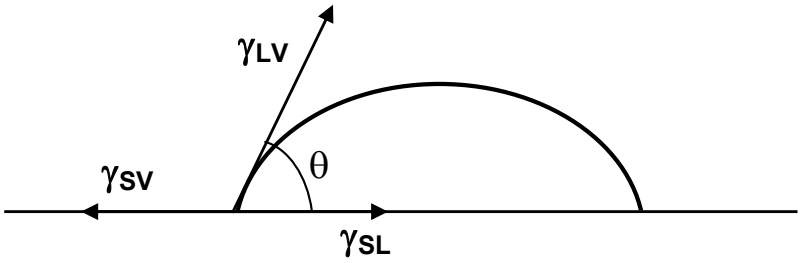

Figure 6: Contact angle equilibrium on an ideal solid substrate.

The wetting kinetics and dynamics of a liquid drop on a substrate is governed by the balance of interfacial, gravitational, inertial and viscous forces. The significance of the effects of gravity, drop inertia and liquid viscosity on the sessile liquid drop could be evaluated by the Bond number (*Bo*), Weber number (*We*) and capillary number (*Ca*), respectively. Equations for the calculation of these numbers are given below (Garnier *et al.,* 1998; Starov *et al.,* 2002).

$$Bo = \text{gravity force / interfacial force} = \rho g L^2 / \gamma \qquad \text{(Equation 6)}$$

$$We = \text{inertial force / interfacial force} = \rho U^2 L / \gamma \qquad \text{(Equation 7)}$$

$$Ca = \text{viscous force / interfacial force} = \eta U / \gamma \qquad \text{(Equation 8)}$$

where L = drop radius, U = velocity of the macroscopic three-phase line = dL/dt, ρ = liquid density, η = liquid viscosity, and g = gravitational acceleration. For small liquid drops, *Bo* and *We* are usually much lower than unity indicating that the gravitational and inertial forces on the dynamic contact angles of the sessile drops are negligible as compared to the viscous and interfacial forces (Garnier *et al.,* 1999). $Bo < 1$ indicates negligible gravitational effect which may render drop distortion, thus a hemispherical section of the liquid drop on the substrate can be assumed (Garnier *et al.,* 1998).

I-C4.2.1.1. Axisymmetric Drop Shape Analysis-Profile (ADSA-P)

ADSA-P, an improved version of axisymmetric drop shape analysis, quantifies the liquid-solid or liquid-liquid interfacial tensions and contact angles from the shape of axisymmetric menisci of sessile or pendant drops based on the drop profile coordinates (Lahooti *et al.,* 1996; Kwok *et al.,* 1998). The most basic theoretical background of ADSA-P is the classical Laplace equation of capillarity (Equation 9) that describes the mechanical equilibrium condition for two homogeneous fluids separated by an interface. The pressure difference across a curved interface to the surface tension and the curvature of the interface, ΔP is given by:

$$\gamma\,(1/R_1 + 1/R_2) = \Delta P \qquad \text{(Equation 9)}$$

where γ = interfacial tension, and R_1, R_2 = the principal radii of curvature. In ADSA-P, a calculated theoretical Laplacian curve is fitted to experimental drop profile obtained from image analysis in order to compute the surface tension, contact angle, drop volume and surface area of a drop. This is illustrated in Figure 7. The apex of the theoretical Laplacian curve is represented by the coordinates (x_0, z_0). The coordinates for the experimental drop profile points, U_i is (X_i, Z_i), and the point on the theoretical Laplacian curve closest to it is (x_i, z_i). The fitting of the theoretical and experimental profile is carried out by comparing the experimental drop profile points U_i, i = 1, 2,..., N, with the theoretical Laplacian curve, u whereby their normal distances, d_i are calculated. This in turn results in an objective function of the deviation between the Laplacian and experimental profiles which is further minimized to generate the output parameters.

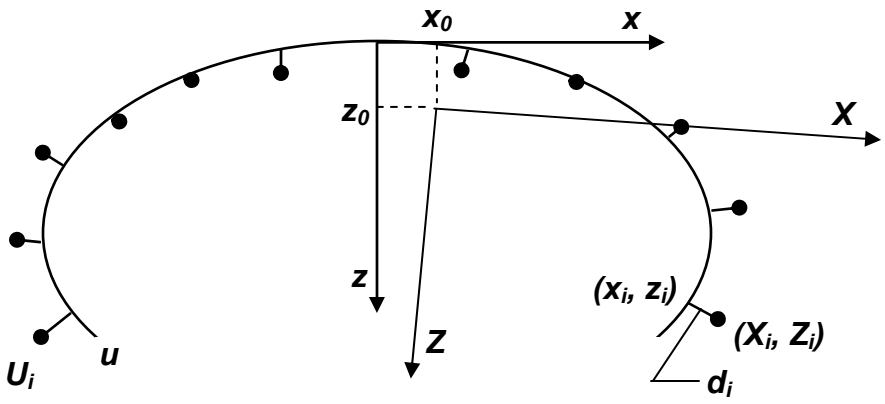

Figure 7: Comparison between experimental points and a calculated Laplacian curve in axisymmetric drop shape analysis-profile.

I-C4.2.2. Assessment of topical gel wettability using contact angle

Static contact angles of water and other liquids have been widely used to characterize wetting properties (Peppas and Mongia, 1997), surface energies (Lehr *et al.,* 1993; Rosa and Pinho, 1997; Oh and Luner, 1999) as well as surface configurations of polymeric films and gels (Yasuda and Okuno, 1994; Yamada *et al.,* 2001; Liu *et al.,* 2004). Experiments involving contact angle measurements on pharmaceutical dosage forms were commonly carried out using casted film samples, dried coatings of gel on glass surfaces or completely solidified blocks of gel. Pre-treatment of gel samples ensures well-defined and flat solid surfaces of uniform thickness which will possibly lead to more reproducible measurements. However, modification of sample surfaces can occur during preparation and this will almost inevitably alter the gel surface properties (Rosilio *et al,* 1998). Besides, the pre-treated gel samples do not necessarily reflect the final usable form of the formulations. On account of these shortfalls, where possible, the use of the

original gel matrices for contact angle measurement will certainly offer a more accurate and physiologically relevant representation of the gel wetting behavior.

I-C5. Gel spreadability

Spreadability is regarded as one of the more important attributes of topical dosage forms that can affect patient acceptability in terms of ease of application and clinical efficacy (Jones *et al.,* 1997b; Tamura *et al.,* 1997). Spreadability is one of the physical parameters commonly characterized in the formulation and development of topical dosage forms (Jones *et al.,* 1997b; Contreras and Sánchez, 2002a; Takayama *et al.,* 1990; Paula *et al.,* 1998). Spreading of topically applied products was reported to affect drug delivery as reflected by dermatopharmacokinetic outcome such as drug concentration in the stratum corneum (Shah, 2005).

I-C5.1. Measurement of spreadability

Spreadability is commonly measured by the sample spread diameter or area that is formed upon application of a known weight for a predetermined time duration on the sample (Contreras and Sánchez, 2002a; Takayama *et al.,* 1990; Paula *et al.,* 1998). However, this method of spreadability measurement was deemed to be time consuming (Jones *et al.,* 1997b). Besides, preparation of samples with standardized shapes and diameters for measurement might be technically difficult considering the sticky nature of most semisolid gels and ointments. Such standardization of shape will not be possible for samples with lower consistencies as a well-defined shape can never be easily attained. The compression test, performed as a part mechanical characterization of semisolid

formulations had recently been employed as a more convenient and less subjective measurement of gel spreadability. This test involves penetration of a probe into a fixed height of a sample and the resultant compressibility values reflect the ease of gel spreading over the probe surface (Jones *et al.,* 1997a and 1997b). While both the abovementioned methods are able to provide a measure of the ease of gel spreading upon application of a shear force, they fail to incorporate the effect of the skin substrate, a pertinent aspect pertaining to spreading of topically applied gel. Therefore, a method taking into account the effect of gel-skin interaction will offer a more physiologically relevant representation of gel spreadability.

I-C5.1.1. Assessment of topical gel spreadability using contact angle

Spreading of a drop of liquid on a solid surface is considered as part of the wetting process, hence the spreading of a drop of polymeric solution on its substrate would also be governed by similar forces as described in Section I-C4.2.1. Contact angle measurements of sessile drops of polymeric solutions or melts on solid substrates have become an alternative means to study the spreading behavior of these materials on their substrates. However, these studies in the literature are very often reports of work carried out for polymeric solutions or melts used for non-pharmaceutical applications and treatments had been largely theoretical (Holman *et al.,* 2002; Nieh *et al.,* 1996; Chen, 1988; Joanny, 2001; Summ and Samsonov, 1999).

I-C6. Drug release behavior

The knowledge of the release characteristic of a drug incorporated within a semisolid gel vehicle is very important as drug release characteristic dictates the ultimate effectiveness of topical drug delivery and its clinical efficacy. Factors governing drug diffusion within the polymeric matrix of a semisolid gel will affect the drug release and effectiveness of the topical drug delivery system. These factors include rheological properties, mechanical properties, gel wettability, drug solubility, drug partition coefficient, effective concentrations and drug diffusivity. The first three factors have been discussed in Sections I-C3.1 and I-C4.1. A more detailed account on the influence of remaining factors on drug release had been reviewed by Barry, 1983.

I-C6.1. Theoretical models

Drug release from polymer-based semisolid gel matrices is largely dependent on molecular diffusion that is modeled either by Fickian or non-Fickian diffusion processes (Peppas, 1987). The controlled drug release behavior at time, t can generally be represented by (Ritger and Peppas, 1987):

$$M_t / M_\infty = Kt^n \qquad \text{(Equation 10)}$$

where M_t / M_∞ = fractional drug release, K = constant, and n = diffusional exponent characteristic of the release mechanism.

One of the earliest and most widely used drug release model based on Fickian diffusion from semisolid formulations was the Higuchi model which demonstrates a direct proportional relationship between the amount of drug release per unit area, Q and the square root of time, $t^{1/2}$ (Kalia and Guy, 2001).

$$Q = [DC_s(2C_o - C_s)\, t]^{1/2} \qquad \text{(Equation 11)}$$

where C_o = original concentration of drug in the semisolid matrix, C_s = solubility of the drug in the semisolid matrix, and D = diffusivity of the drug in the semisolid matrix. The The Higuchi equation (Equation 11) was originally derived to describe the release behavior of drugs dispersed uniformly in an ointment matrix (Higuchi, 1961). This equation describes a system with the following characteristics: (a) the sizes of the suspended drug particles are much smaller than the thickness of the applied layer of semisolid; (b) $C_o >> C_s$; and (c) the surface to which the ointment is applied is immiscible with the ointment and acts as a perfect sink for the released drug. Although the Higuchi equation was derived for semisolid systems, it was later found to be applicable for many other pharmaceutical dosage forms (Higuchi, 1961; Costa and Lobo, 2001). Ritger and Peppas (1987) also found for their exponential diffusion model (Equation 10) that Fickian diffusion from a polymeric film or a slab was characterized by n = 0.5, hence $M_t / M_\infty \propto t^{1/2}$ which is in accordance to the Higuchi model.

The non-Fickian diffusion models for polymeric films includes anomalous transport and case-II transport, as represented by $0.5 < n < 1$ and $n = 1$, respectively (Ritger and Peppas, 1987; Peppas and Sahlin, 1989). These models are useful to describe drug release from polymeric systems where the release mechanism cannot be conclusively fitted into one of the classical models such as the Higuchi model because more than one competing type of release behaviors can occur concurrently (Costa and Lobo, 2001). Drug diffusion and release from such systems are often achieved by the continuous relaxation of the polymer chains in a hydrophilic, swollen gel system (Peppas, 1987; Agrawal *et al.,* 2003). The case-II transport is essentially a zero-order release

mechanism where release rate is constant and independent of time (Peppas, 1987; Costa and Lobo, 2001).

I-D. Formulation and characterization of non-aqueous gel for topical drug delivery

I-D1. Advantage of non-aqueous gel

The polymer-based semisolid gel has been one of the most popular means of topical drug delivery. Aqueous gels are much better studied than non-aqueous gels because hydrophilic gelling agents are readily available. However, the presence of water in aqueous gels may not be desirable when formulating moisture-sensitive drugs as chemical stability problem is almost inevitable when such drugs are incorporated into water-containing systems (Yoshioka *et al.,* 1992; Loukas *et al.,* 1998). The availability of a substantial number of topically useful but moisture-sensitive drugs in the market calls for formulation in suitable vehicles that can ensure drug stability.

I-D2. Model drug

Minocycline hydrochloride (MH), a member of the tetracycline class of antibiotics, was selected as the model drug in this study since it is chemically unstable but useful in the treatment of a host of topical bacterial infections. The tetracyclines are known to be unstable under conditions of low or high pH, heat and high humidity (Wu and Fassihi, 2005; Moreno-Cerezo *et al.,* 2001). The most common reactions that occur are epimerization, a steric rearrangement in the configuration of the dimethylamino function at C_4 to form epi-tetracycline, and dehydration at $C_{5a,6}$ to form anhydrotetracycline (Mitscher, 1978). The epimer is reported to have less than 5% of the

activity of the normal analogue, whereas the anhydro product has the potential to cause kidney damage (Remmers *et al*., 1963). However, dehydration reaction does not occur in MH due to the lack of –OH group at C_6 (Mitscher, 1978).

Tetracycline antibiotics are among the most effective treatment used topically for periodontitis (Greenstein and Polson, 1998) and one of the commonly prescribed systemic agents for long term therapy of acne (Johnsson, 1996). MH demonstrated superior efficacy compared to other members of tetracyclines due to its more efficient absorption and lower level of bacterial resistance (Eady *et al*., 1990 and 1993; Edlund *et al*., 1996; Seaman *et al.,* 2001). MH, like other tetracycline antibiotics, has a broad spectrum of activity and a relatively good safety profile (Johnsson, 1996). In general, the tetracyclines display good activity against many gram-positive and gram-negative bacteria, including obligate anaerobes, chlamydiae, mycoplasmas, rickettsiae and protozoan parasites. Its antibacterial effect is exerted by binding to the 30S ribosomal subunit of bacteria, hence leading to the inhibition of bacterial protein biosynthesis (Chopra, 1995; Chopra and Roberts, 2001; Bouchillon *et al.,* 2005). However, long term systemic administration of MH in acne therapy has been associated with multiple adverse effects such as ecological disturbances of gastrointestinal microflora, candida vaginitis, cutaneous symptoms, dizziness, vertigo, erythema nodosum, hepatitis and hypersensitivity (Goulden *et al*., 1996). In view of the potential toxicity of systemic antibiotics, topical therapy offers the advantage of minimizing or eliminating these side effects by the use of a much lower topical dose compared to the oral dose (Budden, 1988) and by confining the medication specifically to the lesion. On top of that, clinical efficacy may be improved when high drug concentration is achieved in the lesions by the site-

specific topical drug delivery. Among the antibiotics used for treatment of acne, MH and clindamycin have been recommended for topical administration from the ecological point of view (Edlund *et al*., 1996).

Apart from its clinical efficacy, there are other compelling reasons for selecting MH as the model drug for this study. One of the aims of formulating a non-aqueous gel in this study was to stabilize moisture-sensitive drugs. In order to demonstrate the ability of the non-aqueous gel to perform its intended purpose, a moisture-sensitive drug, MH was used as the model drug. The suppression of the moisture-induced epimerization of MH upon incorporation into the non-aqueous gel matrix would be a good indicator of drug stabilization. Another reason for selecting MH was that the main degradant, epiminocycline was reported to be inactive, thus reinforcing the significance of reducing the epimerization reaction.

I-D3. Formulation of non-aqueous MH gel

Non-aqueous gels can be divided into two types, namely the hydrophilic and lipophilic non-aqueous gels formulated using the appropriate solvents and gelling agents. Each type of gel has its own advantages as well as drawbacks. MH is ionic and freely water-soluble (McEvoy, 2006). Therefore, the use of hydrophilic solvent will allow complete drug dissolution in the vehicle and the gel matrix. A drug solution of reasonably high concentration is preferable to provide a better drug release profile. However, a limitation with the hydrophilic solvents is the tendency of hygroscopicity. Although improved drug stability had been reported for some non-aqueous hydroalcoholic gels (Vandenbossche *et al.,* 1991), the hydrophilic nature of these gels can still cause drug

degradation. Hence, to overcome the problem associated with moisture dependent drug degradation, it is important to develop a vehicle that does not contain water but possesses better or similar rheological and mechanical properties as hydrophilic gels. A non-aqueous lipophilic gel will be suitable to address this problem. However, most commonly encountered pharmaceutically acceptable polymers are not able to form gel in the presence of high proportion of hydrophobic solvents. Another potential limitation of lipophilic gel is the inability of MH to dissolve in the vehicle, hence MH will have to exist as drug dispersion within the gel matrix. Drug release and bioavailability may be compromised if the drug is not readily soluble in the vehicle. As both non-aqueous hydrophilic and lipophilic gels warrant their own merits, it is worthwhile to explore the essential properties of both types of gels pertaining to their use as a topical drug delivery vehicle for MH. The properties identified as crucial for MH gels include the ability to stabilize MH and gel rheology. Stability profile of MH incorporated in the gel will determine whether the formulated gel can serve its purpose in protecting moisture-sensitive drugs. Gel rheology is a fundamental property for any gel system as rheological characteristics is a useful indicator of the type of gel present and provides structural information about the gel system.

Commercially available topical MH formulations indicated for treatment of periodontal disease are Dentomycin® (Cyanamid), an ointment containing 2 % MH and Arestin® (OraPharma) consisting of MH incorporated into poly(glycolide-co-dl-lactide) miscrospheres in the form of dry powder. Attempts have been made to formulate tetracycline antibiotics in oleaginous bases for the treatment of periodontal diseases (Uno *et al*., 2002) and in non-aqueous, silicone-based gels for acne (Ritter, 1992). Shigeyama

et al. (1999) formulated and evaluated the release and water absorption properties of various MH-containing hydrophobic and hydrophilic ointments prepared using purified lanolin for the treatment of bedsore. A blend of hydrophilic ointment base and purified lanolin (7:3) was identified as a promising vehicle with high drug release rate and sufficient water absorption ability. Further studies using this ointment base showed that incorporation of β-cyclodextrin enhanced water absorption ability, elution volume and MH release rate of the formulation (Shigeyama *et al*., 2000).

I-D3.1. Solvents and gelling agents

I-D3.1.1. Non-aqueous hydrophilic gel system

The non-aqueous hydrophilic solvent to be used to formulate a gel matrix could be selected from several non-aqueous solvents commonly used for pharmaceutical formulations. These include glycerin, propylene glycol, N-methylpyrrolidone, dimethylformamide, the low molecular weight polyethylene glycols and the short-chain alcohols.

Preliminary studies carried out to identify the polymers that could dissolve in the non-aqueous vehicles employed in this study led to the selection of three types of polymers, namely PNVA, Gantrez S-97 and Plasdone S-630. PNVA is a copolymer of N-vinylacetamide and sodium acrylate. Gantrez is a synthetic copolymer of methylvinyl ether and maleic anhydride. It had been used as a drug delivery system for bromhexidine hydrochloride in the form of a polymeric film (El-Faham, 1994) or an ocular insert (El-Faham and Massoud, 1994). Plasdone S-630 is a copolymer of N-vinyl-2-pyrrolidone and vinyl acetate with the potential to be used in a number of applications such as a tablet

binder, sustained release coating, film coating and film forming agent in topical sprays (Plasdone S-630 Technical Profile). The potential application of PNVA, Gantrez S-97 and Plasdone S-630 polymers as gelling agents has yet to be exploited.

I-D3.1.2. Non-aqueous lipophilic gel system

The lipophilic solvent selected for gel formulation was propylene glycol dicaprylate/dicaprate (Miglyol 840), a hydrophobic diester derivative of propylene glycol. Propylene glycol dicaprylate/dicaprate has been used as a cosmetic ingredient and as an apolar phase in an oil-in-water emulsion. It had been shown to be non-irritating and non-sensitizing in primary skin compatibility tests, hence justifying its use in topical formulations (Bergfeld *et al.,* 1999; Rampon *et al.,* 2004). Its ready solubility in natural oils and most organic solvents indicates the potential of good solvating ability for hydrophobic drugs.

Ethylcellulose (EC) is often used as a polymer for coating, matrix material in controlled-release oral dosage forms (Heng *et al.,* 2003; Romero *et al.,* 1991; Wu *et al.,* 2003), excipient in topical or transdermal films (Shani *et al.,* 1998) and patches (Arora and Mukherjee, 2002), as well as, a particulate emulsion stabilizer owing to its surface active property (Melzer *et al.,* 2003). The flexibility, hydrophobicity and low water permeability of EC films allowed it to be an effective backing material for buccal delivery devices (Remuñán-López *et al.,* 1998). Although EC is a popular polymer in film forming applications, its use in the formulation of non-aqueous gels remains largely unexplored.

Ethocel EC polymers (Dow Chemical, Midland, MI, USA) are classified according to their degree of ethoxylation into the "Standard", "Medium" and "High" ethoxyl type that correspond to ethoxyl content of 48.0 to 49.5 %, 45.0 to 47.0 % and 49.5 to 52.0 %, respectively. Within each class, the polymer is further subdivided into different nominal viscosities. The "Standard" type, which is available as pharmaceutical grade and in fine particle forms, was used in this study. The fine particle form of EC polymer was designed for use in direct compression of controlled release solid dosage forms and has not been previously reported in the literature for gel formulation.

Both EC and Miglyol 840 were employed in the formulation of non-aqueous gels in the present study. They are classified in the literature as safe for use, relatively inert and biocompatible. EC gels prepared using solvents such as ethanol and diester phthalates have been reported (Contreras, 1993; Lee, 1995; Lizaso, 1999a). Ethanol has been successfully used in EC gels to achieve transdermal drug delivery (Contreras, 1993; Lee, 1995) but this solvent suffers the disadvantage of high volatility. Preparation of EC gels using diester phthalates involved the use of a high temperature, at 180 °C, thus entailing considerable technical difficulties and potential problems with drug stability. In the present study, a non-aqueous EC gel formulation was developed using the non-volatile solvent, Miglyol 840. The gel could be readily prepared using a slightly elevated temperature of 60 °C.

I-E. Significance of study

There are two major scientific contributions of this study. They are divided into formulation of a non-aqueous gel system and development of alternative methods for gel characterization.

This study has explored an alternative application for the fine particle grades EC polymer in non-aqueous gel formulation. As these polymers were originally produced for direct compression in tabletting and for film forming applications, their usefulness in gel formulation is largely unexplored. Using the formulated EC gel matrices in this study, a stable MH gel intended for topical application has been successfully produced. MH incorporated into these gel formulations has demonstrated chemical stability and high *in vitro* efficacy against common skin pathogens. Despite its potential clinical benefits, topical formulation of MH for the treatment of acne vulgaris is currently not available in the market yet, probably due to its stability problem. Such formulation is also not widely reported in the literature. The main benefits of employing topical MH for the treatment of acne vulgaris include direct targeting of the skin, that is the site of the disorder and avoidance of multiple side effects arising from long term oral administration of MH. The use of a topical tetracycline hydrochloride solution marketed for the treatment of acne had been discontinued in the United States (McEvoy, 2006). Topical formulations of minocycline available in the market were largely indicated for the treatment of periodontitis. Several studies had reported on formulation of minocycline hydrochloride for the treatment of periodontitis and bedsore. In view of the limited number of studies pertaining to topical gel formulations of MH, the attempt of the current study to explore

the potential usefulness of a non-aqueous gel as a vehicle for topical delivery of MH would contribute interesting insights into this area.

Alternative methods for the characterization of gel wetting and spreading behavior having close association with the *in use* conditions of topical gels have been developed in this study. This is the first study that demonstrated the feasibility of employing dynamic contact angle combined with axisymmetric drop shape analysis-profile as a method to investigate the wetting behavior of non-aqueous gel matrices in their original semisolid forms. The existing methods for gel wetting measurement such as hydration and water penetration studies are deemed to be less applicable for semisolid gel matrices while reported methods based on the contact angle technique often employ pre-treated gel samples which do not represent the final usable form of the semisolid gel. Thus, the use of the original gel matrices for contact angle measurement in this study offers a more accurate and physiologically relevant representation of the gel wetting behavior than the existing methods. This study is also the foremost to explore the possibility of applying dynamic contact angle technique as an alternative approach to measure spreadability of topical gels. This method has the advantage of direct visualization of sample spreading on its substrate. The spreading parameters derived from this method bear direct relevance to topical application as it incorporates the effect of interaction between the sample and a substrate that mimics the human skin. Thus, on top of the gel mechanical properties, an important factor associated with spreadability is taken into account, that is the surface properties of the gel and the skin substrate.

In summary, this study has addressed the major problem of drug stability in the formulation of a topical delivery system for MH indicated for the treatment of acne

vulgaris. This study has also explored the potential of employing the dynamic contact angle technique as a more relevant means for the characterization of wetting and spreading behavior of topical gels.

II. HYPOTHESES

II-A. Background

A topical dosage form should satisfy certain physicochemical and aesthetic criteria to ensure clinical efficacy and patient acceptability. Desirable attributes cited for topical dosage forms include stability of the active ingredient, and optimal rheological and mechanical properties (Barry, 1983). These attributes are often associated with drug release kinetics, bioadhesion and the ability of the dosage form to withstand mechanical stresses due to body movements (Jones *et al*., 1997b).

Rheological and mechanical characterization had been widely reported for aqueous gels because such formulations are more common. Reported studies on non-aqueous gel matrices are much less common. Only three studies were found to report on the rheology of non-aqueous gels, of which, two focused on the carbopol gel systems (Barry and Meyer, 1979b; Islam *et al.,* 2004) and one on EC gel (Lizaso *et al.,* 1999a). The characterization of non-aqueous gels containing hydrophilic polymers used in the current study (PNVA, Gantrez and S-630) had not been previously reported. Although the different aspects of rheological behavior of EC/*m*-cresol lyotropic liquid crystalline solutions have been extensively reported (Santamaría *et al.,* 1997; Lizaso *et al.,* 1999b), there was only one study on the dynamic rheological property of non-aqueous EC gels (Lizaso *et al.,* 1999a) as opposed to the more widely studied aqueous gels of cellulose derivatives (Jones *et al.,* 1997b and 2002). The limited information available on the rheological and mechanical properties of non-aqueous gels warrants more in-depth studies on such gel systems. Thus, this study attempted to investigate the relatively unexplored rheological and mechanical properties non-aqueous gel matrices.

As wettability has a significant predictive role in important processes such as bioadhesion and drug release, it is necessary to gain a deeper understanding of the wetting behavior of the non-aqueous gel matrices in order to correlate performance with their applicability as a topical drug delivery system. Although contact angle measurements have been widely reported for EC films and other cellulose ether films in coating applications (Oh and Luner, 1999; Luner and Oh, 2001), no reported studies on the measurement on semisolid gel matrices intended for topical application were found. As wettability can have profound effect on product performance, the absence of pertinent wettability data on topical gel formulations provided the impetus to investigate the wetting behavior of non-aqueous gel matrices using dynamic contact angle. Besides, measurement technique based on dynamic contact angle also offers a more accurate and physiologically relevant means of determination of gel wetting behavior.

Characterization of topical gel spreadability on a physiologically relevant substrate would be intriguing but there is a lack of such data with pharmaceutical systems. Considering the significant influence of spreadability on the ultimate effectiveness of topical dosage forms as mentioned in Section I-C5, it is essential to dwell deeper into the understanding of the spreadability of EC gel matrices in order to assess its usefulness for topical drug delivery.

The abilities of the non-aqueous gel to stabilize moisture-sensitive drug and release it for its purported action associated with its clinical use are the ultimate aim of formulating the ideal gel system. Hence such performance characteristic needed to be evaluated in order to verify the potential usefulness of the formulated non-aqueous gel as a topical drug delivery system.

II-B. Hypotheses

The present study is performed to test out four hypotheses:

1. A non-aqueous system forms a more appropriate gel vehicle than an aqueous system in providing stability to moisture-sensitive drug such as MH.

As MH is unstable in the aqueous environment, a non-aqueous gel matrix is hypothesized to be a more appropriate gel vehicle for MH because the absence of moisture in the gel matrix will prevent MH degradation. Apart from the well-documented influences of pH, heat and humidity on the stability of tetracycline antibiotics, the nature of the non-aqueous hydrophilic and hydrophobic solvents used in the formulation will also play a significant role in affecting the stability of MH. Since the gelling agents (polymers) used are relatively inert, the stability of MH incorporated in the non-aqueous gel matrix is entirely influenced by the solvent.

2. Physical properties of non-aqueous gel matrices are affected by formulation variables.

Formulation variables such as the type of polymers and polymer concentration and are hypothesized to influence gel physical properties such as rheology, mechanical properties, wettability and spreadability. The rheological properties of many gel systems are known to be governed by the gel network structure. In turn, the network structure is influenced by molecular interactions involving the solvent and polymer molecules. Hence, solvent-polymer interactions are often cited as the basis for the observed difference in gel rheological properties (Lizaso *et al,* 1999a). Polymer-polymer and

solvent-polymer interactions are presumed to affect the rheological and mechanical properties of the non-aqueous gel in the present study and the conformation of the solvent molecule is postulated to be of particular significance to this aspect.

3. Dynamic contact angle combined with axisymmetric drop shape analysis-profile is a feasible method to quantify non-aqueous gel wetting and spreading behavior.

There are various shortcomings associated with the existing methods of gel wettability and spreadability measurements measurement. Methods commonly used for determining gel wettability are hydration and water penetration studies, and for determining gel spreadability are compression test and spread diameter measurement upon application of known weight. It is desirable to develop an alternative method with better relevance to the semisolid gel system under study. Hence, dynamic contact angle combined with axisymmetric drop shape analysis-profile is hypothesized to be a feasible method to investigate and quantify the wetting and spreading behavior of non-aqueous gel system in its original semisolid form. Besides the well known influence of polymer surface properties such as surface configuration, roughness and chemical heterogeneity on the liquid dynamic contact angles, rheological and mechanical properties of the non-aqueous gel matrices will also play a role in the gel wetting and spreading behavior. Rheological and mechanical properties of gel systems are often closely associated with gel network structure, whereas wettability and spreadability are usually deemed as predominantly involving surface phenomena. However, correlation among these properties is postulated to exist in the currently studied non-aqueous gel system.

4. Gel physical properties have an influence on gel performance characteristics.

It is hypothesized that gel physical properties such as rheological and mechanical properties have an influence on performance characteristics in terms of MH stability, MH release and antibacterial efficacy of gel matrices containing MH.

III. OBJECTIVES

The main objective of this study was to develop a non-aqueous gel system for topical drug delivery of moisture-sensitive drugs. To achieve this objective, this study was subdivided into four parts:

1. Formulation of non-aqueous gels that could stabilize the model moisture-sensitive drug, MH.

Both non-aqueous hydrophilic and lipophilic gel matrices were formulated using compatible solvent-polymer combination to produce semisolid gel matrices of visually good consistency. For the formulation of a hydrophilic gel system, appropriate solvents were identified based on their ability to stabilize MH since the likelihood of MH instability in hydrophilic solvents was expected to be higher compared to lipophilic solvents. There were also more choices of solvents and polymers for formulating hydrophilic gel systems. In order to select the appropriate hydrophilic solvent system for MH, the stability of MH in different types of non-aqueous solvents was examined and comparisons were made with a fully aqueous environment (water).

The approach for formulating the lipophilic gel system required greater emphasis on the ability to produce a stable gel matrix since the number of pharmaceutically acceptable hydrophobic polymers that are capable of forming a gel in a lipophilic solvent is comparatively less. To ensure suitability of the lipophilic solvent for MH, stability study of MH in the chosen solvent was also performed.

2. Physical characterization of non-aqueous gel matrices.

To investigate the effects of formulation variables on gel physical properties, non-aqueous gel matrices formulated using different type of non-aqueous solvents, polymers and polymer concentrations were employed in the characterization of gel rheology, mechanical properties, wettability and spreadability.

Rheological and mechanical characterization of the non-aqueous gel matrices were performed with the aim of understanding their network structure and the role of solvent molecular conformation in affecting the molecular interactions leading to the formation of gel network. The relationship between solvent molecular conformation and gel network formation was elucidated using a molecular conformational approach.

3. Development of an alternative method to characterize gel wettability and spreadability based on dynamic contact angle combined with axisymmetric drop shape analysis-profile.

An alternative method based on dynamic contact angle combined with axisymmetric drop shape analysis-profile was developed in the attempt to characterize gel wettability and spreadability. These newly developed methods were deemed to be relevant for the gel system being studied. Gel wettability was determined using sessile drops of pure liquids on the gel surface while gel spreadability was determined using sessile drops of polymer solutions on an appropriate substrate. Measurement of gel wettability and spreadability formed part of physical characterization of the non-aqueous EC gel matrices.

4. Evaluation of performance characteristics of non-aqueous gel.

The performance characteristics of the non-aqueous gel were evaluated by studying the stability of MH incorporated in the gel matrices, *in vitro* MH release and antibacterial efficacy of resultant gel systems. New insights into the factors governing drug release from the non-aqueous gel matrices were elucidated.

IV. EXPERIMENTAL

IV-A. Materials

IV-A1. Formulation of gels

IV-A1.1. Non-aqueous hydrophilic gels

Minocycline hydrochloride (MH) and propylene glycol (PG) were obtained from Sigma (St. Louis, MO, USA); glycerin from BDH (Poole, Dorset, England); and N-methylpyrrolidone (NMP) from ISP Technologies (Wayne, NJ, USA). Magnesium chloride hexahydrate, zinc chloride dihydrate, calcium chloride dihydrate, aluminium chloride hexahydrate, methanol and ethanol were obtained from Merck (Darmstadt, Hessen, Germany). These materials were used for stability study. All solvents used were of analytical grade.

Methyl vinyl ether/maleic acid copolymer (Gantrez S-97) and vinyl pyrrolidone/vinyl acetate copolymer (Plasdone S-630) were obtained from ISP Technologies (Wayne, NJ, USA), and poly N-vinylacetamide (PNVA) from Showa Denko (Tokyo, Honshu, Japan). These polymers were used for formulation of non-aqueous hydrophilic gel matrices.

IV-A1.2. Non-aqueous lipophilic gels

Formulation of EC gels were carried out using three fine particle grades of ethylcellulose (EC) polymers of increasing chain length with ethoxyl content of 48.0-49.5 %: Ethocel Std 7 FP Premium (EC7), Ethocel Std 10 FP Premium (EC10) and Ethocel Std 100 FP Premium (EC100) supplied by Dow Chemical (Midland, MI, USA) and

propylene glycol dicaprylate/dicaprate (Miglyol 840) supplied by Sasol (Witten, Ruhr, Germany). Miglyol 840 was also used for stability study of MH.

IV-A2. Characterization of gels

Liquid paraffin was obtained from BDH (Poole, Dorset, England); silicone elastomer designated as "Transluscent Silicone Rubber" from McMaster-Carr (New Brunswick, NJ, USA); and isopropylmyristate (IPM) from Sigma (St. Louis, MO, USA). Ultrapure water was supplied by the Millipore water purification system (Millipore, Billerica, MA, USA). Sigma Plot version 8.02 software for dynamic contact angle data analysis and curve-fitting was obtained from Systat Software (Point Richmond, CA, USA).

IV-A3. *In vitro* release study and HPLC analysis

Potassium phosphate monobasic, sodium phosphate dibasic and orthophosphoric acid 85 % obtained from Merck (Darmstadt, Hessen, Germany) were used in buffer solutions. HPLC grade methanol and acetonitrile for HPLC analysis were obtained from Fischer Scientific (Loughborough, Leicestershire, England).

IV-A4. Evaluation of *in vitro* antibacterial efficacy

The bacteria employed were *Staphylococcus aureus* (*S. aureus*) and *Propionibacterium acnes* (*P. acnes*), representing aerobic and anaerobic opportunistic pathogens commonly found on human skin. Pure cultures of *S. aureus* (ATCC 6538P) were obtained from Culti-Loops (Oxoid, Basingstoke, Hampshire, UK) and *P. acnes*

(ATCC 11827) from QualiSwab (Becton Dickinson, Cockeysville, MD, USA). The nutrient agar employed for cultivation of *S. aureus* was prepared from Nutrient Broth No. 2 and Purified Agar (Oxoid, Basingstoke, Hampshire, England). *P. acnes* was cultivated on brucella blood agar supplemented with hemin and vitamin K_1 (Becton Dickinson, Cockeysville, MD, USA).

IV-B. Methods

IV-B1. Non-aqueous hydrophilic gels

IV-B1.1. Stability study of MH in water and non-aqueous hydrophilic solvents

A series of hydrophilic non-aqueous solvents suitable for pharmaceutical applications and could dissolve MH were identified from a preliminary screening study. 1 %w/w solution of MH was prepared in water and in the respective non-aqueous solvents such as ethanol, methanol, PG, glycerin and NMP. Samples were stored in sealed ampoules at room temperature of 22 ± 1 °C and relative humidity of 50 ± 3 %. HPLC assay for MH remaining was performed at predetermined time intervals over 105 days.

The influence of different cations on the stability of MH was studied using 1 %w/w MH in a 50:50 mixture of PG and glycerin with an equivalent of 2 moles of cations for every mole of MH. Cations were employed as stabilizing agents for MH. Control samples without any cation were also prepared for the purpose of comparison. Chloride salts of divalent cations, magnesium, calcium and zinc, and a trivalent cation, aluminium, were used. An accelerated stability study was carried out with samples in sealed ampoules, stored at 40 °C and the MH concentrations in the samples assayed at predetermined time intervals for up to at least 4 weeks.

IV-B1.1.1. HPLC analysis

HPLC method development for the analysis of MH and subsequent assays of MH were carried out using the Hewlett-Packard LC 1100 Series equipped with a quaternary pump, a 100 µl loop injector, an autosampler and a diode array multiple wavelength detector from Agilent Technologies (Foster City, CA, USA). Analytical separation was performed using a 150 mm × 4.6 mm, 5 µm particle size reversed phase C_{18} column, Hypersil BDS C_{18} with a 20 mm × 4 mm, 5 µm particle size C_{18} guard column obtained from Thermo Electron (Bellefonte, PA, USA). The mobile phase employed was phosphate buffer (pH 3, 25 mM)-methanol-acetonitrile at a volume ratio of 85:10:5 at a flow rate of 1.5 ml/min.

A 0.1 g sample was dissolved in the HPLC mobile phase in a 10 ml volumetric flask and filtered through a 0.45 µm regenerated cellulose membrane filter. Using a UV/VIS scanning spectrophotometer obtained from Shimadzu (Kyoto, Honshu, Japan), MH was found to exhibit maximum absorbance at 255 nm (λ_{max}), hence, a detection wavelength of 255 nm was employed. An injection volume of 40 µl was used. Calibration samples of MH were freshly prepared for every HPLC run. Linear calibration curves ($r^2 \geq 0.999$) were obtained over the drug concentration range of 5 to 100 µg/ml.

IV-B1.2. Rheological characterization

IV-B1.2.1. Sample preparation

Three different types of polymer, PNVA, Gantrez and S-630 were selected on the basis of their ability to dissolve in the chosen non-aqueous hydrophilic vehicles. Preliminary studies were carried out to establish the approximate range of concentrations

for each polymer to form a gel of reasonable consistency. The gels were then formulated using two levels of concentration, namely low and high. The vehicle consisted of a binary mixture of PG and glycerin in three different ratios designated as low (10 %w/w), medium (25 %w/w) and high (50 %w/w) levels with respect to PG. The compositions of the formulations studied are shown in Table 3. Magnesium chloride was dissolved in glycerin with the aid of heat, followed by the addition of PG upon cooling of the magnesium chloride-glycerin mixture to room temperature. Accurately weighed quantity of polymer was then slowly added in small aliquots into the vehicle mixture with stirring to aid dissolution and gelation. The resultant mixture was kept for 24 hours at room temperature to ensure complete swelling prior to any testing.

Table 3: Compositions of gel formulations investigated [a].

Polymer name	Formulation code	Polymer concentration (%w/w)	Propylene glycol (%w/w)	Glycerin (%w/w)
PNVA	P1	3	10	q.s.
	P2	3	25	q.s.
	P3	3	50	q.s.
	P4	1	10	q.s.
	P5	1	25	q.s.
	P6	1	50	q.s.
Gantrez	G1	10	10	q.s.
	G2	10	25	q.s.
	G3	10	50	q.s.
	G4	5	10	q.s.
	G5	5	25	q.s.
	G6	5	50	q.s.
S-630	S1	20	10	q.s.
	S2	20	25	q.s.
	S3	20	50	q.s.
	S4	10	10	q.s.
	S5	10	25	q.s.
	S6	10	50	q.s.

[a] Each formulation consisted of 0.82%w/w of magnesium chloride equivalent to 2 moles of Mg^{2+} cation for every mole of MH.

IV-B1.2.2. Oscillatory rheometry

Oscillation measurements of gels were performed using a cone-and-plate rheometer (Figure 8), Haake RheoStress 1 obtained from Thermo Electron (Baden-Württemberg, Karlsruhe, Germany). The experiments were performed using a cone angle of 1° and a cone diameter of 35 mm at a controlled temperature of 25 ± 0.5 °C (Haake Circulator DC30). Oscillatory stress sweeps were carried out at a constant angular frequency of 19 rad s^{-1} (3 Hz) in a stress range of 0.5 Pa to 1000 Pa. Oscillatory frequency sweeps were performed over a frequency range of 6 to 100 rad s^{-1} (1 to 15 Hz) at a constant stress amplitude of 10 Pa. The equilibration time before each run was 2 min.

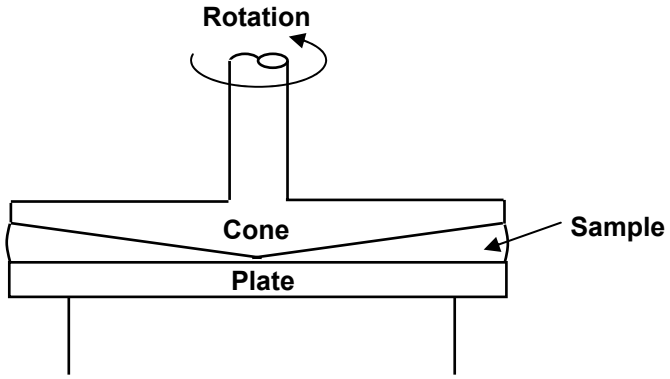

Figure 8: Schematic diagram of a cone-and-plate rheometer.

IV-B2. Non-aqueous lipophilic gels (EC gels)

The model drug, MH was not incorporated in samples employed for physical characterization described in Sections IV-B2.6, IV-B2.7, IV-B2.9, IV-B2.10, IV-B2.15 and IV-B2.17. All samples used for experiments in Sections IV-B2.4, IV-B2.5, IV-B2.13 and IV-B2.16 were incorporated with MH.

IV-B2.1. Preparation of non-aqueous EC gel matrices

EC was dissolved in the non-aqueous solvent, Miglyol 840 with continuous stirring at 60 °C to form a gel. For large volumes of gel samples, mixing was carried out with the aid of a ball mill obtained from Retsch (Haan, North Rhine-Westphalia, Germany). Six formulations of different EC concentrations were prepared from each grade of the polymer as follows: 11 to 16 %w/w for EC7 and EC10, and 7 to 12 %w/w for EC100. Trapped air bubbles were removed from the gel samples using vacuum. The gels were kept for 24 h to ensure complete swelling prior to any testing.

For experiments on gel spreadability, six formulations from 3 to 8 %w/w were prepared from each grade of EC. For EC7 and EC10, better homogeneity was attained when polymer-solvent mixing was carried out with the aid of a ball mill to form a semisolid gel prior to diluting the gel to the required concentration using the solvent. The diluted mixtures were stirred at 60 °C to form homogeneous polymer solutions. The samples were kept for 24 h to ensure complete swelling of polymer prior to any testing. These samples were employed in measurement of gel spreadability using dynamic contact angle and apparent viscosity using continuous shear rheometry.

In order to verify the proposed occurrence of EC chain coiling upon gel hydration, the apparent viscosities of 7 and 12 %w/w EC100 gel matrices incorporated with various amounts of water was measured using continuous shear rheometry. EC100 gels containing 7 and 12 %w/w EC, corresponding to low and high concentrations, respectively, were employed in this study. Hydrated EC100 gels were prepared by incorporating 1, 3, 5, 7 and 10 %w/w ultrapure water into the gel matrices. The gel samples were kept in tightly capped vials for 24 h prior to use.

IV-B2.2. Preparation of EC gel samples containing MH

As the tetracycline class of drugs is known to be thermolabile, MH incorporation into EC gel matrices was carried out only after complete gelation of EC because the elevated temperature employed for gelation would result in drug degradation. MH was found to be readily dispersed within the EC gel matrices by mixing on a glass petri dish using a spatula. Any small occasional clumps of drugs were easily broken to give homogeneous drug dispersion. The MH-containing gels were kept for 24 h to ensure complete swelling prior to any testing. In view of the light sensitivity of tetracyclines, all MH containing samples were protected from light during storage and all experiments involving samples containing MH were carried out under subdued light. The MH standard solutions were prepared immediately before use.

IV-B2.3. Determination of polymer molecular weight

Molecular weights, M_w and M_n (g/mol) and polydispersity, M_w/M_n of EC7, EC10 and EC100 polymer were determined by gel permeation chromatography (Model 2690)

using Styragel column and reflective index detector (Model 2410) obtained from Waters (Milford, MA, USA). Tetrahydrofuran mobile phase, polystyrene standards and column temperature of 40 °C were used. The results expressed as means from duplicate determinations were as follows: EC7, M_w = 54068, M_n = 16469 and M_w/M_n = 3.3; EC10, M_w = 69855, M_n = 27533 and M_w/M_n = 2.5; and EC100, M_w = 130273, M_n = 74740 and M_w/M_n = 1.7.

IV-B2.4. Stability studies

IV-B2.4.1. Stability of MH in Miglyol 840

Samples of 1 %w/w MH in Miglyol were prepared by dispersing 1 mg of MH in 0.1 g of the solvent in 20 ml vials. These samples were stored in the tightly capped vials at room temperature of 22 ± 0.5 °C and relative humidity of 50 ± 3 %. Sampled was carried out at predetermined time intervals for up to 16 weeks. Prior to HPLC analysis, MH was extracted from the oily solvent into 10 ml of phosphate buffer (pH 3, 25 mM) by subjecting the sample-buffer mixture to 5 min sonication in the Elma LC60H ultrasonic bath (Singen, Baden-Württemberg, Germany). Since MH is soluble in water but insoluble in Miglyol, such extraction resulted in the dissolution of MH in the aqueous phase. To separate the oil and aqueous phases, the mixture was centrifuged for 10 min at a speed of 4000 rpm using the Compact Tabletop Centrifuge 2100 from Kubota (Tokyo, Honshu, Japan). The lower aqueous phase containing MH was withdrawn using a long metal needle (20 gauge) and filtered through a 0.45 μm regenerated cellulose membrane filter prior to HPLC assay for amount of MH present. The first few drops of the filtrate were discarded to allow sufficient saturation of the membrane filter with the drug. In order to

investigate and quantify the possible MH degradation due to sample treatment process, the entire extraction and centrifugation cycle was also carried out using 100 μg/ml of freshly prepared MH solution, for each sampling time point for the stability study. The amount of MH originally present in the MH solution was 1 mg of MH in 10 ml of phosphate buffer and was equivalent to the starting amount of MH in the Miglyol samples. The means of triplicate samples were reported.

IV-B2.4.2. Stability of MH in non-aqueous EC gel matrices

1 %w/w MH was incorporated into EC gel matrices containing low and high concentrations of EC corresponding to 11 and 16 %w/w for EC7 and EC10, and 7 and 12 %w/w for EC100, respectively. Gel samples were divided into smaller aliquots of 0.1 g containing approximately 1 mg of MH and they were then stored at room temperature of 22 ± 0.5 °C in individual, tightly capped vials, each of 20 ml capacity, for predetermined time intervals of up to 13 weeks. Prior to HPLC analysis, MH dispersed in the non-aqueous EC gel matrix in each vial was extracted using an aqueous medium of 10 ml phosphate buffer (pH 3, 25 mM). In order to break down the gel matrices to facilitate complete release and dissolution of MH, the EC gel sample in buffer was sonicated in an ultrasonic bath for 5 min followed by manual stirring and kneading of the gel mass. This cycle was repeated twice, resulting in total sonication duration of 15 min for each sample. The disintegrated gel matrix was separated from the aqueous phase by centrifugation at a speed of 4000 rpm for a duration of 10 min. The lower aqueous layer containing MH was withdrawn using a long metal needle and filtered through a 0.45 μm regenerated cellulose membrane filter prior to HPLC assay for amount of MH present. Any possible MH

degradation due to sample treatment was quantified by repeating the entire extraction and centrifugation cycle with 100 μg/ml of freshly prepared MH solution at each sampling time point in the stability study. At each sampling point, duplicate samples were used and reported values represented the means of MH contents.

IV-B2.5. Determination of MH solubility in Miglyol 840

An excess amount of MH (approximately 4 mg) was mixed with about 4 g of Miglyol in a screw cap vial of 20 ml capacity. The sample was placed in the Precision Model 50 shaker bath obtained from Jouan (Winchester, VR, USA) at 32 °C and 50 cycles/min. Approximately 0.8 ml aliquot of the sample containing suspended MH was withdrawn at 1, 2 and 7 days, filtered through a 0.45 μm regenerated cellulose membrane filter to obtained 0.2 g of filtrate for HPLC assay. Saturation of the membrane filter with MH was ensured by discarding several initial drops of the filtrate. Sample treatment procedure prior to HPLC analysis was identical to that employed for stability study of MH in Miglyol as previously described under Section IV-B2.4.1.

IV-B2.6. Rheological measurements

Continuous and oscillatory shear rheometry measurements were performed using a cone-and-plate rheometer (Figure 8) with cone of 60 mm diameter and 1° cone angle, at a controlled temperature of 25 ± 0.5 °C. The gel sample was carefully applied to the lower plate to minimize shearing effects and allowed to equilibrate for about 10 min prior to measurement. Each measurement was carried out using a fresh sample. At least three

samples were measured for each formulation and the mean values of the various rheological parameters reported.

IV-B2.6.1. Continuous shear rheometry

The upward and downward flow curves were measured in the controlled-rate mode by changing the shear rate from 0.001 s^{-1} to 60 s^{-1} over a period of 600 s. The upward flow curves were modeled using the Oswald-de-Waele equation (Macosko, 1994):

$$\sigma = k\nu^{n} \qquad \text{(Equation 12)}$$

where σ = shear stress, ν = shear rate, k = consistency index and *n* = flow behavior index. Estimation of yield stress was done by fitting the data on the upward flow curve to the Casson's model (Macosko, 1994):

$$\sigma^{1/2} = \sigma_y^{1/2} + (\eta\nu)^{1/2} \qquad \text{for } \sigma > \sigma_y \qquad \text{(Equation 13)}$$

where σ_y = yield stress, and η = shear viscosity (creep viscosity). In order to validate the applicability of the rheometer and the Oswald-de-Waele model under the above experimental conditions, the experiment was repeated with liquid paraffin. This liquid should give a rheogram typical of a Newtonian fluid.

For measurement of the apparent viscosities of the hydrated EC100 gel matrices, the shear rate from 0.001 s^{-1} to 30 s^{-1} over a period of 300 s was employed.

IV-B2.6.2. Oscillatory shear rheometry

Oscillatory stress sweeps were performed at a constant angular frequency of 1 rad s^{-1} (0.2 Hz) over a stress range of 0.1 to 500 Pa. Oscillatory frequency sweeps were

carried out over a frequency range of 0.1 to 100 rad s^{-1} (0.02 to 16 Hz) at a constant stress amplitude of 1 Pa. At this stress amplitude, all the gel samples were within linear viscoelastic region as shown by the oscillatory stress sweep profiles. Viscoelastic parameters which included the shear modulus (storage modulus, G′ and loss modulus, G″), loss tangent (tan δ) and complex dynamic viscosity (η*) were obtained.

IV-B2.7. Mechanical characterization

Mechanical characterization of the gel samples were performed using a universal tensile machine, EZ-Tester with a 100 N load cell from Shimadzu (Kyoto, Honshu, Japan). Hardness, compressibility, cohesion and adhesiveness parameters were obtained. The experimental methods were adapted from those employed by Jones *et al.* (1997a). Gel samples were filled into 50 ml beakers, to a fixed height of about 4.5 cm immediately after their preparation. The slightly elevated temperature of the freshly prepared gel resulted in a lower gel consistency that facilitated flow of gel into the beaker. Trapped air bubbles in the gel samples were then removed by vacuum and the samples were stored for 24 h at room temperature of 22 ± 0.5 °C before mechanical testing. The gel was compressed twice by the compression probe of 25 mm diameter to a depth of 15 mm at a rate of 10 mm s^{-1}, with a recovery period of 60 s between the end of the first compression and the start of the second compression. At least three samples were measured for each formulation and the mean values of the various parameters reported. From the force-displacement plot, hardness was defined as the maximum load stress attained on gel compression and cohesion was defined as the minimum load stress on probe withdrawal from the gel. These parameters were measure of the resistance to penetration and to

withdrawal of the probe. Compressibility was defined as the work required to deform the gel through a fixed distance during compression and adhesiveness was defined as the work required to overcome the attractive forces between sample and probe. Hardness and compressibility values from the first and second compression cycles were acceptable when values of coefficients of variation (C.V.) were less than 10 %.

IV-B2.8. Construction of structures for conformational analysis

The molecular structures of diester solvents required for conformational analysis were constructed and minimized with the aid of molecular modeling software PCMODEL Version 7 obtained from Serena Software (Bloomington, IN, USA). The structures were subjected to energy minimization followed by GMMX conformational search protocol using the default settings, to obtain the Global Minimum Energy Conformation (GMEC) and Local Minimum Energy Conformations (LMECs) within 1 Kcal/mole from GMEC. The GMEC and LMECs of each solvent molecule were used in this study since the solvent molecules would generally assume the most energetically favorable conformation in the gel system or in any other chemical system.

IV-B2.9. Dynamic contact angle measurements

All dynamic contact angle measurements of sessile liquid drops on the substrate were performed using the FTÅ200 contact angle analyzer (First Ten Ångstroms, Portsmouth, VA, USA) equipped with a CCD camera (Sanyo, Osaka, Honshu, Japan). The schematic diagram for the experimental setup for dynamic contact angle measurement of sessile liquid drops on gel samples is shown in Figure 9.

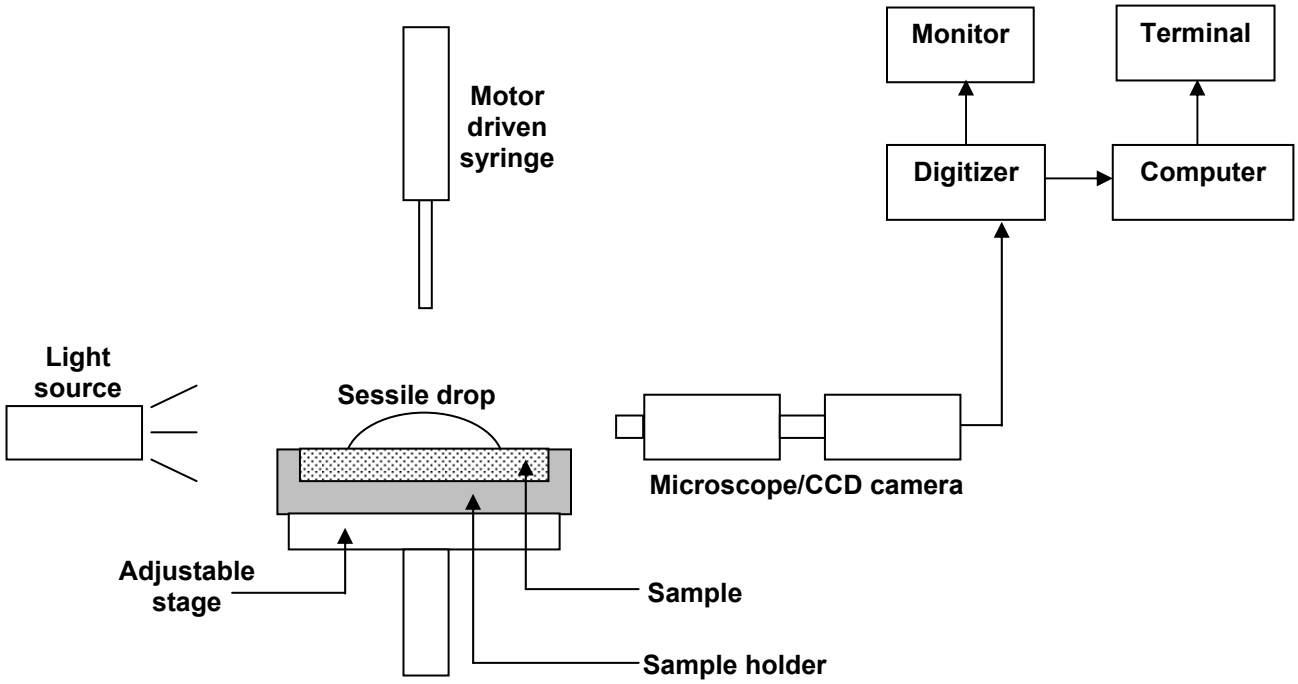

Figure 9: Schematic diagram for the experimental setup for dynamic contact angle measurement of sessile liquid drop on gel sample.

All measurements were performed at 22 ± 0.5 °C in a humidity controlled environment (relative humidity of 50 ± 3 %). The captured images of the sessile liquid drops were analyzed by the axisymmetric drop shape analysis-profile technique using the FTÅ32 V2.0 Software. Image analysis of the experimental drop profile was performed via digital image processing.

IV-B2.9.1. Gel wetting behavior

Approximately 0.3 g of EC gel was carefully filled into a sample holder of the contact angle analyzer to avoid disruption of the gel structure. Excess gel was removed from the rim of the sample holder using a spatula with sharp edges in order to produce a flat gel surface for dynamic contact angle measurement. The sessile drop was dispensed by a syringe pump through a 27-gauge flat tip needle onto a flat surface of the gel. The volume of each drop of water and IPM was approximately 8 μL and 3 μL, respectively. The contact angles at the three-phase contact line, standing volumes and base areas of sessile drops of water (θ_w, V_w and A_w, respectively) and IPM (θ_i, V_i and A_i, respectively) on the gel surface were measured over time periods ranging from 1.5 to 4 min. The mean values of 6 to 10 sessile drops for each test liquid were reported. In order to ensure that effect of sessile water drop evaporation was negligible, dynamic contact angle measurement was also carried out for sessile water drop on an impermeable solid surface and rate of change of standing volume was calculated.

IV-B2.9.2. Gel spreadability

A rectangular (2 cm × 13 cm) strip of silicone elastomer of 3 mm thickness was employed as the substrate for dynamic contact angle measurement of sessile drop of Miglyol or EC polymer solution. The substrate was thoroughly rinsed with distilled water and gently dabbed dry. The sessile drop was dispensed by a syringe pump through a 22-gauge flat tip needle onto the flat surface of the substrate. The volume of each drop of Miglyol or EC polymer solution was approximately 6 μl. The distance between needle tip and substrate was kept low, to approximately 3 to 5 mm in order to ensure negligible effect of drop momentum on spreading and the measured contact angle. The contact angles at the three-phase contact line (θ_s), standing volumes and base areas of sessile drops on the substrate were measured over 620 s. The mean values of 6 to 14 sessile drops for each test solution were reported.

IV-B2.9.3. Wettability of human skin

Dynamic contact angle measurements were repeated using water and IPM as test liquids on both silicone elastomer and human skin as substrates. The drop volume of water was approximately 9 μl and for IPM solution, approximately 4 μl. Clean, untreated dorsal skin surfaces of the hands of six female and two male adult human volunteers aged between 25 to 31 years were used and the averaged values from at least three sessile drops of water and IPM on each volunteer's skin were reported. The area of the skin was cleaned by gentle wiping using lint-free paper wetted with distilled water prior to testing.

IV-B2.10. Determination of EC gel density

A shallow acrylate container, 3 mm depth and 50 mm diameter, with a cover was employed for gel density measurement. Freshly prepared EC gel was filled to slight excess and kept for 24 h at 22 ± 0.5 °C. The cover was carefully put in place and excess gel was removed. The weight of gel was determined. The volume of each container was determined by the weight of water it could hold under the same experimental conditions. The averaged gel density values from at least three samples were reported. Gel density was calculated as follows:

Gel Density = (Weight of Gel / Weight of Water) × 0.998 g/ml [a] (Equation 14)

[a] Density of water at 22 °C (Dean, 1999)

IV-B2.11. Determination of IPM surface tension

The surface tension of IPM was determined at 22 ± 2 °C using the Rosano surface tensiometer obtained from Biolar (North Grafton, MA, USA). The surface tension measurement was based on the Wilhelmy plate method. A correction factor due to thermal expansion of plate was included in the calculation of surface tension.

IV-B2.12. Atomic force microscopy

The surfaces of silicone elastomer and freshly isolated human skin sample from the dorsal surface of the finger with a dimension of approximately 1 cm × 1 cm and 1 mm × 5 mm, respectively were scanned using an atomic force microscope, SPM-9500J from Shimadzu (Kyoto, Honshu, Japan). The samples were secured on the sample holder using an adhesive tape. The surface scanning was carried out using the non-contact dynamic

mode at a frequency of 1 Hz over an area of 25 μm × 25 μm and a *Z* range of 5 μm. The average Ra (arithmetic mean roughness) value of at least five sample areas measured was reported.

IV-B2.13. *In vitro* release study

The *in vitro* MH release studies of different EC gel formulations were carried out using the Hanson Microette® apparatus from Hanson Research (Chatsworth, CA, USA) comprising six vertical automated Franz diffusion cells, each with a orifice diameter of 15 mm and a receptor compartment volume of 7 ml. Sampling was carried out using a six-channel syringe pump connected to an autosampler. The donor compartment for each diffusion cell consists of a Teflon disk with a thickness of 1.5 mm and a central orifice of 15 mm diameter together with a glass cap. Sink condition in each receptor compartment was maintained by a magnetic stirrer and a helix cell mixer controlled by a Variomag Controller (Telemodule C). A bath circulator Model 8005 from PolyScience (Niles, IL, USA) was used to maintain a constant temperature.

EC gels consisting of low and high EC concentrations for each grade of EC were loaded with 3 %w/w MH. EC concentrations employed were as follows: 11 and 16 %w/w for EC7 and EC10, and 7 and 12 %w/w for EC100. The receptor medium, 0.1 M phosphate buffer (British Pharmacopeia 1988) at a pH of 5.5 was degassed before use. The Spectra/Por regenerated cellulose membrane discs with molecular weight cut-off of 12,000 to 14,000 (Spectrum Laboratories, Rancho Dominguez, CA, USA) were pre-soaked in the receptor medium before they were used for the release study. Approximately 0.3 g of MH-loaded EC gel, equivalent to 9 mg MH, was applied to the

donor compartment supported by the membrane. The donor-membrane assembly was carefully placed on top of the receptor compartment in order to ensure absence of air bubble. It was then capped and clamped in place. A temperature of 32 ± 0.5 °C was employed for the release study to mimic the skin temperature. The receptor medium was stirred at 100 rpm. The withdrawal of each 0.5 ml sample from the receptor compartment was preceded with a rinse cycle that flushed the sampling tube with 0.5 ml of receptor medium, termed as waste volume. Samples were collected at fourteen time points over 48 h and 1 ml of fresh receptor medium was replaced automatically and simultaneously at each sampling. The amount of MH release at each sampling time was assayed by HPLC. At least six *in vitro* release replicates for each EC sample were carried out, unless otherwise indicated. The release data were averaged to represent the release profile for each EC sample.

IV-B.2.13.1. Analysis of *in vitro* MH release data

The cumulative amount of MH released from EC gel matrices into the receptor medium over time was calculated based on the following equation (Baker *et al.,* 1990):

$$M_T[n] = V_r \cdot C[n] + V_s \cdot \sum_{i=1}^{i=n-1} \{C[n-1]\} \qquad \text{(Equation 15)}$$

where $M_T[n]$ = cumulative mass of drug transported across the membrane at time t, $C[n]$ = concentration of drug in the receptor medium, $\Sigma\{C[n\text{-}1]\}$ = summed total of the previous measured drug concentrations, $i = 1$ to $i = [n\text{-}1]$, V_r = volume of the receptor medium, and V_s = volume of the sample removed for analysis at each sampling point.

The mechanism of MH release from EC gel was determined by fitting the release data to the following equations (Heng *et al.,* 2001):

$$\text{Zero order equation, } M_G = M_0 - K_0 t \qquad \text{(Equation 16)}$$

where M_G = amount of drug remaining in the gel matrices at time t, M_0 = amount of drug remaining at t = 0, and K_0 = zero order release constant.

$$\text{Higuchi equation, } Q = K_H t^{1/2} \qquad \text{(Equation 17)}$$

where Q = amount of drug release per unit area, and K_H = Higuchi rate constant.

IV-B2.14. HPLC analysis

The HPLC analysis method described here was employed for MH assay in the stability studies, determination of MH solubility and *in vitro* release study described in Sections IV-B2.4, IV-B2.5 and IV-B2.13, respectively. HPLC assay of MH was carried out using the Shimadzu LC-2010A Liquid Chromatograph (Shimadzu, Kyoto, Honshu, Japan) equipped with a quaternary pump, a 100 µl loop injector, an autosampler and a single wavelength detector. Analytical separation was performed using a 150 mm × 4.6 mm, 5 µm particle size reversed phase Hypersil BDS C_{18} column with a 20 mm × 4 mm, 5 µm particle size C_{18} guard column (Thermo, Bellefonte, PA, USA) thermostated at 25 °C. The mobile phase employed was phosphate buffer (pH 3, 25 mM)-methanol at a volume ratio of 55:45 and flow rate of 1 ml/min. As MH was found to exhibit maximum absorbance at 255 nm (λ_{max}), a detection wavelength of 255 nm was employed. An injection volume of 40 µl was used. Calibration samples of MH were freshly prepared for every HPLC run. Linear calibration curves ($r^2 \geq 0.991$) were obtained over the drug concentration range of 4.8 to 100 µg/ml.

IV-B2.15. Determination of moisture uptake

EC gel matrices without any drug added were employed with EC concentrations of 11 and 16 %w/w for EC7 and EC10, and 7 and 12 %w/w for EC100. Moisture uptake by EC gel was determined in an environmental chamber (WTC Binder, Tuttlingen, Baden-Württemberg, Germany) at 32 ± 0.5 °C and 75 % relative humidity. Freshly prepared EC gels were filled slightly below the brim of shallow acrylate container of 3 mm depth and 50 mm diameter. Control samples of the pure solvent, Miglyol, were also included in this study. The samples were kept for 24 h in a desiccator. The weight of gel or Miglyol at an initial time (t = 0), expressed as W_0 was determined at 22 ± 0.5 °C prior to storage in the environmental chamber. Subsequently, weights of the samples at predetermined time intervals, W_t were determined for up to 10 days. Percent moisture uptake by EC gel or Miglyol was calculated as follows:

$$\% \text{ Moisture uptake} = (W_t - W_0) \times 100 / W_0 \qquad \text{(Equation 18)}$$

IV-B2.16. *In vitro* antibacterial efficacy

MH-loaded EC gels of different consistencies as given by low, medium and high EC concentrations were used in the *in vitro* antibacterial testing. The EC concentrations used were 11, 13 and 16 %w/w for EC7 and EC10, and 7, 9 and 11 %w/w for EC100. Antibacterial activity of these gels against *S. aureus* and *P. acnes* was evaluated by the agar diffusion method using surface inoculated agar medium.

Agar plates consisting of 20 ml nutrient agar in sterile petri dishes with diameter of 100 mm were prepared for cultivation of *S. aureus*. For cultivation of *P. acnes*, prepared plates (100 mm diameter) of brucella blood agar supplemented with hemin and

vitamin K_1 were used. The test bacteria, revived to their optimal state, were suspended in sterile water, which was then diluted appropriately. An inoculum size of 0.2 ml, consisting of approximately 10^6 cfu of *S. aureus* or 10^7 cfu of *P. acnes*, was spread on the agar. Three wells, with diameter of 10 mm, were made in the agar and filled with EC gel containing MH, blank EC gel and MH standard solution, respectively. Gel loading into the wells was carried out with care to avoid trapping of air bubbles at the gel-agar interface in order to ensure good contact between the deposited gel and agar. The plates were then incubated at 37 °C and radii of the zones of inhibition produced were measured.

Different conditions were employed in the test against the two bacteria of different nature. The experiments were carried out aseptically, under normal aerobic conditions for *S. aureus* and anaerobic conditions [10 % carbon dioxide, 5 % hydrogen and 85 % nitrogen in the Bactron IV anaerobic chamber (Shellab, Cornelius, OR, USA)] for *P. acnes*. *S. aureus* was cultivated on nutrient agar while *P. acnes* on brucella blood agar supplemented with hemin and vitamin K_1. The zones of inhibition were measured at the same time, within 12 to 18 h for *S. aureus* and 72 h for *P. acnes*. A longer incubation time was required for the slow growing *P. acnes* (Charnock *et al.,* 2004; Hall *et al.,* 1994). Gels and standard solutions consisting of 1 %w/w MH were employed against *S. aureus* while a lower concentration of 0.05 %w/w was used against the more sensitive *P. acnes*.

The antibacterial activity of the EC gel containing MH against both *S. aureus* and *P. acnes* was quantified by $R_{g/s}$, defined as $r_{gel} / r_{standard}$ where r_{gel} was the radius of the inhibition zone produced by EC gel containing MH and $r_{standard}$ was the radius of the

inhibition zone produced by MH standard solution. A higher $R_{g/s}$ value indicated higher antibacterial activity. The mean values of $R_{g/s}$ for at least five samples were reported.

IV-B2.17. Qualitative determination of moisture uptake from nutrient agar

EC gel matrices, incorporated with 0.5 %w/w of pure methylene blue powder as an indicator, were employed to determine whether moisture was absorbed into the gels from the agar media. The EC gel matrices used were composed of 11 and 16 %w/w of EC7 and EC10, and 7 and 11 %w/w of EC100, representing low and high consistencies, respectively. Nutrient agar prepared from Nutrient Broth No. 2 and Purified Agar was used. EC gel samples were loaded into three 10 mm wells in each plate of nutrient agar. At least four samples were tested for each of the six different EC gel matrices. Visual examination of the plates for moisture uptake into EC gel samples was carried out after 1, 2 and 3 days of storage at 37 °C. Moisture uptake was indicated by the appearance of a diffuse blue coloration in the gel which originally contained dispersed dark grey methylene blue particles.

VI-B3. Statistical analysis

All results were evaluated statistically using one-way ANOVA (SPSS 12.0 for Windows, SPSS, Chicago, IL, USA). Post-hoc statistical analyses of the means of individual groups were performed using Tukey's test. For all analyses, $p < 0.05$ denoted significance.

V. RESULTS AND DISCUSSION

V-A. Non-aqueous hydrophilic gels

V-A1. Stability of MH in water and various hydrophilic non-aqueous solvents

V-A1.1. Stability of MH in pure solvents

Figure 10 shows the % MH remaining at different time intervals in the pure solvent systems studied. Water was included in the study to compare with the other non-aqueous solvents. The % MH remaining in the non-aqueous hydrophilic solvents decreased with time and gradually leveled off, indicating that the reaction was approaching an equilibrium state. On the other hand, there was a progressive decline in MH level in water with time without attaining any equilibrium state. Kinetics modeling was carried out using equations describing first-order kinetics and first-order reversible kinetics. The first-order kinetics is represented by Equation 19 (Carstensen, 2000) and the first-order reversible kinetics by Equation 20 (Remmers *et al*., 1963).

$$\ln (A/A_0) = -k_1 t \qquad \text{(Equation 19)}$$

$$\ln (A_0-A_e)/(A-A_e) = (k_1+k_{-1})\, t \qquad \text{(Equation 20)}$$

where A_0 = % MH at time, t = 0, A = % MH at time, t, A_e = % MH at steady state, k_1 and k_{-1} = forward and backward rate constant, respectively. The rate constants, k_1 and k_{-1} were determined using the following relationship (Hussar *et al*., 1968):

$$(100- A_e) / A_e = k_1 / k_{-1} \qquad \text{(Equation 21)}$$

The plot of ln ($A-A_e$) versus t (Figure 11) followed a straight line (correlation coefficient, r = 0.980 to 0.999) with a slope of $-(k_1+k_{-1})$ indicating that loss of MH at the initial phase before plateau in non-aqueous hydrophilic solvents was best described by first-order reversible reaction kinetics, also known as pseudo first-order degradation, a

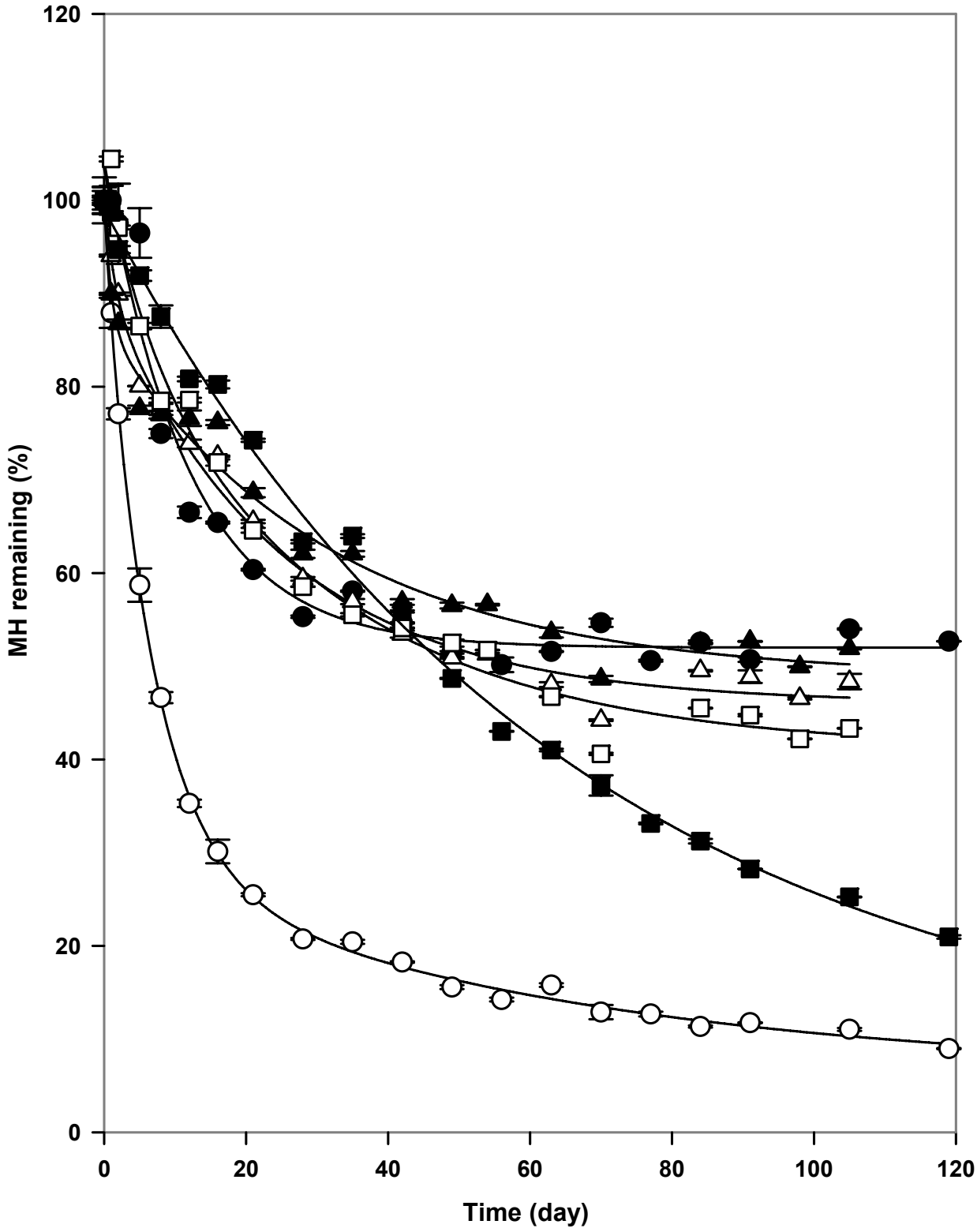

Figure 10: Stability of MH in various solvents. NMP (○), glycerin (●), propylene glycol (△), ethanol (▲), methanol (□) and water (■).

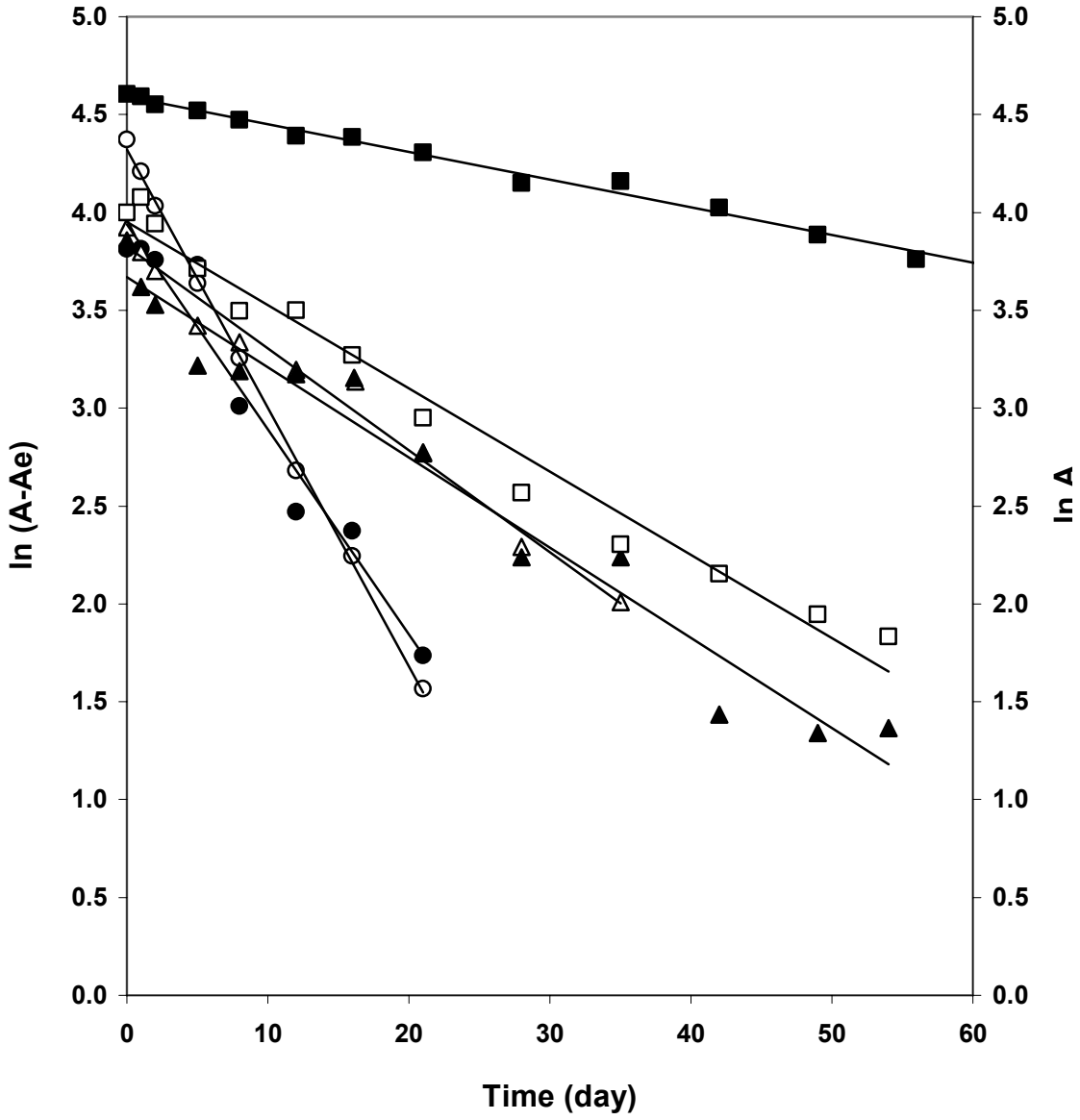

Figure 11: First-order reversible kinetics and first-order kinetics for MH tranformation in non-aqueous hydrophilic solvents and water, respectively. NMP (○, y = -0.132x + 4.323, r = 0.9993), glycerin (●, y = -0.105x + 3.938, r = 0.9801), propylene glycol (△, y = -0.052x + 3.825, r = 0.9905), ethanol (▲, y = -0.046x + 3.671, r = 0.9819), methanol (□, y = -0.043x + 3.952, r = 0.9895) and water (■, y = -0.013x + 4.575, r = 0.9974).

reaction commonly observed for tetracycline (Remmers *et al,* 1963; Wu and Fassihi, 2005). As for MH in water, the rate of MH loss followed the first-order reaction kinetics where the plot of ln A versus t exhibited a straight line (r = 0.997) with a slope of $-k_1$ (Figure 11). A higher k_1 indicated a higher rate of MH transformation and faster attainment of equilibrium MH level over time. From the rate constant, k_1, calculated for MH in various solvent systems (Table 4), MH underwent the highest rate of transformation in NMP, followed by glycerin, PG, methanol, ethanol and water. Water demonstrated the lowest k_1 as this value was derived from the first-order kinetic model where reaction end point was complete MH exhaustion instead of reaching an equilibrium level.

Table 4: Rate constants for MH transformation in various solvents.

	k_1 (day^{-1})		k_{-1} (day^{-1})		k_1+k_{-1} (day^{-1})	
NMP	0.106	± 0.002	0.028	± 0.001	0.133	± 0.003
Glycerin	0.047	± 0.001	0.057	± 0.002	0.105	± 0.004
Propylene glycol	0.026	± 0.001	0.026	± 0.000	0.052	± 0.001
Ethanol	0.021	± 0.000	0.024	± 0.000	0.045	± 0.001
Methanol	0.023	± 0.000	0.019	± 0.000	0.042	± 0.001
Water	0.013	± 0.000	N.A.		N.A.	

The % MH remaining values in different solvents were compared at six different time points (day 2, 8, 28, 49, 70 and 105) which were selected to represent the entire study period. Percent MH remaining in NMP was always significantly lower than the rest of the solvents throughout the study. Although water showed the lowest k_1 value, the first-order reaction kinetics eventually resulted in a significantly lower MH level than the rest of the solvents from day 49 onwards, with the exception of NMP. The steady state

levels of MH obtained by day 70 and day 105 decreased in the order of glycerin > ethanol > PG > methanol > NMP. This reflected the extent of MH transformation in the non-aqueous solvents. However, the trend for extent of MH transformation did not correlate directly to its rate, which increased in the order of ethanol < methanol < PG < glycerin < NMP as indicated by k_1 values. Although equilibrium MH level was attained faster in glycerin as reflected by higher k_1, glycerin was able to maintain a higher amount of MH through a lower extent of MH loss over time.

As the decline of MH level in the non-aqueous solvents followed the first-order reversible reaction kinetics, the most likely mechanism to account for the decline was the transformation of MH by C_4 epimerization, a reaction that had been associated with tetracyclines (Mitcher, 1978; Remmers *et al*., 1963). The HPLC retention times for MH and its epimer (epiMH) peaks were 8 min and 10 min, respectively. Collection and re-injection of the 10 min fraction gave rise to two peaks, corresponding to MH and epiMH. This demonstrated that the epimer was able to revert back to its original form, further supporting the proposed mechanism of MH transformation by a reversible reaction. Such reaction, known as "back epimerization" had been reported for both MH (Nelis and De Leenheer, 1982) and tetracycline (Wu and Fassihi, 2005). For glycerin and PG, epimerization was the predominant mechanism responsible for the decline in MH levels as evident by the chromatograms showing only presence of MH and epiMH peaks (Figure 12). The sum of the % MH and epiMH peaks was always approaching 100 %, indicating the sole presence of these two compounds in the solvents as opposed to the presence of MH in NMP or water which exhibited a progressive decline in total % MH

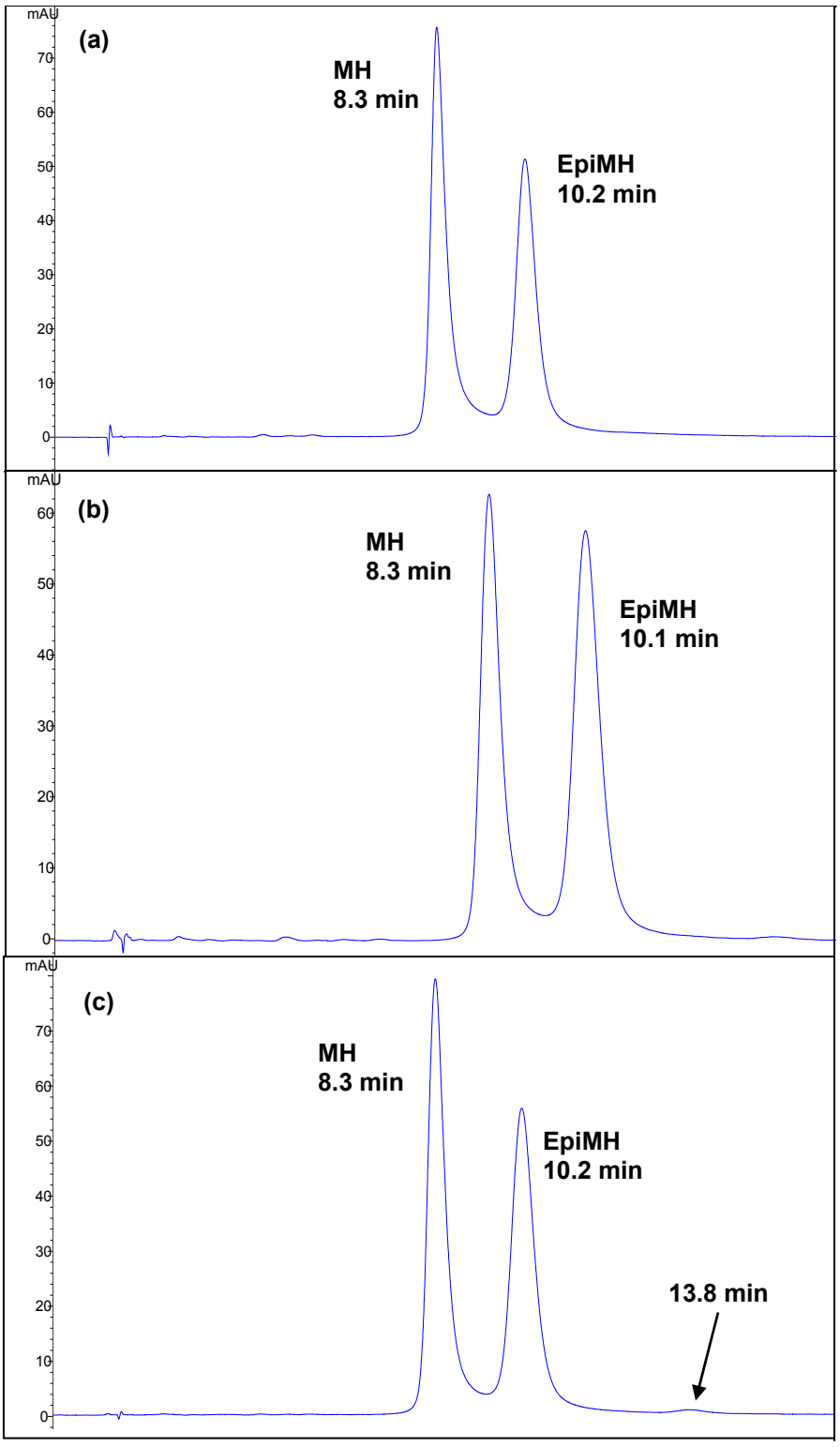

Figure 12: Chromatogram of MH in glycerin (a), propylene glycol (b) and ethanol (c) after 105 days of storage.
(HPLC analysis was performed using the Hewlett-Packard LC 1100 Series as described under Section IV-B1.1.1).

and epiMH over time (Table 5). For ethanol and methanol, total % MH and epiMH exhibited slightly greater deviations of from 100 % (Table 5) as compared to glycerin and PG. This indicated possible occurrence of other modes of MH transformation although epimerization remained the predominant mechanism in these solvents. The plots of the amount of epimer in glycerin, PG, ethanol and methanol also leveled off at around the same time frame for the amount of MH remaining to reach steady state (Figure 13). The amounts of MH remaining in NMP after 28 days and in water after 105 days were only about a quarter of the initial level. The epimer levels in NMP and water also started to decline after 35 and 56 days, respectively (Figure 13). HPLC analysis showed the presence of early extraneous chromatographic peaks which became more prominent with time. This indicated irreversible degradation of MH and epiMH compounds into possibly various low molecular weight degradants. A number of compounds that eluted later than MH and epiMH were also evident in NMP after long storage time indicating the possible occurence of complexation reaction forming high molecular weight compounds. The formation of an insoluble dark colored precipitate was observed over time as a result of MH oxidation, leading to MH polymerization through a free radical intermediate (Nilges *et al.,* 1991). Thus, these irreversible degradative processes accounted for the marked decline of MH concentration on prolonged storage in NMP or water. Although an equilibrium level was achieved for MH in NMP, on close examination of the stability data, the MH level was found to continue to decline very slowly. The rate constants of MH disappearance in NMP served only as an estimate for the rate of initial MH epimerization.

Table 5: Percentage MH remaining and epiMH formed in non-aqueous hydrophilic solvents and water over time.

Day	2			8		
	MH	EpiMH	Total	MH	EpiMH	Total
NMP	77.1 ± 0.6	15.4 ± 0.1	92 .5	46.7 ± 0.6	37.2 ± 0.3	83.9
Glycerin	97.4 ± 4.3	13.6 ± 1.1	111.1	74.9 ± 0.5	30.7 ± 1.7	105.6
Propylene glycol	88.9 ± 0.2	10.5 ± 0.2	99.4	77.6 ± 0.7	24.2 ± 2.0	101.8
Ethanol	85.6 ± 0.4	7.0 ± 0.4	92.6	77.1 ± 0.4	14.5 ± 0.2	91.5
Methanol	95.6 ± 0.2	9.1 ± 0.3	104.7	78.4 ± 0.3	20.4 ± 0.1	98.8
Water	94.7 ± 0.4	6.5 ± 0.1	101.2	87.6 ± 1.2	12.9 ± 0.2	100.5

Day	28			49		
	MH	EpiMH	Total	MH	EpiMH	Total
NMP	20.8 ± 0.1	50.7 ± 0.4	71.5	15.6 ± 0.2	46.4 ± 3.6	62.0
Glycerin	55.3 ± 0.1	49.7 ± 0.4	105.0	51.5 ± 0.1	49.4 ± 0.1	100.9
Propylene glycol	59.4 ± 0.2	42.7 ± 0.2	102.1	50.9 ± 0.1	54.7 ± 0.4	105.7
Ethanol	62.1 ± 0.4	28.5 ± 0.1	90.6	56.6 ± 0.3	38.5 ± 0.3	95.0
Methanol	58.5 ± 0.1	34.7 ± 0.1	93.2	52.5 ± 0.4	46.7 ± 0.4	99.1
Water	63.4 ± 0.2	21.6 ± 0.2	85.0	48.7 ± 0.1	24.3 ± 0.4	73.0

Day	70			105		
	MH	EpiMH	Total	MH	EpiMH	Total
NMP	13.0 ± 0.8	38.9 ± 5.5	51.9	11.0 ± 0.2	26.5 ± 0.0	37.5
Glycerin	54.7 ± 0.5	51.9 ± 0.7	106.6	54.0 ± 0.1	47.0 ± 0.1	101.0
Propylene glycol	44.2 ± 0.1	55.3 ± 0.3	99.5	48.4 ± 0.8	56.2 ± 0.6	104.6
Ethanol	48.7 ± 0.4	41.3 ± 0.1	89.9	51.9 ± 0.1	47.9 ± 0.2	99.8
Methanol	40.6 ± 0.1	48.0 ± 0.2	88.6	43.3 ± 0.1	52.4 ± 0.2	95.7
Water	37.2 ± 1.1	23.1 ± 1.4	60.3	25.3 ± 0.1	15.8 ± 0.1	41.1

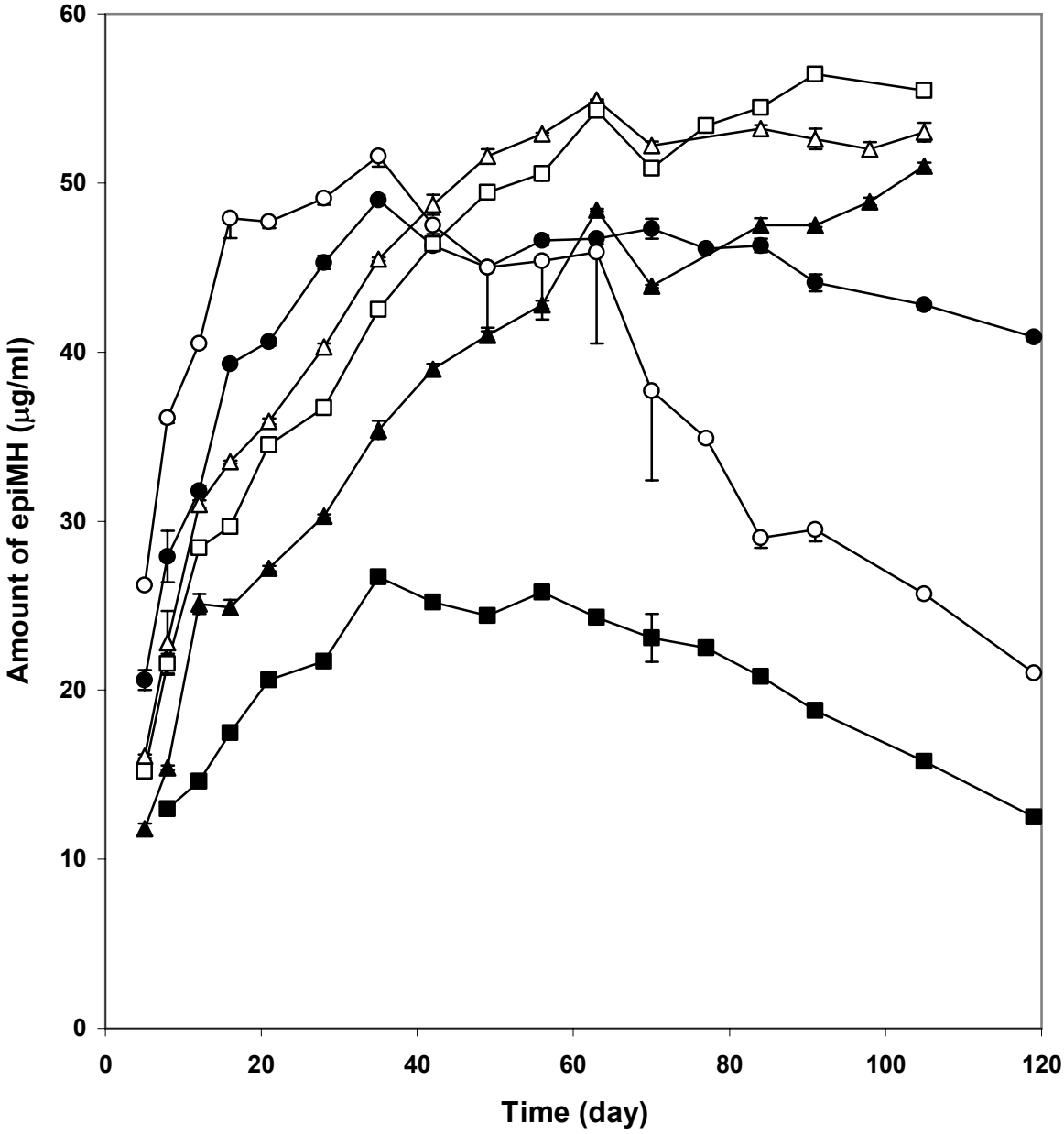

Figure 13: Amount of epiMH formed in non-aqueous hydrophilic solvents and water over time. NMP (○), glycerin (●), propylene glycol (△), ethanol (▲), methanol (□) and water (■).

In summary, the stability of MH was affected by the type of solvent employed and the duration of storage. The rate constants partially determined the stability of MH and they decreased in the following order: NMP > glycerin > PG > methanol > ethanol. The declining levels of MH in the non-aqueous solvents such as glycerin, PG, ethanol and methanol were primarily attributed to reversible C_4 epimerization, hence the rate constants were essentially the rates of epimerization. On prolonged storage in a solvent, equilibrium existed between MH and epiMH. Compared to glycerin, PG, ethanol or methanol, NMP was the non-aqueous solvent that produced markedly lower levels of MH on prolonged storage due to high rate of epimerization and irreversible degradation. Hence, the declining level of MH in a solvent was not directly related to the rate constant. Both the rate and extent of MH transformation must be taken into consideration when selecting a solvent system. The results from the stability study were consistent with literature reports on the instability of tetracyclines in aqueous systems (Mitscher, 1978).

From the findings of the stability study, PG and glycerin were selected as the two exploratory solvents for the development of a gel formulation containing MH. Although ethanol could offer advantages in terms of relatively good MH stability, it was not selected because of some unfavorable properties for use as a vehicle solvent in topical formulations. The higher volatility of ethanol poses potential problems, especially in maintaining a stable drug concentration. Close examination of the chromatogram for ethanol containing MH (Figure 12c) revealed a small peak at retention time of 13.8 min, which corresponded to another transformed product of MH or epiMH. This peak was absent in the chromatograms for PG and glycerin (Figure 12a and 12b). PG was selected for its relatively low rate of MH epimerization as shown by the rate constants. Besides, a

study had demonstrated significant follicular deposition of pyridostigmine bromide formulated with PG (Bamba and Wepiere, 1993). This was attributed to the miscibility of PG with sebum, thereby facilitating drug delivery through the follicular route. Glycerin was also chosen because it maintained a relatively high level of MH at equilibrium. As pure PG employed as a topical vehicle may cause considerable skin irritation (Wolf *et al.*, 2001; Anderson 2001), glycerin was added as a milder base to make up the rest of the vehicle. The use of glycerin could minimize skin irritation potential, hence improving the acceptability of the final gel formulation. Moreover, the combination of PG and glycerin would offer an advantage of low rate and extent of MH epimerization.

V-A1.2. Effect of different cations on MH stability in hydrophilic non-aqueous solvents

Since the main mechanism responsible for MH decline in PG or glycerin was epimerization of MH as demonstrated by the stability study, further attempts were made to improve stability of MH in these solvents by minimizing the epimerization reaction. Successful stabilization of MH in polyhydric alcohols by Mg^{2+} had been reported (Hasegawa *et al,* 1987). Therefore, the effects of different divalent and trivalent cations on the epimerization of MH in the selected solvent system were investigated. This was aimed at identifying the possibility of using cations to prevent or reduce the rate of epimerization of MH in the proposed gel formulation. An accelerated stability study at 40 °C was carried out in view of the long equilibrium time needed for the transformation of MH in the pure solvents at room temperature. Even longer equilibration times were expected with the introduction of complexing ions because the ions were known to

impart stabilizing effect to the systems (Hasegawa *et al,* 1987). Complexation reactions of MH with Mg^{2+} or Ca^{2+} were reported for cation-MH ratios of 1:1 (1 mole of cation to 1 mole of MH) or 2:1 (2 moles of cation to 1 mole of MH). Complexes of 2:1 ratio were being formed at an increased cation concentrations (Schmitt and Schneider, 2000, Wessels *et al.,* 1998). Hence, 2 moles of cation were used for every mole of MH in each sample for this study. A combination of glycerin and PG in the weight ratio of 1:1 was employed as the vehicle because this combination was deemed to be advantageous in terms of MH stability and reduced skin irritation (Section V-A1.1).

There was a general trend of decreasing MH level with time in the plots of % MH remaining versus time (Figure 14) but the rates and extents of MH decline were different in the presence of different cations. The rate constants were not determined in this part of the study because the loss of MH in these systems did not follow any normally applied reaction kinetics as opposed to the findings when pure solvents were used. Hence, the % MH remaining in different samples were compared at four different time points over the duration of the study, namely 1, 7, 14 and 28 days. Over the four time points, samples added with either $MgCl_2$ or $ZnCl_2$ showed significantly higher % MH values than the samples containing either $CaCl_2$ or $AlCl_3$. For the first 7 days, the samples with $CaCl_2$, $AlCl_3$ and the control produced % MH remaining in the following order: $AlCl_3 > CaCl_2 >$ control. After 14 days, % MH remaining in the samples containing $AlCl_3$ and $CaCl_2$ were not significantly different from the control. From day 14 onwards, the sample containing $MgCl_2$ had significantly higher % MH remaining than control and those containing $ZnCl_2$, $CaCl_2$ and $AlCl_3$. The extent of MH epimerization was significantly reduced in the presence of divalent and trivalent cations in the first two weeks of storage. It was found

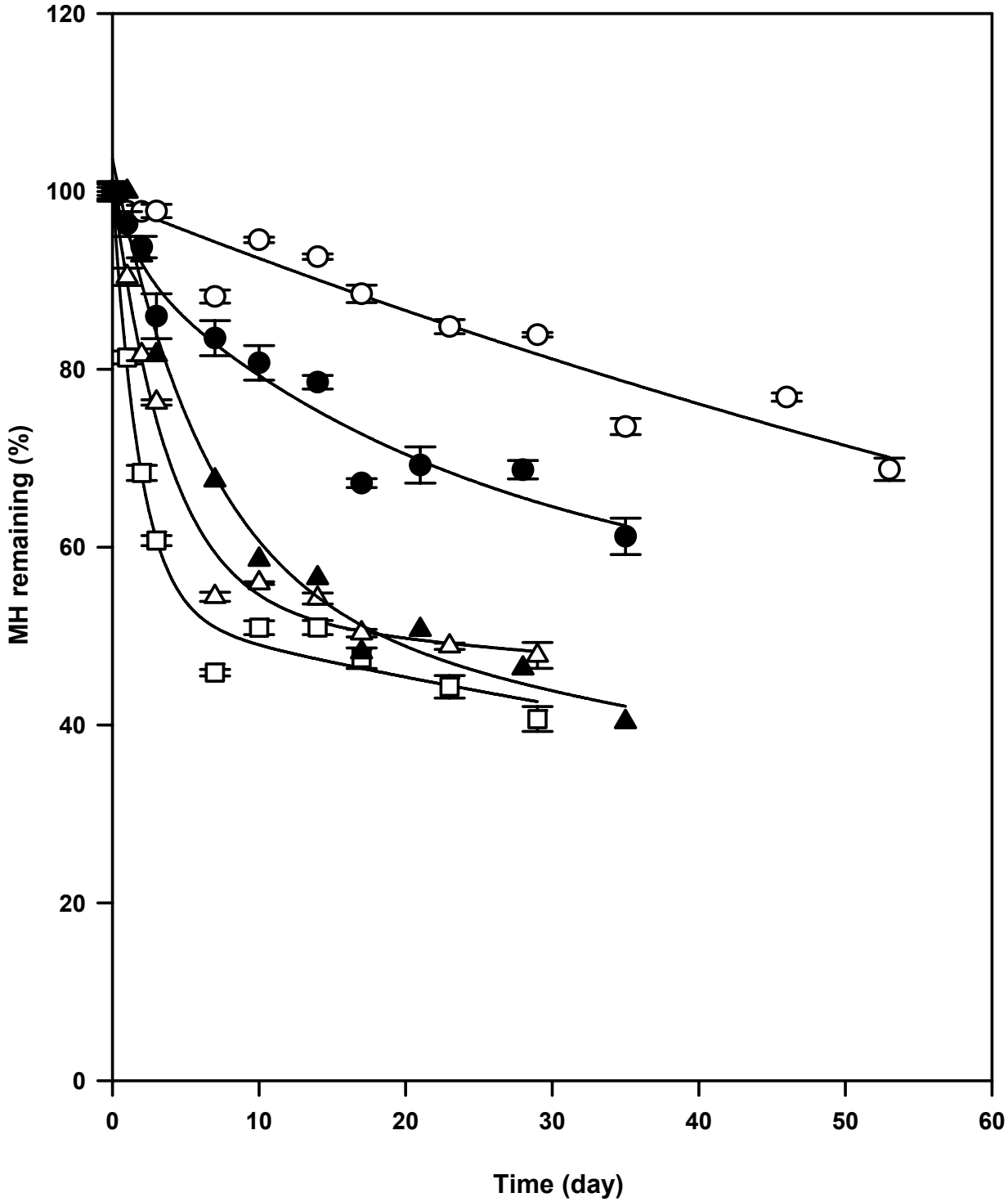

Figure 14: Effect of various cations (2 moles) on stability of MH (1 mole) in propylene glycol-glycerin mixture of 1:1 ratio at 40 °C. $MgCl_2$ (○), $ZnCl_2$ (●), $CaCl_2$ (△), $AlCl_3$ (▲) and control (□).

in this study that $MgCl_2$ and $ZnCl_2$ produced less decline of MH level by epimerization, with $MgCl_2$ being the most effective.

Divalent cations such as Mg^{2+}, Ca^{2+} and Zn^{2+} and trivalent cation such as Al^{3+} were reported to form reversible complexes with the tetracycline class of antibiotics (Wessels *et al*., 1998, Novák-Pékli *et al*., 1996; Lambs and Berthon, 1988) and anhydrotetracycline (De Almeida *et al.,* 1998). Complexation reactions between tetracyclines and metal ions had been widely studied. Tetracyclines were found to be transported in blood plasma mainly as calcium complexes while antibacterial activity was closely associated with the intracellular tetracycline-magnesium complexes (Schmitt and Schneider, 2000, Wessels *et al.,* 1998; Lambs and Berthon, 1988; Chartone-Souza *et al.,* 2005; Berthon *et al.,* 1983). Complex formation between tetracyclines and transition metals such as Cu^{2+} and Pt^{2+} had also received considerable attention as Cu^{2+} played an important role as a cofactor in tetracycline activity (Lambs and Berthon, 1988; Jezowska-Bojczuk *et al.,* 1993) and Pt^{2+} was shown to enhance tetracycline activity against resistant strains of bacteria (Chartone-Souza *et al.,* 2005).

The rate of MH epimerization was influenced by the type of cation present. Differences in size (ionic radius) and ionic strength of the cations had caused differences in binding affinity between cations to MH molecule (Ohyama and Cowan, 1995). The ionic radii followed the order of Ca^{2+} (0.99 Å) > Zn^{2+} (0.74 Å) > Mg^{2+} (0.72 Å) > Al^{3+} (0.535 Å) (Wikipedia; WebElements). Calorimetric studies showed a stronger binding between tetracycline and Mg^{2+} than Ca^{2+} due to the higher charge density of Mg^{2+} (Ohyama and Cowan, 1995), as evident from its smaller ionic radius. Thus, stronger Mg^{2+} binding with MH formed more stable complexes and this was contributory to the

lower rate and extent of MH epimerization. However, ionic radius was not the sole factor responsible for MH stabilization through complexation. This was apparent by comparing the ionic radii with the cations' effectiveness in stabilizing MH which followed the order of $Mg^{2+} > Zn^{2+} > Ca^{2+} \approx Al^{3+}$. This order was indicated by the % MH remaining towards the end of the study. Ca^{2+} and Al^{3+} possessed the highest and lowest ionic radii, respectively, but both of these cations were essentially ineffective at stabilizing MH beyond 14 days. Thus, apart from forming stable complexes, another important factor, the binding action of the cation on MH molecule imparted stability to the configuration of MH at C_4 against epimerization. Depending on the pH and nature of the solvent as well as ionic strength and concentration, tetracyclines can adopt different modes of complexation with metal ions (Wessels *et al*., 1998; Duarte *et al*., 1999). Under different conditions, tetracyclines exist in different tautomeric forms which have binding sites of varying capabilities for complexation (Duarte *et al*., 1999). For example, Mg^{2+} and Ca^{2+} were found to bind at C_{11}-O{M}O-C_{12} and C_4-Me_2N{M}O-C_3 (M denotes metal cation) at pH 7. However, different binding sites, C_{12}-O{Ca}O-C_1 and C_{10}-O(H){Ca}O-C_{11}, were evident for Ca^{2+} at pH 8.5 (Schmitt and Schneider, 2000). Zn^{2+}, on the other hand, had been reported to form a 1:1 complex with oxytetracycline and it was reported to be different from those of Mg^{2+} or Ca^{2+} complexes (Novák-Pékli *et al*., 1996). While the lower effectiveness of Ca^{2+} for stabilizing MH could be attributed to the formation of a less stable complex due to its low charge density, the relative ineffectiveness of Al^{3+} could likely be attributed to a less optimal binding site on MH in that the MH-Al^{3+} complexation was less able to prevent epimerization. Similarly, Zn^{2+} adopted a less

optimal binding site on MH since it exhibited significantly lower effectiveness in MH stabilization than Mg^{2+} despite having only slightly higher ionic radius than Mg^{2+}.

Tetracycline and oxytetracycline free bases were found to exist predominantly as zwitterions in an extended conformation in aqueous solution (Duarte *et al*., 1999; Hughes *et al.,* 1979). In non-aqueous solutions such as ethanol, chloroform and 1-octanol, or in the anhydrous crystalline state, these compounds were found to be nonionic and assumed a "twisted" or "folded" conformation. Hence, it was possible for MH to exist primarily in the "twisted" form on account of the non-aqueous nature of the solvent system used in this study. Reported studies on tetracycline-cation complexation reactions were almost entirely involving the ionized form of the drug in aqueous solutions. Hence, it is doubtful whether the proposed stabilization of MH by cation complexation was a useful explanation because the nonionic form of MH was likely to prevail in the non-aqueous PG-glycerin solvent mixture. However, the significant decrease in MH epimerization with the addition of divalent and trivalent cations in the non-aqueous solvent employed in this study implied that stabilization of the active configuration at C_4 of MH had indeed occurred. The most probable mechanism leading to MH stabilization was complexation. Complexation could occur by direct cation binding to C_4-Me_2N and O-C_3 groups thus locking the C_4-Me_2N functional group in its original configuration. Cations could also bind at C_{11}-O and O-C_{12} groups and this imposed steric hindrance towards C_4-epimerization. Both forms of nonionic and zwitterionic MH existed in equilibrium (Duarte *et al*., 1999; Hughes *et al.,* 1979). Complexation between cations and MH zwitterions would shift the nonionic-zwitterionic MH equilibrium toward producing more zwitterions allowing further complexation with free cations in the system. Hence, the

proposed cation-MH complexation reaction could appropriately account for the reduced MH epimerization in the presence of cations. However, the continuous decline of MH over time especially for systems containing $CaCl_2$ and $AlCl_2$ indicated that Ca^{2+} and Al^{2+} were less effective in stabilizing cation-MH complexes. From this study, Mg^{2+} was found to be the most effective cation in reducing the rate and extent of MH epimerization by forming more stable cation-MH complexes. On this basis, $MgCl_2$ was employed in the formulation of the non-aqueous gel matrix to minimize epimerization of MH.

V-A2. Rheological characterization

V-A2.1. Preparation of non-aqueous hydrophilic gel matrices

Based on visual observation, PNVA, Gantrez and S-630 were able to form clear gels in the non-aqueous vehicles used. All gels completely swelled after 24 hours except S1 (Table 3), which only became fully swollen to form a clear gel after 72 hours of storage. This could be attributed to the high proportion of polymer used. Consequently, longer time was needed for the complete swelling of polymer in the vehicle. Table 3 shows the amount of polymer employed to form a gel with suitable consistency based on visual observation. The minimum amount of PNVA needed for gel formation was the lowest followed by Gantrez and S-630. Thus, PNVA demonstrated the best gel-forming property in the non-aqueous vehicles whereas S-630 was the poorest.

V-A2.2. Oscillatory rheometry

The oscillatory stress sweep showed relatively constant values of the shear modulus and δ over 0.5 Pa to 100 Pa for most of the gel systems tested. Consequently,

stress amplitude of 10 Pa was selected for the oscillatory frequency sweep experiments since this stress amplitude laid within the linear viscoelastic region for all the tested systems. The consistency of S6 was very low and the shear modulus promptly decreased with the application of shear stress. Consequently, stable shear modulus was not attainable in the stress sweep. Thus, subsequent evaluation was not carried out for this formulation.

The viscoelastic properties of the gels prepared from the three different polymers at different concentrations are illustrated in the oscillatory frequency sweep profiles (Figures 15 to 17). In general, there was an increase of G′ and G″ as a function of increasing oscillatory frequency for all the formulations studied. This was consistent with the generalized Maxwell model employed to explain the behavior of semisolid materials under oscillatory shear as discussed previously (Section I-C2.2.1). A decrease in η* was observed for Gantrez and PNVA gels whereas η* remained relatively constant for S-630 gels over the frequency range examined (Figure 16).

The plots of G′ and G″ against oscillatory frequency for 3 %w/w PNVA system (Figure 15) demonstrated the predominance of G′ over G″ for all the three PG levels used, indicating the presence of relatively strong physical gels. The dominant elastic behavior was also shown by the low tan δ of less than 1 for a frequency sweep of up to 10 Hz. However, when the polymer concentration was reduced to 1 %w/w, G″ predominated for all the different vehicle ratios used. A transition from weak gel behavior to that of a concentrated polymer solution was evident with the reduction of polymer concentration. However, the elastic character still had a significant contribution since the tan δ value was still relatively low (less than 2). Low polymer concentration did not allow extensive

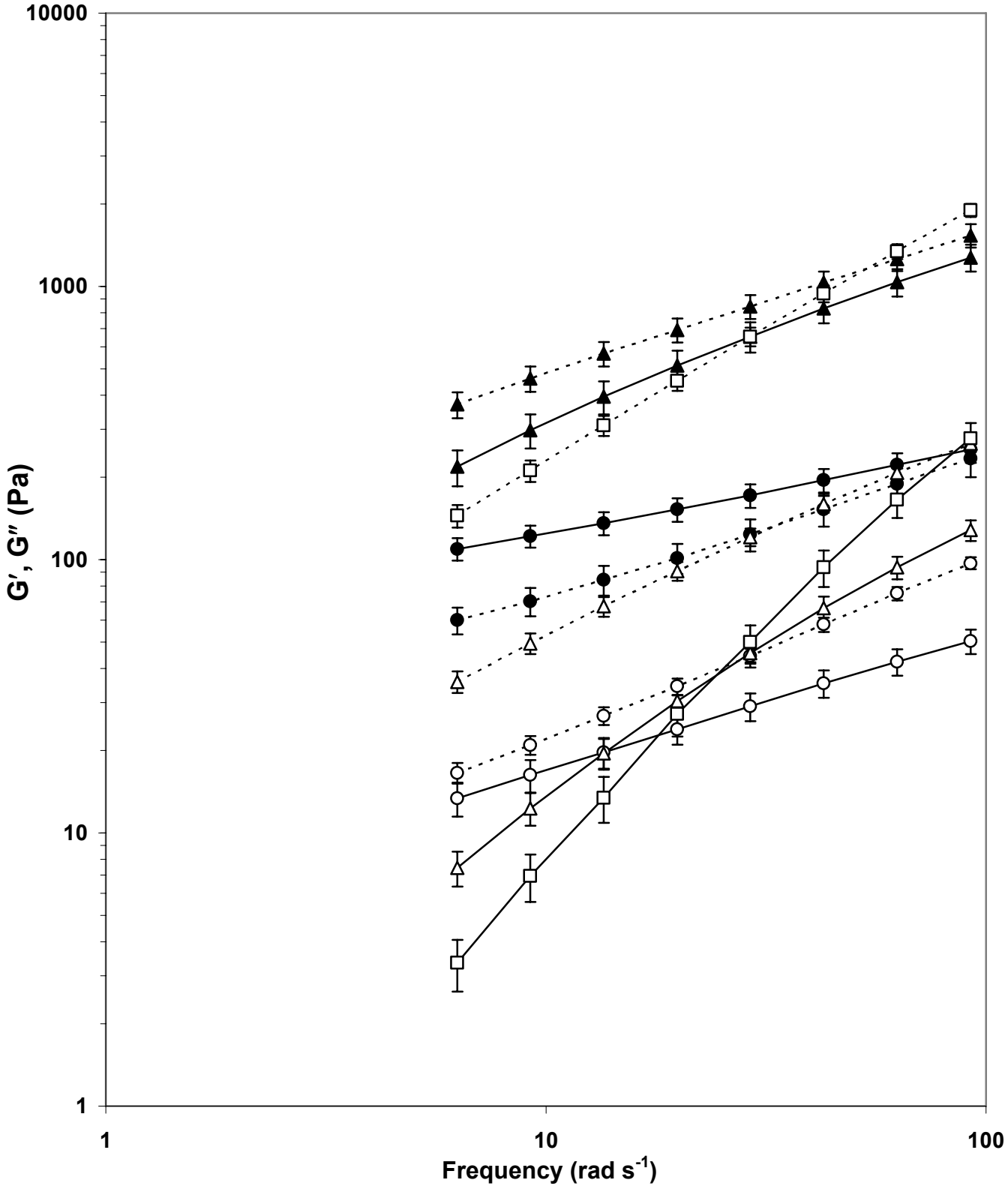

Figure 15: Storage modulus, G′ (solid lines) and loss modulus, G″ (broken lines) of PNVA, Gantrez and S-630 gels as a function of radial frequency in the oscillatory frequency sweep. P1 (●), P4 (○), G1 (▲), G6 (△) and S1 (□).

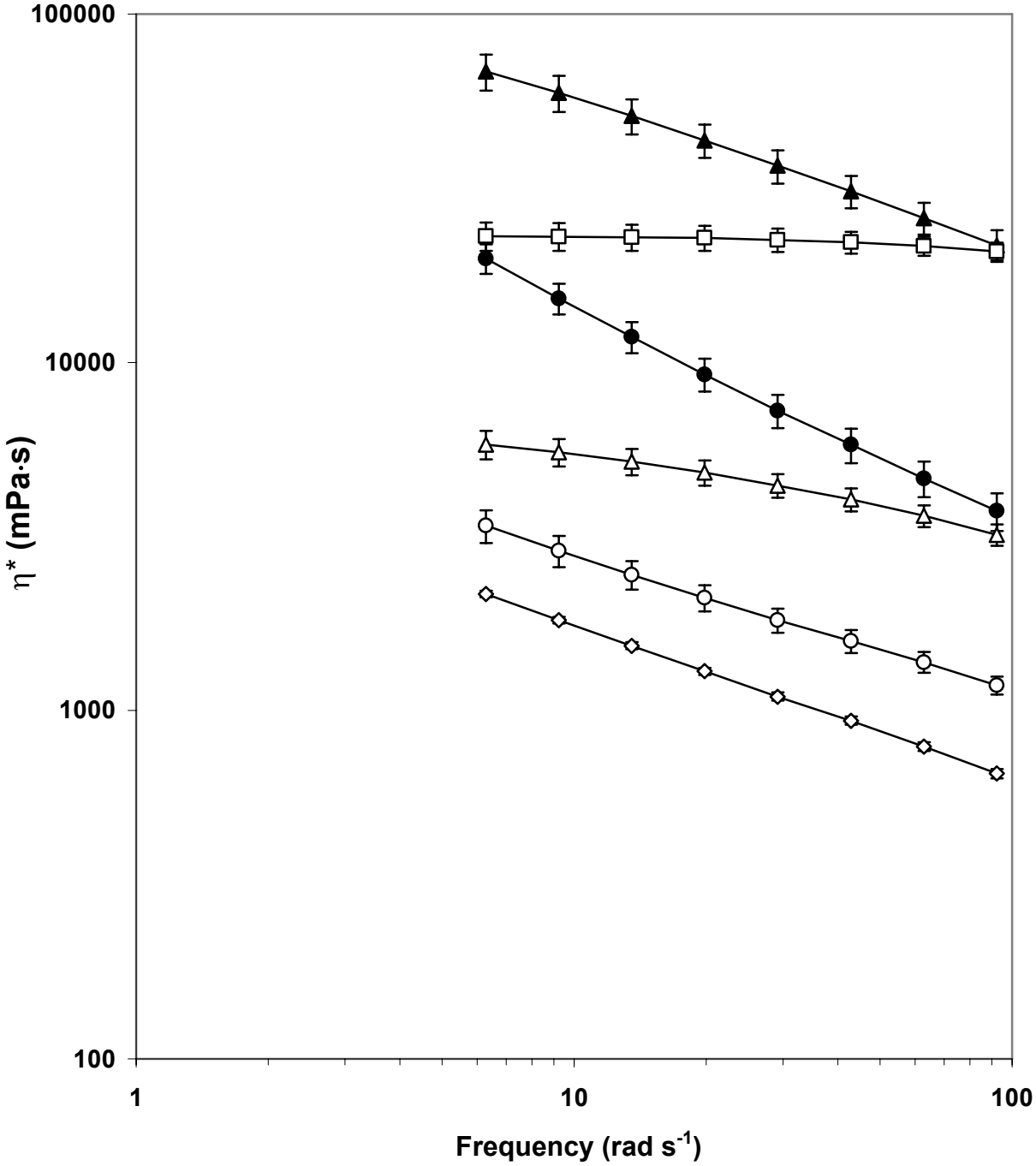

Figure 16: Complex dynamic viscosity, η* of PNVA, Gantrez and S-630 gels as a function of radial frequency in the oscillatory frequency sweep. P1 (●), P4 (○), P6 (◇), G1 (▲), G6 (△) and S1 (□).

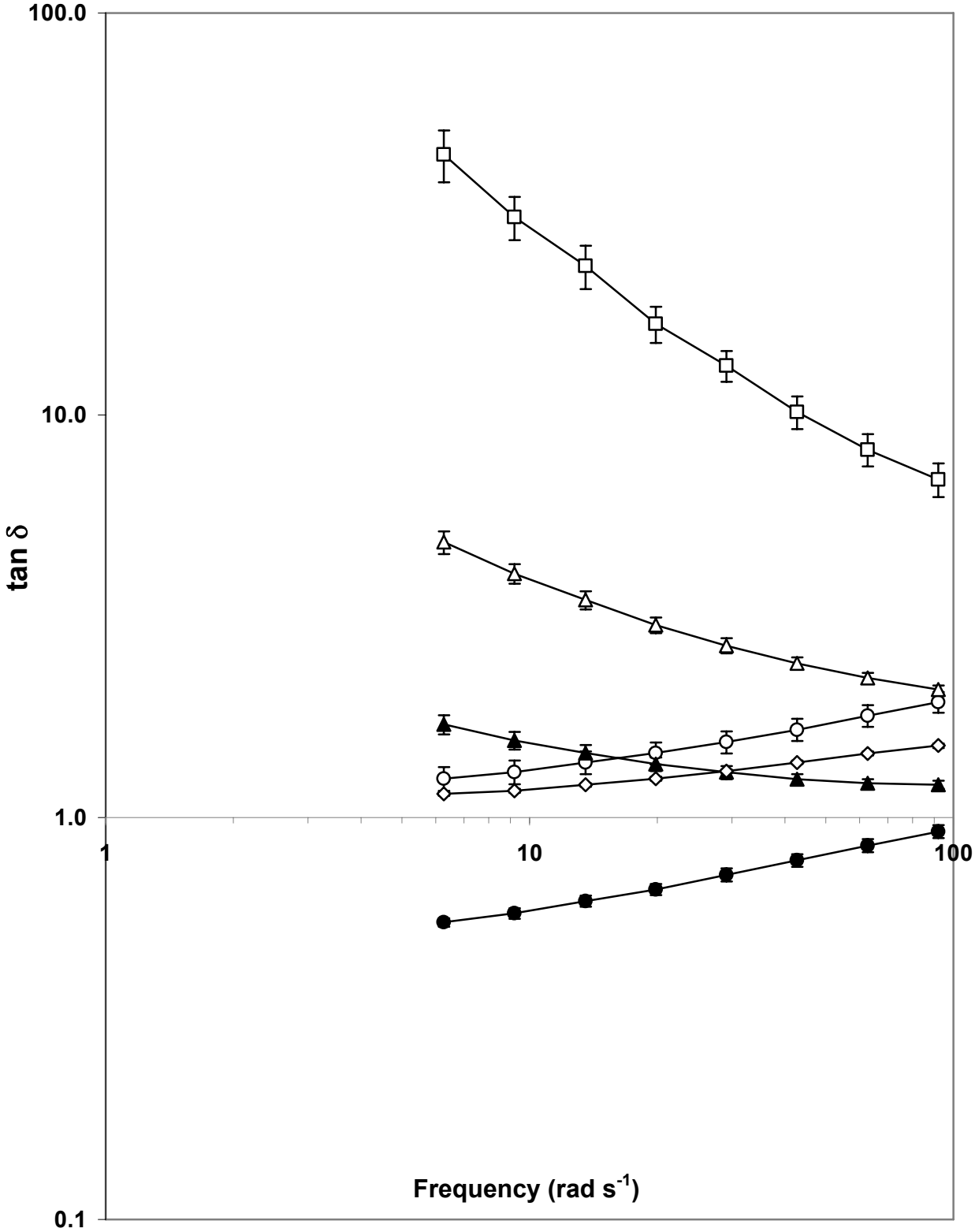

Figure 17: Loss tangent, tan δ of PNVA, Gantrez and S-630 gels as a function of radial frequency in the oscillatory frequency sweep. P1 (●), P4 (○), P6 (◇), G1 (▲), G6 (△) and S1 (□).

entanglements of polymer molecules that would give the system a rigid three-dimensional gel structure. For the same reason, η* was significantly higher in the presence of higher polymer concentration as higher extent of polymeric chain entanglements resulted in a higher resistance to flow (Figure 16). For formulations with high polymer concentration (3 %w/w), G′ was significantly higher for gel systems with a low level of PG (10 %w/w) than systems with a high level of PG (50 %w/w). However, no significant difference in G′ was observed between the gel systems with intermediate level of PG (25 %w/w) and systems with low or high levels of PG. In systems with low polymer concentration (1 %w/w), the level of PG did not significantly influence the values of G′. The same observation applied for G″, G* and η*. PG level appeared to have a significant role in governing the viscoelastic characteristic of PNVA systems with a high polymer concentration.

For Gantrez formulations, G″ was higher than G′ as illustrated in Figure 15, indicating a more pronounced viscous behavior of the systems at all the polymer concentrations tested. They behave like concentrated polymer solutions, with both G′ and G″ dependent upon frequency. The values of the viscoelastic parameters of Gantrez system were significantly different at various PG levels and polymer concentrations used. A higher polymer concentration increased solution viscosity and produced a more solid-like character (higher G′) to the gel system. Gantrez system was more sensitive to the level of PG in the formulations, in that, the viscoelastic parameters such as G′, G″ and η* decreased and tan δ increased with increased level of PG (Figure 15). The change in vehicle viscosity as vehicle ratio was altered probably caused the observed differences in the viscoelastic properties. The decrease in tan δ with increase in polymer concentration

and decrease in PG concentration again pointed to the polymer and PG concentration-dependent increase in elastic behavior for Gantrez systems (Figure 17).

S-630 formulations demonstrated strong dependency of G′ and G″ on frequency with a much higher G″ compared to G′, ranging from approximately 8 to 180 fold. In addition, the slopes for G′ and G″ in the double logarithmic plots of G′, G″ versus frequency for S1 were approaching 2 and 1, respectively (Figure 15). Similar observation also applied for S2 system. The frequency sweep profiles of S1 and S2 indicated a typical rheological behavior of a polymer solution (Section I-C2.2.3.2). The G′/G″ slope ratio of 1.64 for S3 deviated slightly from 2, the theoretical slope ratio for a polymer solution, due to the presence of high level of PG which exerted dilution effect on the polymer solution. Formulations with low polymer concentration (10 %w/w) showed extremely low G′ (below 10 Pa) at all PG levels. In general, the low G′ in S-630 systems suggested a purely viscous polymer solution behavior with insignificant elastic contribution to the system. This point was further strengthened by the observation of constant η* throughout the frequency range used in the test for all the formulations containing S-630 (Figure 16). There was a significant increase in η* with increased polymer concentration and/or decreased PG concentration. The large δ values approaching 90° exhibited by the S-630 systems were characteristic of a purely viscous system. It was suggested that even if there were very little molecular entanglements as in a polymer solution, elasticity would still be demonstrated. Distortions of the coiled molecules by the shear regions gave rise to re-alignment of some of the molecular segments, resulting in flow. Upon cessation of flow, the deformed molecule will relax back to their normal coiled state (Gupta, 2000). This phenomenon could justify the existence of G′ for S-630 systems even though they were

considered as purely viscous solutions from their rheological profiles. Hence, a highly concentrated, viscous polymer solution could be obtained using high polymer concentration of S-630 but gelation would not occur in the system regardless of polymer concentration. This was consistent with the visual observation that even the most concentrated formulation of S-630 systems could still flow upon tilting of the container because the polymer molecules easily slipped pass each other to initiate flow.

Comparing across the different polymer types, Gantrez systems showed the highest G′ at each polymer concentration tested (Figure 15). It is interesting to note that Gantrez systems showed significantly higher G′ than PNVA gels at any particular polymer concentration or PG level used although Gantrez systems lacked a physically crosslinked gel structure. Gantrez systems demonstrated the profile of a polymer solution but the absence of characteristic slope values for G′ and G″ curves, equivalent to 2 and 1 respectively, suggested that the state of true polymer solution was not attained. This indicated that Gantrez systems possessed physical characteristics in between the structured gel PNVA and polymer solution S-630. PNVA exhibited the lowest frequency dependence with regard to G′ and tan δ. For S-630 systems, these parameters were most strongly frequency dependent as shown by their steep slopes (Figures 15 and 17). Gantrez systems were slightly more frequency dependent than PNVA systems. Hence, PNVA systems were relatively more stable to oscillatory shear stresses as compared to Gantrez and S-630 systems. The ability to withstand changes due to shear was a desirable property of the PNVA systems for the formulation of a topical vehicle. Taking the oscillatory frequency of 3 to 10 Hz as a representative frequency range used in the oscillatory shear measurement experiments, PNVA gels were found to exhibit greater

overall elastic contribution than Gantrez. This was evident from the lower tan δ values of PNVA gels which ranged from 0.6 to 1.7 as compared to that of Gantrez systems which ranged from 1.2 to 3.0.

The differences in rheological properties among the different types of polymers could be attributed to differences in molecular structures of the polymers, resulting in different nature and strength of polymer interaction. The greater stability of PNVA gel systems under oscillatory shear stresses suggested the presence of stronger interactions between polymer molecules either by the formation of more contact points or stronger intermolecular attractive forces. PNVA is a neutralized system with the acidic hydrogen of the carboxyl group replaced by a sodium ion. The charge imparted to the polymer molecules by this neutralization process allowed the formation of stronger ionic bonds between the polymer molecules. Gantrez and S-630 are unneutralized systems, hence intermolecular forces are composed mainly of hydrogen bonds that are more easily disrupted under shear stress (Barry and Meyer, 1979b). This observation is consistent with that of Barry *et al*. (1979a) and Tamburic and Craig (1995) who found that unneutralized samples of the carbopol gels were significantly weaker than their neutralized counterparts. Jones *et al.* (1997b) investigated the rheological properties of the non-ionic hydroxyethylcellulose and the ionic sodium carboxymethylcellulose gels. Greater stability was observed in the ionic gel system.

The three different types of polymers resulted in non-aqueous systems with different rheological properties as evident from the different oscillatory stress sweep and frequency sweep profiles. This supported the notion that choice of polymer was the most important factor in determining the rheological properties of gel systems (Tamburic and

Craig, 1995). Polymer concentration significantly affected the viscoelastic properties of PNVA gel such that typical three-dimensional gel structure was only formed at polymer concentration of 3 %w/w. Viscoelastic properties of PNVA gel systems were not sensitive to change in vehicle ratio at 1 %w/w polymer concentration. Gantrez gel systems exhibited both the properties of a concentrated polymer solution and a viscoelastic gel. They possessed high G′ values showing the presence of a solid-like, elastic character but at the same time, showed pronounced viscous behavior. The polymer concentration and vehicle ratio exerted significant effect on the viscoelastic properties. Thus, a different PG-glycerin ratio and/or polymer concentration can be employed to change the rheological properties of Gantrez gel formulations at a particular polymer concentration. S-630 formed a purely viscous polymer solution with little elastic contribution and its viscosity was dependent mainly on the polymer concentration and PG-glycerin ratio. This property rendered pure S-630 not ideal for formulation into a topical dosage form because oscillatory shear stresses encountered at the site of application will initiate flow, hence preventing retention of product on the skin as an adhesive gel for drug delivery.

V-A3. Usefulness of non-aqueous hydrophilic gel as a gel vehicle for moisture-sensitive drugs

The stability of MH was shown to be affected by the type of non-aqueous solvents used and this led to the selection of glycerin and propylene glycol as potential vehicles with magnesium chloride as a stabilizing agent in the test gel formulations. A 3 %w/w PNVA gel was demonstrated to possess the desirable gel rheological properties. Although

the glycerin-propylene glycol and magnesium cation combination appeared as a good choice of non-aqueous hydrophilic vehicle in terms of MH stability, an almost 30 % reduction in MH level were still present in this solvent system. As a gel matrix, the best candidate found for topical gel formulation was PNVA but it was only able to form a structured gel at a polymer concentration around 3 %w/w. Preliminary study using PNVA concentrations beyond 3 %w/w resulted in extremely hard and stiff gels that were unlikely to possess any practical value as topical gel matrices. This indicated that the working range of PNVA concentration for gel formation with the chosen solvent system was very narrow. Owing to the limited ability of the hydrophilic gel system in the current study to stabilize MH and the failure of the polymer to form a reasonably wide range of gel samples with suitable consistency for further investigations, it was concluded that the non-aqueous hydrophilic gel formulations were still inadequate to fully accomplish the overall objectives of this study. Thus, a non-aqueous lipophilic gel system was formulated and studied in the quest of a gel system that would provide a more stable formulation containing MH as well as a more favorable gel network structure to be used as a semisolid topical gel.

V-B. Non-aqueous lipophilic gels

V-B1. Preparation of non-aqueous lipophilic gel matrices

A clear mixture was obtained by stirring ethylcellulose (EC) in propylene glycol dicaprylate/dicaprate (Miglyol 840) at 60 °C. Solidification of the mixture to form an opaque gel occurred upon cooling to ambient temperature. In contrast to the present study, preparation of EC gels using Ethocel Med. 100 in diester phthalate solvents by Lizaso *et al.* (1999a) involved heating mixture to 180 °C and this would entail great technical difficulty. The fine particle form of EC powders used in the present study had probably facilitated wetting due to its high overall surface area (Agrawal *et al.,* 2003a), leading to ease of dispersion and solvation of the polymer particles in Miglyol, thus enabling a lower temperature for gel formation. The gel samples formed were also more homogeneous as compared to those formed using coarser EC particles. It was difficult to wet the coarser EC particles completely, often resulting in clumps in the solvent at 60 °C.

V-B2. Stability of MH in Miglyol 840 and EC gel matrices

MH was found to be stable without visual color change in both Miglyol solvent and EC gel matrices throughout the duration of the stability study as % MH remaining over approximately three months was at least 92.6 % and 94.2 %, respectively (Tables 6 and 7). MH was also shown to be stable regardless of the EC grade and concentration present in the gel matrices. The non-aqueous gel matrices with minimal or absence of hygroscopicity towards the ambient moisture served as a barrier to protect MH from potential moisture-induced degradation.

Table 6: Percentage of MH remaining in Miglyol 840 over time.

Time (day)	% MH remaining
0	98.2 ± 13.7
5	106.7 ± 12.0
7	96.9 ± 26.6
14	99.6 ± 22.8
20	85.7 ± 10.6
27	112.0 ± 10.1
42	92.6 ± 6.5
56	107.6 ± 9.8
70	107.9 ± 23.4
91	108.0 ± 17.2
112	104.3 ± 17.3

Table 7: Percentage of MH remaining in EC gel matrices over time.

EC (%w/w)	% MH remaining [a]							
	Week							
	0	1	2	3	4	6	9	13
EC7								
11	100.0	100.4	103.5	101.8	103.6	103.5	104.8	99.5
16	100.0	102.4	105.4	104.1	105.4	105.3	105.2	100.0
EC10								
11	100.0	98.5	100.3	103.7	101.9	109.2	108.6	102.5
16	100.0	100.0	100.4	103.1	103.1	105.1	107.0	101.6
EC100								
7	100.0	102.3	101.7	104.3	116.9	97.8	98.8	94.2
12	100.0	97.5	105.6	103.2	104.4	103.7	103.8	99.0
Mean [b]	102.6							
S.D.	3.6							
C.V. (%)	3.5							

[a] Amount of MH in the EC gel has been normalized to the amount of MH in the standard solution.
[b] Determined by averaging all data points in Table 7.

V-B2.1. Effect drug solubility on MH stability

In the determination of MH solubility in Miglyol, no MH was detected by HPLC analysis of samples tested for up to 7 days. Hence, solubility of MH in Miglyol as well as the resultant EC gel matrices was likely to be insignificant. This was not unexpected since Miglyol is an oily solvent while MH is a drug present as a hydrochloride salt form that is freely soluble in water (McEvoy, 2006). The relative insolubility of MH in Miglyol was probably the main reason behind the stability of MH in this solvent and in EC gel matrices.

V-B2.2. Effect of sample pretreatment on MH stability

In the stability study, sample pretreatment involving ultrasonication and centrifugation performed before HPLC assay for amount of MH remaining had resulted in pretreatment-induced MH degradation. This phenomenon was evident from the lower amount of MH present in the standard MH solution after it was subjected to identical sample pretreatment as the samples employed for stability study. The original concentration of the standard MH solution was 100 μg/ml. The amount of MH remaining in this standard solution was 93.8 ± 2.5 μg/ml after similar pretreatment as that of MH in Miglyol and 91.4 ± 2.4 μg/ml after similar pretreatment as that of MH in EC gel matrices. Hence, pretreatment accounted for 6.2 % degradation of MH in Miglyol and 8.6 % degradation of MH in EC gel matrices. This degradation was essentially caused by epimerization as evident from the chromatogram which exhibited a small epimer peak (Figure 18). Ultrasonication was employed to extract MH from Miglyol and EC gel matrices into the aqueous solvent while centrifugation was employed to separate the

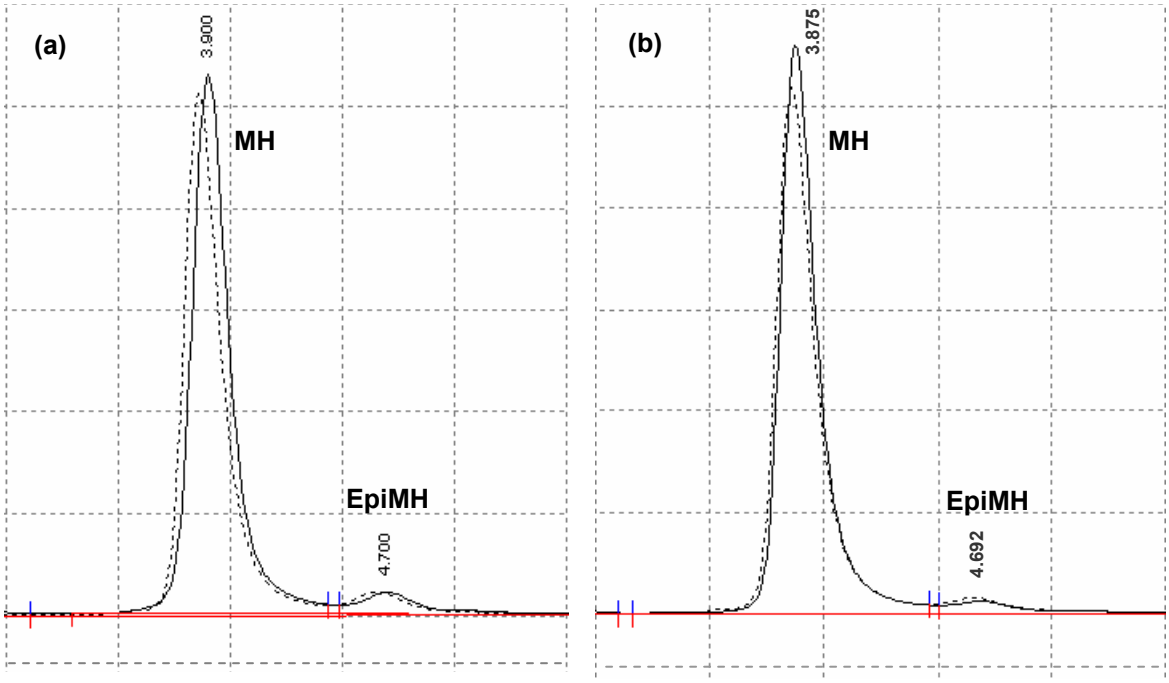

Figure 18: Chromatograms of freshly prepared 100 µg/ml standard MH solution and MH remaining in EC gel matrices after 13 weeks of storage (a), and MH remaining in Miglyol 840 after 10 weeks of storage (b). Both the standard solution (solid lines) and the samples (broken lines) had been subjected to identical treatment process before assay.
(HPLC analysis was performed using the Shimadzu LC-2010A Liquid Chromatograph as described under Section IV-B2.14).

aqueous phase containing MH from the oily phase consisting Miglyol and EC.

The main driving force for MH epimerization was the heat generated within the sample during the ultrasonication and centrifugation processes. Another possible cause of decrease in MH level during the pretreatment period was the exposure of MH to the aqueous solvents. Thus, the amount of MH loss caused by each factor needed to be accounted. A control study with MH solution not subjected to ultrasonication and centrifugation processes needed to be carried out. The data obtained from the stability study with 1 %w/w MH in water (Section V-A1.1, page 80 and Figure 11, page 82) served as the control for samples not subjected to ultrasonication and centrifugation processes prior to being assayed. The amount of MH loss due to exposure to aqueous solvent could be determined from the linear regression of ln (% MH remaining) *versus* time, $y = -0.013x + 4.575$, as shown in Figure 11 (page 82). The total durations of the pretreatment process were typically 30 min for MH in Miglyol and 60 min for MH in EC gel matrices. Substituting these time durations into x of the linear regression would result in % MH remaining of 97.00 and 96.98 %, respectively. Considering that the initial level of MH ($x = 0$) was 97.03 %, the amounts of MH lost after 30 and 60 min were only 0.03 and 0.05 %, respectively. Thus, MH loss due to exposure to the aqueous solvent was negligible. From the assay of standard MH solution subjected to the pretreatment processes, total MH loss was 6.2 % for MH in Miglyol and 8.6 % for MH in EC gel matrices and this could be attributed almost entirely to sample exposure to heat during the ultrasonication and centrifugation processes. The higher extents of MH loss in EC gel samples (8.6 %) were brought about by longer durations of ultrasonication process, resulting in greater heat exposure. As these amounts of degradation were shown to be

brought about by sample pretreatment (heat) alone, the assayed amounts of MH in the samples were normalized to the assayed amount of MH in the standard solution at each sampling time point in order to reflect the actual amounts of MH that were supposed to be present in the samples before the pretreatment processes.

V-B2.3. Homogeneity of drug distribution

Apart from demonstrating MH stability in EC gels, the variability of the values presented in Table 7 was useful to demonstrate the homogeneity of drug distribution within the gel matrices. Since % MH remaining in the EC gel samples over time appeared fairly constant (approximately 100 %) as shown in Table 7, a single coefficient of variation (C.V.) was computed for all data points obtained at different sampling time. The C.V. value indicated the variability of the % MH remaining in all EC gel samples and it also reflected the homogeneity of drug distribution within the gel matrices. The low C.V. of 3.5 % verified the uniformity of distribution of MH particles within the EC gel matrices. It should be noted that % MH remaining in 7 %w/w EC100 gel at week 4 was unusually high (116.9 %). Since there was only one unusual value out of all the 48 data points, it was reasonable to attribute it to random weighing error.

It was acknowledged that the variability of % MH remaining in Miglyol (Table 6) was rather high. However, for most days, the % MH remaining was still fairly close to 100 %. The data on Table 6 was compared statistically using one-way ANOVA and not found not to be significantly different ($p > 0.05$). Thus, the unusually low (85.7 %) and high (112.0 %) values on days 20 and 27, respectively, could be attributed to some weighing errors with the low amount (1 mg) of drug involved. Each 0.1 g sample

contained 1 mg MH in Miglyol and had to be prepared separately. It appeared that a method to achieve higher drug content accuracy was to prepare in bulk a stock of MH-Miglyol mixture and subsequently subdivide the stock mixture into smaller aliquots for stability study. However, subdivision of the MH-Miglyol bulk suspension mixture into the required 0.1 g aliquots would inherently result in considerable content variations owing to difficulties of subdividing suspended MH particles. On the contrary, the EC gel samples containing MH could be prepared in bulk prior to subdivision into 0.1 g aliquots because well-wetted MH could be uniformly distributed in the gel matrices in view of the good gel consistency that provided good drug suspending capability.

Comparing between the EC gel and the non-aqueous hydrophilic gel, the EC gel was shown to be superior in ensuring the stability of MH, hence achieving one of the objectives of this study to formulate a gel system that could protect moisture-sensitive drugs from hydrolysis. In light of the potential usefulness of EC gel matrices, it was worthwhile to perform in-depth evaluations of its physical properties in the attempt to develop it into a topical drug delivery system.

V-B3. Rheological measurements

V-B3.1. Continuous shear rheometry

Rheograms obtained from continuous shear rheometry provided information on the flow pattern and the degree of structural change in the gel systems upon shearing action. In accordance with a Newtonian fluid, liquid paraffin showed a complete overlap of up-curve and down-curve and a directly proportional relationship between shear stress and shear rate with a slope or *n* value approaching unity when the data was modeled using the Oswald-de-Waele equation (Figure 19). This showed that the rheometer and Oswald-de-Waele model were appropriate for the experimental conditions employed in this study.

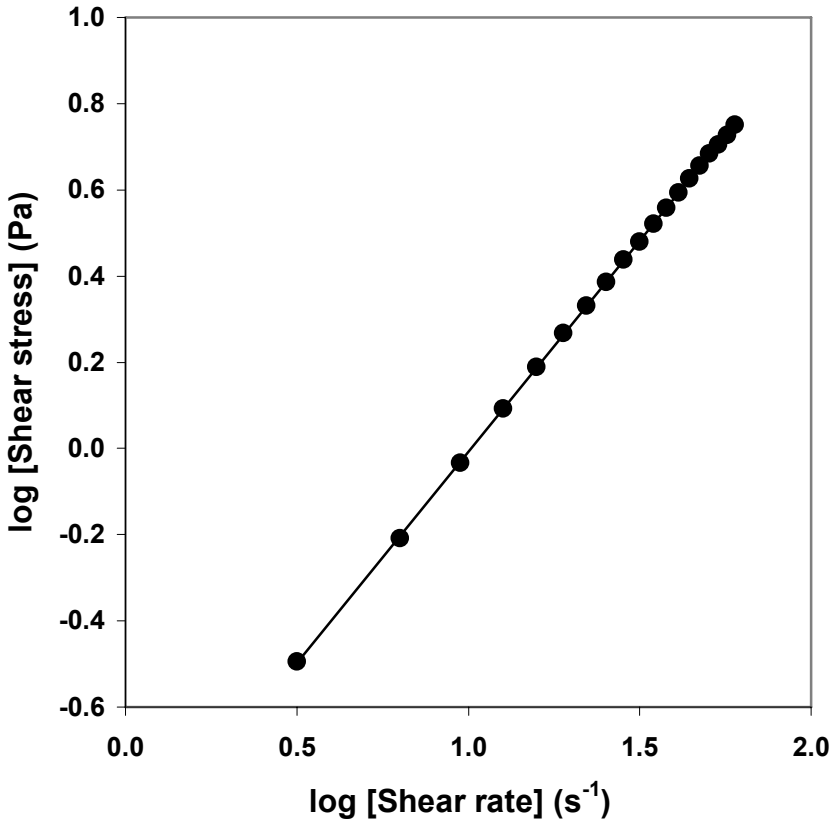

Figure 19: Rheogram of liquid paraffin as modeled using the Oswald-de-Waele equation, $y = 0.980x - 0.988$, $r^2 = 0.9999$.

The convex shapes of the rheograms of shear stress versus shear rate of the EC gels are typical of a shear-thinning system (Figure 20). The decrease in viscosity with increasing shear rate and the presence of hysteresis loops reflected the thixotropic nature of the gel systems. All the rheograms obtained conformed to the power law relationship of shear stress versus shear rate, expressed by the Oswald-de-Waele equation ($r > 0.98$). The *n* values of less than 1 for all the gel samples (Table 8) indicated shear-thinning behavior (Chang *et al.,* 2002).

The extrapolation of shear stress (σ) to zero shear rate ($\nu = 0$) in the Casson's plot of $\sigma^{1/2}$ versus $\nu^{1/2}$ gave the upper limit of the yield stress, σ_y (Talukdar *et al.,* 1996), which is the minimum stress required to be exerted to the gel before it can flow. Yield stress is regarded as a parameter that represents the rigidity and cohesion between molecules forming a three-dimensional gel structure (Contreras and Sánchez, 2002a). Increased EC concentration and polymeric chain length resulted in a stronger gel structure, as reflected by the increased yield stress, apparent viscosity at a shear rate of 10 s^{-1} and consistency index values (Table 8). The relationship of polymer concentration with yield stress, apparent viscosity and consistency index respectively was fairly linear for all the EC gels ($r = 0.9274$ to 0.9709). The concentration dependence of yield stress was observed to increase in the order of EC7 (slope = 19.94) < EC10 (slope = 49.52) < EC100 (slope = 67.48). The apparent viscosity and consistency index values exhibited similar trends. The markedly greater enhancement of yield stress (strength), apparent viscosity and consistency index in EC gels with longer polymeric chains implied that the polymeric chain length exerted a greater influence than the polymer concentrations used in this study.

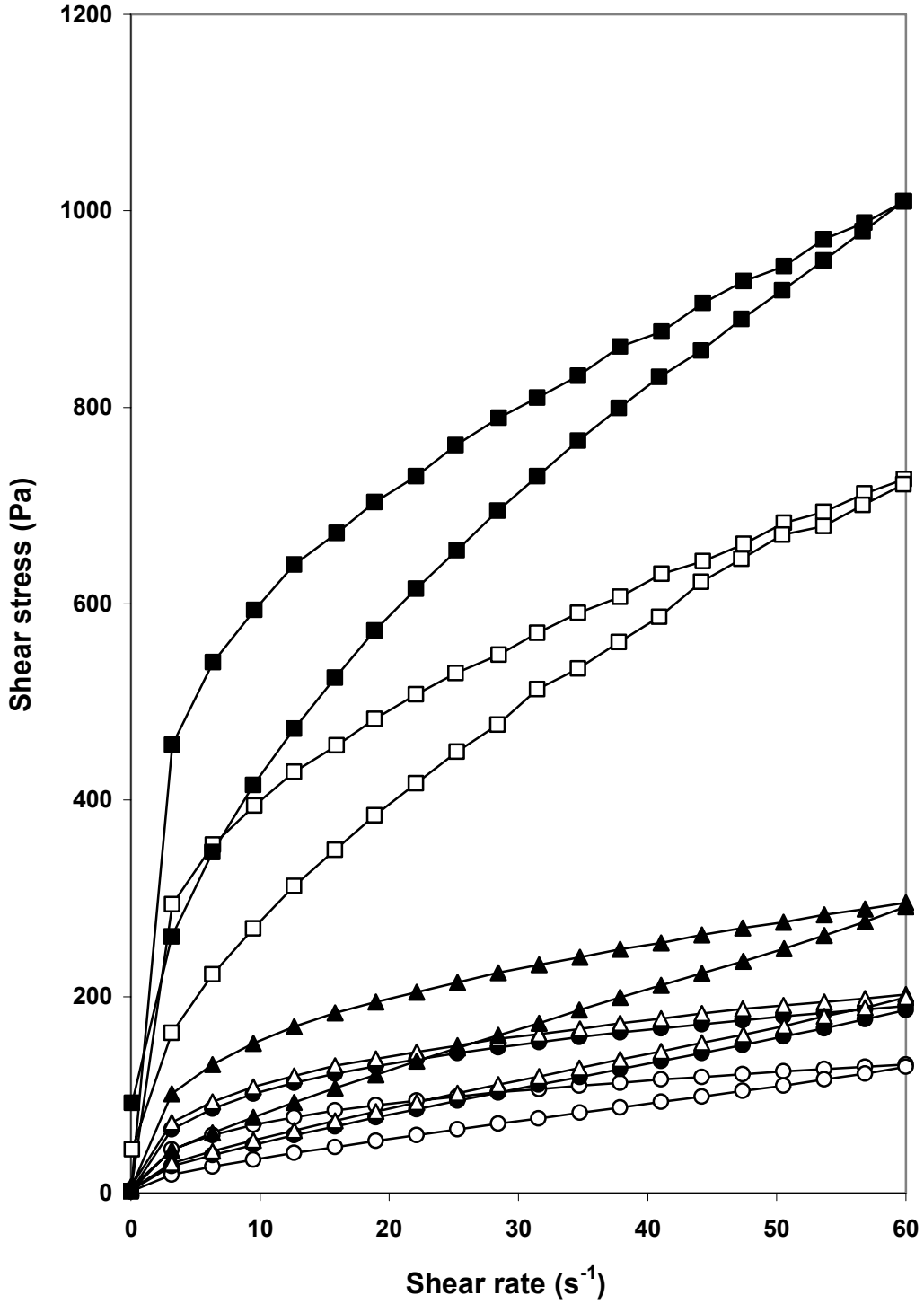

Figure 20: Rheograms showing thixotropic behavior of EC gels and effects of different EC grades and concentrations on the shear stress and thixotropic break down. EC7 (○,●), EC10 (△,▲) and EC100 (□,■). Open symbols and closed symbols represent EC concentrations of 11 and 12 %w/w, respectively.

Table 8: Rheological properties of EC gels.

EC (%w/w)	Flow behavior index, *n*	Consistency index, k ($Pa \cdot s^n$)	Apparent viscosity [a] (mPa·s)	Yield Stress (Pa)	Hysteresis area ($Pa \cdot s^{-1}$)
EC7					
11	0.361 ± 0.025	28.51 ± 3.21	7154 ± 768	36.17 ± 6.09	1515 ± 217
12	0.358 ± 0.017	44.62 ± 2.82	10359 ± 354	52.51 ± 3.79	2207 ± 211
13	0.356 ± 0.005	66.26 ± 2.41	15306 ± 601	77.48 ± 2.72	3066 ± 124
14	0.375 ± 0.006	89.20 ± 2.17	21415 ± 373	103.30 ± 2.69	4006 ± 171
15	0.423 ± 0.008	95.45 ± 1.35	25623 ± 373	107.09 ± 2.21	4084 ± 49
16	0.441 ± 0.004	124.19 ± 2.37	34342 ± 642	137.80 ± 2.78	4772 ± 166
EC10					
11	0.345 ± 0.014	49.06 ± 6.60	12225 ± 171	63.08 ± 8.14	2263 ± 147
12	0.360 ± 0.019	67.35 ± 3.97	16017 ± 744	85.42 ± 4.86	3064 ± 216
13	0.376 ± 0.011	82.34 ± 4.64	19833 ± 1154	102.75 ± 5.79	3727 ± 321
14	0.383 ± 0.009	116.44 ± 1.97	28525 ± 1106	142.35 ± 1.90	4660 ± 284
15	0.405 ± 0.011	162.54 ± 6.46	41466 ± 1402	200.07 ± 11.44	5838 ± 516
16	0.377 ± 0.010	254.01 ± 12.24	60616 ± 1855	333.00 ± 18.36	7093 ± 419
EC100					
7	0.432 ± 0.022	12.09 ± 1.37	3250 ± 235	12.80 ± 1.83	575 ± 86
8	0.339 ± 0.015	36.95 ± 2.74	8086 ± 361	41.63 ± 3.37	1428 ± 91
9	0.314 ± 0.010	75.60 ± 4.74	15589 ± 660	85.19 ± 5.70	2334 ± 175
10	0.309 ± 0.006	127.02 ± 4.21	25789 ± 509	143.42 ± 5.03	3363 ± 151
11	0.313 ± 0.013	196.62 ± 5.81	40278 ± 790	222.26 ± 7.91	4090 ± 377
12	0.272 ± 0.012	322.30 ± 17.85	60600 ± 2607	365.16 ± 19.70	5311 ± 493

[a] Apparent viscosity at a shear rate of 10 s^{-1} and a temperature of 25 °C.

The hysteresis area, H of the rheogram (Table 8), which is associated with the energy required to break down the gel structure, was linearly correlated with concentration, c of the gel system as shown by the following equations:

$H = 653.17c - 5542.5$ (r = 0.9838) for EC7

$H = 954.38c - 8443.0$ (r = 0.9925) for EC10

$H = 934.02c - 6022.6$ (r = 0.9983) for EC100

Thixotropic behavior of the EC gels also increased with the increase in polymeric chain length, with the hysteresis areas of 11 and 12 %w/w EC100 greater than those of EC7 and EC10 by at least 2.4 and 1.7 fold, respectively (Table 8). An increase in hysteresis area reflected a more extensive three-dimensional network structure (Pena *et al.,* 1994). Both larger macromolecules (longer chain length) and higher polymer concentrations allowed the formation of more extensive intermolecular interactions per unit volume, which in turn required higher energy levels to break the network.

V-B3.2. Oscillatory shear rheometry

The EC formulations exhibited a "gel" mechanical spectrum as $G' > G''$ and tan $\delta < 1.0$ in both the oscillatory stress sweep and frequency sweep, indicating a predominant elastic behavior (Tamburic and Craig, 1995). This is typical of a structured, three-dimensional physical gel network. In the oscillatory stress sweeps, the stress independence of the shear modulus and tan δ spanned over a wider stress range with an increase in polymeric chain length and concentration (Figure 21). The upper limit of linear viscoelastic behavior ranged from approximately 15 Pa (11 %w/w EC7) to 300 Pa (12 %w/w EC100). The breaking stress, namely the stress amplitude when $G'' > G'$

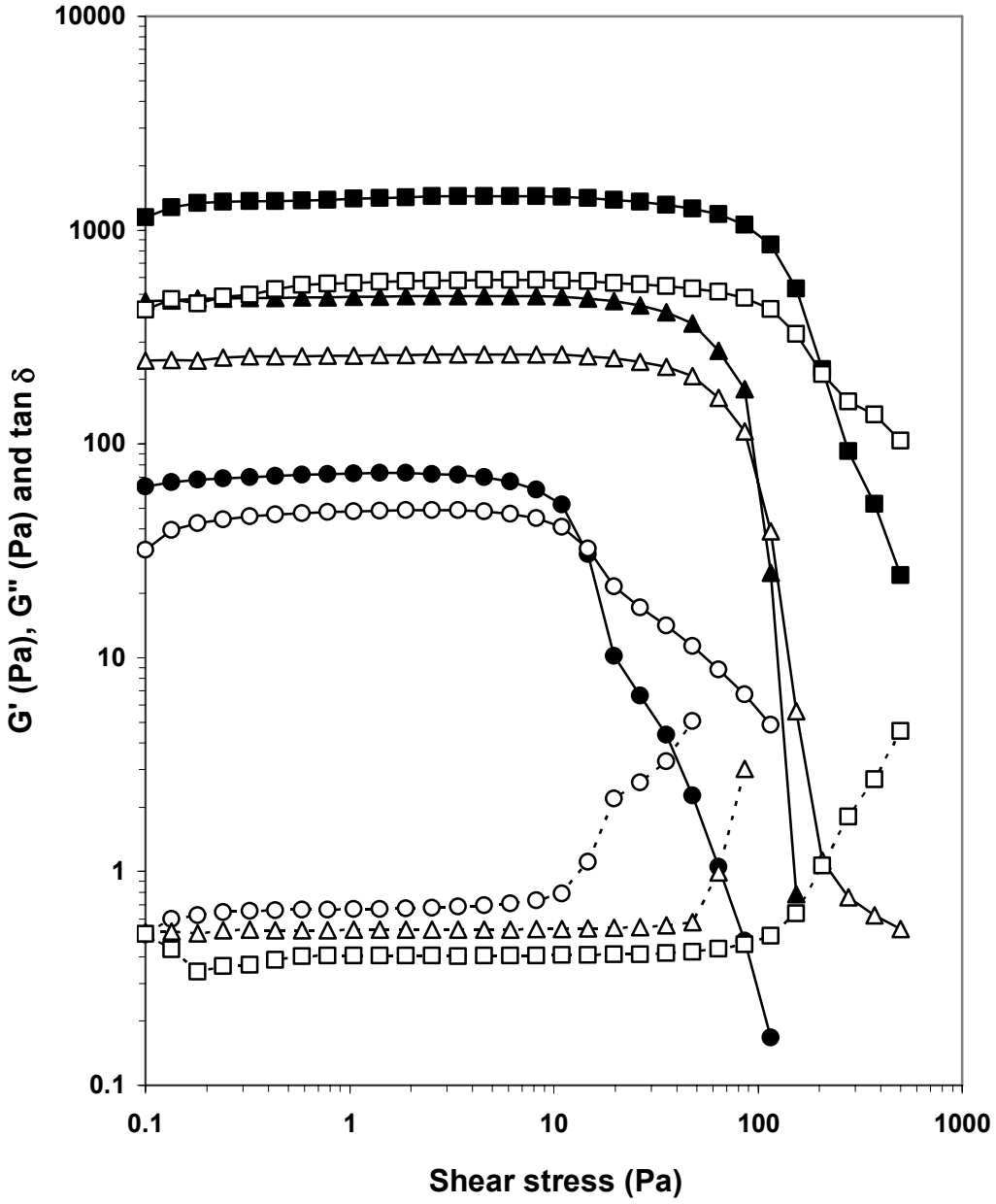

Figure 21: Storage modulus, G′ (closed symbols and solid lines), loss modulus, G″ (open symbols and solid lines), and loss tangent, tan δ (open symbols and broken lines) as a function of shear stress in the oscillatory stress sweep of 11 %w/w EC7 (○,●), EC10 (△,▲) and EC100 (□,■) gels.

(Lizaso *et al.,* 1999a), also exhibited similar dependence on polymeric chain length and concentration. In the viscoelastic region, the polymeric chains were mobilized upon application of shear stress until a critical point was attained, where they were maximally extended. The polymeric chain would eventually be pulled out of the entangled region with further increase in stress, and hence, begin to slide, resulting in a steep decrease in G′ (Chiu and Wang, 1998).

The oscillatory frequency sweep profiles (Figure 22) showed a power-law response of log G′ versus log ω where $G' \propto \omega^s$ (ω = radial frequency and *s* = slope of the double logarithmic plot). The frequency dependence of G′ in different gel systems could be represented by the values of *s*. A lower *s* value reflected a greater degree of structuring in the gel system (Contreras and Sánchez, 2002b). The *s* values of the EC gels were low, increasing in the order of EC100 (8 %w/w and above) < EC10 < EC7, where *s* = 0.266 to 0.277, *s* = 0.365 to 0.372 and *s* = 0.375 to 0.395, respectively. Therefore, degree of gel structuring increased with an increase in polymeric chain length due to the formation of a stronger and more orderly gel network. The *s* value of 7 %w/w EC100 was found to be relatively high (*s* = 0.320) compared to the other concentrations of EC100. This could be attributed to insufficient amount of polymer for extensive intermolecular interactions to produce a strong gel.

EC gels could be classified as physical gels which formed reversible physical crosslinks, as shown by their low *s* values, indicating only slight frequency dependence (Stading *et al.,* 1995). As described under Section I-C2.2.3, for a network of entangled polymer chains (pseudogel) or a polymer solution, G″ > G′ where $G' \propto \omega^2$ and $G'' \propto \omega^1$ at low frequency. On the other hand, the G′ and G″ for a strong, irreversible covalently

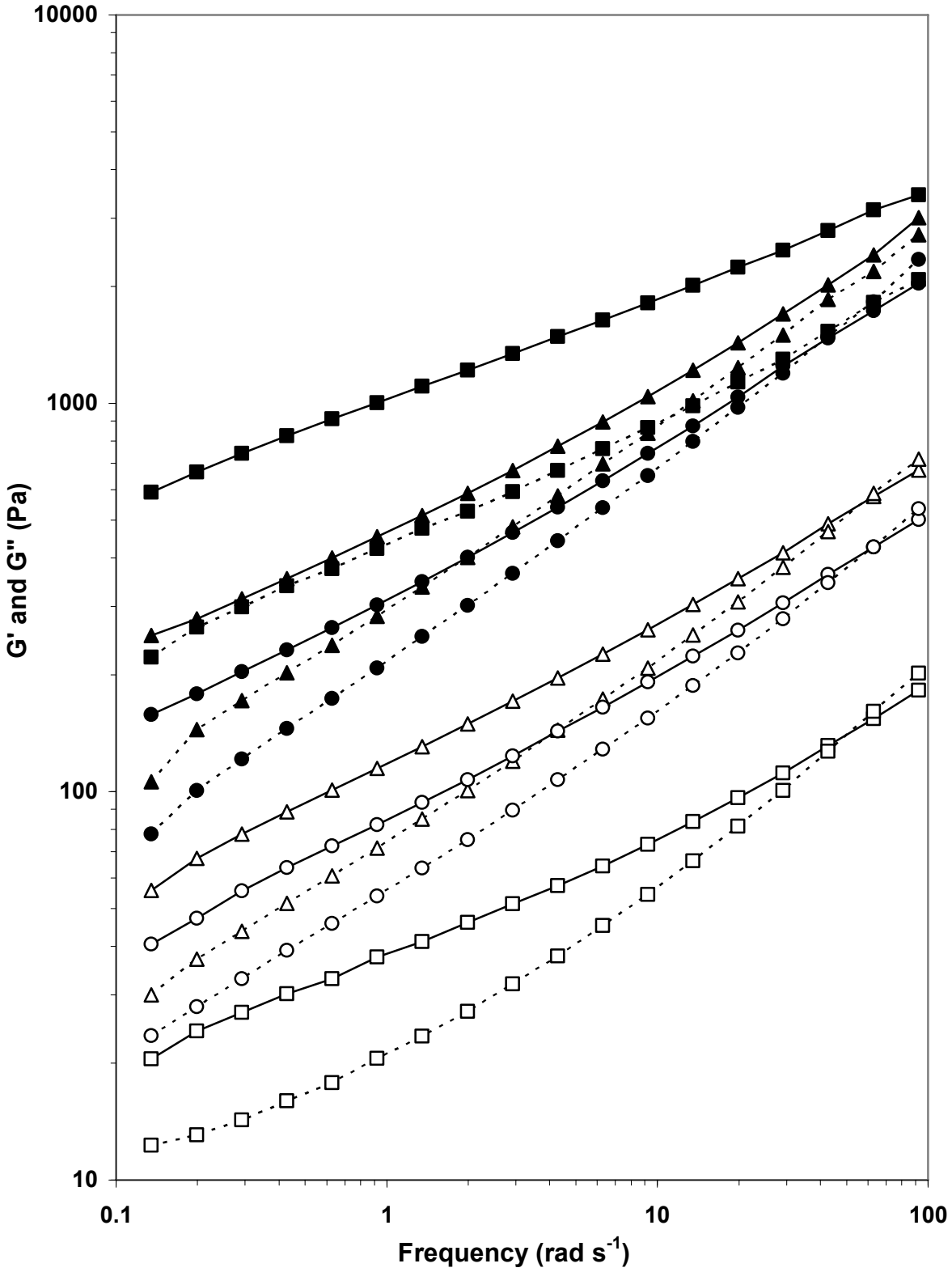

Figure 22: Storage modulus, G′ (solid lines) and loss modulus, G″ (broken lines) of EC7 (○, 11 %w/w; ●, 16 %w/w), EC10 (△, 11 %w/w; ▲, 16 %w/w) and EC100 (□, 7 %w/w; ■, 12 %w/w) as a function of radial frequency in the oscillatory frequency sweep.

crosslinked gel is relatively insensitive to frequency. In 11 to 16 %w/w EC7, 11 to 15 %w/w EC10 and 7 %w/w EC100, there was an obvious crossover of shear moduli at high frequency where G″ > G′, as opposed to EC100 (8 %w/w and above) where no crossover was apparent even up to the maximum frequency of 100 rad s^{-1} used in the test (Figure 22). The crossover indicated a transition from a structured physical gel behavior to that of a concentrated polymer solution at high oscillation frequency. The convergence of G′ and G″ curves of 16 %w/w EC10 with increasing frequency was consistent with the general behavior of EC10 gels. The change in behavior of EC7 and EC10 gel required very high oscillatory frequency which is unlikely to be encountered under normal situations when a gel is used. Hence, these gels would be deemed to exhibit good rheological properties under normal conditions of use.

The steady shear viscosity, $\eta(\nu)$ and complex dynamic viscosity, $\eta^*(\omega)$ profiles obtained for the gels using continuous and oscillatory rheological tests, respectively, were not superimposable, with $\eta^*(\omega) > \eta(\nu)$ as shown in Figure 23. The gel systems did not obey Cox-Merz superposition principle for ordinary polymer solutions, which states that the shear rate dependence of $\eta(\nu)$ is equal to the frequency dependence of $\eta^*(\omega)$, such that $\eta(\nu)$ and $\eta^*(\omega)$ are superimposable (Macosko, 1994; Kavanagh and Ross-Murphy, 1998). This observation reinforced the fact that EC gels formed a more extensive and stronger structural network than just a weak entanglement of polymeric chains.

The effects of polymeric chain length and polymer concentrations on the viscoelastic properties of the gels were statistically evaluated at four representative frequencies, namely 0.199, 0.428, 1.987 and 4.281 rad s^{-1} (Table 9). The EC gel systems generally showed a predictable increase in G′, G″ and η^* with an increase in EC

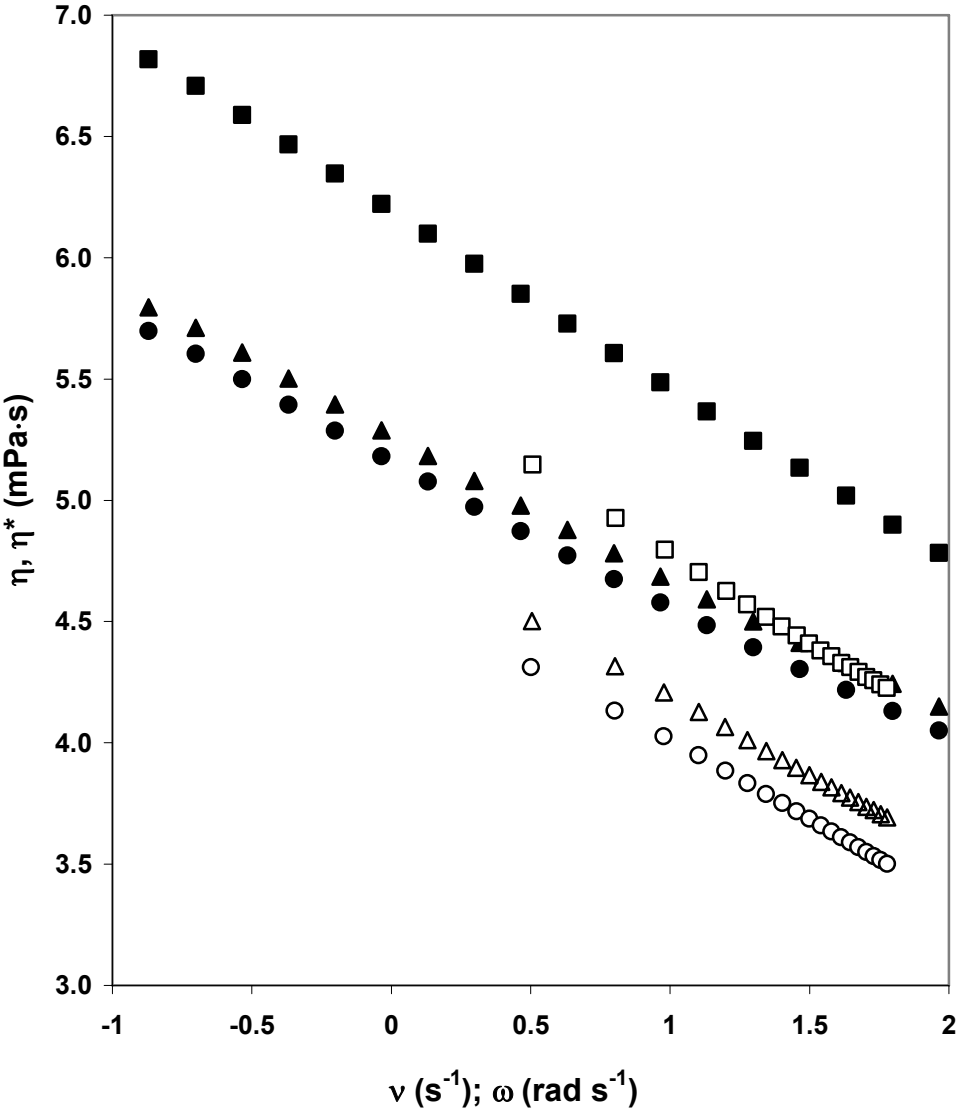

Figure 23: Combined plots of steady shear viscosity, η (closed symbols) versus shear rate, ν and dynamic viscosity, η* (open symbols) versus radial frequency, ω for 12 %w/w of EC7 (○,●), EC10 (△,▲) and EC100 (□,■) gels.

Table 9: Dynamic rheological properties of EC gels.

EC	Dynamic rheological properties of EC gel at ω = 0.199 rad s^{-1}			
(%w/w)	G′ (Pa)	G″ (Pa)	tan δ	η* (mPa·s)
EC7				
11	47.12 ± 6.15	27.89 ± 1.76	0.599 ± 0.070	275789 ± 29982
12	69.62 ± 4.82	38.89 ± 2.26	0.559 ± 0.011	401389 ± 26647
13	88.93 ± 4.84	48.67 ± 2.44	0.547 ± 0.009	510256 ± 27150
14	121.67 ± 10.25	66.47 ± 7.18	0.546 ± 0.028	697944 ± 61570
15	152.22 ± 6.18	84.98 ± 4.24	0.558 ± 0.011	877200 ± 37339
16	178.67 ± 8.06	100.59 ± 5.35	0.563 ± 0.010	1032389 ± 47450
EC10				
11	67.30 ± 8.95	37.05 ± 4.78	0.551 ± 0.017	386700 ± 50789
12	89.79 ± 12.81	48.49 ± 5.71	0.542 ± 0.025	513713 ± 69949
13	114.23 ± 11.46	60.95 ± 5.34	0.534 ± 0.022	651683 ± 62525
14	174.80 ± 8.88	90.75 ± 5.76	0.519 ± 0.010	991100 ± 52763
15	208.78 ± 26.17	113.72 ± 11.33	0.547 ± 0.019	1196833 ± 142679
16	278.68 ± 19.07	144.50 ± 8.46	0.519 ± 0.017	1579833 ± 102548
EC100				
7	24.20 ± 2.06	13.04 ± 0.59	0.541 ± 0.028	138380 ± 10313
8	160.03 ± 13.95	68.20 ± 4.83	0.427 ± 0.013	875700 ± 73745
9	212.28 ± 18.54	86.66 ± 6.76	0.409 ± 0.006	1154160 ± 99140
10	343.24 ± 32.25	137.71 ± 10.67	0.402 ± 0.014	1861857 ± 169292
11	664.41 ± 55.87	265.33 ± 20.08	0.400 ± 0.007	3600889 ± 298289
12	937.61 ± 93.08	387.68 ± 41.64	0.413 ± 0.021	5107111 ± 505130

.....continued from above.

EC	Dynamic rheological properties of EC gel at ω = 0.428 rad s^{-1}			
(%w/w)	G′ (Pa)	G″ (Pa)	tan δ	η* (mPa·s)
EC7				
11	63.70 ± 4.19	39.03 ± 2.05	0.613 ± 0.01	174500 ± 10813
12	91.08 ± 5.28	54.41 ± 2.64	0.598 ± 0.01	247800 ± 13565
13	115.00 ± 6.71	69.98 ± 3.78	0.609 ± 0.005	314433 ± 17986
14	152.78 ± 9.72	92.66 ± 5.54	0.606 ± 0.006	417700 ± 26106
15	196.67 ± 8.70	121.74 ± 4.55	0.619 ± 0.005	540422 ± 22391
16	231.33 ± 10.84	145.5 ± 6.52	0.629 ± 0.007	638211 ± 29644
EC10				
11	88.70 ± 12.56	51.52 ± 7.29	0.581 ± 0.008	239667 ± 33924
12	117.74 ± 16.42	67.94 ± 7.91	0.579 ± 0.017	317575 ± 42412
13	148.62 ± 15.22	85.57 ± 8.08	0.576 ± 0.015	400617 ± 40045
14	222.60 ± 11.59	126.00 ± 6.48	0.567 ± 0.008	597725 ± 30602
15	271.75 ± 32.41	159.00 ± 17.22	0.585 ± 0.008	735167 ± 85615
16	353.78 ± 19.81	202.33 ± 11.45	0.572 ± 0.007	951900 ± 53159
EC100				
7	30.18 ± 2.77	15.96 ± 0.83	0.531 ± 0.023	79768 ± 6591
8	196.8 ± 14.49	83.77 ± 4.83	0.426 ± 0.007	499667 ± 35533
9	265.98 ± 23.05	109.5 ± 9.11	0.411 ± 0.005	671860 ± 57718
10	420.89 ± 37.41	174.43 ± 12.77	0.415 ± 0.011	1064586 ± 91791
11	823.5 ± 71.63	338.78 ± 29.58	0.412 ± 0.012	2080444 ± 179883
12	1153.27 ± 111.43	487.58 ± 56.25	0.423 ± 0.021	2925556 ± 286793

.....continued on next page.

.....continued from previous page.

EC	Dynamic rheological properties of EC gel at ω = 1.987 rad s^{-1}			
(%w/w)	G′ (Pa)	G″ (Pa)	tan δ	η* (mPa·s)
EC7				
11	107.47 ± 6.91	75.16 ± 4.15	0.699 ± 0.007	66041 ± 4019
12	153.67 ± 8.56	106.59 ± 4.96	0.695 ± 0.009	94093 ± 4941
13	195.78 ± 12.11	140.73 ± 7.68	0.719 ± 0.006	121400 ± 7189
14	262.67 ± 18.06	189.19 ± 12.69	0.720 ± 0.007	163000 ± 11110
15	338.67 ± 14.27	249.89 ± 8.29	0.738 ± 0.008	211800 ± 8249
16	400.89 ± 18.50	301.57 ± 13.52	0.752 ± 0.006	252544 ± 11462
EC10				
11	576.18 ± 28.62	316.17 ± 17.41	0.549 ± 0.013	330817 ± 16537
12	637.26 ± 44.32	358.60 ± 22.73	0.563 ± 0.010	368040 ± 24948
13	599.80 ± 66.82	330.20 ± 34.02	0.551 ± 0.006	344600 ± 37692
14	664.56 ± 49.13	372.00 ± 20.89	0.560 ± 0.012	383300 ± 26697
15	653.26 ± 34.80	378.71 ± 19.75	0.580 ± 0.002	380043 ± 20154
16	872.80 ± 61.22	511.86 ± 30.47	0.587 ± 0.009	509286 ± 34220
EC100				
7	46.04 ± 3.90	27.18 ± 1.19	0.592 ± 0.027	26914 ± 1975
8	293.23 ± 20.50	131.33 ± 8.26	0.449 ± 0.005	161733 ± 11080
9	393.76 ± 34.47	175.00 ± 14.12	0.445 ± 0.005	216880 ± 18764
10	622.61 ± 51.94	277.57 ± 19.10	0.447 ± 0.011	343114 ± 27623
11	1218.22 ± 106.22	526.67 ± 45.83	0.432 ± 0.007	667989 ± 58085
12	1718.89 ± 170.56	744.84 ± 73.50	0.433 ± 0.008	942778 ± 93176

.....continued from above.

EC	Dynamic rheological properties of EC gel at ω = 4.281 rad s^{-1}			
(%w/w)	G′ (Pa)	G″ (Pa)	tan δ	η* (mPa·s)
EC7				
11	143.00 ± 9.35	107.29 ± 6.03	0.752 ± 0.008	41721 ± 2572
12	203.11 ± 10.93	152.16 ± 6.79	0.750 ± 0.010	59260 ± 3007
13	261.33 ± 16.48	203.23 ± 11.04	0.778 ± 0.008	77350 ± 4635
14	351.00 ± 24.30	274.28 ± 18.50	0.782 ± 0.007	104048 ± 7115
15	454.44 ± 18.08	363.98 ± 11.15	0.801 ± 0.008	136033 ± 4892
16	540.56 ± 23.69	442.20 ± 19.35	0.818 ± 0.006	163189 ± 7136
EC10				
11	196.22 ± 31.39	143.83 ± 22.39	0.734 ± 0.005	56840 ± 9008
12	259.78 ± 34.06	192.63 ± 20.11	0.744 ± 0.024	75563 ± 9163
13	327.33 ± 35.04	246.33 ± 23.42	0.754 ± 0.018	95720 ± 9765
14	484.98 ± 21.33	358.50 ± 14.46	0.740 ± 0.013	140900 ± 5869
15	602.08 ± 68.35	456.67 ± 47.78	0.759 ± 0.014	176567 ± 19428
16	774.20 ± 44.30	578.17 ± 35.35	0.747 ± 0.006	225700 ± 13213
EC100				
7	57.20 ± 4.94	37.76 ± 1.68	0.662 ± 0.031	16012 ± 1157
8	356.80 ± 24.05	169.33 ± 9.67	0.475 ± 0.006	92280 ± 6025
9	479.52 ± 42.01	229.00 ± 19.21	0.478 ± 0.007	124120 ± 10774
10	759.57 ± 62.01	363.57 ± 25.11	0.479 ± 0.011	196729 ± 15528
11	1485.78 ± 130.82	671.00 ± 54.23	0.452 ± 0.007	380833 ± 33010
12	2090.22 ± 204.64	936.02 ± 87.96	0.448 ± 0.008	535067 ± 51957

concentration and polymeric chain length in the order of EC100 > EC10 > EC7 whereas the reverse order applied to tan δ. A lower tan δ value indicates a higher degree of elastic behavior in a gel. Over the representative frequencies used for evaluation, the tan δ for EC100 (8 %w/w and above), EC10 and EC7 laid in the respective ranges: 0.400 to 0.479, 0.519 to 0.759 and 0.546 to 0.818. The range of tan δ values for 7 %w/w EC100 was particularly high (0.531 to 0.662) compared to those for higher EC100 concentrations (8 % w/w and above) as the low polymer concentration did not provide sufficient interaction points for the formation of a structured gel. In general, the ranges of tan δ values (less than 1.0) indicated the predominance of elastic behavior over viscous behavior in all the EC gels tested. The observed trends of G′ and tan δ showed that the higher polymeric chain length of EC100 resulted in a higher degree of elastic contribution to the overall character of the gels. From the comparison of average C.V. of G′, G″, tan δ and η* in the oscillatory frequency range of 0.199 to 62.83 rad s^{-1} for each EC gel sample, tan δ showed the lowest average C.V. (less than 4 %). Hence, tan δ could be regarded as a relatively more reliable indicator of the viscoelastic character of the EC gels. Nonetheless, it must be emphasized that the average C.V. values exhibited by other viscoelastic parameters were within an acceptable range (3 to 15 %) with 83 % of these values having C.V. < 10 %.

The polymer concentration-dependent increase in shear modulus was consistent with the macromolecular entanglement phenomenon where viscoelastic properties increased correspondingly with increased polymer concentrations due to higher entanglement density associated with the number of intermolecular contacts per unit volume (Talukdar *et al.,* 1996). This reduced polymer mobility and enhanced stability of

the system (Chiu and Wang, 1998). Increased entanglement density could also be the reason for the significantly more viscous gels with higher polymeric chain lengths as longer chains tend to entangle.

Apart from polymeric chain length and concentration, the influence of polydispersity on rheology of colloidal dispersions had been well documented. Increase in polydipersity was reported to reduce elastic modulus, viscosity, yield stress and shear-thinning properties by increasing the maximum packing fraction, defined as the concentration at which uniformly distributed particles touch each other (Luckham and Ukeje, 1999; Greenwood *et al.,* 1997; Kalyon *et al.,* 2002). Similar trend was observed in EC gel as values of rheological parameters decreased in the order of EC100 > EC10 > EC7 with the increased EC polydispersity (1.7, 2.5 and 3.3, respectively). EC7 and EC10 were expected to possess higher maximum packing fraction as smaller polymer molecules could fit in the interstitial spaces of larger molecules, hence reducing their intermolecular interactions (Luckham and Ukeje, 1999). The resistance to flow was decreased due to increased free volume for the movement of smaller molecules (Greenwood *et al.,* 1997).

The EC gel matrices were able to form structured gel networks over the entire concentration range, from samples of low to high consistencies as opposed to the non-aqueous hydrophilic gel matrices of PNVA which possessed a narrow concentration range for structured gel network formation. It was apparent that EC gel matrices had greater versatility in terms of gel formulation as well as rheological properties, hence would be a prospective useful topical vehicle.

V-B4. Mechanical characterization

In general, there were significant trends ($p < 0.05$) of increasing hardness, compressibility, cohesion and adhesiveness with increased polymer concentrations (Table 10 and Figure 24). All four mechanical parameters demonstrated similar profiles.

Table 10: Mechanical properties of EC gels.

EC (%w/w)	Hardness (mN)	Compressibility (N mm)	Cohesion (mN)	Adhesiveness (N mm)
EC7				
11	263 ± 26	3.1 ± 0.3	113 ± 4	2.98 ± 0.21
12	414 ± 31	5.3 ± 0.5	180 ± 21	4.44 ± 0.36
13	1395 ± 136	17.4 ± 1.6	620 ± 43	13.38 ± 0.71
14	1993 ± 129	26.1 ± 2.2	947 ± 49	20.96 ± 1.46
15	2402 ± 150	31.2 ± 2.5	1215 ± 139	26.73 ± 2.59
16	3277 ± 69	43.4 ± 2.1	1738 ± 37	36.71 ± 2.53
EC10				
11	1522 ± 73	19.5 ± 1.5	689 ± 124	13.40 ± 2.15
12	1829 ± 154	22.7 ± 2.0	794 ± 66	16.79 ± 2.15
13	2163 ± 211	28.5 ± 2.6	992 ± 140	20.76 ± 3.24
14	2536 ± 164	33.0 ± 2.9	1289 ± 94	27.77 ± 1.63
15	3244 ± 114	42.3 ± 1.9	1688 ± 93	37.87 ± 1.47
16	6031 ± 436	76.7 ± 7.4	2922 ± 117	61.87 ± 5.59
EC100				
7	383 ± 11	4.8 ± 0.2	140 ± 10	3.20 ± 0.45
8	674 ± 61	8.7 ± 0.8	301 ± 18	7.01 ± 0.18
9	1298 ± 90	17.1 ± 1.4	648 ± 33	14.48 ± 0.71
10	2314 ± 232	29.9 ± 3.8	1168 ± 142	25.66 ± 3.38
11	3778 ± 95	49.9 ± 2.2	2055 ± 87	47.52 ± 3.38
12	5098 ± 349	67.1 ± 6.6	2926 ± 172	68.78 ± 5.18

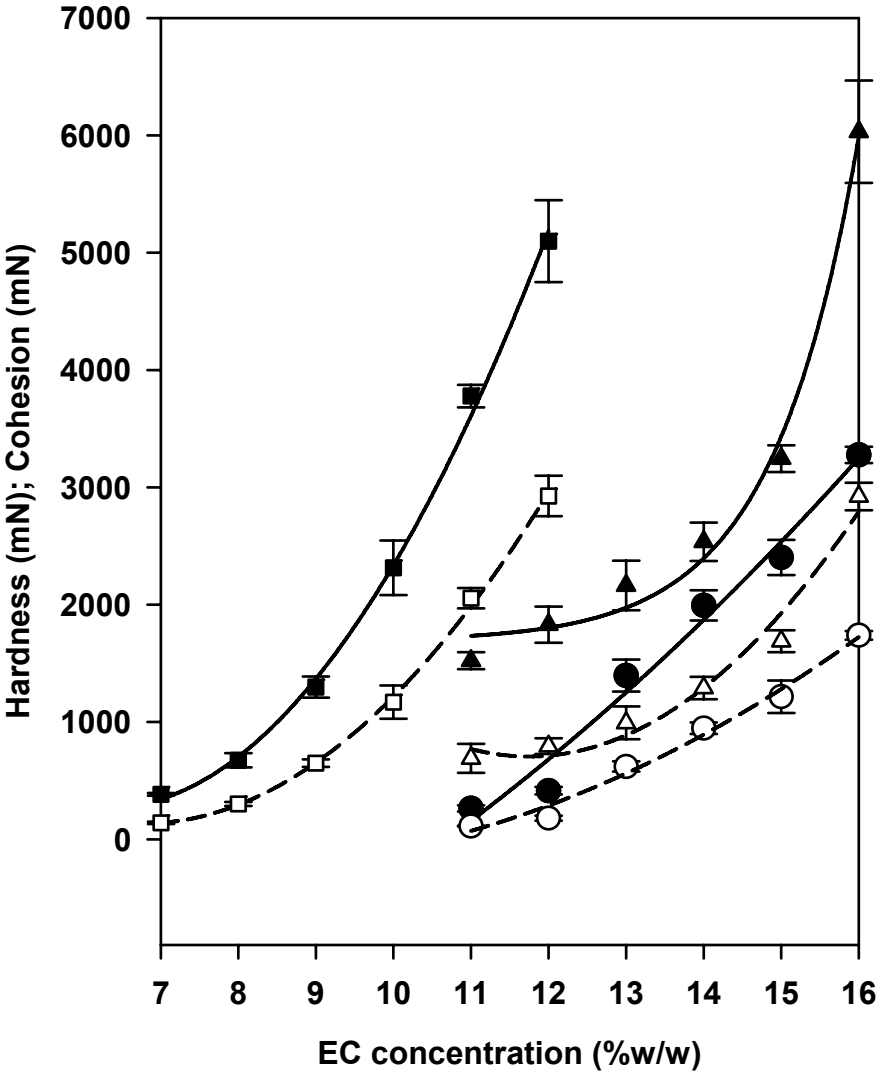

Figure 24: Change of hardness (closed symbols and solid lines) and cohesion (open symbols and broken lines) of EC7 (○,●), EC10 (△,▲) and EC100 (□,■) gels with EC concentration.

Linear correlation were obtained between G′, at the representative oscillatory frequencies of 0.199, 0.428, 1.987 and 4.281 rad s^{-1}, and the corresponding mechanical properties, namely hardness, compressibility, cohesion and adhesiveness, with r values ranging from 0.9292 to 0.9965. The mechanical properties and continuous shear properties, namely the apparent viscosity and yield stress, were better correlated (r = 0.9611 to 0.9897) compared to that between mechanical properties and viscoelastic property (G′) since the former could be described by a single regression line irrespective of the grade of EC (Figure 25). Among the mechanical parameters compared, adhesiveness was best correlated with both viscoelastic and continuous shear properties (Table 11). The linear correlations obtained between the rheological and mechanical parameters were not unexpected since the relationships between these seemingly unrelated entities have been previously described for aqueous gels (Jones *et al.,* 2002; Tamburic and Craig, 1995 and 1997; Bromberg *et al.,* 2004).

Table 11: Rheological-mechanical properties correlation.

	r-value		
Mechanical parameters	G′ at 0.199 rad s^{-1}	Apparent viscosity	Yield stress
Hardness	0.9347	0.9804	0.9611
Compressibility	0.9419	0.9824	0.9625
Cohesion	0.9604	0.9897	0.9747
Adhesiveness	0.9723	0.9896	0.9813

The increase in hardness, compressibility, cohesion and adhesiveness values with an increase in EC concentration and polymeric chain length in the order of EC7 < EC10 < EC100 was attributed to the formation of more viscous and more elastic gels as indicated by the linear relationship of apparent viscosity and G′ with mechanical

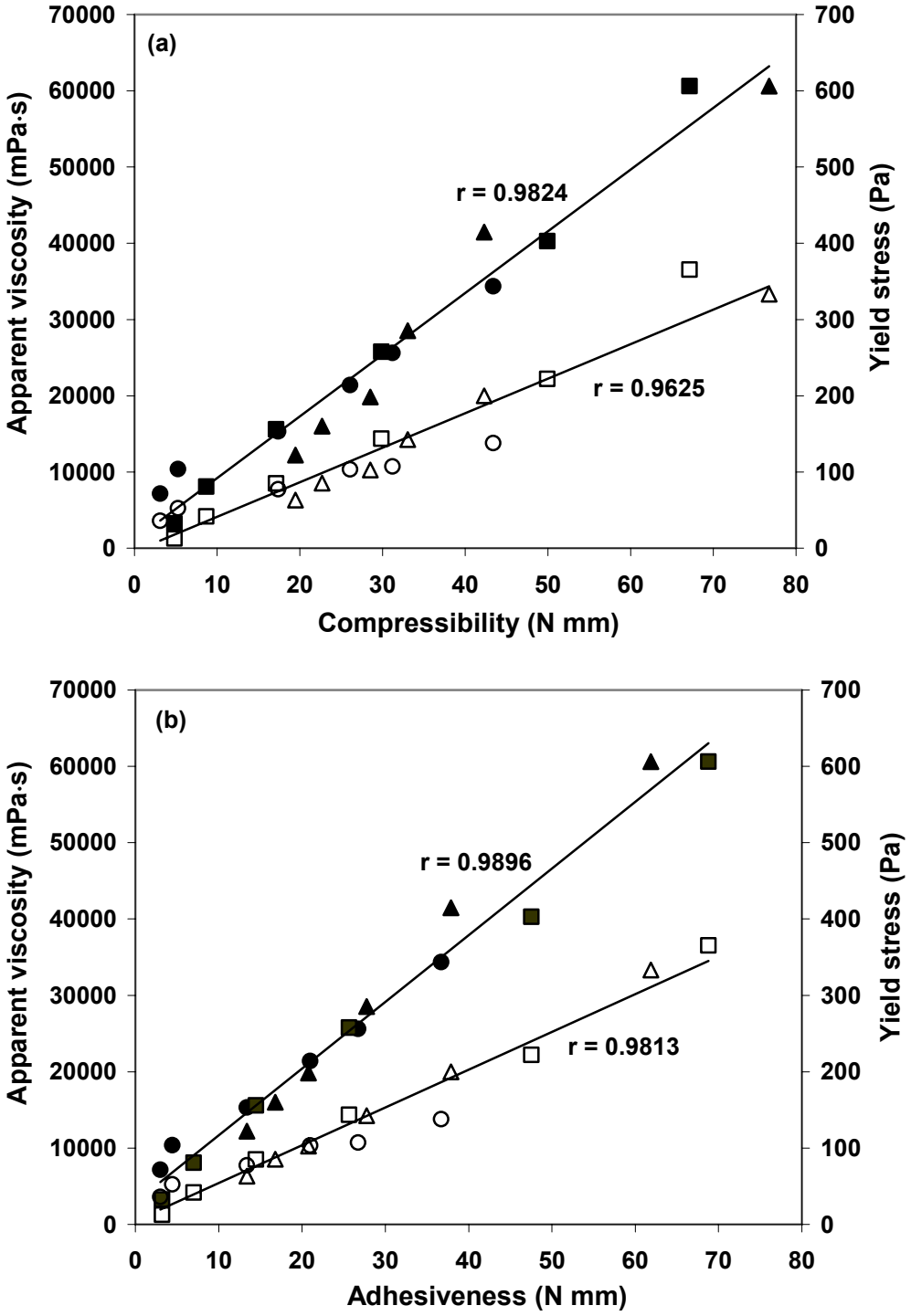

Figure 25: Linear regressions of continuous shear properties (apparent viscosity and yield stress) with compressibility (a), and continuous shear properties with adhesiveness (b) for the entire concentration range of EC7 (○,●), EC10 (△,▲) and EC100 (□,■) gels. Closed symbols represent apparent viscosity and open symbols represent yield stress.

parameters. EC gels with higher G′ presented a stronger and more solid-like structure whereas gels with higher viscosity gave higher resistance to deformation. These resulted in higher compressibility due to the increased work required to displace the probe by a certain distance into the gel during compression. Cohesive bonds within the gel matrices were broken when the probe was lowered into the gel during compression cycle. A more pronounced elastic character resulted in higher rate of gel structure recovery after compression through reversible reformation of internal cohesive bonds. This in turn resulted in higher sample tack and increased work done to induce cleavage of the cohesive bonds upon probe removal from the gel matrices, hence giving rise to higher adhesiveness values (Jones *et al.,* 1997a). Needleman *et al.* (1998) had also concluded that presence of a gel structure was indeed favorable for adhesion. Increased adhesiveness at a higher EC concentration and longer polymeric chain was also attributed to the presence of more functional groups capable of reversible bond formation with the probe surface.

Each mechanical parameter gives important information on the textural property of the gel. The ease of gel removal from a container and application onto a substrate was reflected by the properties of hardness and compressibility (Jones *et al.,* 1996b). Compressibility was regarded as a more convenient measure of gel spreadability as compared to other reported methods. In earlier reported methods, spreadability was obtained by measuring the diameter of gel spreading with the application of known weights (Jones *et al.,* 1997b; Contreras and Sánchez, 2002a). Adhesiveness is an important property used to assess product retention or bioadhesion at the site of application (Jones *et al.,* 1997b). It was cited as a reliable gauge for the ability of topical

formulations to adhere to non-mucous surfaces such as the skin (Jones *et al.,* 1996a), considering the non-mucoid nature of the analytical probe used for measurement.

V-B5. Elucidation of molecular interactions within EC gels by conformational analysis

The interaction forces responsible for entanglement and subsequent gelation of EC include intermolecular hydrogen bonding between the EC polymer molecules as well as dipole-dipole interaction between the monomer units and solvent molecules. Both types of interaction involved the hydroxyl group at the C-6 position of the anhydroglucose units of EC backbone (Jones *et al.,* 1996b; Rodriguez *et al.,* 2001; Itagaki *et al.,* 1997; Sekiguchi *et al.,* 2003; Kondo and Miyamoto, 1998). Diester solvent molecule was postulated to serve as a bridge between EC polymeric chains through dipole-dipole interaction between the positively polarized hydrogen atom on the C-6 hydroxyl group ($^{\delta-}$O-H$^{\delta+}$) of EC and the negatively polarized oxygen atom on the two carbonyl groups ($^{\delta+}$C=O$^{\delta-}$) of the diester solvent molecule. Increase in polymer-polymer interactions instead of polymer-solvent interactions gave a favorable effect towards gel elasticity (Lizaso *et al.,* 1999a).

As the frequency sweep profiles of the reported EC/diester phthalate gels were relatively insensitive to oscillation frequency (Lizaso *et al.,* 1999a), they formed stronger gel networks than the currently studied EC/diester caprylate or diester caprate gels which were marginally frequency dependent. The observed discrepancy in gel behavior when different solvents were used could be explained by examining the molecular

conformations of the solvent molecules which played an influential role in the nature of the solvent-polymer interaction in the EC gel systems.

The solvent used in the present study consisted of propylene glycol diester of caprylic (C_8) and capric (C_{10}) fatty acids. The fatty acids were made up of freely rotating single bonds (Figure 26) that possessed higher degree of molecular flexibility than the diester phthalates used by Lizaso *et al.* (1999a), namely diethyl phthalate, dibutyl phthalate and di(2-ethylhexyl) phthalate. The diester phthalates are rotationally restricted due to the necessity to maintain planarity with respect to the phenyl ring for effective electron delocalization in order to form stable chemical structures (Figure 26). Restricted rotation in turn stabilized the orientation of the carbonyl groups. Visual examination of the space-filled CPK (Corey-Pauling-Koltun) structures revealed that the two carbonyl groups involved in the polymer-solvent interaction were exposed on the surface of the solvent molecules, hence, making the dipole-dipole interaction with EC possible, hence led to the formation of gel network. However, different types of diester solvent assumed different conformations which in turn affected the orientation of the carbonyl groups and resulted in an unparalleled degree of bonding within the gel network. The carbonyl oxygen in the propylene glycol diester solvent molecules (Figure 27) was sterically hindered by the long and bulky dicaprylate and dicaprate chains as these chains protruded slightly above the exposed surface of the carbonyl oxygen atoms. This had compromised the EC $^{\delta-}O\text{-}H^{\delta+}\cdots{}^{\delta-}O{=}C^{\delta+}$ alignment as the interacting functional groups could not come very close in proximity. In contrast, examination of the Global Minimum Energy Conformation (GMEC) of diethyl phthalate and dibutyl phthalate (Figure 28) revealed that the carbonyl oxygen resided along the sides of the molecule opposite to each other.

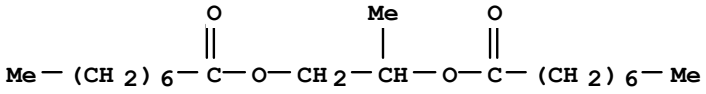

(a)

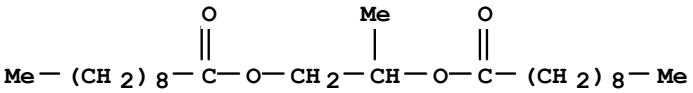

(b)

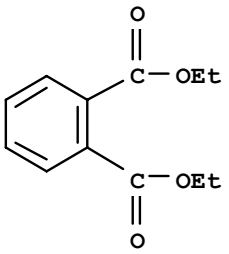

(c)

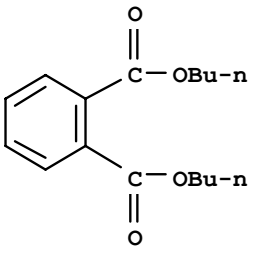

(d)

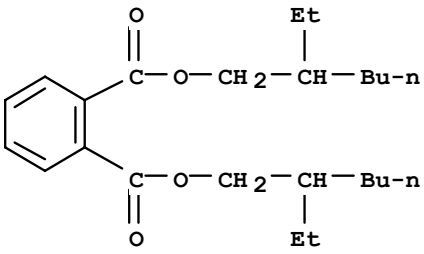

(e)

Figure 26: Molecular structures of propylene glycol dicaprylate (a) and dicaprate (b) showing the freely rotating single bonds which served as a basis for molecular flexibility. Molecular structures of diethyl phthalate (c), dibutyl phthalate (d) and di(2-ethylhexyl) phthalate (e) showing the rotationally restricted carbonyl groups due to the presence of phenyl rings.

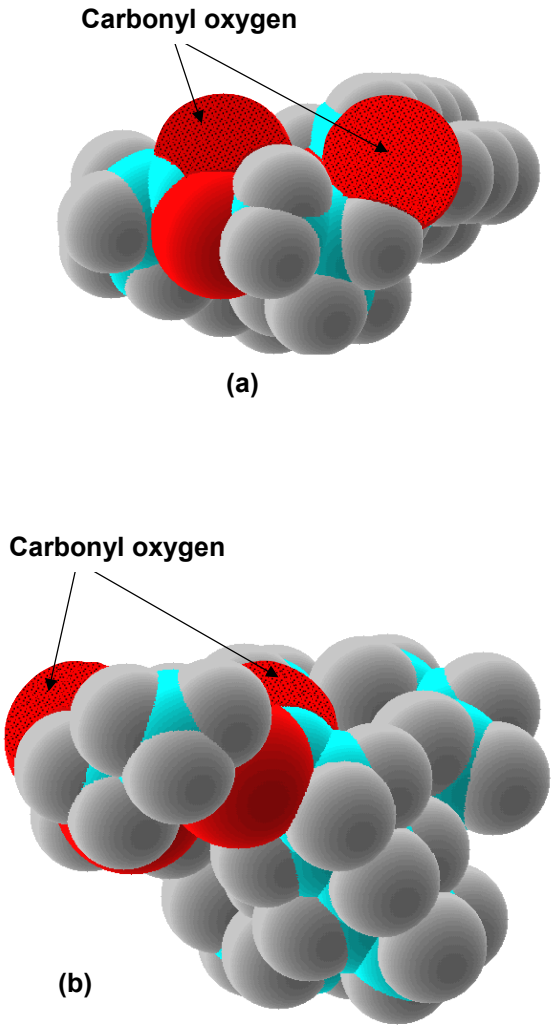

Figure 27: CPK structures of propylene glycol dicaprylate (a) and dicaprate (b) showing the exposed surface of carbonyl oxygen (shaded atoms) for interaction with 6-OH groups of EC polymer chains. The slightly protruding side chain (on the right side of the molecules) imposed a certain degree of steric hindrance towards the solvent-polymer interaction.

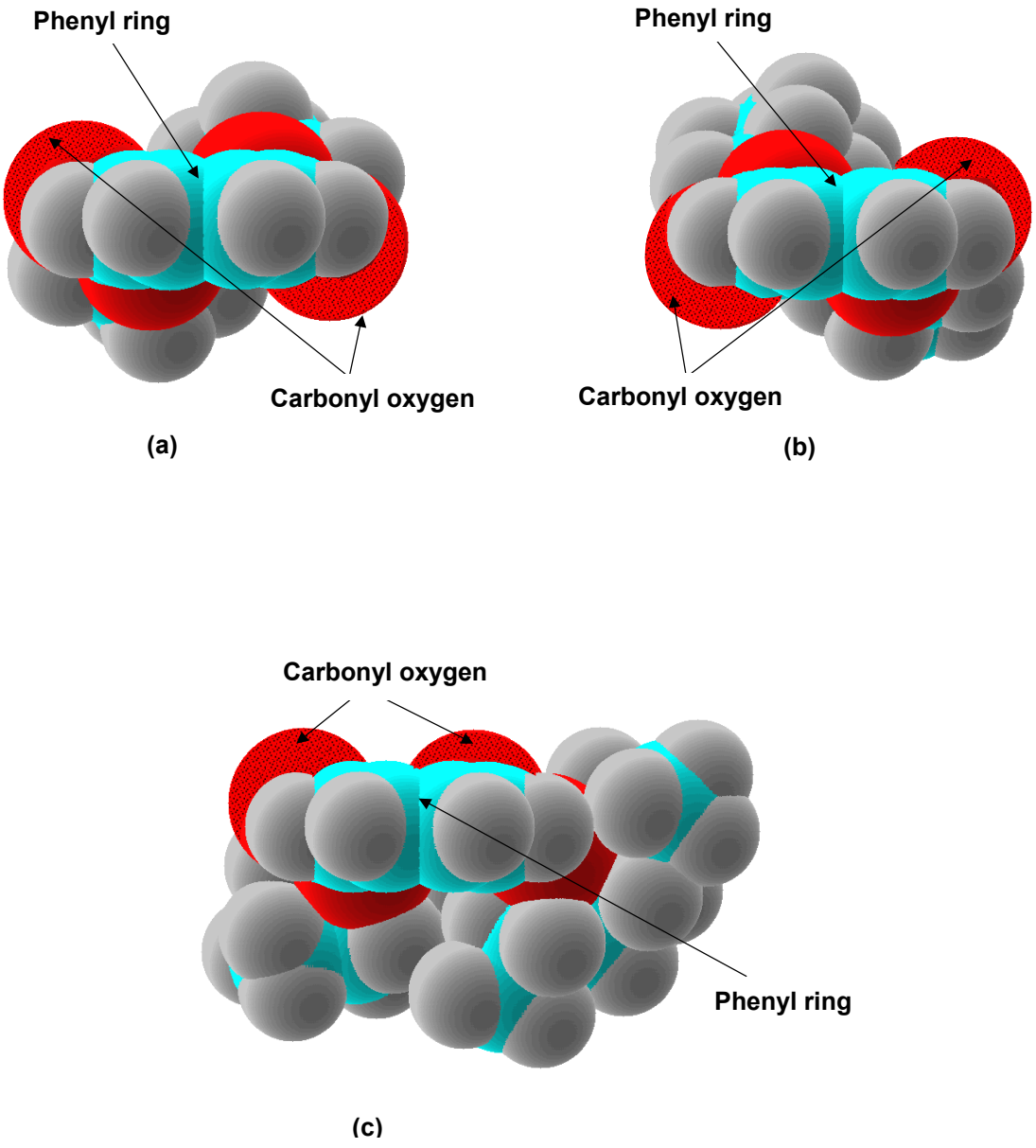

Figure 28: CPK structures of diethyl phthalate (a), dibutyl phthalate (b) and di(2-ethylhexyl) phthalate (c) showing the unhindered surfaces of carbonyl oxygen (shaded atoms) for interaction with 6-OH groups of EC polymer chains.

This appeared to be a more energetically favorable conformation since the ester groups were orientated close to planarity with respect to the phenyl ring. The carbonyl groups of di(2-ethylhexyl) phthalate deviated from planarity due to difficulty in accommodating the bulky side chains. However, the side chains were in an orientation such that steric hindrance to the carbonyl groups was minimal (Figure 28). Similar conformations were observed for some of the Local Minimum Energy Conformations (LMECs) of diethyl phthalate and dibutyl phthalate. The unhindered carbonyl groups in the diester phthalate molecules would allow more effective and closer EC $^{\delta-}O\text{-}H^{\delta+}\cdots{}^{\delta-}O{=}C^{\delta+}$ alignment, hence resulting in stronger dipole-dipole interaction with the EC chains since the strength of dipole-dipole attraction is greatly distance dependent. Therefore, phthalate molecules were postulated to form more rigid bridges to embrace adjacent EC polymer chains into a closely packed three-dimensional network. When the polymeric chains were held closer together by rigid bridges at certain points, the free non-ethoxylated 6-OH groups on the anhydroglucose units along the same polymer chains were brought closely together, thus facilitating intermolecular hydrogen bonding. On the contrary, the slight sterically hindered conformations and the flexibility assumed by the diester caprylate and diester caprate molecules by virtue of their freely rotating single bonds rendered the formation of less rigid bridges between the EC polymer chains. These less rigid bridges would impart a certain degree of mobility to the adjacent EC polymer chains, thus compromising the ease of intermolecular hydrogen bond formation. As a result, a less rigid EC gel network formed with propylene glycol dicaprylate/dicaprate than diester phthalates, hence decreasing the elastic modulus and improving the spreadability of the eventual EC gel. Although the proposed conformational flexibility effect of solvent molecules seemed to

be able to account for the difference in the dynamic rheological behavior of EC gels between the two studies, it should be borne in mind that contribution of other factors may not be inconsequential, given that different polymer grades and experimental conditions were used in both of these studies.

V-B6. Gel wetting behavior

The surfaces of EC gel matrices used for the dynamic contact angle measurement were observed to be distinct and flat to give a well-defined baseline for drop shape analysis. The wetting of EC gels by water and IPM was interpreted in terms of the extent and rate of wetting. For small liquid drops like those employed in this study, wetting phenomenon was only governed by interfacial forces. Other forces acting on the liquid drop were negligible for reasons explained in Section I-C4.2.1. On this basis, a hemispherical section could be assumed for liquid drop on the gel surface. Several captured images at different time points during the dynamic contact angle experiments on 16 %w/w EC7 gel matrices using water and IPM are shown in Figures 29 and 30, respectively.

V-B6.1. Wetting of EC gels by sessile water drops

For all EC gels studied, plots of contact angle of sessile water drop on EC gel surface (θ_w) versus time, and the corresponding standing volume of the sessile water drop (V_w) followed an exponential decay towards an equilibrium value. The base area of the sessile water drop, A_w was observed to rise exponentially with time towards a plateau (Figure 31). However, it should be noted that the reported contact angles were possibly in

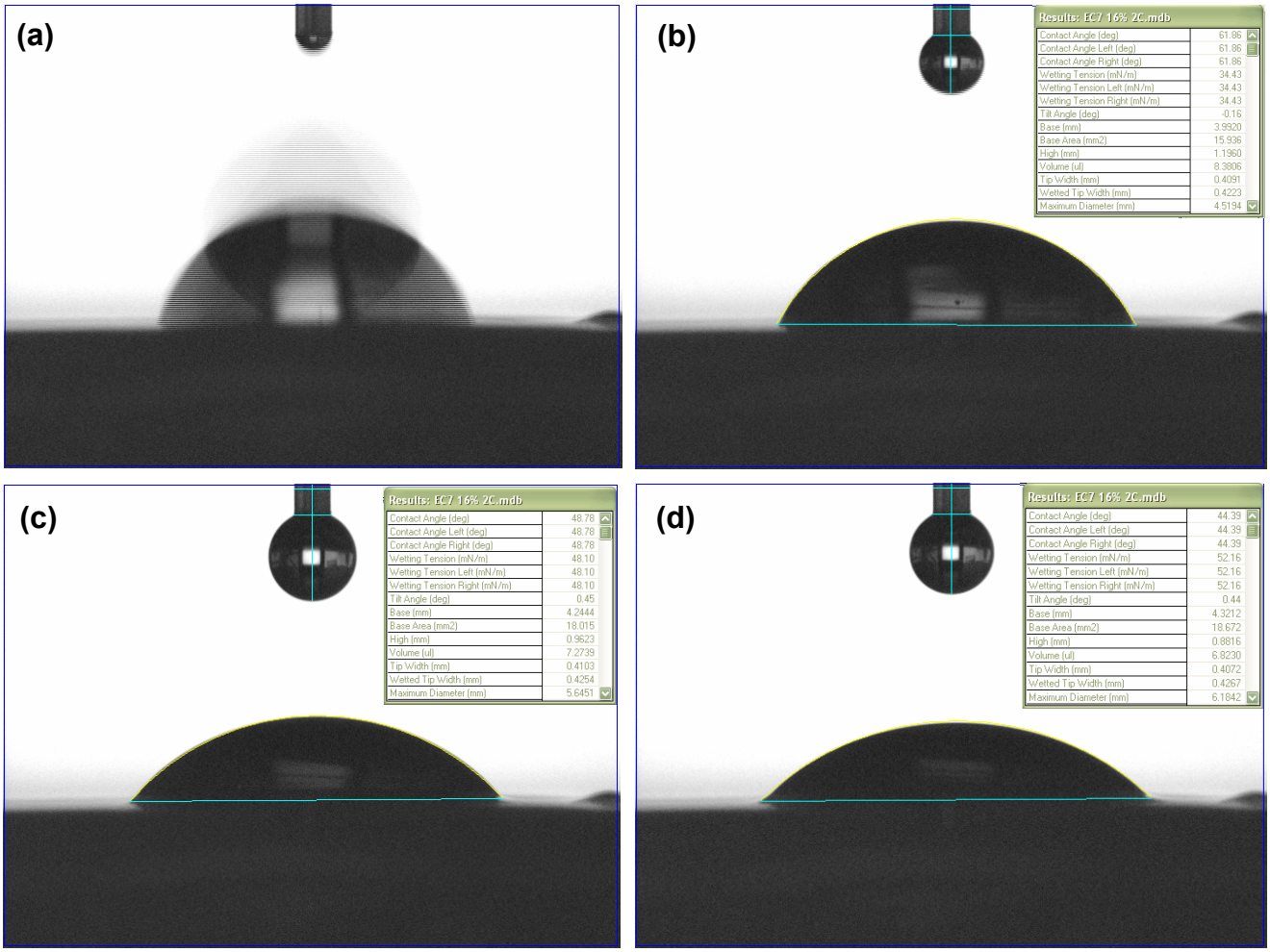

Figure 29: Captured images from dynamic contact angle measurement on 16 %w/w EC7 gel showing the image of water drop detaching from the needle tip (a), and images of sessile water drop at time, t = 0 (b), t = 62.6 s (c), and t = 238.7 s (d).

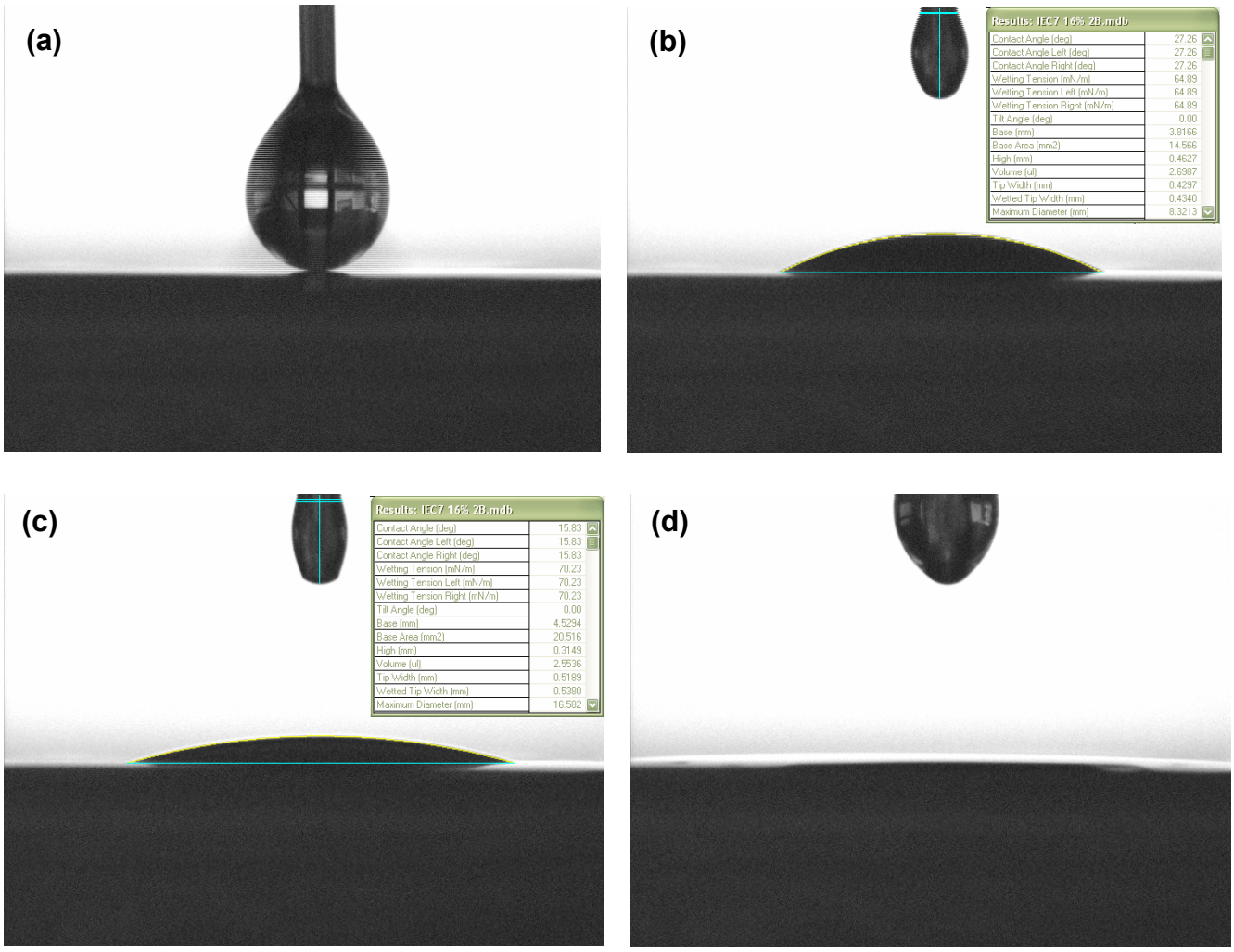

Figure 30: Captured images from dynamic contact angle measurement on 16 %w/w EC7 gel showing the image of IPM drop before detachment (a), and images of sessile IPM drop at time, t = 0 (b), t = 0.2 s (c), and t = 101.1 s where complete IPM absorption had occurred (d).

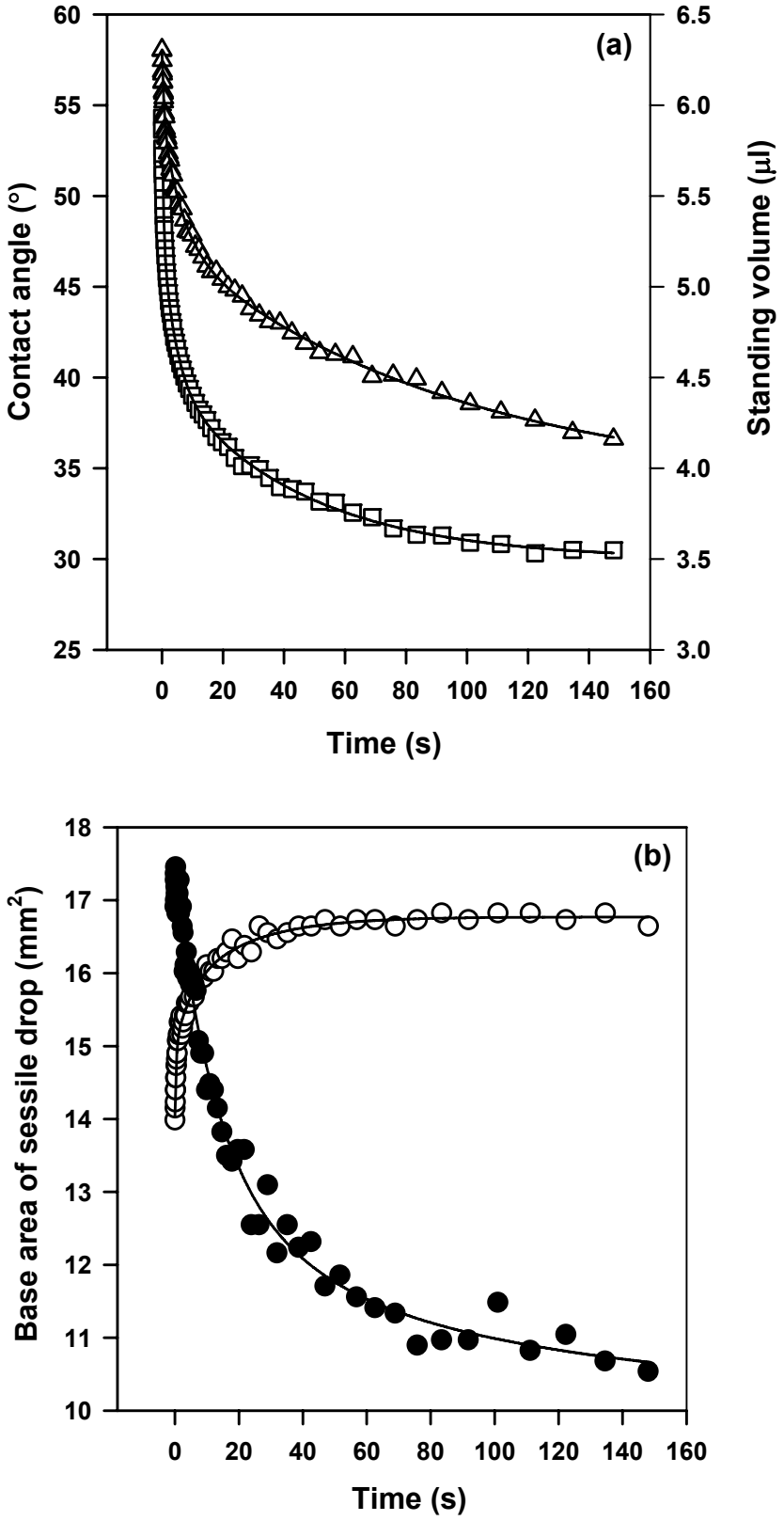

Figure 31: (a) Contact angle (□) and standing volume (△) versus time profiles of sessile water drop on 12 %w/w EC10 gel matrices. (b) Base area versus time profiles of sessile water drop on 12 %w/w EC10 (○) and 7 %w/w EC100 (●) gel matrices.

the metastable equilibrium state instead of the true stable equilibrium state since the latter could only be obtained on an ideal solid surface (Wu, 1982). The θ_w, V_w and A_w profiles were best fitted to an exponential model, $f(x) = y_0 + ae^{-bx} + ce^{-dx} + ge^{-hx}$ with y_0, a, b, c, d, e, g and h as constants. This model was used to compute the equilibrium θ_w, V_w and A_w values at t = 300 s, which represented the extent of EC gel wetting by water. This time point was chosen for the purpose of standardization across all the different EC gel formulations with the assumption that 300 s was sufficiently long for the sessile water drop contact angle to achieve equilibrium. Effect of water drop evaporation was insignificant as the rate of decrease of sessile water drop standing volume on an impermeable solid surface was only 0.002 μl s^{-1}, an amount to cause only an inappreciable effect. The reliability of the proposed exponential model to extrapolate θ_w, V_w and A_w accurately to t = 300 s had been validated by axisymmetric drop shape analysis of images of the same samples taken as snapshots (single images) after 300 s. The mean measured values of θ_w, V_w and A_w of sessile water drops on EC gels obtained over a range of time after 300 s were presented in Table 12. The low percentage deviation ($\leq$ 8.6 %) of the predicted (extrapolated) values from the measured values of θ_w, V_w and A_w for the samples verified the accuracy of the equilibrium values obtained from extrapolation to t = 300 s.

The initial (t = 0) and equilibrium (t = 300 s) θ_w, V_w and A_w, as well as the ratio and % change of these parameters were employed to describe the extent of EC gel wetting by water (Table 13). The initial θ_w ($\theta_{w/0}$), equilibrium θ_w ($\theta_{w/e}$) and $\theta_{w/e}$:$\theta_{w/0}$ ratio exhibited an upward trend with an increase in polymer concentration for all the EC gels while the % change of θ_w ($\Delta\theta_w$) exhibited the opposite trend (Table 13). The decrease of

Table 12: Comparison between the predicted and measured equilibrium contact angle, base area and standing volume of sessile water drops on EC gels.

EC (% w/w)	Contact angle (°)			Base area (mm^2)			Standing volume (µl)			Time range[b] (s)	N[c]
	Predicted[a]	Measured	% Deviation	Predicted[a]	Measured	% Deviation	Predicted[a]	Measured	% Deviation		
EC7											
11	32.5	31.6 ± 1.6	2.8	19.8	19.4 ± 0.7	2.1	4.7	4.9 ± 0.4	4.1	586 - 817	9
16	43.2	41.9 ± 0.9	3.1	18.2	18.6 ± 0.4	2.2	6.3	6.3 ± 0.2	0.0	575 - 718	9
EC10											
11	29.0	27.8 ± 1.4	4.3	18.1	17.2 ± 1.0	5.2	3.8	3.5 ± 0.3	8.6	390 - 576	9
16	43.5	43.2 ± 0.7	0.7	18.0	18.0 ± 0.3	0.0	6.3	6.3 ± 0.2	0.0	318 - 318	9
EC100											
8	35.8	36.0 ± 1.4	0.6	17.7	17.9 ± 1.8	1.1	4.8	5.0 ± 0.6	4.0	377 - 471	9
12	48.3	46.1 ± 0.9	4.8	17.9	18.8 ± 0.6	4.8	7.5	7.2 ± 0.3	4.2	298 - 390	10

[a] Equilibrium contact angle, base area and standing volume values are adapted from Table 13.
[b] The range of time where snapshots of sessile water drop were taken.
[c] Sample size.

Table 13: EC gel wetting parameters by water as represented by sessile water drop contact angle (θ_w), standing volume (V_w), base area (A_w) and rate constant for contact angle ($K_{\theta w}$).

EC (%w/w)	Initial θ_w (°)	Equilibrium θ_w (°)	θ_w change (%)	$\theta_{w/e} : \theta_{w/0}$ ratio	Initial V_w (µl)	Equilibrium V_w (µl)	V_w change (%)	$V_{w/e} : V_{w/0}$ ratio
EC7								
11	56.1 ± 1.4	32.5 ± 1.9	42.1	0.58 ± 0.02	7.3 ± 0.2	4.7 ± 0.4	35.3	0.64 ± 0.04
12	55.5 ± 0.9	32.2 ± 1.9	42.0	0.58 ± 0.03	7.3 ± 0.3	4.8 ± 0.4	33.6	0.67 ± 0.06
13	57.2 ± 1.6	35.3 ± 1.9	38.2	0.62 ± 0.04	7.2 ± 0.5	5.0 ± 0.5	30.7	0.72 ± 0.09
14	60.6 ± 1.1	37.9 ± 1.5	37.4	0.63 ± 0.03	7.5 ± 0.3	5.8 ± 0.5	22.2	0.78 ± 0.05
15	60.5 ± 1.1	41.2 ± 1.7	31.9	0.68 ± 0.03	7.7 ± 0.3	6.1 ± 0.3	20.6	0.79 ± 0.04
16	61.4 ± 1.0	43.2 ± 0.9	29.7	0.70 ± 0.02	7.8 ± 0.2	6.3 ± 0.4	19.9	0.80 ± 0.04
EC10								
11	52.5 ± 0.6	29.0 ± 1.9	44.8	0.55 ± 0.03	6.3 ± 0.3	3.8 ± 0.4	39.3	0.60 ± 0.04
12	55.4 ± 1.9	33.0 ± 2.4	40.5	0.60 ± 0.04	6.4 ± 0.3	4.1 ± 0.5	35.1	0.65 ± 0.06
13	57.3 ± 1.3	36.0 ± 1.6	37.2	0.63 ± 0.03	6.7 ± 0.6	5.0 ± 0.5	25.9	0.74 ± 0.03
14	58.7 ± 1.2	38.3 ± 1.0	34.6	0.65 ± 0.02	7.5 ± 0.3	5.7 ± 0.4	24.1	0.76 ± 0.04
15	59.0 ± 1.0	42.7 ± 0.9	27.7	0.72 ± 0.01	7.8 ± 0.3	6.1 ± 0.3	21.7	0.78 ± 0.01
16	59.8 ± 1.0	43.4 ± 0.7	27.3	0.73 ± 0.01	7.6 ± 0.3	6.3 ± 0.2	17.3	0.83 ± 0.02
EC100								
7	44.4 ± 2.4	19.3 ± 2.6	56.5	0.43 ± 0.04	5.6 ± 0.5	1.4 ± 0.5	75.5	0.24 ± 0.07
8	52.9 ± 1.4	35.8 ± 2.5	32.3	0.68 ± 0.04	6.4 ± 0.5	4.8 ± 0.5	24.5	0.74 ± 0.07
9	55.7 ± 1.5	39.3 ± 1.3	29.4	0.71 ± 0.03	6.8 ± 0.5	5.4 ± 0.6	20.3	0.79 ± 0.08
10	58.1 ± 1.8	43.3 ± 1.7	25.4	0.75 ± 0.01	6.8 ± 0.7	6.1 ± 0.6	10.6	0.85 ± 0.04
11	60.2 ± 1.9	46.9 ± 1.5	22.1	0.78 ± 0.02	7.4 ± 0.3	6.8 ± 0.5	8.8	0.91 ± 0.04
12	61.4 ± 1.3	48.3 ± 1.1	21.3	0.78 ± 0.02	8.1 ± 0.5	7.5 ± 0.5	8.2	0.92 ± 0.03

.....continued from previous page.

EC (%w/w)	Initial A_w (mm^2)	Equilibrium A_w (mm^2)	A_w change (%)	$A_{w/e} : A_{w/0}$ ratio	$K_{\theta w}$ (s^{-1})
EC7					
11	16.1 ± 0.3	19.8 ± 0.7	22.9	1.23 ± 0.04	0.043 ± 0.003
12	16.0 ± 0.6	19.8 ± 1.0	23.4	1.23 ± 0.05	0.042 ± 0.007
13	15.2 ± 0.7	18.6 ± 1.7	22.6	1.22 ± 0.08	0.040 ± 0.004
14	15.0 ± 0.4	19.2 ± 1.1	27.8	1.28 ± 0.07	0.039 ± 0.003
15	15.4 ± 0.4	18.6 ± 0.7	20.9	1.21 ± 0.03	0.031 ± 0.003
16	15.3 ± 0.3	18.2 ± 0.5	19.0	1.19 ± 0.02	0.029 ± 0.003
EC10					
11	15.3 ± 0.5	18.1 ± 1.2	18.0	1.18 ± 0.06	0.057 ± 0.006
12	14.8 ± 0.5	17.7 ± 0.7	19.5	1.20 ± 0.06	0.050 ± 0.004
13	14.8 ± 0.8	18.0 ± 1.3	22.0	1.22 ± 0.04	0.047 ± 0.004
14	15.6 ± 0.5	19.0 ± 0.8	21.9	1.22 ± 0.05	0.032 ± 0.004
15	15.6 ± 0.3	18.4 ± 0.5	17.6	1.18 ± 0.03	0.026 ± 0.002
16	15.4 ± 0.6	18.0 ± 0.4	16.6	1.17 ± 0.03	0.025 ± 0.002
EC100					
7	17.0 ± 0.7	11.5 ± 2.2	-31.9	0.68 ± 0.12	0.069 ± 0.011
8	15.4 ± 0.7	17.7 ± 1.5	15.2	1.15 ± 0.07	0.041 ± 0.006
9	15.2 ± 0.6	18.1 ± 1.3	18.7	1.19 ± 0.05	0.040 ± 0.003
10	14.7 ± 0.6	17.4 ± 1.2	18.8	1.19 ± 0.04	0.042 ± 0.004
11	15.0 ± 0.7	18.0 ± 0.7	20.0	1.20 ± 0.04	0.049 ± 0.004
12	15.7 ± 0.7	17.9 ± 1.7	14.0	1.21 ± 0.03	0.053 ± 0.006

θ_w over time was a result of absorption and/or spreading of the sessile water drop upon contact with the gel matrices. Absorption was manifested by a decrease of V_w while spreading by an increase of A_w over time.

The initial V_w ($V_{w/0}$), equilibrium V_w ($V_{w/e}$), $V_{w/e}$:$V_{w/0}$ ratio and % change of V_w (ΔV_w) demonstrated similar concentration dependent trend as the corresponding parameters for θ_w. As EC concentration was increased, ΔV_w decreased from 35 to 20 % for EC7, 39 to 17 % for EC10 and 76 to 8 % for EC100. This indicated that water was absorbed into all the EC gel matrices such that lower degrees of water absorption were observed for gels with higher EC concentrations.

The extent of spreading of the sessile water drop was described by initial A_w ($A_{w/0}$), equilibrium A_w ($A_{w/e}$) and $A_{w/e}$:$A_{w/0}$ ratio. The A_w profile of 7 %w/w EC100 followed an exponential decay instead of the typical profiles of exponential rise to plateau as shown by other concentrations and grades of EC gels (Figure 31b). Spreading was limited by enhanced degree of water absorption into this gel matrix, hence drop spreading was not observed for this particular formulation. Unlike the other parameters, $A_{w/0}$, $A_{w/e}$ and $A_{w/e}$:$A_{w/0}$ ratio did not show any significant trend with EC concentration and polymeric chain length for all EC gels. $A_{w/e}$:$A_{w/0}$ ratio was about 1.2 for all the EC gels tested except for 7 %w/w EC100 which showed $A_{w/e}$:$A_{w/0}$ ratio of 0.7. $A_{w/e}$:$A_{w/0}$ ratio of greater than 1 indicated spreading while the ratio of less than 1 indicated absorption of sessile water drop.

$\theta_{w/0}$, $\theta_{w/e}$, $\theta_{w/e}$:$\theta_{w/0}$ ratio, $\Delta\theta_w$ and the corresponding parameters for V_w exhibited linear relationship with EC concentration for 11 to 16 %w/w EC7 and EC10, and 8 to 12 %w/w EC100 (Figure 32). Most of these parameters for 7 %w/w EC100 were found to be

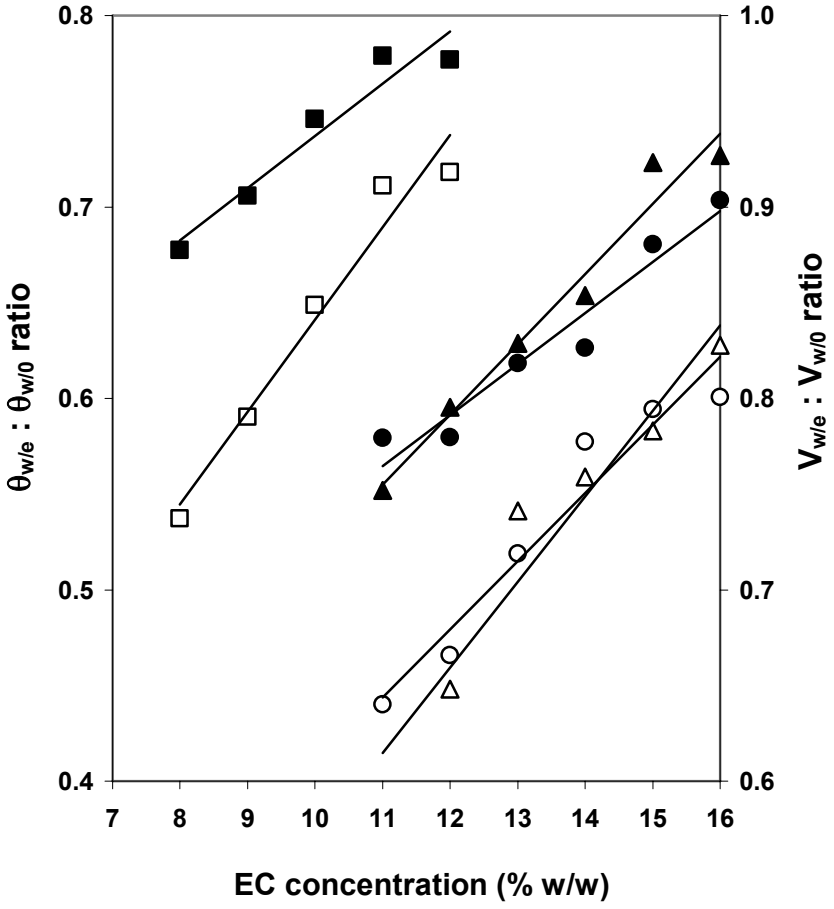

Figure 32: Linear relationship of equilibrium:initial contact angle ratio ($\theta_{w/e}$:$\theta_{w/0}$) and equilibrium:initial standing volume ratio ($V_{w/e}$:$V_{w/0}$) of sessile water drop with EC concentration for EC7 (○,●), EC10 (△,▲) and EC100 (□,■) gels. Correlation coefficients, r = 0.9696 (●), r = 0.9691(○), r = 0.9846 (▲), r = 0.9716 (△), r = 0.9655 (■) and r = 0.9797 (□). Closed symbols represent $\theta_{w/e}$:$\theta_{w/0}$ and open symbols represent $V_{w/e}$:$V_{w/0}$.

exceptionally low. $A_{w/e}$ was less than $A_{w/0}$, indicating water absorption without spreading for 7 %w/w EC100. The change of θ_w observed in the rest of the EC gel samples could be accounted by both spreading and absorption. The relatively low θ_w and V_w values for 7 %w/w EC100 were more apparent at equilibrium as compared to initial state since some time was needed for significant absorption into the gel matrices to take place. $\theta_{w/e}$:$\theta_{w/0}$, $V_{w/e}$:$V_{w/0}$ and $A_{w/e}$:$A_{w/0}$ ratio were regarded as relatively more accurate parameters to indicate extent of wetting as possible errors caused by small change in drop volume could be avoided.

Comparing the influence of different polymeric chain lengths, EC100 was found to have much higher $\theta_{w/e}$:$\theta_{w/0}$ and $V_{w/e}$:$V_{w/0}$ ratios (Figure 32), as well as lower $\Delta\theta_w$ and ΔV_w than EC7 and EC10 (Table 13). These parameters were not significantly different ($p > 0.05$, one-way ANOVA) between EC7 and EC10, probably because the difference in their molecular weights was relatively small. The absolute values of θ_w and V_w of EC100 were also much higher. The concentration dependence of $V_{w/0}$ and $V_{w/e}$ increased in the order of EC7 < EC10 < EC100 as shown by the slope values for $V_{w/0}$ of 0.1211 for EC7, 0.3251 for EC10 and 0.4122 for EC100, and the slope values for $V_{w/e}$ of 0.3549 for EC7, 0.5387 for EC10, and 0.6913 for EC100. This implied that reduction in water absorption capacity was more sensitive to EC concentration as polymeric chain length increased, hence reflecting the considerable role of polymeric chain length in the wetting property of EC gels. Similar trends were demonstrated by the slopes of $\theta_{w/0}$ and $\theta_{w/e}$ versus concentration profiles with the exception of $\theta_{w/0}$ profiles between EC7 and EC10 which did not exhibit statistically significant difference in their slopes. Since A_w did not show

any significant trend with EC concentration or polymeric chain length, the concentration dependence of $\theta_{w/0}$ and $\theta_{w/e}$ could be primarily attributed to water absorption.

The rate of EC gel wetting by water was determined by kinetic modeling of the rate of change of θ_w, V_w and A_w from 2 to 12 s. The change of these values slowed down markedly after 10 s. The decline of θ_w with time followed first-order kinetics (Wilkinson and Elliott, 1974) as linear plots of ln (θ_w-$\theta_{w/e}$) versus time were obtained for all the EC gels (correlation coefficient, r = 0.9359 to 0.9951) with rate constants of $K_{\theta w}$ (Figure 33). Both V_w and A_w fitted into the same kinetic model. Despite the acceptable r-values, it should be noted that direct kinetic modeling as shown above might not be adequate to study the wetting kinetics of EC gels accurate since the wetting process involved both water spreading and absorption at the same time. However, kinetic constants derived from such simple modeling could still provide useful comparison among the different gel formulations. $K_{\theta w}$ was generally low, with values ranging from 0.025 to 0.069 s^{-1}. There was a slight decrease in rate of gel wetting by water at higher concentration ranges of both EC7 and EC10 (Table 13). It was interesting to note that $K_{\theta w}$ values of 11 and 12 %w/w EC100 were significantly higher than those of 8 to 10 %w/w, indicating more rapid wetting at higher EC100 concentration. EC100 gel at 7 %w/w exhibited a particularly high $K_{\theta w}$ due to its absorption-dominated mechanism of wetting. The $t_{50\%}$ values, defined as the time taken to for $\theta_{w/0}$, $V_{w/0}$ and $A_{w/0}$ to change to a value corresponding to $(\theta_{w/0} + \theta_{w/e})/2$, $(V_{w/0} + V_{w/e})/2$, and $(A_{w/0} + A_{w/e})/2$, respectively, were also useful in describing the rates of EC gel wetting. The same mathematical model, $f(x) = y_0 + ae^{-bx} + ce^{-dx} + ge^{-hx}$ was used to determine $t_{50\%}$ values. Although $t_{50\%}$ values derived from the plots of θ_w, V_w and A_w versus time were found to be less reproducible, they

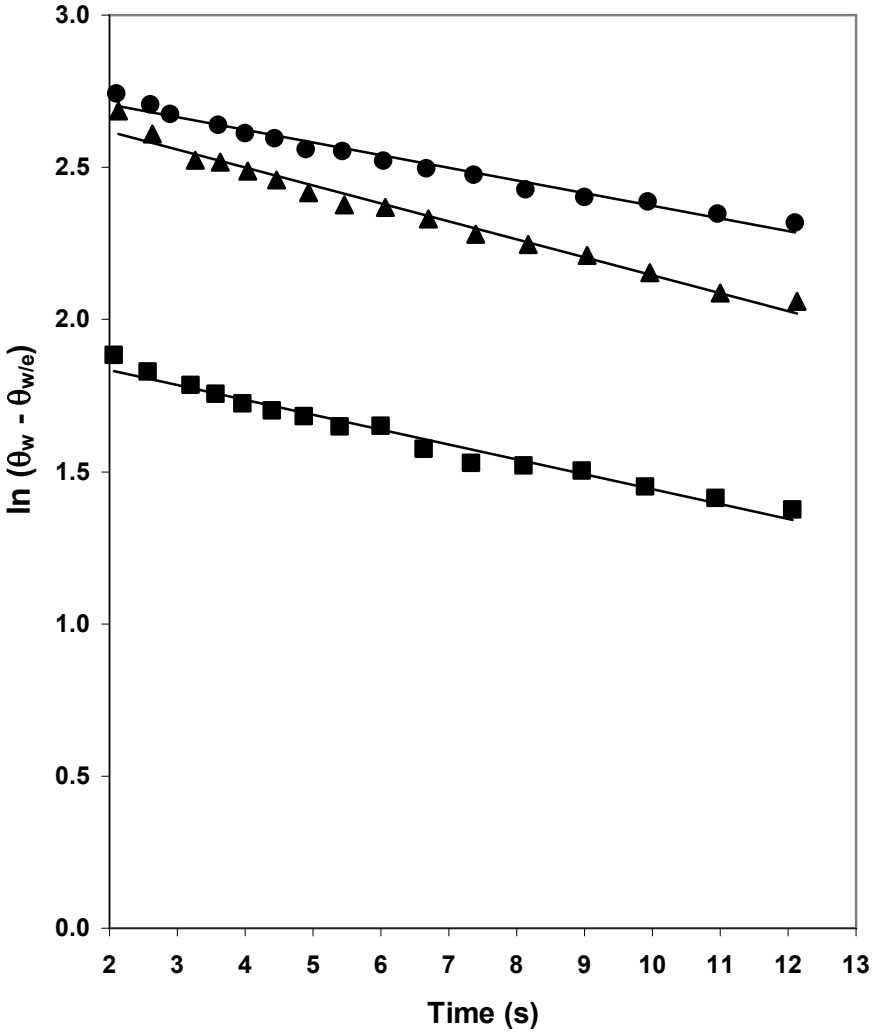

Figure 33: Decline in contact angle, θ_w of sessile water drop on 11 %w/w EC7 (●, y = -0.0416x + 2.7886, r = 0.9880), EC10 (▲, y = -0.0589x + 2.7349, r = 0.9882) and EC100 (■, y = -0.049x + 1.9323, r = 0.9864) gels with time according to first-order kinetics. First-order rate constants are given by slopes of the linear regressions.

exhibited trends that could aid in interpretation of the rate constants. The trends of $K_{\theta w}$ versus EC concentration were supported by the $t_{50\%}$ values of θ_w, which showed a concomitant concentration dependant increase for EC7 and EC10, and concentration dependant decrease for EC100 from 8 %w/w onwards (Figure 34). The main process responsible for the observed trend of $K_{\theta w}$ could be envisaged by examining the rate of water absorption and spreading. The $t_{50\%}$ values for V_w indicated a decrease in rate of water absorption with an increase in EC concentration for all the gels studied (Figure 34). The $t_{50\%}$ values for A_w and θ_w showed similar trends as $K_{\theta w}$, indicating that the rate of spreading played a major role in influencing $K_{\theta w}$. Therefore, the faster wetting of gels with higher EC100 concentration was primarily attributed to faster liquid spreading rather than faster liquid absorption. It should be noted that the rate of wetting only reflected how rapidly the sessile water drop attained equilibrium state. Higher rate of wetting did not necessarily indicated higher extent of wetting. For example, the rate of wetting of EC100 gels was found to be higher in gels with higher EC concentration but the extent of wetting was still lower.

Classically, the wetting process is described by three different stages, that is, adhesional, immersional and spreading wetting. The free energy change involved in the respective stages of wetting is represented by *Wa* (work of adhesion), *At* (adhesion tension) and *Sc* (spreading coefficient), which are defined as follows (Rosen, 1989):

$$Wa = \gamma_{LV} (\cos\theta + 1) \qquad \text{(Equation 22)}$$

$$At = \gamma_{LV} \cos\theta \qquad \text{(Equation 23)}$$

$$Sc = \gamma_{LV} (\cos\theta - 1) \qquad \text{(Equation 24)}$$

where γ_{LV} = surface tension of the wetting liquid, and θ = contact angle. It should be

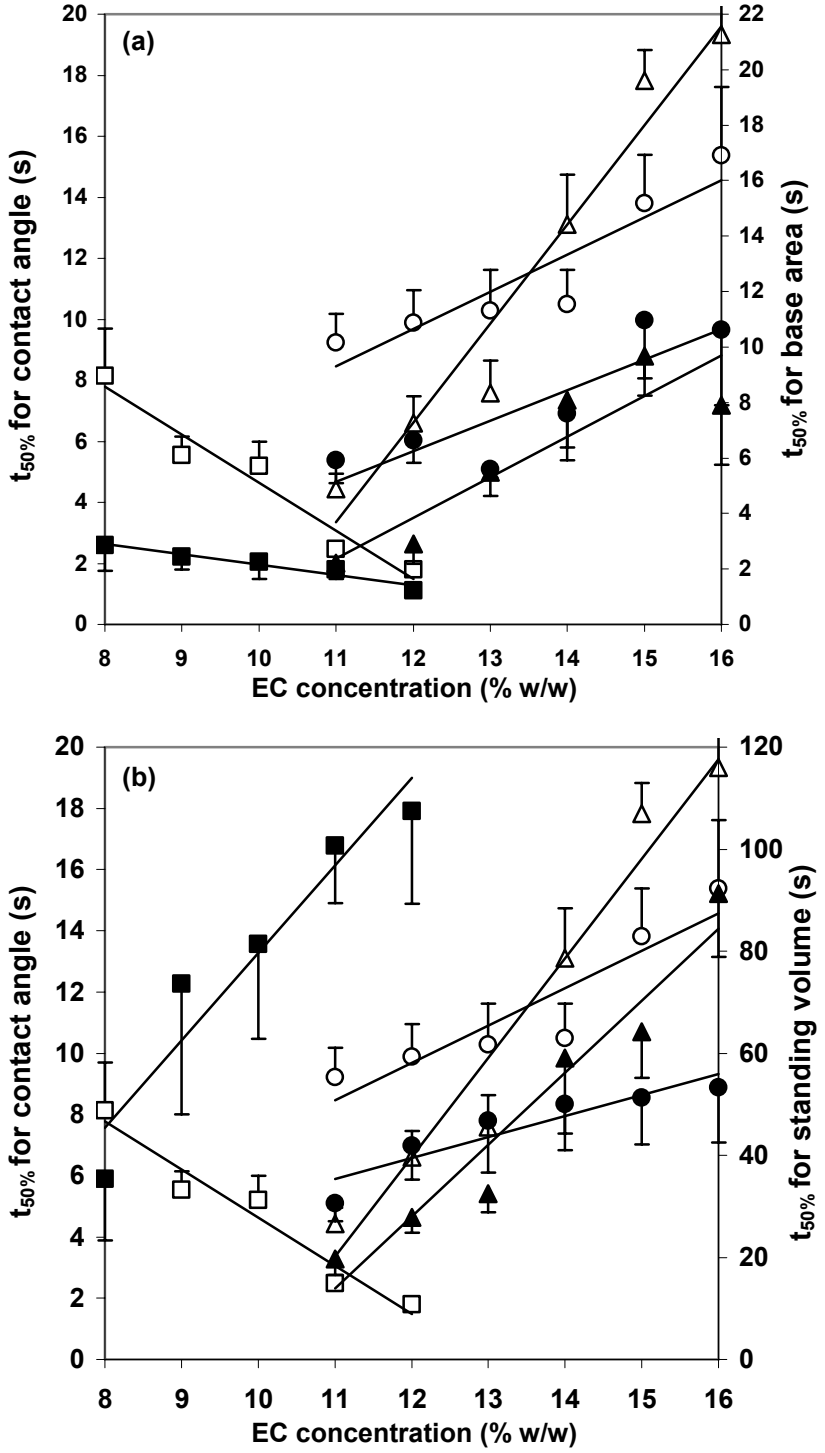

Figure 34: Change in contact angle and base area $t_{50\%}$ (a), and contact angle and standing volume $t_{50\%}$ (b) of sessile water drop with EC concentration for EC7 (○,●), EC10 (△,▲) and EC100 (□,■) gels. Correlation coefficients for contact angle, r = 0.9226 (○), r = 0.9777 (△), r = 0.9744 (□); base area, r = 0.8742 (●), r = 0.9082 (▲), r = 0.9697 (■); and standing volume, r = 0.9220 (●), r = 0.9697 (▲), r = 0.9550 (■). Closed symbols represent base area or standing volume and open symbols represent contact angle.

Table 14: The free energy change involved in adhesional, immersional and spreading wetting of EC gels by water sessile drop.

EC (%w/w)	Work of adhesion[a] (mJ m^{-2})	Adhesion tension[a] (mJ m^{-2})	Spreading coefficient[a] (mJ m^{-2})
EC7			
11	134.2 ± 1.3	61.4 ± 1.3	-11.4 ± 1.3
12	134.4 ± 1.3	61.6 ± 1.3	-11.2 ± 1.3
13	132.2 ± 1.4	59.4 ± 1.4	-13.4 ± 1.4
14	130.2 ± 1.2	57.4 ± 1.2	-15.4 ± 1.2
15	127.6 ± 1.5	54.8 ± 1.5	-18.0 ± 1.5
16	125.9 ± 0.8	53.1 ± 0.8	-19.7 ± 0.8
EC10			
11	136.5 ± 1.2	63.7 ± 1.2	-9.3 ± 1.1
12	133.8 ± 1.7	61.0 ± 1.7	-12.4 ± 1.4
13	131.7 ± 1.1	58.9 ± 1.1	-13.9 ± 1.1
14	129.9 ± 0.8	57.1 ± 0.8	-15.7 ± 0.8
15	126.3 ± 0.8	53.5 ± 0.8	-19.3 ± 0.8
16	125.6 ± 0.7	52.8 ± 0.7	-20.0 ± 0.7
EC100			
7	141.5 ± 1.1	68.7 ± 1.1	-3.6 ± 0.6
8	131.8 ± 1.8	59.0 ± 1.8	-14.2 ± 1.6
9	129.2 ± 1.0	56.4 ± 1.0	-16.4 ± 1.0
10	125.7 ± 1.5	52.9 ± 1.5	-19.9 ± 1.5
11	122.5 ± 1.4	49.7 ± 1.4	-23.1 ± 1.4
12	121.8 ± 1.1	49.0 ± 1.1	-23.8 ± 1.1

[a] Water surface tension, γ_{LV} = 72.8 mN m^{-1} was employed for calculation.

noted that *Wa*, *At* and *Sc* for EC gels at equilibrium (t = 300 s) as presented in Table 14 might not necessarily be the true free energy values as the abovementioned equations employed for calculation were derived from Young's equation (Equation 5) for a solid substrate with ideal smooth surface. However, these energy values could be employed as a relative gauge on the mechanism involved in EC gel wetting and as a means of comparison among the different EC gels studied for the same wetting liquid. Positive *Wa* and *At* (Table 14) reflected spontaneous adhesional and immersional wetting of EC gels by water while negative *Sc* indicated absence of complete water drop spreading. There was a significant decrease ($p < 0.05$) in *Wa*, *At* and *Sc* when EC concentration was increased in the EC gels. *Wa*, *At* and *Sc* values were comparable for most concentrations of EC7 and EC10 gels but were significantly lower in EC100 gels. Hence, the thermodynamic driving force for each type of wetting decreased with increase in EC concentration and polymeric chain length.

V-B6.2. Wetting of EC gels by sessile IPM drops

Plots of θ_i, V_i and A_i versus time followed an exponential decay and were also found to be best fitted to the same exponential model as that for water. Instead of forming an equilibrium sessile drop on the EC gel surface, IPM was completely absorbed into the gel matrices (Figure 30). Therefore, the extent of EC gel wetting by IPM could only be evaluated by the $\theta_{i/0}$ and $V_{i/0}$, namely θ_i and V_i at t = 0, respectively (Table 15). $\theta_{i/0}$, with C.V. of less than 10 % for most formulations, was relatively more consistent than $V_{i/0}$ which exhibited C.V. ranging from 4 to 20 % with the higher C.V. occurring in gels at lower concentration range of EC. There was a fairly linear concentration dependent trend

Table 15: EC gel wetting parameters by IPM as represented by sessile IPM drop contact angle (θ_i), standing volume (V_i) and rate constant for contact angle ($K_{\theta i}$).

EC (%w/w)	Initial θ_i (°)	Initial V_i (µl)	$K_{\theta i}$ (s^{-1})
EC7			
11	17.3 ± 1.3	2.2 ± 0.3	0.32 ± 0.02
12	21.7 ± 1.9	2.2 ± 0.2	0.31 ± 0.03
13	23.1 ± 2.0	2.3 ± 0.3	0.32 ± 0.03
14	23.7 ± 1.8	2.4 ± 0.2	0.31 ± 0.03
15	25.2 ± 1.5	2.5 ± 0.2	0.33 ± 0.03
16	27.2 ± 1.1	2.6 ± 0.2	0.31 ± 0.03
EC10			
11	18.3 ± 1.6	2.5 ± 0.3	0.44 ± 0.07
12	20.6 ± 2.2	2.5 ± 0.3	0.35 ± 0.04
13	21.5 ± 1.8	2.6 ± 0.1	0.34 ± 0.03
14	21.0 ± 2.6	2.5 ± 0.1	0.33 ± 0.04
15	23.6 ± 1.7	2.8 ± 0.3	0.33 ± 0.03
16	26.5 ± 1.8	2.8 ± 0.2	0.33 ± 0.05
EC100			
7	15.8 ± 1.3	2.1 ± 0.3	0.90 ± 0.09
8	21.4 ± 2.0	2.4 ± 0.2	0.44 ± 0.08
9	23.2 ± 1.8	2.5 ± 0.1	0.39 ± 0.03
10	26.4 ± 1.7	2.7 ± 0.2	0.30 ± 0.04
11	29.2 ± 1.9	2.7 ± 0.1	0.28 ± 0.03
12	31.0 ± 2.1	2.8 ± 0.2	0.23 ± 0.02

for both $\theta_{i/0}$ ($r \geq 0.9385$) and $V_{i/0}$ ($r \geq 0.8780$) for the entire range of EC concentrations used in the study. For IPM, $\theta_{i/0}$ and $V_{i/0}$ of 7 %w/w EC100 were able to fit into the respective linear regressions as opposed to the observation made on water because the wetting of EC gel by IPM was dominated by the same mechanism for the entire concentration range of EC100, namely absorption. For gel concentrations of 11 and 12 %w/w, EC100 showed significantly higher $\theta_{i/0}$ than both EC7 and EC10. The base area for IPM sessile drops was rather erratic as observed from the high C.V., due to the fast absorption of this liquid by EC gel. Therefore, base area was not employed to describe the extent of gel wetting by IPM as it was deemed to be less reliable.

The rate of EC gel wetting by IPM could be described by the rate constant, $K_{\theta i}$ (Table 15) and time taken for complete IPM absorption, t_a. These two parameters basically described the rate of IPM absorption. Linear plots of ln θ_i versus time were obtained from 0.1 to 3 s ($r = 0.8686$ to 0.9917), indicating wetting of EC gels by IPM according to first-order kinetics. The initial rapid decline of θ_i was observed to slow down after approximately 3 s for all the EC gel formulations. No significant trend between $K_{\theta i}$ and EC concentration was observed for all the formulations of EC7 and EC10, except 11 %w/w EC10. On the contrary, a significant decrease in $K_{\theta i}$ was exhibited with an increase in EC100 concentration. This showed that the rate of wetting of EC gels with longer polymeric chain was more sensitive to polymer concentration than those of shorter polymeric chains. Time taken for complete absorption of IPM ranged from 12.5 to 220.3 s. EC7 and EC10 showed linear increases of t_a with increase in polymer concentration (Figure 35). For EC100, the increase of t_a was exponential and the influence of EC concentration was much more pronounced above 9 %w/w EC100.

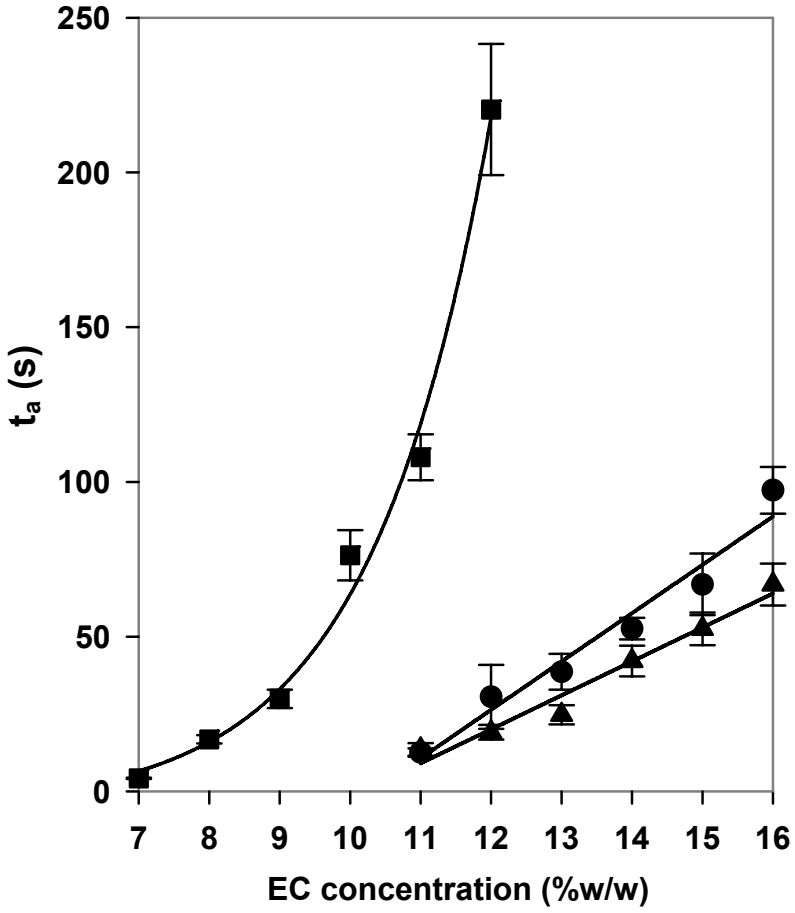

Figure 35: Time for complete absorption of sessile IPM drops into EC7 (●), EC10 (▲) and EC100 (■) gel matrices, t_a as a function of EC concentration.

The spontaneous adhesional wetting, *Wa* and spreading wetting, *Sc* values of IPM with EC gels were 58.1 and 0.0 mJ m^{-2}. Calculations of *Wa* and *Sc* were based on $\theta = 0°$ due to the complete wetting of EC gels by IPM, and $\gamma_{LV} = 29.0$ mN m^{-1} as determined for IPM using the Wilhelmy plate method. For $\theta \leq 0°$, adhesion tension, *At* could not be determined from contact angle. It required alternative methods such as calorimetry to measure the heat of immersion (Rosen, 1989) which was not performed in this study. Nevertheless, immersional wetting of EC gels was evident since *At* would be positive as long as $\theta < 90°$ (Parfitt, 1981).

Comparison was made for the wetting of EC gel by water and IPM. The initial contact angles of water sessile drop on EC gel matrices were 2 to 3 fold higher than those of IPM, indicating a higher extent of EC gel wetting by IPM. The rates of wetting by IPM were 4 to 13 fold higher than water in all the EC gels studied (Table 16). The much higher rate of gel wetting by IPM was visually apparent from Figures 29 and 30.

V-B6.3. Wetting of human skin by sessile IPM drops

IPM were found to be readily absorbed into human skins with initial contact angles, $\theta_{i/h}$ ranging from 22.5 to 35.2° and a mean $\theta_{i/h}$ of 30.1 ± 3.3°. Times taken for complete absorption indicated the rates of IPM absorption and they ranged from 2.3 to 35.2 s. Such a wide range in absorption time could be attributed to biological variables in different individuals' skin such as skin thickness, hydration level and hair density.

Table 16: Comparison of the extent and rate of EC gel wetting by water and IPM. Difference in extent of wetting is expressed as ratio between the initial contact angle of water, $\theta_{w/0}$ and IPM, $\theta_{i/0}$ while difference in rate of wetting is expressed as ratio between the contact angle rate constant of IPM, $K_{\theta i}$ and water, $K_{\theta w}$.

EC	Ratio	
(%w/w)	$\theta_{w/0} : \theta_{i/0}$	$K_{\theta i} : K_{\theta w}$
EC7		
11	3.2	7.4
12	2.6	7.2
13	2.5	8.0
14	2.6	8.0
15	2.4	10.5
16	2.3	10.9
EC10		
11	2.9	7.7
12	2.7	7.1
13	2.7	7.2
14	2.8	10.3
15	2.5	13.0
16	2.3	13.2
EC100		
7	2.8	13.1
8	2.5	10.8
9	2.4	9.7
10	2.2	7.2
11	2.1	5.7
12	2.0	4.4

V-B6.4. Density of EC gel matrices

Densities of EC7, EC10 and EC100 gels ranged from 0.935 to 0.981, 0.939 to 0.993 and 0.927 to 1.032 g/ml, respectively. The C.V. values ranged from 0.06 to 1.26 % for all samples. The densities of all the EC gels were lower than that of water (0.998 g/ml) at 22 °C, except for 12 %w/w EC100 which were slightly denser (1.032 ± 0.003 g/ml). Gel densities increased linearly with EC concentration for EC7 (r = 0.9782) and EC10 (r = 0.9909) but increased exponentially for EC100 (Figure 36).

V-B6.5. Correlation of EC gel wetting behavior with rheological and mechanical properties

It was postulated that the rheological and mechanical properties of EC gels would affect their wetting behavior. Hence, an attempt was made to correlate by linear regression the wetting parameters with the rheological and mechanical parameters of EC gels. Oscillatory rheological parameters (elastic moduli), continuous rheological parameters (apparent viscosity at shear rate of 10 s^{-1}, yield stress and area of hysteresis) and mechanical parameters (hardness and adhesiveness) were employed in the linear regression analysis (Tables 8 and 10). These parameters were adopted from the study on EC gel rheology and mechanical properties (Sections V-B3 and V-B4). The contact angles (θ_w and $\theta_{i/0}$) and standing volumes (V_w and $V_{i/0}$) generally exhibited satisfactory linear correlation with both rheological and mechanical parameters, with r-values ranging from 0.7314 to 0.9956 (Figure 37). Comparing between rheological and mechanical parameters, the former (mean r = 0.9318) showed a better correlation with wetting parameters than the latter (mean r = 0.9150). $\theta_{w/e}$ and $\theta_{i/0}$ could be correlated with

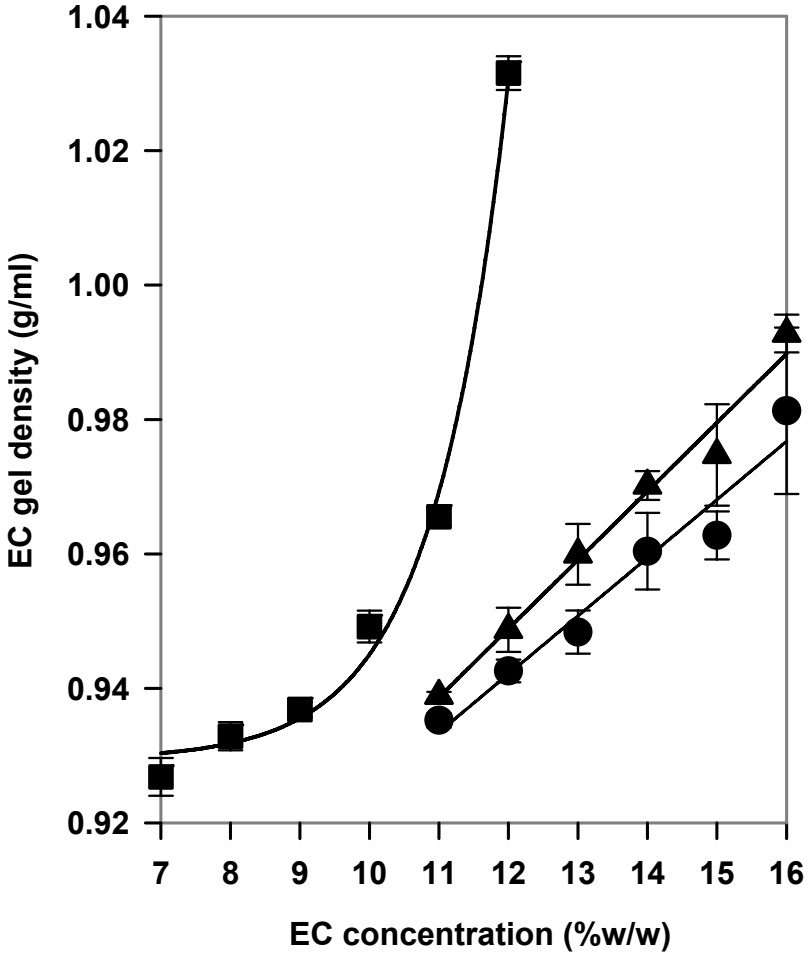

Figure 36: Change of EC7 (●), EC10 (▲) and EC100 (■) gel density as a function of EC concentration.

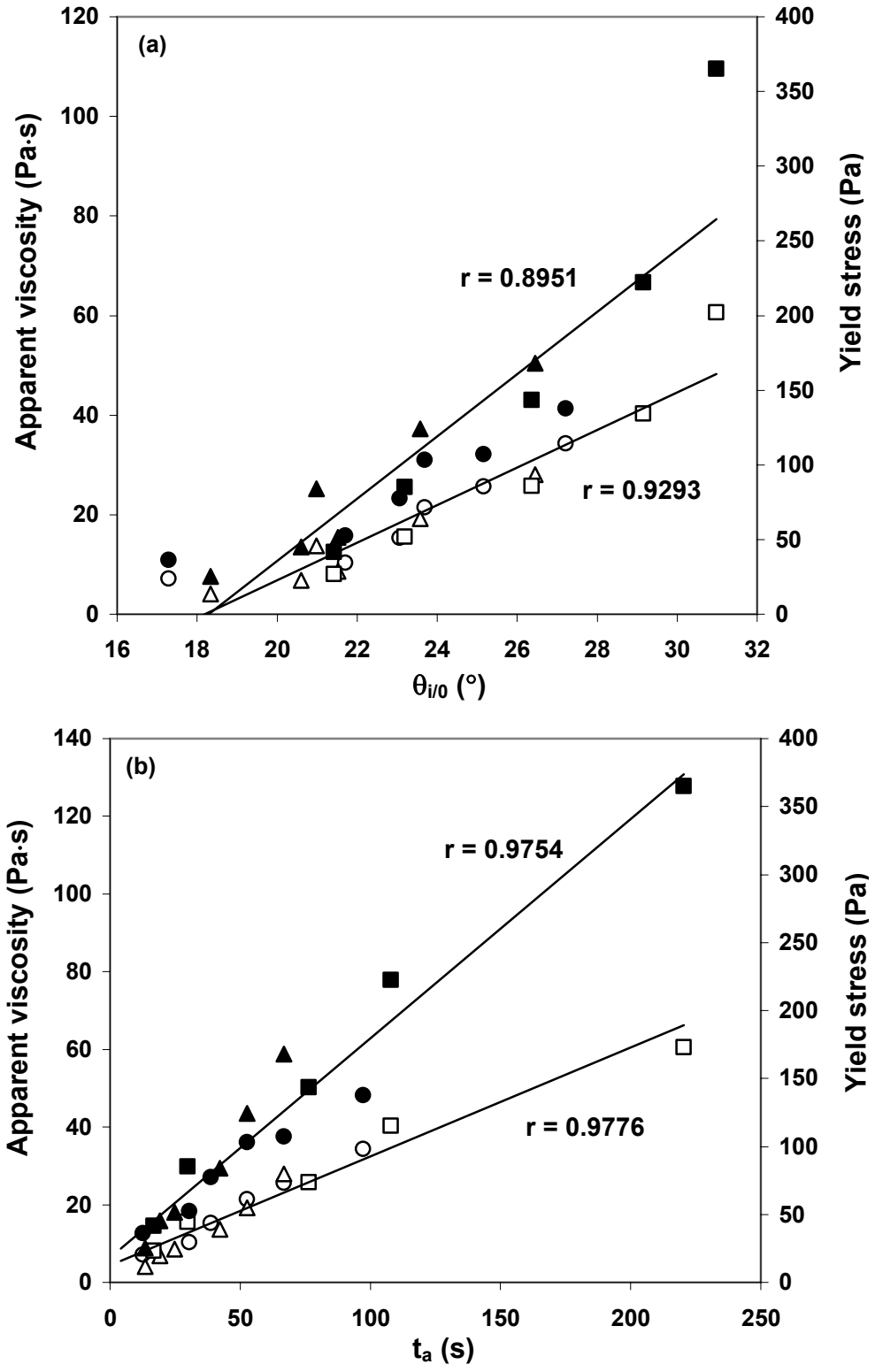

Figure 37: Linear regressions of apparent viscosity and yield stress with initial contact angle of sessile IPM drop, $\theta_{i/0}$ (a), and time for complete IPM absorption, t_a (b) for the entire concentration range of EC7 (○,●), EC10 (△,▲) and EC100 (□,■) gels. Closed symbols represent yield stress and open symbols represent apparent viscosity.

apparent viscosity and yield stress by a single regression line irrespective of the grade of EC. For linear regressions of $\theta_{i/0}$-apparent viscosity, r = 0.9293 and $\theta_{i/0}$-yield stress, r = 0.8951 (Figure 37) while for $\theta_{w/e}$-apparent viscosity, r = 0.8844 and $\theta_{w/e}$-yield stress, r = 0.8624. From the higher r-values, $\theta_{i/0}$ demonstrated better correlation with apparent viscosity and yield stress than $\theta_{w/e}$. Among the parameters that represented rate of wetting, t_a showed the most satisfactory linear correlation with the rheological and mechanical parameters, with r ranging from 0.9133 to 0.9979 (Figure 37).

V-B6.6. Wetting behavior of EC gel matrices

The dynamic contact angles measured for the sessile liquid drops in the current study were advancing contact angles formed when the liquid front advanced on the gel-air interface. There are different definitions for the state of wetting based on contact angle (θ) values. Complete wetting is defined by $\theta = 0°$ but partial wetting is defined either by $0° < \theta < 90°$ (Garnier *et al.,* 1998) or $0° < \theta < 180°$ (Myers, 1999). The non-aqueous EC gels studied were thus partially wetted by water and completely wetted by IPM.

V-B6.6.1. Wetting behavior as an indicator of gel surface properties

Information about surface configuration and hydrophilic-lipophilic properties of EC gels could be obtained from the dynamic contact angle profiles of water and IPM on the gel surfaces. Water is commonly used as a liquid possessing good hydrophilic property. IPM is the isopropyl ester of myristic acid (C_{14}) and is predominantly a lipophilic solvent. The ability of both water (hydrophilic) and IPM (lipophilic) to form sessile drops with contact angles of 44 to 61° and 16 to 31°, respectively upon contact

with EC gels proved that the gel matrices possessed both hydrophilic and lipophilic properties, with the predominance of lipophilic property. This observation agreed with the non-aqueous nature of the gel. IPM is usually employed to represent the polar/non-polar nature of the skin (Jaiswal *et al.,* 1999; Baker *et al.,* 1990; Hadgraft *et al.,* 1986; Poulsen *et al.,* 1968). It was used as a vehicle in partition coefficient experiments to predict the amount of drug partitioning into the skin (Panchagnula, 1996). The good skin compatibility of IPM was demonstrated in the current study by the relatively low initial contact angle (≤ 35.2°) and short time for complete absorption (≤ 35.2 s) of IPM drops placed on the skin of human subjects. The ready absorption of sessile IPM drops into EC gels and the overlap of the range of IPM contact angle values on EC gels (16 to 31°) with those on human skins (23 to 35°) implied a certain degree of similarity of the gel with the skin. This in turn reflected the good compatibility of the non-aqueous EC gel with human skin if formulated as a topical gel.

V-B6.6.2. Mechanism underlying gel wetting

EC is known to be a water-insoluble, hydrophobic polymer due to the hydrophobic ethyl substitution on its hydrophilic cellulose backbone. The observed wetting behavior of polar and non-polar solvents on EC gel matrices could be explained partially by the change of EC gel surface configuration upon contact with liquid sessile drops. The tendency of reorientation of polymeric moieties on gel surfaces to establish equilibrium with the surrounding medium in order to minimize interfacial free energy is well recognized. When the gel was exposed to air, a hydrophobic gel-air interface would exist where hydrophobic segments of the polymer and solvent chains were orientated

towards the air phase and hydrophilic moieties, namely the unethoxylated hydroxyl groups on the C-6 position of the anhydroglucose units of the EC backbone were buried in the interior of the gel matrix (Peppas and Mongia, 1997; Yasuda and Okuno, 1994; Yamada *et al.,* 2001; Liu *et al.,* 2004; Xu *et al.,* 1997; Hogt *et al.,* 1985; Park *et al.,* 1995). The reasonably low water contact angle, θ_w observed for EC gels indicated the presence of hydrophilic moieties at the gel-water interface. This could be explained by reorientation by molecular rotation of flexible parts of the polymer and solvent to direct the unethoxylated and hydrophilic C_6 –OH groups of EC directly beneath the drop towards the gel-water interface upon contact of EC gel surface with the sessile water drop. The difference in wetting property as represented by different water and ethanol contact angles observed on hydroxypropylcellulose powder compact had been attributed to the influence of different solvent polarities on polymer hydration and macromolecular rearrangements (Bajdik *et al.,* 2005). As surface mobility of functional groups was often observed in polymeric materials at room temperature (Park *et al.,* 1995; Tretinnikov and Ikada, 1994; Tan *et al.,* 2004; Ferguson and Whitesides, 1992), such reorientation was highly possible for EC gel surfaces. This was even more favorable in semisolid gels as the gel surfaces were highly perturbable (Suzuki and Kobiki, 1999). The time-dependence of the dynamic contact angle could also be partially explained by this phenomenon since time was needed for polymeric reorientation and attainment of equilibrium contact angle (Tretinnikov and Ikada, 1994). Such reorientation was not required in gel wetting by IPM since there was already favorable hydrophobic polymeric orientation at the EC gel-air interface.

V-B6.6.3. Influence of gel network structure on wetting behavior

Polymeric chain length and concentration dependent trends for the extent and rate of wetting were observed for all the EC gels studied. Higher EC concentration and greater polymeric chain length resulted in lower extent of wetting by water as reflected by lower θ_w and $\theta_{w/e}$:$\theta_{w/0}$ but higher V_w and $V_{w/e}$:$V_{w/0}$ values. The effect of polymeric chain length was only apparent between EC with large difference in molecular weights such as between EC100 and EC7 or EC100 and EC10. Increased EC concentration and polymeric chain length gave rise to a higher degree of inter-polymeric interactions to form a stiffer gel network due to the increased entanglement density associated with the number of intermolecular contacts per unit volume of EC gel (Section V-B3.2). The resulting decrease in chain mobility would impose greater difficulties to rotational reorientation of C_6 –OH groups, hence reducing the number of –OH groups available to interact with the water sessile drop. This rendered a more lipophilic gel surface, leading to higher water contact angle.

More lipophilic EC gel matrices (higher EC concentration and/or polymeric chain length) were expected to show greater affinity for lipophilic solvents such as IPM. However, IPM demonstrated similar wetting trends as water where the extent and rate of gel wetting decreased despite the more lipophilic EC gel matrices. The general contention that wetting is predominantly a surface phenomenon which is mainly influenced by surface properties is supported by some reported studies. In a study involving relatively solid substrates, it was found that contact angle was a function of surface properties but relatively independent of other bulk properties of the substrate (Hogt *et al.,* 1985). The spreading of some organic liquids on hydrogels of poly(2-acrylamido-2-methylpropane-

sulfonic acid) was independent of polymer concentration and network mesh size for the physical gels and covalently crosslinked gels but liquid spreading was affected by these factors in the polymer solutions when $G'/G'' < 1$ (Kaneko *et al.*, 2005). However, in another study, the dependence of contact angle on polymer gel bulk structures was observed (Suzuki and Kobiki, 1999). Hence, it was postulated that apart from hydrophilic-lipophilic properties, rheological and mechanical properties of EC gel matrices had also influenced their wetting behavior.

Rheological and mechanical characteristics exerted significant effects on the overall physical properties of EC gels (Sections V-B3 and V-B4). Such characteristics were important predictors of gel product performance such as drug release kinetics (Talukdar *et al.,* 1996; Jones *et al.,* 1996a) and bioadhesion (Needleman *et al.,* 1998; Tamburic and Craig, 1997). The direct positive linear correlations of θ_w, V_w, $\theta_{i/0}$ and $V_{i/0}$ with rheological and mechanical parameters verified the influence of these parameters on the wetting behavior of EC gel matrices. The absorption-dominated wetting of 7 %w/w EC100 by water sessile drop could be attributed to the weaker gel network structure due to lower polymer concentration and the lack of compact polymeric network for extensive intermolecular interactions (Section V-B3.2). EC polymer polydispersity was another factor that had affected gel wetting through its effect on gel viscosity as described under Section V-B3.2. Thus, the more polydispersed EC7 ($M_w/M_n = 2.5$) and EC10 ($M_w/M_n = 3.3$) produced less viscous gels that were more readily wetted by water and IPM as compared to the less polydispersed EC100 ($M_w/M_n = 1.7$). Despite their differences in polydispersity, the wetting behaviors of EC7 and EC10 were similar due to their similarity in M_w, hence demonstrating the stronger influence of polymeric chain length.

The polymeric network mesh size representing the average distance between consecutive physical entanglements provided a measure of porosity of the network (Lowman and Peppas, 2000; Baumgartner *et al.,* 2002; Gemeinhart and Guo, 2004). Gel with higher mesh size occupied higher volume for a particular mass of gel and this had resulted in a lower gel density. Gel densities determined using EC gel samples in their swollen states were assumed to be inversely related to mesh size. Hence, gel density values were employed as an indirect measure for EC gel mesh size in this study. A more structured gel network would possess lower mesh size due to more extensive polymeric chain entanglements, producing a denser gel network. A decrease in mesh size with an increase in EC concentration and polymeric chain length was reflected by higher gel density at higher EC concentration (Figure 36). This in turn imparted greater resistance to liquid penetration into the gel matrices, thereby decreasing the extent of water and IPM absorption. Since wetting by IPM necessitated the absorption of the solvent into the gel matrices without appreciable IPM drop spreading, it was reasonable to expect that gel rheology and mesh size exerted a more direct influence on the wetting process. This explained the higher rheology-wettability correlation observed with IPM, r = 0.9293 and 0.8951, as compared to water, r = 0.8844 and 0.8624 (Section V-B6.5). The rates of water absorption as reflected by $t_{50\%}$ for V_w and IPM absorption as reflected by t_a, also decreased due to the reduction in mesh size. Since EC gel was shown to be highly compatible with IPM due to their lipophilic properties, gel lipophilicity was the secondary factor influencing the wetting behaviors of the EC gels by IPM. The exponential increase of t_a for EC100 mirrored the exponential trend of EC100 density (Figures 35 and 36), highlighting the strong influence of mesh size on the rate of IPM

absorption. Hence, the observed difference in wetting behavior of different EC gels could be explained by the mesh size factor. For EC gel wetting by water, increased mesh size rendered spreading of sessile water drop more difficult due to higher propensity of water absorption. The increased rate of water spreading of higher concentration range of EC100 gels as indicated by greater $K_{\theta w}$ and lower $t_{50\%}$ for A_w was attributed to low mesh size. Such drastic reduction of mesh size especially for 12 %w/w EC100 (Figure 36) was able to induce slippage of the sessile water drop on the gel surface, hence facilitating more rapid spreading despite the higher lipophilicity of 12 %w/w EC100 gels. The lower density of 8 to 10 %w/w EC100 gave rise to higher mesh size, hence lower rate of water spreading. Since the concentration dependant increase in gel density of EC100 was exponential, at the lower concentration range of 8 to 10 %w/w, the increase in gel density was not sufficient to result in significant difference in rate of water spreading among the gel samples (Figure 36). EC7 and EC10 gels exhibited opposite trends in the rates of water spreading with respect to EC concentrations as reflected in the $t_{50\%}$ values for A_w (Figure 34). Densities of EC7 and EC10 gels were much lower than that of 12 %w/w EC100 gels even at a higher concentration range of 14 to 16 %w/w as shown by the more gradual linear density-concentration trends (Figure 36). Consequently, the reduction in mesh size at increased EC concentrations was not sufficient to induce the water drop slippage phenomena on the gel surfaces as described for 12 %w/w EC100. Thus, mesh size factor did not exert significant effect on rate of water spreading in EC7 and EC10 gels while gel lipophilicity appeared to play a prominent role in this case. A higher polymer concentration gave rise to higher gel surface lipophilicity. This resulted in lower rate of water spreading as the rapid movement of water front along the gel surface was

impeded by high lipophilicity. Unlike IPM, water was less compatible with EC gels and the lipophilicity of EC gel matrices was a limiting factor in wetting by water. Mesh size and lipophilicity of the gel demonstrated opposing effects on the rate and extent of EC gel wetting by water. Higher EC concentration and/or chain length resulted in gels of higher lipophilicity, a factor that decreased water spreading. However, the mesh size in these gels was lower, and this would promote water spreading. Hence, the interplay of mesh size and lipophilicity on the extent of water spreading gave rise to a stable base area ratio of 1.2 irrespective of the different formulations of EC gel.

V-B6.6.4. Influence of other factors on EC gel wetting

Surface chemical heterogeneity due to the presence of microscopic patches of hydrophobic and hydrophilic groups with differing surface energies, and surface topography such as roughness had been reported to affect contact angle of sessile liquid drops on solid polymeric materials (Park *et al.,* 1995; Ferguson and Whitesides, 1992; Rangwalla *et al.,* 2004). Surface chemical heterogeneity was found to inhibit uniform wetting (Tretinnikov and Ikada, 1994) while surface roughness reduced the observed contact angle when $\theta < 90°$ (Wu, 1982). The significance of these factors was dependent on the polymeric system being studied. Roughness was not regarded as an important factor for well prepared polymer surfaces because such surfaces were shown to be smooth (Tretinnikov and Ikada, 1994; Rangwalla *et al.,* 2004). Polymer surfaces with different surface roughness and heterogeneity were shown to have the same advancing contact angles (Grundke *et al.,* 2001). Kwok *et al.* (1998) observed that in axisymmetric drop shape analysis-profile, contact angles was less sensitive to surface roughness and

heterogeneity as compared to surface tensions measured using sessile drops. In general, surface roughness below 0.1 to 0.5 μm or heterogenous patch below 1 μm would give negligible effect on the observed advancing contact angle (Wu, 1982; Grundke *et al.,* 2001). While the influence of these factors on the contact angle of polymeric systems was acknowledged, their effect on EC gel wetting was not investigated in the current study. The influence of gel lipophilicity, rheological and mechanical properties on EC gel wetting behavior were the main focus of this study.

The observed dynamic contact angle of sessile liquid drop could be partly attributed to slight solvation of gel components which affected the liquid drop surface tension and consequently, the contact angle. However, the insolubility of EC and immiscibility of Miglyol 840 with water coupled with the small sessile drop volume ensured negligible solvation effect. Greater solvation of the non-aqueous gel components was expected for IPM due to the common lipophilic properties of IPM and EC gels, hence resulting in lower sessile drop contact angle as compared to water. However, given the enormous proportion of polymer and solvent relative to the sessile liquid drop, same degree of solvation was expected to occur in each drop of liquid. Hence, while solvation factor was important to explain the lower IPM contact angle observed on EC gel surfaces as compared to water, this factor was deemed to be trivial in explaining the relative trends of wetting of different EC gel formulations.

V-B6.6.5. Stages of wetting and mechanism of liquid absorption

Adhesional wetting is represented by the free energy change for a liquid to make contact and adhere to the subtrate (Rosen, 1989; Parfitt, 1981). Immersional wetting is

represented by the free energy change for a substrate to be completely immersed in the liquid. Spreading wetting is represented by the free energy change for a liquid which is already in contact with the substrate to increase its area of contact. These concepts were applied in the currently studied EC gel wetting behavior. Liquid absorption by EC gel was reflected by immersional wetting. From the values of *Wa* representing adhesional wetting, *At* representing immersional wetting and *Sc* representing spreading wetting (Table 14), the propensity for these three stages of wetting of EC gel was inversely related to EC polymeric chain length and concentration for a particular wetting liquid. Unlike water, IPM did not exhibit equilibrium wetting as it was completely absorbed into EC gels, therefore *Wa*, *At* and *Sc* between water and IPM were not directly comparable. Besides, for a liquid which does not demonstrate equilibrium wetting such as IPM, rate of wetting ($K_{\theta i}$ and t_a) was a more important determinant of the gel wetting behavior (Rosen, 1989).

The mechanism responsible for absorption of either water or IPM into EC gel matrix was likely to be molecular diffusion. The affinity of water molecules for the non-aqueous EC gel was provided by the unethoxylated and hydrophilic C_6-OH groups on EC backbone. The presence of a sessile water drop on EC gel surface would result in diffusion of water molecules into the gel matrix to interact with C_6-OH by hydrogen bonding. However, the lipophilic groups that abundantly dominated the overall property of EC gel would impart resistance to the diffusion of water molecules, thus resulting in only limited water absorption. Unlike water, IPM had the requisite lipophilicity for affinity towards EC gel. Also, the miscibility of IPM with Miglyol greatly increased the ease for molecular diffusion of IPM into EC gel matrix to result in a complete absorption.

V-B6.6.6. Summary on EC gel wetting behavior

Wetting of non-aqueous EC gel matrices could be represented by the extent and rate of wetting. These parameters could be quantitatively derived from the time-lapse dynamic contact angle measurements. Extent of wetting by a hydrophilic liquid such as water which formed an equilibrium sessile drop on the gel matrix could be represented by initial and equilibrium contact angles, standing volumes and base areas. The initial:equilibrium ratios of these parameters were more reliable when comparing the same type of EC gel. For lipophilic liquid like IPM that was completely absorbed into the EC gel matrix, extent of wetting was described by initial contact angle and standing volume. Base area, indicating spreading of the sessile IPM drop was not a meaningful parameter due to the absorption-dominated wetting of EC gel. The initial rate of wetting of EC gel by either water or IPM was represented by the first-order rate constant for contact angle and it was found to be more reproducible than the rate constants from standing volume and base area. The derived $t_{50\%}$ values were complementary in their ability to provide information on whether the observed trend for each rate constant was governed by rate of spreading or absorption. Time taken for complete absorption was another useful parameter to describe the rate of IPM absorption into an EC gel matrix. The average C.V. values of the raw data for θ, A and V of water and IPM were compared as an assessment criteria to determine the order of suitability of each parameter as a potential predictor of EC gel wetting. Both water and IPM exhibited similar trends: $C.V._{\theta} < C.V._{A} < C.V._{V}$. This indicated that contact angle were the best overall parameter in providing a more reliable assessment of the wetting behavior of the EC gel matrices. Average C.V. values of θ, A and V for water were 3.3, 4.4 and 7.5 %, respectively and

they were approximately 3 fold lower than the corresponding C.V. values for IPM. The lower C.V. values of water wetting parameters indicated that a more hydrophilic liquid of lower absorption tendency improved reproducibility of wettability measurement using dynamic contact angle.

Dynamic contact angle measurement confirmed the lipophilic nature of the non-aqueous EC gel. The lipophilic EC gel surface would potentially ensure minimal ambient moisture absorption, hence protecting moisture-sensitive drugs incorporated in the gel matrices from hydrolysis. When wetted by water, rapid changes of EC gel surface configuration occurred, allowing wetting and moderate water uptake into the gel matrix. Therefore, a certain degree of water-associated gel hydration was possible despite the non-aqueous nature of the gel formulations. The ability of the non-aqueous EC gel to be wetted and slightly hydrated upon contact with water would be essential for bioadhesion (Peppas and Buri, 1985; Lehr *et al.,* 1992; Toledano *et al.,* 1999; Esposito *et al.,* 1994) and for drug release from the gel matrices (Buckton, 1990; Buckton *et al.,* 1991; Spireas and Sadu, 1998; Bodmeier and Paeratakul, 1991; Rosilio *et al.,* 1998). Gel hydration was found to be especially important for water-soluble drug such as MH which had existed as a suspension in EC gel. For such formulations, drug dissolution in the aqueous medium was required for its transport out from a gel matrix to the aqueous environment associated with the physiological/biological systems. The ease of wetting and IPM uptake into EC gel matrices signified good compatibility of the EC gel with the skin and this served as a prerequisite for bioadhesion.

V-B7. Gel spreadability

An alternative technique based on dynamic contact angles of sessile drops of EC samples on silicone elastomer had been employed to evaluate EC gel spreadability. The advancing contact angles were measured for sessile drops in the current study as indicated by their advancing liquid fronts along the substrate-air interfaces. For small drops of pure liquids such as water, IPM and Miglyol employed in this study, effects of gravity, drop inertia and liquid viscosity on the dynamic contact angles of the sessile drops were negligible as compared to interfacial forces (Garnier *et al.*, 1998 and 1999). Owing to the smallness of drop, only negligible gravitational effect was present and unlikely to cause drop distortion, thus verified the assumption of a hemispherical section of the liquid drop on the substrate. As for the EC samples studied, the small drop sizes indicated that the sessile drops were free from the influence of gravitational and inertial forces (Garnier *et al.*, 1998 and 1999). On the other hand, viscous forces were expected to have an influence on sessile drops of EC samples in view of the concentrated nature of the EC polymer solutions, especially for samples with higher consistencies.

V-B7.1. Evaluation of the applicability of silicone elastomer as human skin mimic for dynamic contact angle measurement of EC samples

The surface of the silicone elastomer employed in this study is an inert, non-porous and hydrophobic material that mimics human skin in term of hydrophilic/lipophilic property. The surface of the silicone elastomer showed a distinct baseline for accurate drop shape analysis and was observed to be smooth under the atomic force microscope as reflected by very low mean Ra value of 15.9 ± 2.0 nm. The

human skin sample with mean Ra value of 354.1 ± 29.4 nm was about 22 times rougher than the silicone elastomer (Figure 38). The smooth silicone elastomer surface would reduce tremendously any error in contact angle measurement due to surface roughness.

Although human skin appeared to be an obvious choice of substrate for spreadability measurement, its biological variability and scarce supply would necessitate the use of a substitute that can mimic the skin. Silicone elastomer, an inert and biocompatible polymer was proposed to be an appropriate substrate for spreadability measurements of EC polymer solutions using dynamic contact angle as this commonly used material in skin grafts (Bertolami *et al.,* 1991) was deemed to be similar to human skin in term of hydrophilic/lipophilic property. This presumption was tested by comparing the wetting behavior of silicone elastomer and human skin using water and IPM as test liquids.

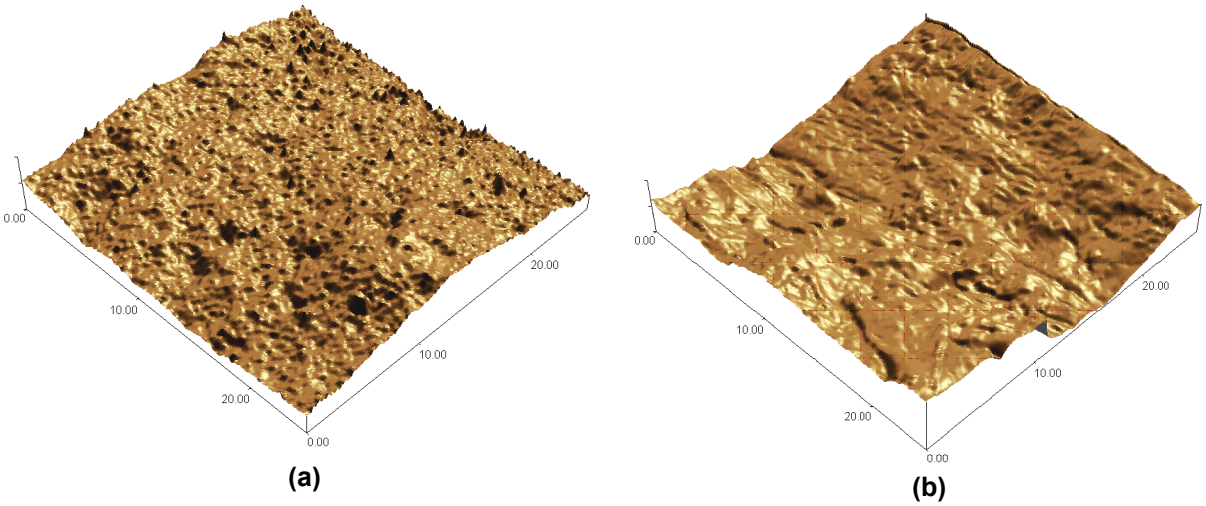

Figure 38: AFM topograph of silicone elastomer (a) and human skin (b).

The initial and mean contact angles were employed to describe wetting with water. Initial contact angle was defined by t = 0, the time when the first stable image of the sessile drop observed upon drop deposition on the substrate. Mean contact angle was determined by averaging the water contact angle values obtained over the measurement period of about 620 s. Unlike water contact angle which remained relatively constant over the measurement period, IPM contact angle decreased exponentially with time, hence mean contact angle would not serve as an accurate parameter to characterize the wetting of the substrate with IPM. Instead, the initial (t = 0) and final IPM contact angle formed at t = 620 s were employed for this purpose.

Water is a known hydrophilic liquid whereas IPM is predominantly a lipophilic solvent. The relatively high initial and mean water contact angles (Table 17) indicated that both the substrates were not very well wetted by the water drop. On the contrary, IPM exhibited good wetting on silicone elastomer and human skin as shown by the relatively low initial IPM contact angles of 32.5° and 30.1°, respectively and final contact angles of 17.4° and 0°, respectively. The decline in IPM contact angle on human skin was markedly faster than that of silicone elastomer (Figure 39a) due to rapid absorption of IPM into the skin as indicated by the decline in standing volume of the sessile IPM drop. Complete absorption ($\theta = 0°$) occurred in 35.2 s or less. Conversely, absorption did not occur in silicone elastomer due to its non-porous surface. Hence, decline in IPM contact angle on silicone elastomer could be associated solely to drop spreading. This was verified by Figure 39b which demonstrated concomitant increase in base area with decrease in contact angle but without any change in standing volume with time. The poor wetting by water but good wetting by IPM indicated that both the substrates were

Table 17: Comparison of wetting behavior between silicone elastomer and human skin as substrates using contact angles of sessile drops of water and IPM.

Substrate	Contact angle (°)			
	Water		IPM	
	Initial	Mean	Initial	Final
Silicone elastomer	104.1 ± 3.1	95.0 ± 4.9	32.5 ± 0.4	17.4 ± 0.9
Human skin	98.1 ± 10.2	95.1 ± 11.3	30.1 ± 3.3	0.0

predominantly more lipophilic in nature. The lipophilicity of human skin was attributed to the stratum corneum, the outermost skin layer forming the main barrier of the skin (Loth, 1991). The similarity of silicone elastomer and human skin in term of hydrophilic/lipophilic property was established by the fact that they demonstrated identical mean water contact angle (95°) and close initial water and IPM contact angle values with only 6.1 % and 8.0 % deviations, respectively. Apart from its predominantly lipophilic property, the purpose of employing IPM was its good compatibility and similarity to the human skin in term of the polar/non-polar nature of the skin as reflected by complete skin wetting in a short period of time (Sections V-B6.3 and V-6.6). Hence, the low IPM contact angle on silicone elastomer (17.4°) was indicative of the similarity of this substrate with the nature of the human skin. This study had verified that the hydrophilic/lipophilic property of silicone elastomer was close to that of human skin, at least with respect to the outermost stratum corneum layer. Thus, the silicone elastomer could be employed as a convenient substitute to human skin in order to characterize spreadability of EC gels using dynamic contact angle measurement. Besides, higher reproducibility could be obtained as silicone elastomer was not subjected to biological variability present in human skin and possible solvent effects, if re-used.

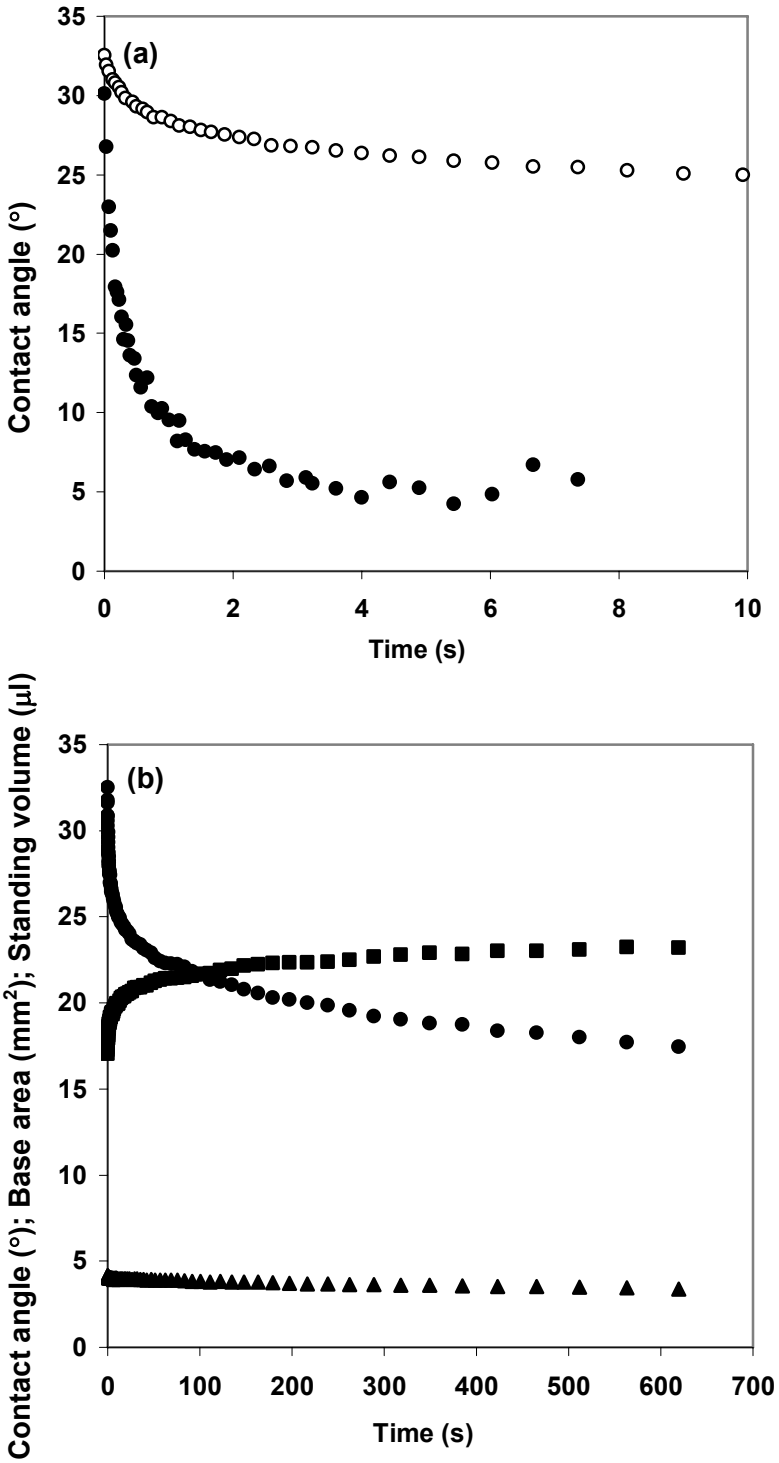

Figure 39: (a) Contact angle versus time profiles of sessile IPM drop on silicone elastomer (open symbols) and human skin (closed symbols). (b) Contact angle (●), base area (■) and standing volume (▲) versus time profiles of sessile IPM drop on silicone elastomer.

It should be noted that silicone elastomer would not be totally comparable to human skin in terms of surface roughness and chemical heterogeneity which might have some influence on contact angle and thus EC gel spreadability. The difference in surface roughness of silicone elastomer and human skin was apparent from their Ra values. As it was technically not realistic to produce a substrate with similar roughness and chemical heterogeneity, these factors could not be investigated in the current study. Hence, silicone elastomer and human skin was compared only with respect to their hydrophilic/lipophilic property.

V-B7.2. Dynamic contact angle of EC samples and the influence of viscosity on spreadability

Several captured images at different time points during the dynamic contact angle experiments with 5 %w/w EC7 polymer solution on silicone elastomer are shown in Figure 40. Plots of contact angle versus time of Miglyol and EC samples on silicone elastomer followed an exponential decay towards an equilibrium value while base area increased exponentially with time towards a plateau indicating drop spreading (Figure 41). It was interesting to note that sessile drops containing 7 and 8 %w/w EC100 exhibited slight recoil at around 10 to 15 s. The contact angles increased by approximately 1.7° for 7 %w/w EC100 and 2.5° for 8 %w/w EC100 before decreasing again and then leveling off. However, the drop recoil was not reflected in the base area profiles since the contact angle change was only momentary and marginal (Figure 41). The standing volume of sessile drops of Miglyol and all EC samples remained relatively unchanged at about 6 µl with an average coefficient of variation of 9.04 %. This was

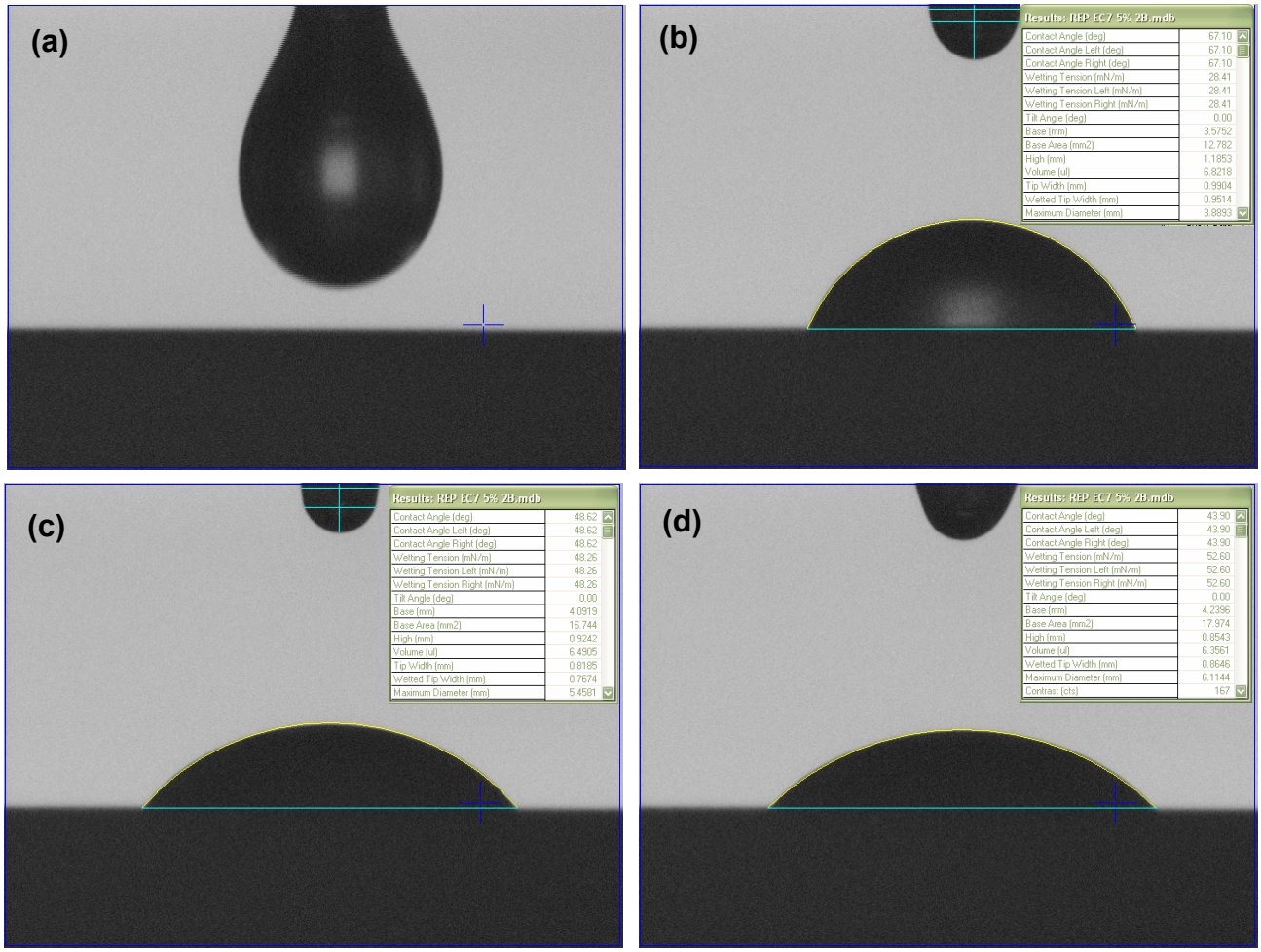

Figure 40: Captured images from dynamic contact angle measurement of 5 %w/w EC7 sample on silicone elastomer showing the image of the drop before detachment (a), and images of sessile sample drop at time, t = 0 (b), t = 62.6 s (c), and t = 619.7 s (d).

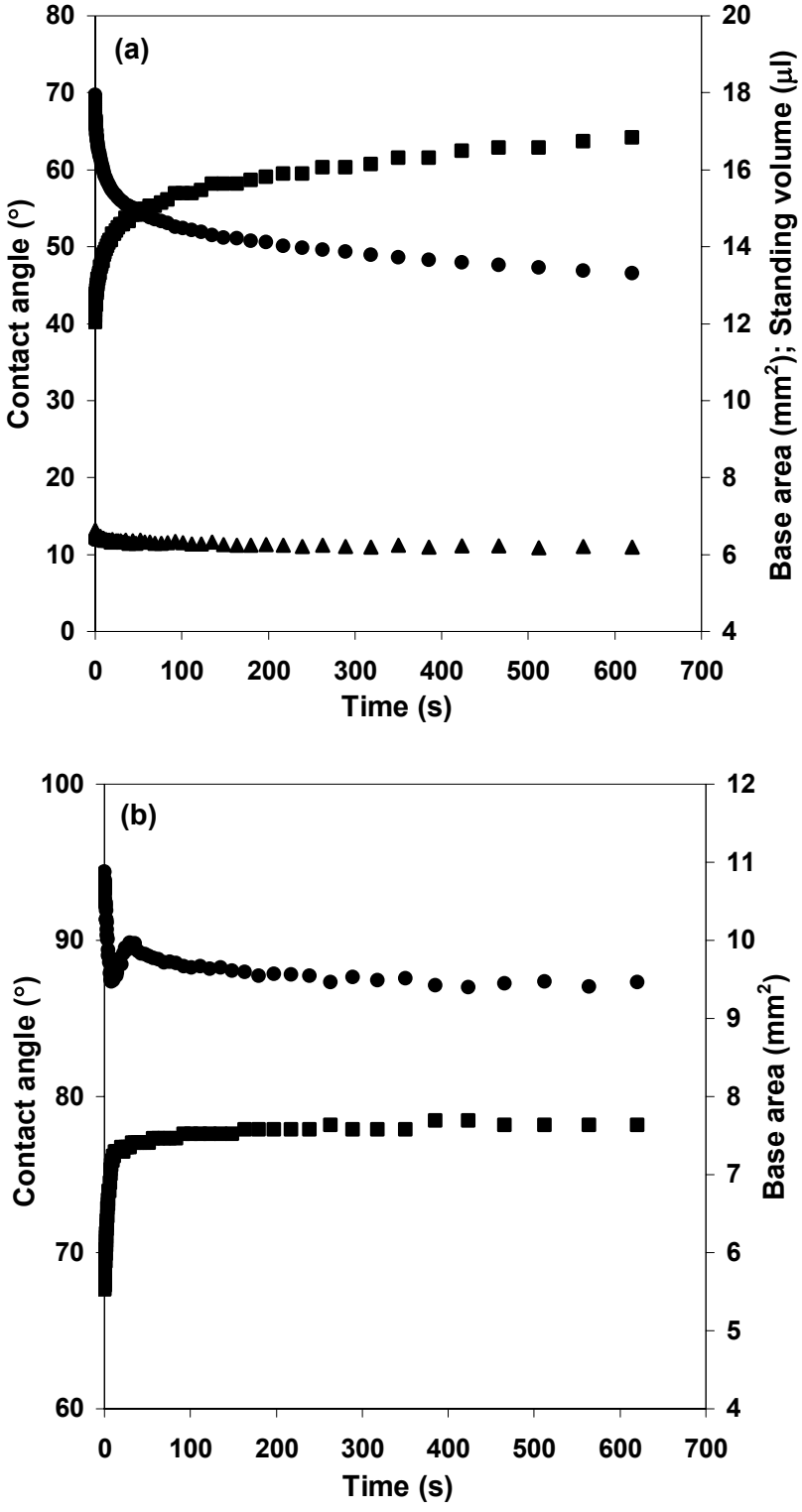

Figure 41: Contact angle (●), base area (■) and standing volume (▲) versus time profiles of sessile drop of 5 %w/w EC10 (a) and 8 %w/w EC100 (b) on silicone elastomer. Standing volume of 8 %w/w over time could not be accurately obtained.

attributed to the non-porous surface of the silicone elastomer (Figure 41). The initial and equilibrium contact angles and base areas were employed to describe the spreadability of the sessile drops of EC samples. Equilibrium values for contact angle and base area were obtained by averaging readings after 300 s when changes in the physical properties of the sessile drops for all EC samples had already leveled off.

The initial and equilibrium contact angles of all EC samples studied exhibited linear relationships with EC concentrations from 3 to 8 %w/w (Table 18). The linear relationship for equilibrium contact angle was deemed to be more robust as it extended to zero EC concentration which corresponded to the equilibrium contact angle of pure Miglyol (32.8°). For the initial contact angle of EC samples, linearity was only observed from 3 %w/w EC onwards possibly due to the non-equilibrium state of the sessile drops at initial time. Equilibrium base area decreased linearly with EC concentration (Table 18), parallel to the concomitant increase in contact angle indicating a lesser extent of spreading of the sessile drops with increase in the EC concentration. Unlike the equilibrium contact angle which was relatively independent of the drop volume, the accuracy of the base area measurements might be affected by small fluctuations in generating drop volumes. Therefore, the base areas of EC7, EC10 and EC100 were normalized with respect to the average drop volumes for each EC grade. The resultant plots of base area:volume ratio versus EC concentration also exhibited similar linear trends (Figure 42). EC100 showed significantly higher equilibrium contact angle and lower base area:volume ratio as compared to EC7 and EC10. This could be accounted by the much higher M_w of EC100 (130273). However, no significant difference in equilibrium contact angle and base area:volume ratio was observed between EC7 and

Table 18: Apparent viscosity of EC samples and spreading parameters as represented by initial and equilibrium contact angles (θ_s), and equilibrium base area of sessile drops of EC samples on silicone elastomer. Correlation of the respective parameter with EC concentrations is given by the linear regressions and correlation coefficients, r.

EC (%w/w)	Initial θ_s (°)	Equilibrium θ_s (°)	Equilibrium base area (mm^2)	Apparent viscosity (mPa·s)
EC7	y = 5.35x+38.0 r = 0.951	y = 2.39x+30.9 r = 0.969	y = -0.64x+21.0 r = 0.852	y = 0.254x+1.5 r = 0.993
0	60.9 ± 1.2	32.8 ± 1.7	20.2 ± 1.0	Not determined
3	58.3 ± 9.2	36.0 ± 2.5	19.5 ± 1.1	154 ± 8
4	55.3 ± 8.5	38.3 ± 3.6	18.8 ± 1.7	360 ± 16
5	65.1 ± 4.4	43.3 ± 2.4	18.2 ± 0.5	647 ± 18
6	68.4 ± 3.9	46.8 ± 4.8	16.7 ± 1.4	1105 ± 60
7	73.4 ± 5.4	48.6 ± 6.5	18.1 ± 1.4	2078 ± 189
8	84.2 ± 1.9	49.9 ± 7.7	14.2 ± 1.3	2910 ± 328
EC10	y = 4.49x+43.8 r = 0.944	y = 2.48x+31.2 r = 0.976	y = -0.76x+21.1 r = 0.899	y = 0.254x+1.7 r = 0.998
0	60.9 ± 1.2	32.8 ± 1.7	20.2 ± 1.0	Not determined
3	54.3 ± 5.5	36.9 ± 2.9	19.0 ± 1.8	259 ± 24
4	65.9 ± 3.9	41.4 ± 1.5	18.4 ± 0.5	535 ± 37
5	67.5 ± 4.2	42.2 ± 2.9	17.7 ± 1.1	964 ± 52
6	69.4 ± 8.8	45.6 ± 8.0	18.2 ± 2.0	1803 ± 52
7	72.0 ± 6.9	47.8 ± 5.4	15.0 ± 2.0	2960 ± 140
8	81.6 ± 0.7	53.3 ± 5.4	13.7 ± 1.2	4923 ± 206
EC100	y = 6.76x+40.2 r = 0.978	y = 6.37x+32.3 r = 0.999	y = -1.53x+20.6 r = 0.990	y = 0.375x+1.3 r = 0.986
0	60.9 ± 1.2	32.8 ± 1.7	20.2 ± 1.0	Not determined
3	62.0 ± 0.4	50.6 ± 2.0	16.1 ± 0.8	185 ± 5
4	64.6 ± 1.5	57.6 ± 6.3	14.6 ± 1.8	731 ± 20
5	72.2 ± 0.4	64.8 ± 0.9	13.3 ± 0.2	1842 ± 51
6	85.5 ± 0.7	70.7 ± 1.4	12.5 ± 0.6	4705 ± 137
7	87.1 ± 5.0	75.8 ± 4.3	9.3 ± 0.8	8577 ± 112
8	93.1 ± 1.7	84.1 ± 4.7	7.8 ± 0.5	14785 ± 326

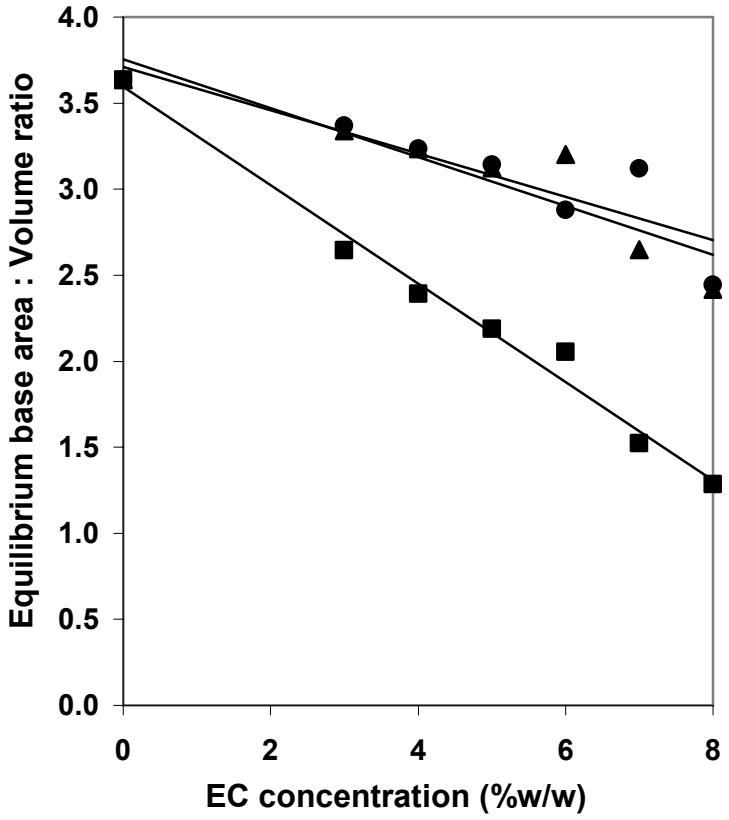

Figure 42: Linear regressions between equilibrium base area:volume ratio and EC concentrations for sessile drops of EC7 (●, y = -0.126x + 3.711, r = 0.896), EC10 (▲, y = -0.142x + 3.756, r = 0.917) and EC100 (■, y = -0.286x + 3.594, r = 0.993) samples.

EC10 because the difference in their molecular weights (54068 and 69855) was relatively small. The higher gradients for the linear plots of EC100 for both contact angle and base area:volume ratio versus EC concentration indicated that spreading of sessile drops of EC samples on silicone elastomer was more sensitive to EC concentration as polymeric chain length increased, hence reflecting the prominent role of polymeric chain length in the spreadability of these samples. In general, spreadability of EC7 and EC10 samples on silicone elastomer could be regarded as reasonably good especially for samples at lower concentration range as observed from their equilibrium contact angles ranging from 36° to 53°. EC100 samples had equilibrium contact angles ranging from 51° to 84°, hence demonstrated moderate spreadability at the higher concentration range. The non-aqueous nature and predominantly lipophilic EC samples resulted in attractive interaction between the sample gel surface and the lipophilic substrate and this served as the driving force for sample spreading.

Rheological measurements of EC samples were carried out in order to investigate the potential effect of viscosity on the observed trends of spreading as reflected by the dynamic contact angles. Apparent viscosity at a low shear rate of 10 s^{-1} on the upward curve of the rheogram was employed to represent the viscosity of the sessile drops of EC samples on silicone elastomer. Apparent viscosity was used in order to mimic more closely the sheared state of the samples after extrusion from the needle tips. Besides, difficulty and inaccuracy involved in the calculation of zero shear viscosity also limited its use in this situation. Apparent viscosity of EC samples increased with EC concentration from 3 to 8 %w/w. The plots of logarithm of apparent viscosity versus EC concentration was linear for EC7, EC10 and EC100 with slope values, S = 0.254, 0.254

and 0.375 mPa·s, respectively (Table 18). The apparent viscosities for each corresponding EC concentrations increased in the order of increasing polymeric chain lengths of EC where EC7 < EC10 < EC100. From the higher S value, the concentration dependence of apparent viscosity for EC100 was markedly higher as compared to EC7 and EC10, implying a greater influence of polymeric chain length than the polymer concentration. Besides polymeric chain length, the decrease in polydispersity in the order EC7 (3.3) < EC10 (2.5) < EC100 (1.7) was also a contributory factor to the increase in apparent viscosity (Section V-B3.2).

The linear relationships between equilibrium contact angles and logarithm of apparent viscosities for 3 to 8 %w/w EC concentrations verified the direct influence of the sample viscosity on its dynamic contact angle and hence spreadability on silicone elastomer (Figure 43). The steeper slope of EC100 (16.9) as compared to EC7 (11.7) and EC10 (11.6) implied a stronger influence of viscosity on spreadability, highlighting again the role of polymeric chain length in this phenomenon. Higher polymeric chain length and polymer concentration imparted higher viscosity due to an increase in degree of polymeric chain entanglement, resulting in higher resistance to flow upon shearing. This in turn led to the lower extent of sessile drop spreading as indicated by higher equilibrium contact angle. The dependence of contact angle on viscosity as reported for aqueous cellulose solutions (Twitchell *et al.,* 1995) further supported the observed trend for EC samples in the current study. The decrease in equilibrium contact angles in less viscous EC samples could be partly attributed to the increase in polydispersity as this also played a role in the viscosity decrease. However, influence of polymeric chain length remained more prominent than polydispersity as EC7 and EC10 with relatively small difference in

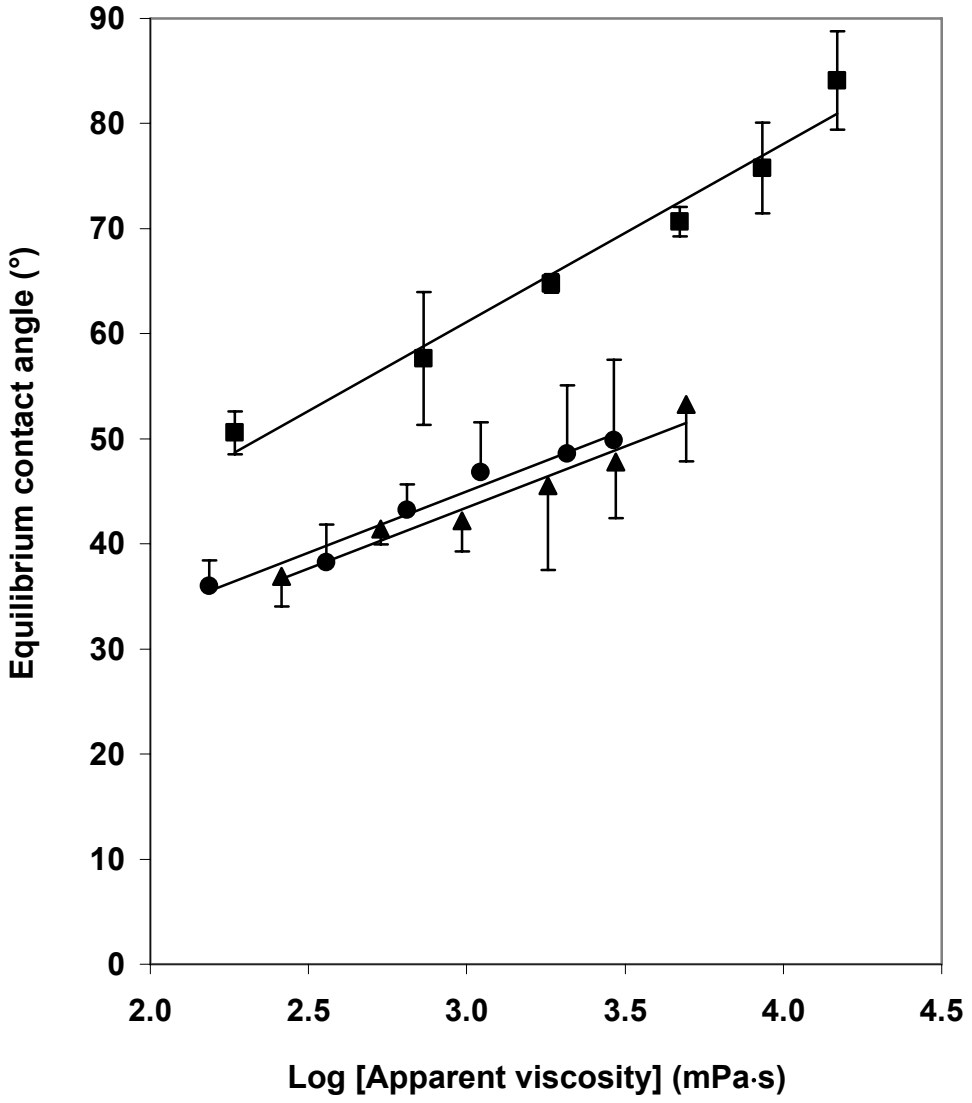

Figure 43: Linear relationship between equilibrium contact angle and logarithm of apparent viscosity of sessile drops for EC7 (●, y = 11.7x + 10.0, r = 0.985), EC10 (▲, y = 11.6x + 8.6, r = 0.976), EC100 (■, y = 16.9x + 10.4, r = 0.986) samples.

M_w did not demonstrate significant difference in equilibrium contact angle despite their difference in polydispersity.

The observed spreading of the sessile drop of EC sample could be explained by chemical interaction and viscosity factor. The propensity of gel surfaces to reorientate and the establishment of a hydrophobic gel-air interface has been described in detailed in Section V-B6.6.2. Since EC concentrations were low in most of the samples used in this study, less extensive polymeric chain entanglements would occur, producing concentrated polymer solutions instead of semisolid gels. Changes of surface configuration were expected to occur more readily in these polymer solutions since molecular rotations would be easier in the absence of rigid gel matrices. This could be well substantiated by dynamic surface tension studies on polymeric solutions ranging from low to high concentrations of the non-ionic cellulose, hydroxypropylmethylcellulose and ethylhydroxyethylcellulose. Molecular diffusion and reorientation at sample-air interface were always cited as reasons for the observed decrease in surface tensions of the samples with time (Um *et al.,* 1997; Persson *et al.,* 1999; Machiste and Buckton, 1996; Nahringbauer, 1995). It was established in the current study that the surface of the silicone elastomer substrate used was predominantly lipophilic. Upon contact of a drop of EC sample with the silicone elastomer, reorientation of polymeric moieties would take place by molecular rotations of flexible parts of the polymer chains and solvent molecules to direct their hydrophobic segments, namely the non-polar ethyl substituents of EC as well as the capric and caprylic acid substituents of Miglyol towards the drop-air interface and the drop-substrate interface in order to establish the hydrophobic interactions. On the contrary, the unethoxylated and

hydrophilic C_6 –OH groups of EC and carbonyl oxygen of Miglyol would be directed preferentially into the interior of the sessile drop where intermolecular hydrogen bondings and dipole-dipole interactions would take place. Apart from the well documented reorientation phenomenon demonstrated by polymeric solutions exposed to the non-polar air phase, high extent of adsorption and gradual conformational rearrangement of ethylhydroxyethylcellulose at a hydrophobic silica surface had been observed by means of in situ ellipsometry. The increased extent of adsorption with increased hydrophobicity of the silica surface implied hydrophobic interactions as the main driving force for adsorption (Malmsten and Lindman, 1990). This has provided a basis for associating the spreading of sessile drops of EC samples with molecular reorientations and hydrophobic interactions with the surface of silicone elastomer. The time dependency of the dynamic contact angle profile of the sessile drop could be attributed to time needed for air displacement and reorientation of polymeric moieties and reestablishment of intermolecular interactions until the attainment of equilibrium upon which advancement of the drop front would cease. The equilibrium contact angle was attained when interaction forces between the sessile drop and silicone elastomer which acted to reduce the contact angle was balanced by the viscous forces within the drop which acted to maintain the contact angle. For more viscous samples, stronger intra-droplet cohesive forces produced by more extensive interpolymeric interactions. This resulted in stronger network structures within the samples and entrapping much of the continuous phase within. Thus, stronger network structures accounted for the lower extent of spreading in samples with higher EC concentrations and polymeric chain lengths.

From Young's equation (Equation 5), contact angle is known to be a function of surface tension where higher surface tension results in higher sessile drop contact angle on a particular substrate (Wu, 1982). However, the observed EC concentration and polymeric chain length dependent increase in contact angle in the current study could not be attributed to increased surface tension of the EC polymer solution. This is because surface tension of the EC polymer solution was expected to decrease with increase in EC concentration and polymeric chain length due to increased ordering of polymer segments at the interfaces as commonly observed for both dilute and concentrated aqueous solutions of cellulose polymers (Um *et al.,* 1997; Persson *et al.,* 1999; Machiste and Buckton, 1996). Hence, the increase in contact angle observed for sessile drop of EC gel sample was essentially the result of increased viscosity. Increases in sessile drop viscosity and surface tension were also cited as reasons for sessile drops recoil from solid surfaces (Bhola and Chandra, 1999; Pasandideh-Fard *et al.,* 1996). Since surface tension was the unlikely dominating factor for reasons discussed above, the slight drop recoil observed for EC100 samples at higher concentration was possibly related to a certain degree of viscous recovery as 7 and 8 %w/w of EC100 had been shown to be thixotropic (Section V-B3.1) and their high viscosities would attempt to hold the sessile drops in shape.

Besides the commonly cited reasons for drop recoil, one could argue that other phenomena related to trapped air and transient syneresis as possible cause for the slight recoil of high concentrations of EC100 samples. Although elucidating the main mechanism responsible for the observed drop recoil was not the focus of the current study, it was still worthwhile to consider other possibilities in order to pave the way for further investigations and understanding of gel spreadability. Upon contact of the sessile

drop with the substrate, a layer of air originally present on the substrate surface could be trapped beneath the highly viscous sessile drop due to incomplete air displacement and the slow escape of this layer of air later on resulted in drop recoil. However, there was also no observable bubble or air space beneath the drop during the dynamic contact angle measurement. In view of the very thin layer of adsorbed air on the substrate surface and the high mobility of air molecules, air displacement was assumed to be rapid and complete as is usually the case for wetting of smooth solid substrates. Furthermore, the highly smooth and flat surface of the silicone elastomer facilitated easy air displacement and avoided trapped air due to surface irregularities. On the other hand, the surfaces of drops produced from the syringe tip were observed to be even and free from any undulation that could create air pockets upon contact with the substrate. Also, contact with substrate began at the droplet tip and gradually increase in contact circumference, thus eliminating the likelihood of entrapping air.

As external pressure was known to be one of the factors causing gel syneresis (Tesch *et al.,* 1999), in the same manner, transient syneresis could be induced by the pressure exerted on the more viscous EC100 sample in order to produce a drop from the syringe tip. In this situation, continuous phase displacement could take place where small amount of solvent or solvent-rich fraction was expelled in the front of the drop followed by a more concentrated polymer-rich fraction. The solvent-rich fraction would exhibit a faster decrease in contact angle until it was reabsorbed into the bulk phase of the sample and re-equilibrated. Reabsorption of the continuous phase was expected to take a slightly longer time for more viscous samples and was manifested as drop recoil when it occurred. The dependence of rate of solvent reabsorption on EC sample viscosity was

implied from Section V-B6 which showed a decrease in rate of lipophilic solvent absorption into EC gel matrices of higher viscosities. However, contrasting evidence to the above supposition on transient syneresis and drop recoil was present from previous studies on methylcellulose, hydroxypropylmethylcellulose and chitin gels. These studies reported a reduced or absence of syneresis in gels prepared from higher concentrations of these polymers. Syneresis was suppressed by the increased viscosity and crosslinking density which rendered in more rigid gel network with low polymeric chain mobility (Ford and Mitchell, 1995; Vachoud *et al.,* 2000; Gérentes *et al.,* 2002). Syneresis was also not observed for polymeric solutions where polymer concentrations were below those required for gel formation (Vachoud *et al.,* 2000; Gérentes *et al.,* 2002). On this basis, transient syneresis might not occur at all in the viscous EC100 samples as well as the other samples composed of lower EC concentrations that existed as polymeric solutions. Although the existence and the role of transient syneresis in drop recoil of EC samples was unclear and it was not easy to be demonstrated in the current study given the dynamics of the speed of measurement, such phenomenon would still remain as a possibility for very viscous samples subjected to extrusion and this could be an interesting subject which merits further exploration but beyond the scope of this study.

V-B7.3. Characterization of EC gel spreadability by dynamic contact angle measurement

EC gel compressibility has been regarded as a convenient measure of gel spreadability (Section V-B4). In order to verify the feasibility of employing dynamic contact angle as a means of determining EC gel spreading, a correlation study was carried out between the equilibrium contact angle and compressibility of semisolid EC gel. Dynamic contact angle measurements performed in this study employed low EC concentrations of 3 to 8 %w/w in order to facilitate sample extrusion through the narrow tip of the syringe to obtain reproducible sessile drops. Extrusion of samples with higher EC concentrations was not possible due to high consistencies of the semisolid gels.

The graphs of equilibrium contact angle versus EC concentration of EC7, EC10 and EC100 were extrapolated according to the linear regressions given on Table 18 in order to obtain contact angle values over the EC concentration ranges employed for the determination of gel compressibility, namely 11 to 16 %w/w for EC7 and EC10, and 7 to 12 %w/w for EC100. The compressibility values for EC gels at the given concentrations (Table 19) were adopted from the study on EC gel mechanical properties (Section V-B4). The extrapolated equilibrium contact angles for EC gels, θ_e, ranged from 57.3° to 70.8° for EC7 and EC10, and 76.9° to 108.7° for EC100 (Table 19). According to definition (Section V-B6.6), these θ_e values indicated partial wetting for all the EC gels on the substrate and could be interpreted as moderate spreadability. Spreadability of 10 to 12 %w/w EC100 gels was regarded as relatively poor as θ_e values were above 90°. Their dense network structures imparted high viscosities and spreading was hindered due to more restricted rotational reorientation of polymeric moieties upon contact with the

Table 19: Compressibility values and extrapolated equilibrium contact angles, θ_e of EC gels.

EC (%w/w)	Compressibility [a] (N mm)	θ_e (°)
EC7		
11	3.1 ± 0.3	57.3
12	5.3 ± 0.5	59.7
13	17.4 ± 1.6	62.1
14	26.1 ± 2.2	64.4
15	31.2 ± 2.5	66.8
16	43.4 ± 2.1	69.2
EC10		
11	19.5 ± 1.5	58.4
12	22.7 ± 2.0	60.9
13	28.5 ± 2.6	63.4
14	33.0 ± 2.9	65.9
15	42.3 ± 1.9	68.4
16	76.7 ± 7.4	70.8
EC100		
7	4.8 ± 0.2	76.9
8	8.7 ± 0.8	83.3
9	17.1 ± 1.4	89.6
10	29.9 ± 3.8	96.0
11	49.9 ± 2.2	102.4
12	67.1 ± 6.6	108.7

[a] Data adopted from Table 10.

substrate.

Correlation between EC gel contact angle and compressibility was carried out by means of linear regression of θ_e:S ratio versus compressibility where S was defined as the slope values of the linear plots of logarithm of apparent viscosity versus EC concentration for EC7, EC10 and EC100 as shown in Table 18. The use of θ_e:S ratio to establish the linear correlation could be rationalized by the dependence of equilibrium contact angles of EC samples on viscosity as exhibited by Figure 43. It was shown that the relationship between θ_e:S ratio and compressibility for EC7, EC10 and EC100 could be described by a single linear regression with a correlation coefficient, r = 0.914 (Figure 44). The slope value of close to unity (0.988) showed that both θ_e:S ratio and compressibility was affected to the same extent by EC concentration. Hence, the positive linear relationship between θ_e:S ratio and compressibility of EC gels suggested the feasibility of adopting θ_e:S ratio as a parameter to predict gel spreadability.

The proposed linear relationship of θ_e:S ratio versus compressibility was validated by performing compression test on two additional samples of EC gels for each grade of EC at polymer concentrations of 12.5 and 17.0 %w/w for EC7 and EC10, and 8.5 and 14.0 %w/w for EC100. The detailed methodology for the compression test could be found in the mechanical characterization of EC gels described under Section IV-B2.7. In order to demonstrate the robustness of the proposed relationship, EC concentrations that were different from those used to obtain the compressibility data on Table 19 were employed for the validation. For each grade of EC, one concentration within the lower concentration range and another beyond the highest concentration of EC were selected (Table 20). The predicted compressibility values from the linear regression of θ_e:S ratio

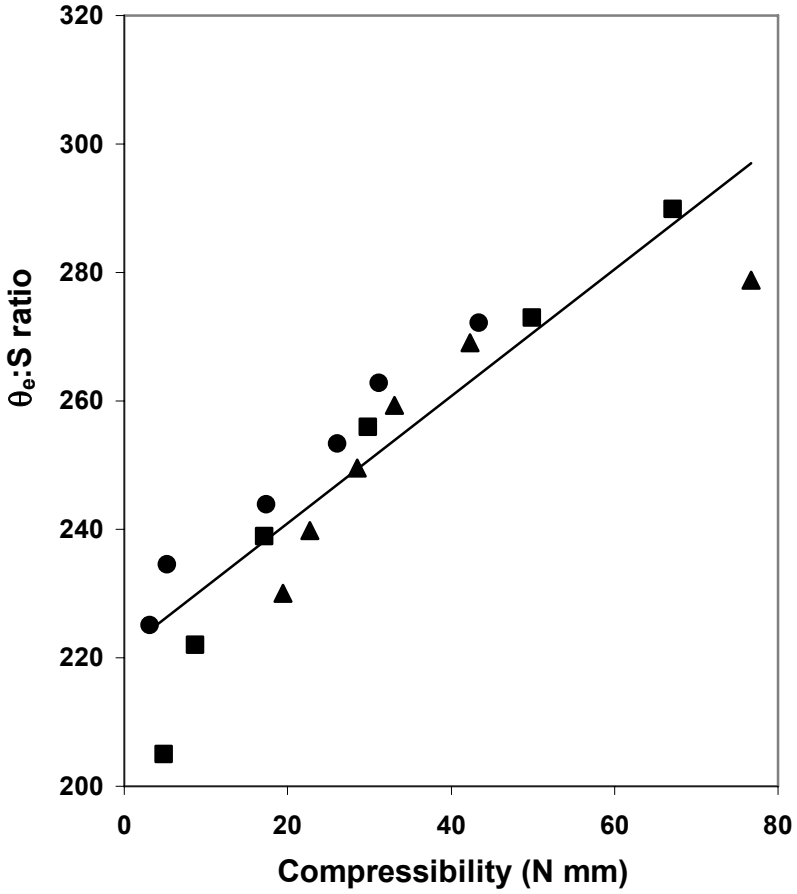

Figure 44: Linear regression (y = 0.988x + 221.2, r = 0.914) between θ_e:S ratio and compressibility of EC7 (●), EC10 (▲) and EC100 (■) gels where θ_e is defined as the extrapolated equilibrium contact angles for EC gels and S is defined as the slope values of the linear plots of logarithm of apparent viscosity versus EC concentration.

versus compressibility were compared with the measured compressibility values of EC gel samples used for validation. The percentage deviation was within the acceptable range (0.7 to 11.2 %), hence verifying the applicability of the proposed relationship to EC gels at concentrations beyond those being used to derive the relationship (Table 20). Thus, the usefulness of dynamic contact angle measurement as an alternative to compression test to measure EC gel spreadability was established in this study where higher θ_e:S ratio reflected lower spreadability. Equilibrium contact angle instead of base area was employed in the correlation with EC gel compressibility as contact angle in its equilibrium state was independent of variation in drop volume (Wu, 1982). Thus, it was deemed to be a more accurate and direct measurement as compared to base area. Since the silicone elastomer substrate was non-porous, the change in sessile drop contact angle parallelled the change in its base area, hence the area of spreading could be accurately represented by the contact angle.

Table 20: Comparison between gel compressibility values obtained from direct measurement and from the linear plot of θ_e:S ratio versus compressibility where θ_e is defined as the extrapolated equilibrium contact angles for EC gels and S is defined as the slope values of the linear plots of logarithm of apparent viscosity versus EC concentration.

	EC (%w/w)	θ_e (°)	Compressibility (N mm)		Deviation from measured compressibility (%)
			Predicted	Measured	
EC7	12.5	60.9	18.20	17.45	4.3
	17.0	71.6	61.07	54.91	11.2
EC10	12.5	62.2	23.69	26.32	10.0
	17.0	73.3	68.15	66.80	2.0
EC100	8.5	86.4	9.32	8.86	5.2
	14.0	119.8	99.34	100.08	0.7

It should be noted that there were several fundamental differences between compression test and dynamic contact angle applied as techniques for determining gel spreadability. Compression test measured the work required to deform a gel through a fixed displacement of the compression probe with a shear force applied on the gel to elicit the compressibility value. More viscous gels imparted higher resistance to the deformation force exerted by the probe and resulted in higher compressibility values. The higher compressibility results were correlated to lower spreadability. Apart from gel viscous property, compressibility value was also dependent on the rate of shear which in turn, was dependent on the probe speed. For dynamic contact angle measurement, the shearing force came from sample extrusion through the syringe tip but the contact angle values were not dependent on the shear applied. It was governed by sample properties such as viscosity, hydrophilic/lipophilic property as well as the compatibility between sample and substrate through the extent of attractive interactions. Dynamic contact angle was a more direct approach to determine spreadability. This method took into consideration the sample-substrate compatibility which was more directly relevant to the final application of the gel on its substrate. It also allowed visualization of the actual spreading process upon contact of the sample sessile drop with the substrate.

V-B8. *In vitro* release of MH from EC gel matrices

V-B8.1. Release kinetics

The release behavior of EC gel matrices were determined using gel samples containing 3 %w/w MH. The amount of MH released over time was markedly different among the different grades of EC, decreasing in the order of EC7 > EC10 > EC100 (Figure 45). The mechanism of MH release was best described by the Higuchi model (Higuchi, 1961) as indicated by the high coefficients of determination, r^2, from linear regression analyses, which ranged from 0.9760 to 0.9959 (Figure 46 and Table 21). The Higuchi model describes drug release from a non-erodible matrix containing the drug as dispersed phase of a viscous suspension. The linear cumulative MH release versus square root of time relationship implied a diffusion-controlled release of MH from EC gels. This suggested that the gel formulation was in control of the release process (Shah *et al.,* 2003). A negligible lag time as obtained by the small x-intercept value of the Higuchi's plot indicated an instantaneous MH release upon contact of the gel samples with receptor medium. It was most likely that drug particles were present on the gel surface. Two important requirements for an *in vitro* release study that had to be met for a valid Higuchi release model were the maintenance of sink condition and a cumulative percentage drug released less than 30 % of the amount of drug present in the donor compartment (Rapedius and Blanchard, 2001). These requirements were easily achieved for the manner of MH released from EC gels. Sink condition was facilitated by continuous stirring of the receptor medium. The requirement for cumulative drug release below 30 % was met by the modest proportion of MH released ranging from 3.2 to 16.6 % after 48 h (Table 22), indicating a sustained drug release behavior of EC gels.

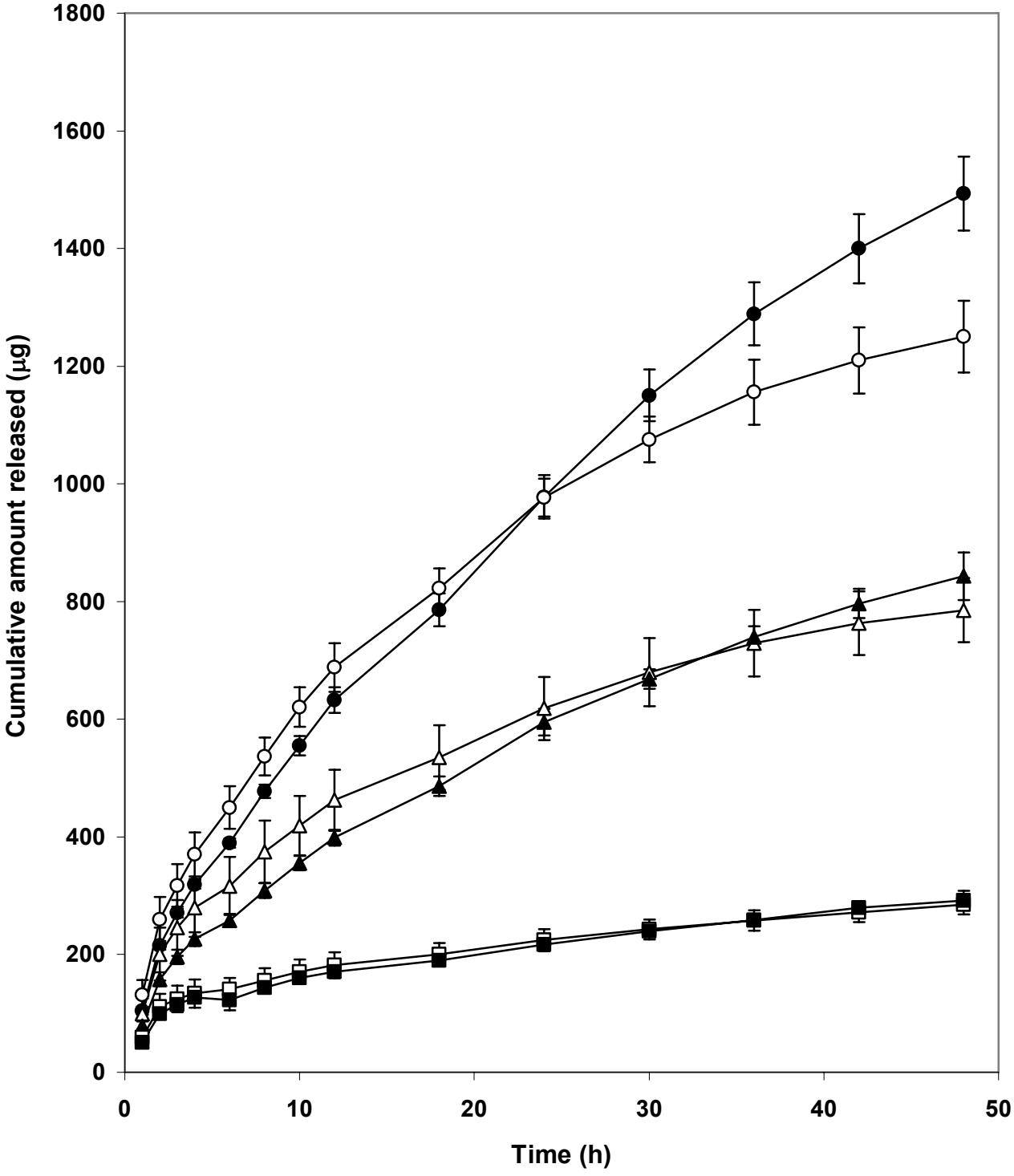

Figure 45: Cumulative amount of MH released over time from EC7 (11 %w/w, ○; 16 %w/w, ●), EC10 (11 %w/w, △; 16 %w/w, ▲) and EC100 (7 %w/w, □; 12 %w/w, ■) gels.

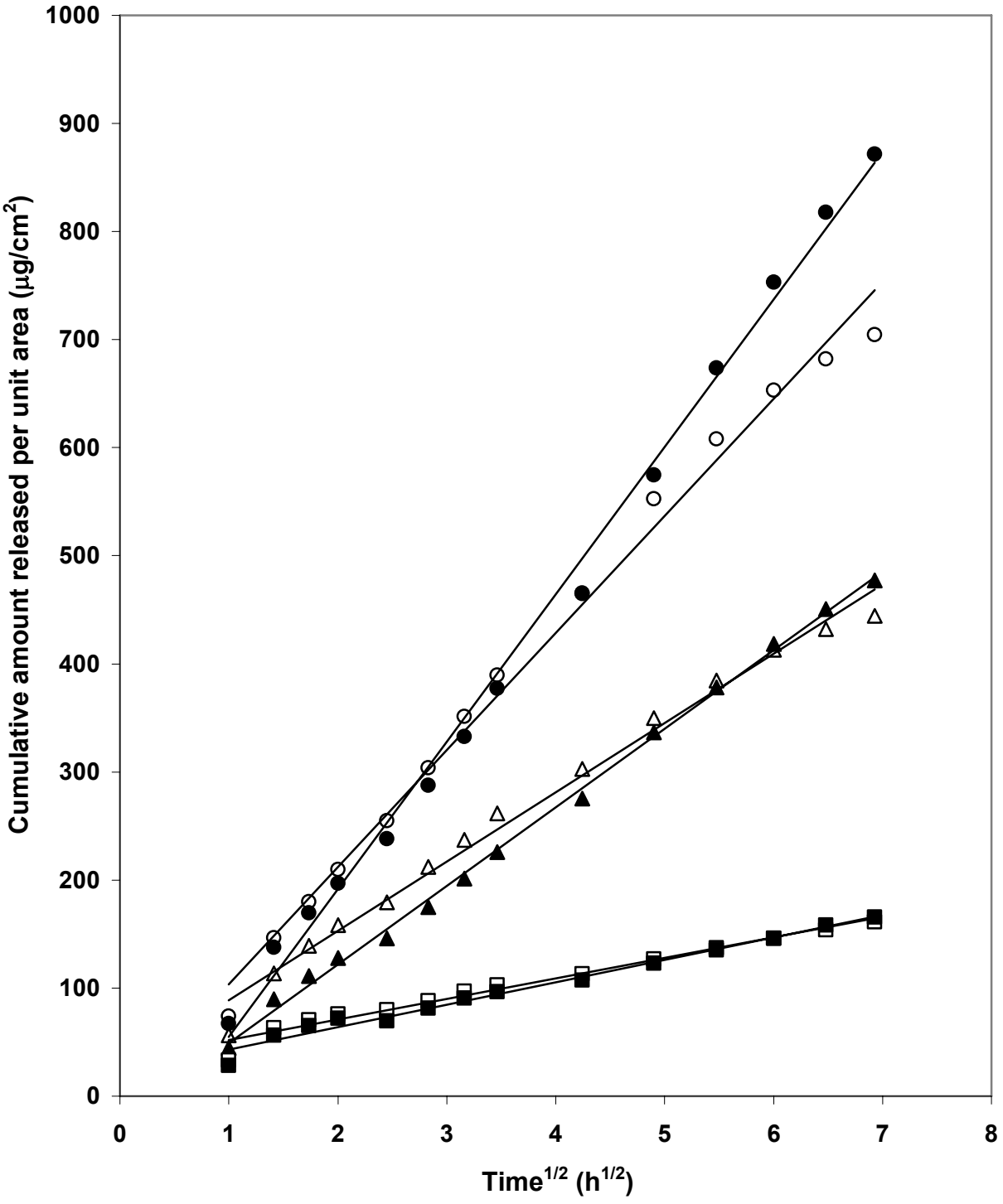

Figure 46: Higuchi's plots for MH release from EC7 (11 %w/w, ○; 16 %w/w, ●), EC10 (11 %w/w, △; 16 %w/w, ▲) and EC100 (7 %w/w, □; 12 %w/w, ■) gels. MH release rates are given by the slope of Higuchi's plots (Table 21).

Table 21: Kinetic parameters of MH release from EC gel matrices.

EC	Zero order equation		Higuchi equation	
(%w/w)	K_0	r^2	K_H	r^2
EC7				
11	0.2544 ± 0.0094	0.9272	108.36 ± 3.84	0.9920
16	0.3284 ± 0.0194	0.9787	136.41 ± 8.13	0.9959
EC10				
11	0.1486 ± 0.0029	0.9178	64.23 ± 1.88	0.9886
16	0.1747 ± 0.0107	0.9504	73.66 ± 4.06	0.9956
EC100				
7	0.0446 ± 0.0031	0.9071	19.04 ± 1.27	0.9760
12	0.0491 ± 0.0024	0.9351	20.73 ± 0.95	0.9822

Table 22: Cumulative amount and percentage of MH released at different time points [a].

Time (h)	**EC7** (% w/w)			
	11		16	
	Cumulative amount released (µg)	% release	Cumulative amount released (µg)	% release
1	131.1 ± 25.4	1.5	104.4 ± 6.6	1.2
4	370.4 ± 37.7	4.1	319.3 ± 7.1	3.5
8	537.0 ± 32.3	6.0	477.8 ± 11.2	5.3
12	687.9 ± 41.5	7.6	632.4 ± 21.7	7.0
24	976.5 ± 32.5	10.9	977.7 ± 37.1	10.9
48	1244.6 ± 52.3	13.8	1493.0 ± 62.7	16.6

.....continued from above.

Time (h)	**EC10** (% w/w)			
	11		16	
	Cumulative amount released (µg)	% release	Cumulative amount released (µg)	% release
1	99.2 ± 26.4	1.1	73.1 ± 8.8	0.8
4	279.6 ± 49.2	3.1	225.2 ± 13.2	2.5
8	374.6 ± 53.5	4.2	313.3 ± 13.5	3.5
12	462.5 ± 51.9	5.1	421.6 ± 26.8	4.7
24	618.2 ± 53.4	6.9	607.1 ± 23.0	6.7
48	785.1 ± 54.5	8.7	844.0 ± 54.4	9.4

.....continued from above.

Time (h)	**EC100** (% w/w)			
	7		12	
	Cumulative amount released (µg)	% release	Cumulative amount released (µg)	% release
1	59.3 ± 13.1	0.7	50.9 ± 6.3	0.6
4	133.9 ± 23.8	1.5	125.4 ± 12.0	1.4
8	155.7 ± 21.5	1.7	146.5 ± 12.1	1.6
12	181.8 ± 21.7	2.0	174.6 ± 13.8	1.9
24	224.5 ± 18.5	2.5	229.4 ± 18.9	2.5
48	284.6 ± 15.9	3.2	306.6 ± 34.3	3.4

[a] Total amount of MH present in 7 ml of receptor medium in the receptor compartment of the Franz diffusion cell.

V-B8.2. Influence of MH concentration

Preliminary release studies were conducted using MH concentrations of 0.05, 1, 3 and 5 %w/w dispersed in EC100 gels containing either 7 %w/w EC (n = 2) or 12 %w/w EC (n = 3) to determine a suitable MH concentration to be employed in the *in vitro* release study. EC100 were expected to demonstrate the lowest rate of drug release as it possessed the highest molecular weight among the three grades of EC. Thus, EC100 gels were employed in the preliminary release studies. MH release was found to be affected by the concentration of MH present in the EC gel matrices. Gels containing 0.05 and 1 %w/w MH failed to result in detectable level of MH in the receptor fluid even after 24 h. However, MH release from these gels could not be ruled out as it occurred at a much lower rate and extent but not detectable by the routine HPLC analysis. MH release was detectable after the first hour for gels containing 3 or 5 %w/w MH. For gels containing 5 %w/w MH, $K_H = 55.44 \pm 1.10$ μg/cm^2/h$^{1/2}$ ($r^2 = 0.9051$) for 7 %w/w EC100 gel and $K_H = 55.35 \pm 7.07$ μg/cm^2/h$^{1/2}$ ($r^2 = 0.9726$) for 12 %w/w EC100 gel. The 5 %w/w MH gels demonstrated higher rates (Higuchi model) and amounts of MH released than 3 %w/w MH gels throughout the 48 h run period (Table 23). Similar to EC100 gels containing 3 %w/w MH, release rates of EC100 gels containing 5 %w/w MH were also independent of EC concentrations. It could be inferred from this preliminary study that although amounts and rates of MH release were dependent on MH concentration, influence of EC concentrations on MH release behavior remained the same regardless of MH concentration present in the EC gel matrices. The minimum inhibitory concentration (MIC) of MH for bacterial infections ranged from < 4 to 16 μg/ml (Micromedex Healthcare Series). The cumulative amount of MH released from EC gels into the 7 ml

Table 23: Cumulative amount and percentage of MH released at different time points from EC100 gels containing 5 %w/w MH [a].

Time (h)	**EC100** (% w/w)			
	7		12	
	Cumulative amount released (μg)	% release	Cumulative amount released (μg)	% release
2	220.21 ± 76.15	1.5	85.48 ± 27.45	0.6
4	391.30 ± 138.12	2.6	206.92 ± 36.62	1.4
8	539.98 ± 138.55	3.6	312.53 ± 36.74	2.1
12	634.86 ± 140.19	4.2	400.52 ± 40.44	2.7
24	716.04 ± 133.66	4.8	492.74 ± 36.90	3.3
48	848.84 ± 130.90	5.7	671.90 ± 52.10	4.5

[a] Total amount of MH present in 7 ml of receptor medium in the receptor compartment of the Franz diffusion cell.

receptor compartment of the Franz diffusion cell after 4 h was at least 125 μg which corresponded to a MH concentration of 18 μg/ml (Table 22). Since the level of MH that was released from EC gels containing 3 %w/w MH was higher than the reported MIC for bacterial infections, 3 %w/w MH gel was deemed to be adequate for clinical use. Thus, this MH concentration was employed in the *in vitro* release study for the EC gels studied.

V-B8.3. Influence of EC grade and concentration

The MH release rate or steady-state flux as given by the slope of Higuchi's plot decreased in the order of EC7 > EC10 > EC100, indicating that EC gels with longer polymeric chains resulted in a slower MH release. However, despite the well known effect that high polymer concentration slowed drug release from polymeric gel matrices by increased viscosity or network tortuosity (Lee *et al.,* 1995; Jones *et al.,* 1996a and 2000; Mitchell *et al.,* 1993), significantly higher release rates ($p < 0.05$) were observed in EC7 and EC10 containing 16 %w/w EC as compared to a lower 11 %w/w EC concentration. Statistically similar release rates were obtained for EC100 gels with 7 and

12 %w/w polymer in the preliminary studies. These findings indicated that EC gel viscosity itself was not the dominant determinant for MH release. The order of release rates (EC7 > EC10 > EC100) appeared to be in agreement with the general trend of EC gel rheological parameters where EC7 < EC10 < EC100, hence it could be argued that rheological parameters were important. Nevertheless, a closer examination of the rheological parameters of the EC gels in Table 8 revealed that no consistent trend could be observed between rheological parameters and MH release rates. For example, the apparent viscosities of 12 %w/w EC100 (60600 mPa·s) and 16 %w/w EC10 gels (60616 mPa·s) were comparable. However, the rate and amount of MH released from 12 %w/w EC100 gel was much lower than those of 16 %w/w EC10 gel (Tables 21 and 22). The apparent viscosity of 7 %w/w EC100 gel was the lowest among the EC gels employed in the release study but EC100 gels produced the slowest MH release. These examples provided strong evidence that gel rheology per se was not the dominant property of EC gels affecting drug release.

V-B8.4. Influence of moisture uptake

The ability of MH to be released despite its negligible solubility in the non-aqueous gel vehicle was intriguing. This suggested a mechanism whereby drug molecules were mainly released by dissolving in moisture present within the non-aqueous gel matrix through water absorption upon exposure of the gel to the receptor medium employed in the release study. EC matrix hydration had also been cited as the basis for dissolution and subsequent release of theophylline from EC matrix tablets (Chambin *et al.,* 2004). The ability of the non-aqueous gel EC matrix to imbibe water in spite of its lipophilicity had

been demonstrated in the earlier studies on water wetting behaviors of EC gels (Section V-B6). Differences in the water absorption behavior of the EC gel matrices employed for the release study were also identified as the important phenomenon responsible for the observed release profiles of MH from EC gel matrices. For verification of such proposition, a moisture uptake experiment was performed to assess the ability of the non-aqueous EC gel matrices to absorb water. All the gel matrices tested were shown to absorb limited amount of moisture over time with a total moisture uptake of less than 1 % of sample weight after 10 days (Table 24 and Figure 47). The extent and rate of water uptake for gels used in release study were expected to be much higher due to direct contact with the aqueous environment of the receptor medium. However, moisture uptake study was conducted at only 75 % relative humidity in an environmental chamber but in not under 100 % aqueous environment owing to the technical difficulty and possible errors associated with weight determination of the wetted gel matrices, particularly for gels of lower consistencies. These gels possessed higher flowability and could not maintain a well defined shape to facilitate measurement. Furthermore, the use of relative humidity beyond 80 % in the environmental chamber resulted in variable degree of condensation that could compromise experimental accuracy. The rate of moisture uptake in the environmental chamber was much lower since water was only available as vapors, hence an extended duration of the experiment was employed in the moisture uptake study. Although the absolute amount of moisture absorbed by EC gel matrices in the environmental chamber could be very different from that of the *in vitro* release study, the relative trends of moisture uptake observed from the moisture uptake studies would still provide invaluable clue for explaining the release behavior of MH from EC gel matrices.

Table 24: Moisture uptake by EC gel matrices over time.

Time (h)	Moisture uptake (%) by EC gel matrices of different polymer concentrations					
	EC7		EC10		EC100	
	11 %w/w	16 %w/w	11 %w/w	16 %w/w	7 %w/w	12 %w/w
4	0.348 ± 0.022	0.408 ± 0.018	0.308 ± 0.014	0.394 ± 0.029	0.310 ± 0.021	0.291 ± 0.020
8	0.408 ± 0.019	0.497 ± 0.025	0.374 ± 0.009	0.458 ± 0.022	0.405 ± 0.018	0.395 ± 0.021
24	0.537 ± 0.037	0.610 ± 0.035	0.486 ± 0.014	0.576 ± 0.013	0.562 ± 0.027	0.549 ± 0.020
48	0.585 ± 0.017	0.686 ± 0.024	0.552 ± 0.024	0.654 ± 0.014	0.664 ± 0.021	0.638 ± 0.024
96	0.691 ± 0.031	0.796 ± 0.034	0.648 ± 0.032	0.748 ± 0.019	0.776 ± 0.037	0.734 ± 0.039
240	0.804 ± 0.009	0.937 ± 0.004	0.752 ± 0.016	0.905 ± 0.055	0.883 ± 0.071	0.817 ± 0.063

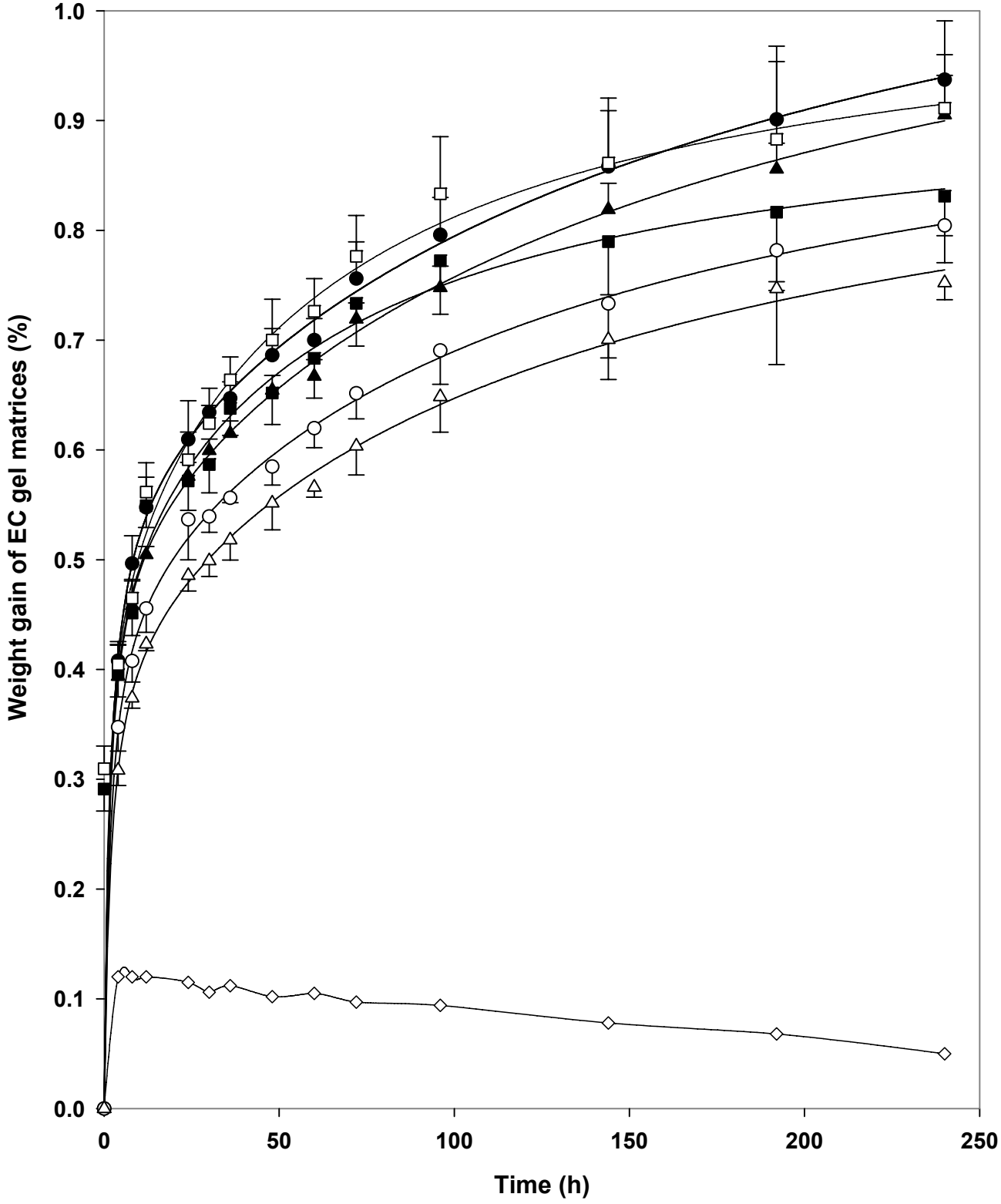

Figure 47: Water uptake of Miglyol 840 (◇), and EC7 (11 %w/w, ○; 16 %w/w, ●), EC10 (11 %w/w, △; 16 %w/w, ▲) and EC100 (7 %w/w, □; 12 %w/w, ■) gel matrices as given by percentage weight gain over time.

Water of hydration in polymers has been widely classified into three types: I. free or unbound water, also known as freezing water, II. loosely bound freezing water, and III. non-freezing bound water. The thermal properties and the significance of these different types of water in hydrated polymer powders as well as in gel matrices had been detailed elsewhere (McCrystal *et al.,* 1999; Ford and Mitchell, 1995; Joshi and Wilson, 1993; Zografi, and Kontny, 1986; Agrawal *et al.,* 2003b). Hydrated EC was largely associated with types I and III water (Joshi and Wilson, 1993; Agrawal *et al.,* 2003b). Moisture uptake into the non-aqueous EC gel matrices was caused by the propensity of water molecules to interact with the hydrophilic –OH groups on the EC backbone by hydrogen bonds (Joshi and Wilson, 1993; Agrawal *et al.,* 2003b), in particular, with the unethoxylated C_6 –OH groups which were cited as the sites of hydration (Zografi and Kontny, 1986). Increased exposure of EC to aqueous environment increased the availability of primary water binding sites on the EC backbones and these allowed binding for larger number of water molecules to the detriment of intermolecular hydrogen bonds between the EC polymer chains. Further binding of water molecules to other water molecules bound to the primary sites in turn led to the consequential increase in free water content within the gel matrices (Zografi and Kontny, 1986; Agrawal *et al.,* 2003b).

The observed moisture uptake by EC gel matrices could be attributed almost entirely to EC polymer instead of Miglyol as indicated by the negligibly low moisture uptake over time for Miglyol (Figure 47). For EC7 and EC10, the increase in moisture uptake with an increased EC concentration from 11 to 16 %w/w (Figure 47) was a result of an increased number of –OH groups when higher amount of EC was present in the gel matrices. Concentration and molecular weight dependent increase in gel matrix hydration

had been commonly observed for EC polymers and other cellulose-based polymeric gels as thermal analysis revealed higher proportions of bound water that directly interacted with the polymeric chains (McCrystal *et al.,* 1999; Ford and Mitchell, 1995; Agrawal *et al.,* 2003b). Statistically significant difference in moisture uptake was not observed between EC7 and EC10 containing the same EC concentration probably due to the relatively small differences in their molecular weights, hence the proportion of –OH groups did not differ greatly enough to cause an observable difference with regard to moisture uptake. This observation was in parallel to the wetting behavior of EC gels where significant difference in wettability between EC7 and EC10 was not demonstrated (Section V-B6). It should be noted that the moisture uptake profile for EC100 was not directly comparable to EC7 and EC10 due to the different amount or weight of EC present in the EC100 gel matrices and the relatively higher molecular weight of EC100. Unlike EC7 and EC10, statistical significance in moisture uptake was not seen for EC100 gel matrices with low and high EC concentrations despite the higher –OH content in the latter. This could be explained by considering the polymeric mesh size and network rigidity of EC100 gel matrices as reflected by the gel density and elastic modulus, respectively (Section V-B6.6.3). EC gel containing 12 %w/w EC100 possessed exceptionally high density (Figure 36) which had resulted in considerable reduction in polymeric mesh size. Its remarkably high elastic modulus (Section V-B3.2) and degree of gel structuring (s = 0.268) imparted a considerable degree of rigidity to the gel network. These factors in turn gave rise to a certain extent of impediment to molecular diffusion for water molecules in the gel matrix, thus accounting for the consequential decrease in moisture uptake. On the contrary, the diffusion of water molecules into 7 %w/w EC100

was possibly less impeded owing to its larger polymeric mesh size as indicated by the lower gel density and low network rigidity as shown by the low elastic modulus and degree of gel structuring (s = 0.320). Difference in matrix porosity was believed to affect water uptake and the subsequent drug release profiles of poly (L-Lactic acid) matrices (Miyajima *et al.,* 1997). This observation could further substantiate the influence of polymeric mesh size proposed to explain the moisture uptake behavior of EC100 gel on the basis that gel network porosity was reflected by its polymeric mesh size (Lowman and Peppas, 2000; Baumgartner *et al.,* 2002; Gemeinhart and Guo, 2004). For 12 %w/w EC100 gel matrices, the opposing effects of the abovementioned factors that hindered water absorption/diffusion had compromised its presumably higher affinity for moisture in view of the abundance of –OH groups, proportionally-wise, and would have favored higher moisture absorption as compared to 7 %w/w EC100. These opposing effects had resulted in similar extent of moisture uptake for EC100 gels despite the use of different EC concentrations. Unlike EC100, polymeric mesh size did not exert such a pronounced effect on the moisture absorption ability for EC7 and EC10 gels since the increases in density from the low to the high EC concentration for EC7 (4.9 %) and EC10 (5.7 %) gel matrices were relatively lower than that of EC100 (11.3 %). The relatively less drastic increase in network rigidity was reflected by the lower change in elastic modulus from the lowest to the highest EC concentration for EC7 (273 %) and EC10 (300 %), as opposed to the much greater change for EC100 (3671 %). This accounted for the lower dominance of network rigidity on moisture uptake in EC7 and EC10. Therefore, –OH content was more important than polymeric mesh size and network rigidity in dictating the moisture uptake capacities of EC7 or EC10 gels.

The observed release profiles of MH from EC gel matrices were related to their moisture uptake behaviors. The increase in moisture uptake capacity for EC7 and EC10 gels containing higher EC concentration (16 %w/w) implied an enhanced hydration of EC gel matrices by the receptor solution during the release study. The presence of higher moisture content would in turn facilitate dissolution of a higher amount of the MH particles dispersed within the non-aqueous gel matrix. This resulted in greater availability of the drug to diffuse out from the gel matrix, thus producing an increased MH release rate. Diffusion of solute molecules through bound water within starch-based matrices had been observed (Zografi and Kontny, 1986), hence suggesting the feasibility of MH molecule diffusion and release by means of EC gel hydration. The statistically similar release rates of the low and high concentrations of EC100 gels were due to similar degrees of moisture uptake by these gel matrices. Consequently, the amount of MH dissolved and became available in the molecular form which were diffusible through the gel matrices would essentially be similar. Thus, the increase in release rate with an increase in EC concentration in EC7 and EC10, as well as the similar release rate observed with different EC100 concentrations could be accounted by their hydration behavior. The difference in the rheological behaviors of EC7 and EC10 gels containing different EC concentration appeared to be less important as compared to the moisture uptake capacity in affecting MH release from these gel matrices.

V-B8.4.1. Moisture uptake from environmental chamber versus wetting by sessile water drop

Apparent discrepancy was observed between the moisture uptake behavior of EC gels in the environmental chamber and the wetting behavior of the EC gels obtained from sessile water drops in that the moisture uptake in the environmental chamber increased but water wettability by sessile water drops decreased in gels containing higher EC concentrations. Such discrepancy could be explained by considering that the amounts of water available and the time durations for both the water uptake studies were greatly different. For moisture absorption in the environmental chamber, there was continuous supply of water vapors for an extended period of time (10 days). Long exposure times allowed diffusion of water molecules into the interior of the gel matrices. This facilitated hydration and binding of water molecules to the hydrophilic –OH groups of EC via hydrogen bond for attaining homogeneous distribution of water molecules within the gel matrices. Although increased EC concentration rendered higher gel surface lipophilicity as evident by the dynamic contact angle measurements, sufficient exposure time for gels to absorb water vapor allowed gradual equilibration of water-gel system which eventually resulted in higher amount of moisture uptake by gels with EC higher concentration. Besides, storage of EC gel in high humidity environment resulted in less lipophilic gel surfaces due to the reorientation of polymeric moieties on gel surfaces to repel hydrophobic ethyl groups on the EC backbones and encouraged the exposure of the hydrophilic –OH groups towards the gel-air interface. The moisture uptake study related more closely to the actual release study environment as both of these studies had in common two important criteria, namely the unlimited availability of moisture supply and

long exposure time to water. Therefore, MH release behavior was better explained by correlating it to the moisture uptake behavior from the environmental chamber.

In the study of EC gel wetting behavior using dynamic contact angle of sessile water drops, the gel matrices were exposed to only small amount of water (approximately 8 μL) over a limited period of time (not more than 4 mins). This experimental setup was more appropriate to reflect surface phenomena occurring on EC gel matrices upon exposure to water. Thus, the data obtained was more useful for the prediction of bioadhesion to skin or mucous membrane as this process usually began immediately upon contact of the gel with its substrate (short time exposure) and involved very limited amount of water.

V-B8.5. Polymer-drug interaction and polymer chain coiling

Although gel matrix hydration was able to account for the observed release rate for different EC concentrations within the same grade of EC, this factor alone was not sufficient to explain the trend for release rates from gels containing different grades or polymeric chain lengths of EC. As mentioned previously, the release rates decreased in the following order: EC7 > EC10 > EC100. The MH release rates of EC7 gels were much higher than those of EC10 gels but the amounts of moisture absorbed over time by these gel matrices at each EC concentration were not significantly different. As for EC100 gels, the levels of moisture uptake were considerably higher but MH release rates were among the lowest of the three grades of EC gels. This finding indicated that MH release from EC gels was not as straightforward as expected and was dependent on the interplay among several counteracting factors.

Polymer-drug interactions as well as polymer chain coiling were commonly observed in polymeric matrices and these phenomena were likely to play a role in governing MH release from EC gels. The chemical properties of MH were important and needed to be understood for their basis of interaction with EC. MH (Figure 48) possesses a linear fused tetracyclic nucleus with multiple ionizable functional groups which are described by four pK_a values, namely 3.2, 7.8, 9.3 and 5.1 for the tricarbonyl system on the A ring, the phenolic β-diketone system, the quarternary proton of the 4-dimethylamino group and the quarternary proton of the 7-dimethylamino group (Nilges *et al.,* 1991; Pinsuwan *et al.,* 1999). In some reports, pK_a values ranging from 10.7 to 12.0 were assigned to the phenolic group in ring D for the tetracyclines (Tavares and McGuffin, 1994; Chen and Lin, 1998). As the release study was performed at pH 5.5, the tricarbonyl system (pK_a = 3.2) would be deprotonated and assumed a negative charge while 4-dimethylamino group (pK_a = 9.3) remained protonated, thus imparting a positive charge. The phenolic group in ring D would be unionized due to its protonated state at

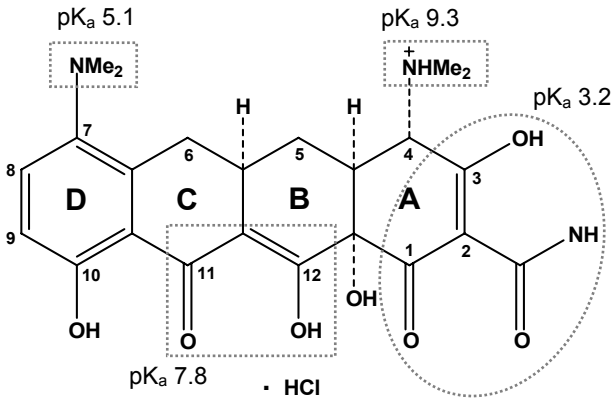

Figure 48: Molecular structure of MH.

this pH. Approximately 25 % of MH molecules within the gel matrices had their 7-dimethylamino group protonated, hence imparting a net positive charge (cationic) to MH. The remaining 75 % of MH existed as zwitterions due to the negative and positive charges imparted by the tricarbonyl system and the 4-dimethylamino group, respectively. The percentage of MH ionization was calculated based on the Henderson-Hasselbach equation for a weak base in a solvent at pH 5.5 as follows (Kim, 2004):

$$[\text{unionized}] / [\text{ionized}] = 10^{(\text{pH-pKa})} \qquad \text{(Equation 25)}$$

The isoelectric point reported for tetracycline hydrochloride was 5.6 (Dietz, 1989) and the isoelectric point of MH would likely to be close to this value since it was structurally very similar to tetracycline hydrochloride. Thus, it was most reasonable to have the majority proportion of MH as neutral zwitterions at pH 5.5 as this pH was very close to the isoelectric point. Since EC gels were hydrated by the receptor fluid at pH 5.5, the MH dissolved within the gel matrices would follow the abovementioned degree of ionization. The individual non-ionized hydrophilic groups of MH such as the phenolic β-diketone system and part of the 7-dimethylamino group formed hydrogen bonds with the –OH groups on the EC backbones while the ionized groups interacted with EC by dipole-dipole interaction. Hydrophobic interactions also existed between ethyl substituents of EC and tetracyclic ring system of MH. Such interactions were possibly enhanced in the zwitterionic form of MH as it did not bear a net charge. Since the zwitterions formed a major proportion of MH within the EC gel matrix, the hydrophobic drug-polymer interaction would be substantial. Besides, MH itself was considered a relatively lipophilic drug due to its tetracyclic ring structure and it was reported to have enhanced lipophilicity compared to other tetracyclines (Nelis and De Leenheer, 1982). From the comparison of

partition coefficients which were cited as hydrophobic parameters for drug compounds (Chen and Lin, 1998), MH exhibited the highest lipophilicity among the commonly available tetracyclines (Table 25). Thus, hydrophobic interactions between MH and EC chains were also facilitated by the inherent lipophilicity of MH molecule.

Table 25: Octanol/water partition coefficient, $P_{o/w}$ of tetracycline antibiotics [a].

Drug	$P_{o/w}$
Minocycline	1.12, 1.4 [b]
Chlortetracycline	0.41
Doxycycline	0.95
Demeclocycline	0.25
Tetracycline	0.09
Oxytetracycline	0.08

[a] Adopted from Chen and Lin, 1998
[b] Adopted from Böcker *et al.,* 1991

Apart from drug-polymer interactions, another important factor to be considered in the attempt to explain the trend of MH release from EC gels was the polymeric chain coiling. The propensity of long chain polymers, especially uncharged polymeric chains, to form coiled conformation was well recognized (Meyer *et al.,* 1991; Sarkar and Somasundaran, 2004; Gosselet *et al.,* 1999). Increased degree of chain coiling of the higher molecular weight fractions of hydroxypropylcellulose was reported to affect the degree of indomethacin substitution on the polymeric backbones (Meyer *et al.,* 1991). The possibility of polymeric chain coiling in the EC gel matrices was further substantiated by the well known tendency of polymer chains to coil in the presence of a poor solvent (Romeu *et al.,* 1997; Madkour, 2001) and the random coil conformation explanation had been used to describe EC chains in films casted from a relatively poor

solvent of EC (Rosilio *et al.,* 1998). Hydration of EC gel matrix set up a relatively more hydrophilic environment for the EC polymeric chains from the purely lipophilic base provided by the oily solvent, Miglyol. More hydrophilic conditions were certainly less favorable for EC molecules which were inherently not water soluble due to the presence of hydrophobic ethyl substituents on the EC backbones. This rendered in the formation of coiled conformation of the EC chains with the hydrophobic segments forming the interior of the coil conformers. Water of hydration was known to have plasticizing effect to the EC polymeric systems (Lippold *et al.,* 1989). Moreover, the ability of EC-bound water molecules to disrupt hydrogen bonding between polymer chains was intensified with exposure to higher water content in the gel matrices (Agrawal *et al.,* 2003b). These phenomena imparted greater degree of flexibility to the EC polymeric chains, thus further facilitating chain coiling. The progressive coiling of EC chains as induced by an increased amount of water absorbed by the gel matrix upon prolonged exposure to the receptor solution during the release study would trap MH molecules within the hydrophobic interior of the coils, in particular the major hydrophobic zwitterionic forms of MH. As an increase in polymer molecular weight was known to cause a higher extent of polymeric chain coiling, the extent of EC chain coiling would be expected to follow the order of EC100 > EC10 > EC7. EC100 was expected to exhibit more intense coiling than both EC7 and EC10 as its molecular weight was much higher, indicating the presence of much higher number of ethyl substituents in the longer polymeric chains of EC100, hence favoring a higher degree of coiling. EC polydispersity which followed the order of EC100 < EC10 < EC7 indicated the dominance of the long polymeric chain fraction in EC100, another factor facilitating chain coiling. On the contrary, the more

widely distributed EC7 would contain a high proportion of shorter polymeric chain fractions and substantial coiling was less likely. Diffusion of entrapped MH molecules through the coiled conformers within the gel matrices were more hindered, resulting in retarded release rate. Thus, the more coiled the polymeric chains, the more hindered was the diffusion and release of MH from EC gels.

In order to verify the proposed occurrence of EC chain coiling upon gel hydration, the apparent viscosities of 7 and 12 %w/w EC100 gel matrices incorporated with various amounts of water (1, 3, 5, 7 and 10 %w/w) was measured. EC100 gel was used for this study as it was deemed to possess the highest propensity for coiling. EC100 gels at the various hydration levels studied demonstrated significantly lower apparent viscosities ($p < 0.05$) than the non-hydrated gels (Figure 49). With the introduction of only 1 %w/w water into the EC100 gel matrices, a drastic drop of apparent viscosities to approximately half of those of the non-hydrated EC100 gels was observed. The uncoiling of polymeric chains in gel systems had been associated with an increase in apparent viscosity as more functional groups were exposed for interpolymeric chain interactions among the uncoiled polymeric chains resulting in a stronger gel network (Barry and Meyer, 1979b). Thus, the significant drop in EC gel viscosities observed upon gel hydration could be attributed to EC chain coiling since coiled polymers rendered less extensive interpolymeric chain interactions.

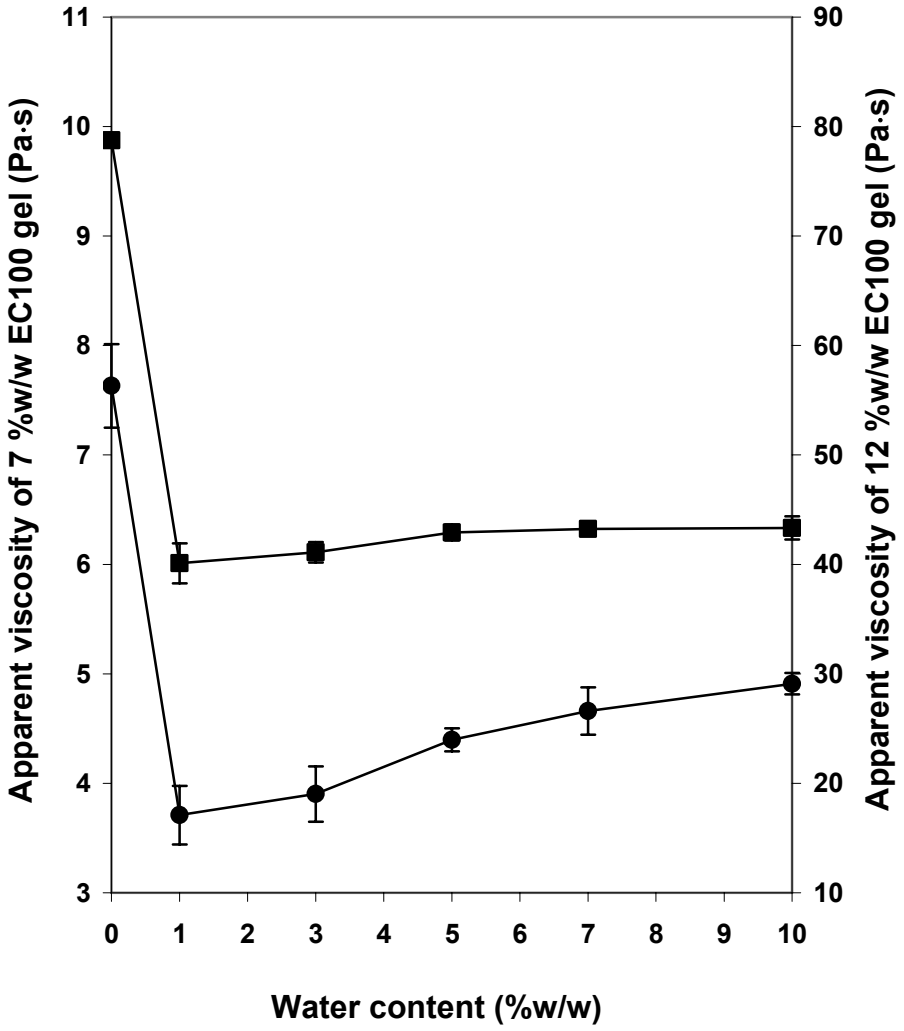

Figure 49: Apparent viscosity at a shear rate of 10 s^{-1} of 7 %w/w (●) and 12 %w/w (■) EC100 gel matrices at various hydration levels.

V-B8.6. Summary on *in vitro* release of MH from EC gel matrices

The *in vitro* release of MH from EC gel matrices was mainly governed by the interplay among several factors, identified as gel matrix hydration, drug-polymer interaction and polymeric chain coiling. Increased gel hydration in EC7 and EC10 gels containing high EC concentrations resulted in increased MH release rates from these gel matrices due to the availability of higher amounts of dissolved MH within the gel matrices for release. Hence, it followed that similar extents of hydration in both the low and high polymer concentrations in EC100 resulted in an insignificant difference in the release rates between the EC100 gel matrices. While the degree of gel hydration served as a satisfactory explanation for the observed release rates for gels containing low and high EC concentrations within the same grade of EC, additional factors involving MH-EC interactions and EC chain coiling had to be considered in order to account fully for the MH release rates among EC gels containing different grades of EC. The MH molecules were expected to interact with the –OH groups and ethyl substituents on the EC polymeric chains via hydrogen bonding and hydrophobic interactions, respectively. EC gel hydration over time led to the coiling of hydrophobic segments of EC chains. This had occurred in response to a relatively more hydrophilic gel continuous phase which was deemed to be less favorable for the polymer. MH zwitterions, forming the major proportion of the dissolved drug molecules within the gel matrix, would be trapped in the interior of the coiled polymers, hence drug diffusion was severely hindered. As the degree of polymeric chain coiling was known to increase with polymer molecular weight, the more extensive coiling of higher molecular weight EC resulted in a concomitant decrease in MH release rate when higher molecular weight EC was used to prepare the

EC matrix. In general, EC gel rheology was found to be a poor predictor of MH release probably due to gel network changes induced by prolonged periods of hydration during the release study. The roles of gel polymeric mesh size and rheological parameters such as elastic modulus on MH release were largely indirect as they only affected the extent of gel hydration and apparent effects of these factors were seen only in EC100 gels.

V-B8.7. Comparison of drug release performance of EC gels with other gel systems

Better appreciation of the relevance of the MH release data obtained from the present study could be made by comparing the drug release performance of EC gel with other reported gel systems employing either similar model drug (tetracycline antibiotics) or polymer matrices (EC). Although differences in the type of excipients, dosage forms, drug doses as well as experimental procedures would likely to invalidate such comparisons, it is still worthwhile to have a brief review on the drug release performance of related polymeric systems. The absolute amount of MH released from EC gel matrices after 48 h ranged from 285 to 1493 μg which corresponded to 3.2 to 16.6 % release from the original amount of MH present in the gel (3 %w/w or 9 mg). Elkayam *et al.* (1988) had reported minocycline release of approximately 35 to 75 % after 30 h from a sustained release EC polymer films with 30 %w/w drug content casted from different types of solvents. On the contrary, polymer films made of ethylene vinyl acetate (EVA) copolymer and 10 %w/w drug demonstrated much lower minocycline release (1 %) but minocycline release increased to 6.65 % when combined with another drug, nystatin in the film (Kalachandra *et al.,* 2002). However, tetracycline incorporated in the same system showed a release of up to 56 % (Kalachandra *et al.,* 2002), possibility owing to its

relatively more hydrophilic structure (Table 25). The studies reported by Shigeyama *et al.* (1999 and 2000) on formulation of MH into ointment bases for treatment of bedsore was probably the most relevant with respect to the current study. The highest release rate achieved for 1 % MH formulated in the hydrophilic ointment base with and without cyclodextrin additive was reported to be 10.16 and 9.92 $\mu g/ml/cm^2/h^{1/2}$, respectively. When the Franz diffusion cell volume of 7 ml was taken into consideration, release rates of MH from EC gels in the present study was estimated to range from 2.96 (12 %w/w EC100) to 19.49 (16 %w/w EC7) $\mu g/ml/cm^2/h^{1/2}$. Hence, the EC gels prepared seemed to be able to achieve higher rates of MH release but it should be noted that higher concentration of MH was employed. *In vivo* tetracycline release from a cellulose membrane impregnated with 400 μg of the drug was found to be the highest (54.5 %) after 1 day of peritoneal implantation in mice (Markman *et al.,* 1995). Cellulose-based hydrogel loaded with 5 %w/w tetracycline showed cumulative *in vitro* releases ranging from 20 to 100 % after 30 h or less (Jones *et al.,* 2000). The percentage of doxycycline prepared as saturated solutions in pure ethanol, 2:1 ethanol:Miglyol 840 mixture and 1:1 ethanol:Miglyol 840 mixture that had permeated through full thickness skin after 48 h was 0.07, 0.35 and 0.84 %, respectively (Perkins and Heard, 1999). The amount permeated from the heat-separated epidermal membrane was 10 fold higher. As for EC-based non-aqueous gels, Lee *et al.* (1995) reported theophylline permeation of 45 to 69 % through hairless mouse skin after 24 h from gels composed of ethanol, panasate 800 (tricaprylin), 3 to 10 %w/w EC and 0.2 to 1.0 % w/w drug with or without the presence of lauric acid enhancer. In another study (Contreras *et al.*, 1993) using ethanol-containing EC gels (15 or 20 %w/w EC) incorporated with 5 %w/w naproxen, the observed

naproxen release through a hydrophilic-lipophilic double layer synthetic membrane after 6 h ranged from 13 to 21 %. From the brief review above, it could be seen that most sustained release semisolid delivery systems containing tetracycline antibiotics demonstrated much higher percentage of drug released than the currently studied EC gels. This could be due to the lower MH load employed and the highly lipophilic continuous phase (Miglyol 840) of EC gels in the present study. The significant release retarding effect of Miglyol 840 was also seen in the liquid formulation of doxycycline, as reported by Perkins and Heard (1999). The use of ethanol in EC gels (Lee *et al.,* 1995; Contreras *et al.,* 1993) facilitated drug solubility in the continuous phase and served as one of the contributory factors that had resulted in higher drug release as compared to the currently studied EC gels where MH did not dissolve in the gelling solvent.

The non-aqueous EC gels successfully retarded and controlled the release of MH. This is important as the high dissolution rates of highly water soluble drugs in the aqueous media had posed a great challenge in their formulation into sustained release dosage forms.

V-B9. *In vitro* antibacterial efficacy of non-aqueous EC gel matrices containing MH

V-B9.1. Antibacterial activity

Figure 50 shows the zones of inhibition produced by EC gel samples and MH standard solutions against *S. aureus* and *P. acnes*. *P. acnes* demonstrated much higher sensitivity to MH than *S. aureus* in this study. In the antibacterial test against *S. aureus*, the gel used contained 1 %w/w MH and the bacterial load consisted of 10^6 cfu. To avoid excessively large zones of inhibition for *P. acnes*, the MH concentration used had to be

reduced by twenty fold to 0.05 %w/w and the bacterial load increased to 10^7 cfu. The absolute inhibition zones produced by the MH standard solutions and MH-loaded EC gels were observed to be larger for *P. acnes* than for *S. aureus* (Table 26). The absence of any observable zone of inhibition for the blank EC gel indicated that antibacterial activity was attributed solely to MH present in the EC gel matrices and the standard solutions (Figure 50).

Antibacterial activity of the gel containing MH was represented by $R_{g/s}$ value, defined as the ratio of the inhibition zone radius produced by the gel over that of MH standard solution. A high $R_{g/s}$ value indicated high bacterial growth inhibition. Significant polymer concentration-dependent trend was not shown in the $R_{g/s}$ values of EC7, EC10 and EC100 gels prepared from three different EC concentrations. Thus, a common $R_{g/s}$ value was derived for each grade of EC gel, namely EC7, EC10 and EC100 by averaging the $R_{g/s}$ values obtained from different EC concentrations (Table 27). This would simplify data interpretation and increase the power of statistical test due to increased sample size.

The $R_{g/s}$ values of the gels ranged from 0.75 to 0.78 against *S. aureus* and 0.62 to 0.80 against *P. acnes* and the order of antibacterial activity against the respective bacteria were EC7 = EC10 > EC100 and EC7 > EC10 > EC100. Lower antibacterial activity for the gel samples as compared to the MH standard solutions was expected due to the retarded release of MH from the gel matrices. The dependence of antibacterial activity on the grade of EC indicated that MH release and the ensuing bacterial growth inhibition were controlled by the ease of drug diffusion through the polymeric matrices.

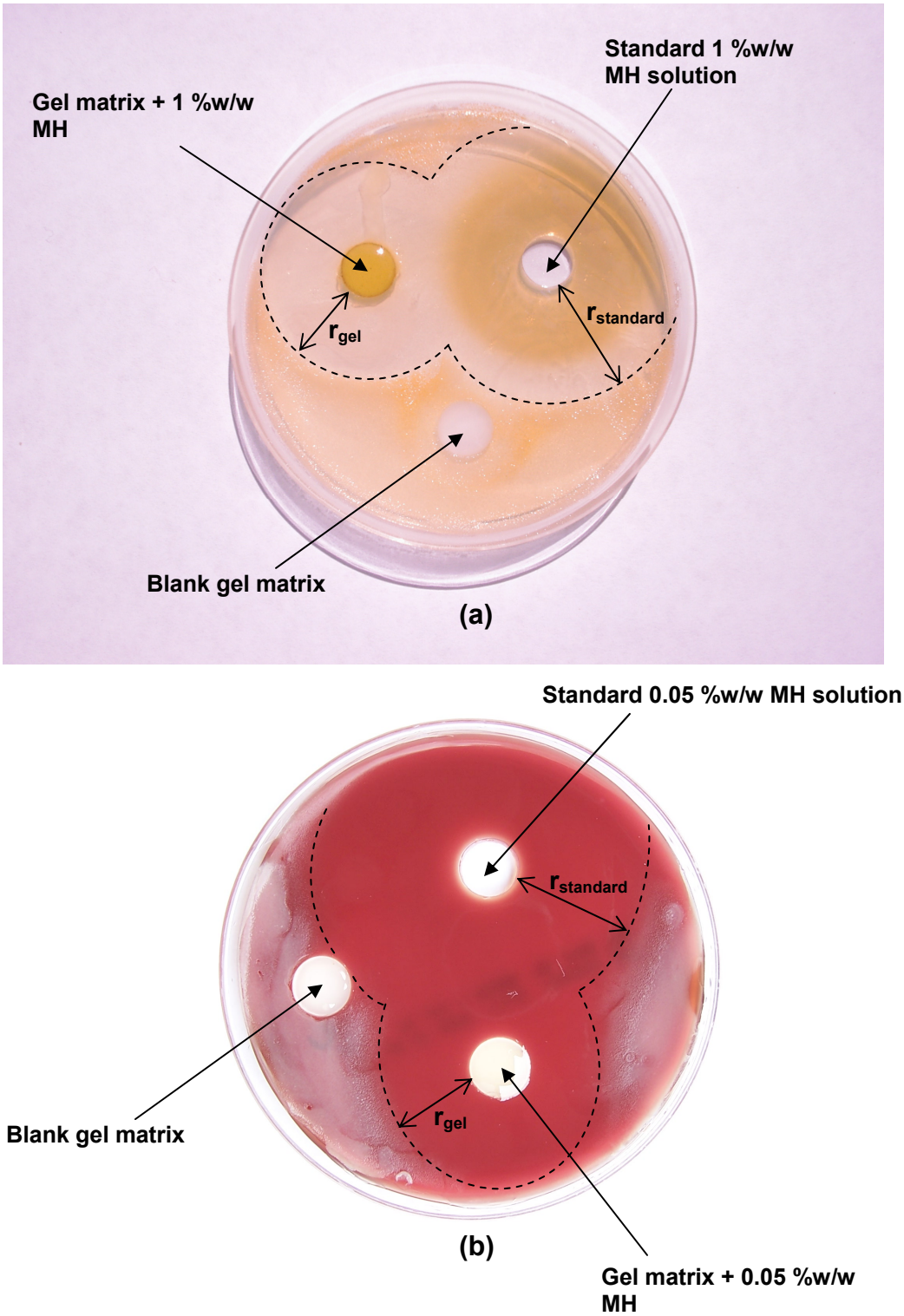

Figure 50: Growth inhibition of *S. aureus* (a) and *P. acnes* (b) by 11 %w/w EC100 gel samples. Broken lines outline zones of inhibition produced by EC gel and MH standard solution and the radius of the respective zone of inhibition is designated by r_{gel} and $r_{standard}$.

Table 26: Zones of inhibition for MH-loaded EC gels and MH standard solutions.

	Zone of inhibition (mm)			
	S. aureus		*P. acnes*	
	Gel with 1% w/w MH	Standard solution of 1% w/w MH	Gel with 0.05% w/w MH	Standard solution of 0.05% w/w MH
EC7	17.17 ± 1.63	22.02 ± 2.03	20.59 ± 2.36	25.98 ± 2.68
EC10	15.97 ± 1.41	20.52 ± 2.15	19.84 ± 2.22	27.12 ± 2.67
EC100	16.24 ± 1.24	21.47 ± 1.81	15.72 ± 1.98	24.75 ± 2.54

Table 27: The ratio of the radius of the zone of inhibition produced by MH-loaded EC gel over that of MH standard solution, $R_{g/s}$, for EC7, EC10 and EC100 gels.

EC (%w/w)	$R_{g/s}$	
	S. aureus	*P. acnes*
EC7		
11	0.769 ± 0.019	0.819 ± 0.045
13	0.794 ± 0.042	0.787 ± 0.061
16	0.776 ± 0.036	0.778 ± 0.036
Overall	0.780 ± 0.035	0.795 ± 0.051
EC10		
11	0.761 ± 0.036	0.735 ± 0.053
13	0.793 ± 0.032	0.711 ± 0.021
16	0.791 ± 0.026	0.730 ± 0.049
Overall	0.783 ± 0.034	0.725 ± 0.042
EC100		
7	0.733 ± 0.013	0.640 ± 0.047
9	0.745 ± 0.018	0.596 ± 0.026
11	0.758 ± 0.029	0.636 ± 0.039
Overall	0.748 ± 0.025	0.624 ± 0.041

V-B9.2. Relationship between antibacterial activity and *in vitro* drug release

The observed trends of antibacterial activity of EC gel samples could be attributed to MH release behavior from EC gel matrices and the inherent sensitivity of the bacteria to MH. In the antibacterial testing, the mechanism of MH release from EC gels into the agar medium was likely to be the same as that for the *in vitro* MH release in the Franz diffusion cell (Section V-B8). The prerequisite for MH release in these systems was gel hydration. Upon exposure to the agar medium, EC gel matrix was gradually hydrated by absorbing moisture from the water-rich agar medium which served as a water reservoir for gel hydration. Dissolution of the dispersed MH particles occurred in the hydrated gel matrix and this was followed by diffusion of MH molecules into the agar which functioned as an aqueous receptor compartment for MH. To verify this postulation, experiments were conducted to determine whether EC gel hydration occurred when the gels were placed into the wells of the agar medium. Pure methylene blue powder, employed as an indicator for moisture absorption, was incorporated into EC gel matrices as a dispersion (Section IV-B2.17). After 1 day of EC gel incubation, the methylene blue particles exhibited partial dissolution, producing a diffuse blue coloration in the gel and the surrounding agar medium (Figure 51). The partial dissolution and color change of the methylene blue particles from dark grey (original) to blue indicated the presence of water in the gel matrices. This verified the occurrence of gel hydration brought about by diffusion of water molecules from nutrient agar into EC gel matrices. The subsequent diffusion of the dissolved methylene blue from the gel matrices to the agar medium resulted in blue coloration in the surrounding agar medium. The area of blue coloration on the surrounding agar medium became larger with longer incubation time (up to 3

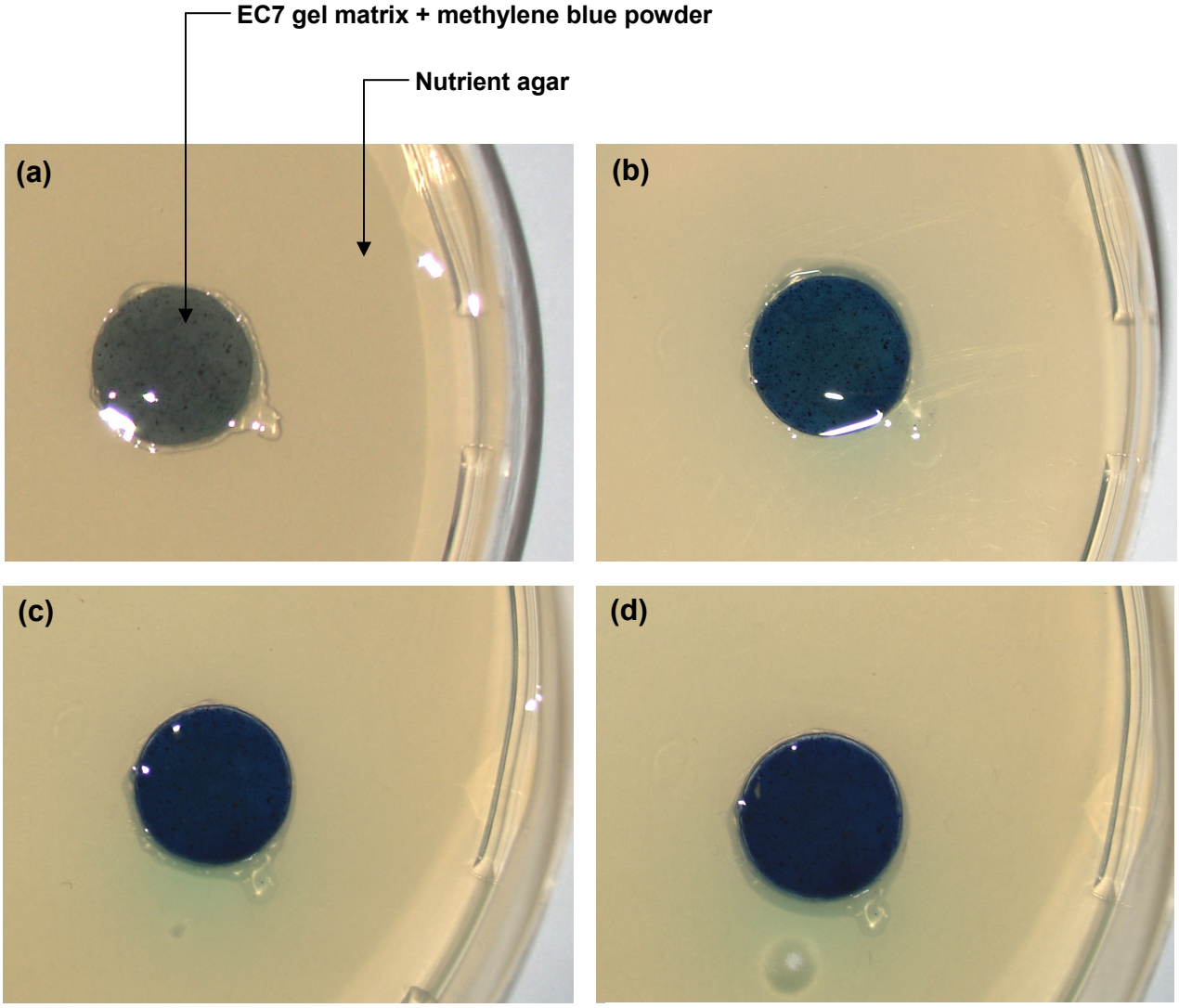

Figure 51: Enlarged images of 16 %w/w EC7 gel containing 0.5 %w/w methylene blue powder loaded in a 10 mm well of the nutrient agar. Before incubation, the gel appeared dark grey due to the presence of methylene blue powder (a). Gel hydration was indicated by a diffuse blue coloration in the gel and the surrounding agar medium after 1 day (b), 2 days (c) and 3 days (d) of incubation. The area of blue coloration on the surrounding agar medium increased from (b) to (d) indicating an increased extent of gel hydration with time.

days) indicating an increased extent of gel hydration with time, hence facilitating greater extent of methylene blue dissolution and diffusion. The likelihood of ambient moisture absorption in contributing to EC gel hydration was ruled out by the absence of any color change to the original EC gels containing methylene blue even after prolonged period of storage. Preliminary study also demonstrated that Miglyol did not diffuse into the agar medium as volume change of the pure Miglyol loaded in the agar wells was not observed even after 24 h incubation. This was in contrast to the complete absorption or removal of water from the agar wells in less than 2 h after loading. The inability of Miglyol to diffuse into the agar medium was not unexpected in view of the incompatibility of the lipophilic solvent with the aqueous-based agar medium. Hence, the possibility that MH release was mediated by solvent (Miglyol) diffusion from EC gel into the agar medium was ruled out.

The presence of significant bacterial growth inhibition indicated that the amount of MH released from these EC gels containing 0.05 and 1 %w/w MH was adequate for antibacterial activity. However, in the *in vitro* release studies, EC gels containing similar concentrations of MH failed to demonstrate any detectable level of MH in the HPLC analysis of the receptor fluid (Section V-B8.2). It is acknowledged that the use of different MH concentrations in the EC gel samples for the *in vitro* release study (3 %w/w MH) and the antibacterial testing (1 and 0.05 %w/w MH) was a limitation of this study. Standardization of MH concentration in the different types of experiments was not possible due to limitations imposed by the inherent bacterial sensitivity to MH and the analytical sensitivity of HPLC as detailed in Sections V-B9.1 and V-B8.2, respectively.

The amounts and rates of MH released were expected be to be lower in the antibacterial testing due to lower MH concentration used. An attempt was made to explain the antibacterial activity of EC gels containing MH using the MH release parameters determined in the *in vitro* release study on the assumption that relative trends of MH release from gel samples made from different EC grades and concentrations were similar regardless of MH concentration present in the gel matrices. This assumption was drawn from preliminary studies on the influence of MH concentrations on MH release from EC100 gels (Section V-B8.2). From Table 21, the change of MH release rate for gels from low to high EC concentration was 25.9 % for EC7, 14.7 % for EC10 and 8.9 % for EC100. The mean change of MH release rate for gels made from different EC grades was much higher, namely 43.4 % for EC7 to EC10, 71.1 % for EC10 to EC100, and 83.6 % for EC7 to EC100. The relatively lower release rate changes resulted in only small difference in the amounts of released MH between gels of low and high EC concentration at any particular time during the antibacterial testing, hence accounting for the lack of significant effect of EC concentrations on antibacterial activities. In contrast, pronounced effect of EC polymer grade on antibacterial activities against *P.acnes* (EC7 > EC10 > EC100) and *S. aureus* (EC7 = EC10 > EC100) was observed. This could be attributed to the larger difference in release rates of the different EC grades. However, similar antibacterial activity was exhibited by EC7 and EC10 gels against *S. aureus*. This indicated that the difference in MH release rate between EC7 and EC10 (43.5 %) was not sufficiently high to result in a significant difference in antibacterial activity due to the lower sensitivity of *S. aureus* towards MH. Owing to the much higher sensitivity of *P.*

acnes to MH, the differences in MH release rates among the EC gels made from different EC grades were fully reflected in the trends of antibacterial activity against *P. acnes*.

Since MH release from EC gels into the agar media followed the same mechanism as that described for the *in vitro* release study, factors governing MH release such as difference in degree of hydration, drug-polymer interaction and polymeric chain coiling, and the dependence of these factors on EC gel concentration and polymeric chain length would be expected to affect MH release in the same manner as described under Section V-B8 for the *in vitro* MH release in the Franz diffusion cell. Since EC gel rheological properties were not found to impart prominent influence on MH release, any difference in antibacterial activities among the EC gel samples could not be attributed to rheological properties of the gel matrices. The polymeric chain length (EC grade) dependence but concentration independence of antibacterial activity highlighted the lack of prominent influence of EC gel rheological properties on bacterial growth inhibition.

V-B9.3. Applicability of EC gels containing MH for topical antibacterial therapy

The use of *P. acnes* in the antibacterial testing could directly address the aim of this study to formulate a stable non-aqueous MH gel for topical treatment of acne vulgaris. While *P. acnes* is known to be the main causative agent of acne vulgaris, the coagulase-positive *S. aureus* is often implicated in a host of suppurative skin infections such as impetigo, furunculosis, cellulitis and ecthyma (Maisch *et al.,* 2004; Sasaki *et al.,* 2003). *S. aureus* was also reported as one of the predominant aerobic isolates from the pustular acne lesions of human subjects (Brook *et al.,* 1995). Thus, the use of *P. acnes* and *S. aureus* in the antibacterial testing for EC gels incorporated with MH would be

useful to verify the potential application of this gel in the topical therapy of acne vulgaris as well as other skin infections.

The three types of organisms that are predominantly present on the face and comedones were *P. acnes*, the coagulase-negative staphylococci, mainly *Staphylococcus epidermidis* and the lipophilic yeast of the genus *Pitysporum*. Among these organism, *P. acnes* was the only organism implicated in the pathogenesis of the inflammatory lesions of acne vulgaris due to its immunostimulatory property (Plewig and Kligman, 1993; Burkhart *et al.,* 1999; Jappe, 2003; Brook *et al.,* 1995). The inability of the aerobes (staphylococci and yeast) to reside in the anaerobic condition of the deeper infrainfundibulum of the pilosebaceous units led to the monopolistic presence of *P. acnes*. *P. acnes* is more accurately considered as a microaerophilic bacterium which grows best under strictly anaerobic conditions (Plewig and Kligman, 1993; Gribbon *et al.,* 1994). The number of viable *P. acnes* isolated from human skin varies from 10^2 to 10^6 cm^{-2} (Jones and Collins, 1986) and *P. acnes* count of up to 10^7 from a single pilosebaceous unit had been reported (Burkhart *et al.,* 1999). The formation of zones of inhibition on the surface inoculated agar indicated radial drug diffusion, hence the applied EC gel would not only exert antibacterial effect on the skin just beneath the site of application but also on its surrounding area (Lee *et al.,* 2003). The relative lipophilicity of MH molecules especially at the physiological pH would facilitate its diffusion through the lipophilic skin barrier (Nelis and De Leenheer, 1982; Lee *et al.,* 2003) and its ready penetration into the sebaceous follicles (Thiboutot, 2000). This would be followed by MH diffusion through the lipid bilayer of the bacterial cytoplasmic membrane to exert its antibacterial effect (Chopra and Roberts, 2001; Ito *et al.,* 2001). The minimum inhibitory

concentrations (MIC) of MH against *P. acnes* ranged from 0.125 to 0.2 μg/ml for sensitive strains and 2 to 4 μg/ml for more resistant strains (Gardner *et al.,* 1997; Kurokawa *et al.,* 1999; Ross *et al.,* 2001; Eady *et al.,* 1993). The MIC against *S. aureus* ranged from ≤ 0.25 to > 8 μg/ml (Bouchillon *et al.,* 2005). The amount of MH released from the EC gels within 4 h ranged from 125 to 370 μg which corresponded to MH concentration of 18 to 53 μg/ml in the receptor media (Table 22). This amount of MH released would most probably be sufficient to achieve MIC *in vivo* against both *P. acnes* and *S. aureus* after considering the additional diffusional resistance imparted by the skin barrier to the *in vivo* drug delivery. As the amount of MH released was shown to increase with time, higher amount of MH released could be achieved by allowing the gel to remain at its site of application for a longer duration during its use.

The ability of the EC gel samples containing low level of MH (0.05 %w/w) to exhibit satisfactory antibacterial activity against *P. acnes* clearly demonstrated the usefulness of EC gel as a delivery system. The lack of direct predictive role of EC gel rheology on *in vitro* MH release and antibacterial activity should not undermine the role of rheology in the overall effectiveness of the gel formulation. This is because modifying rheological properties had been shown to be valuable in controlling the gel wettability and spreadability. In turn, wettability and spreadability could affect the ease of gel application, bioadhesion and gel retention at the site of action.

It should be noted that the full potential and benefit of the prominently sustained release character of the EC gel matrices would not be realized in applications such as treatment of acne although *in vivo* antibacterial activity might be attainable. Acne skin conditions would plausibly require frequent gel application as gel removal from the skin

surfaces during routine washing and cleaning was inevitable. These activities would prevent gel retention on the skin for a time duration long enough to enable accumulation of high level of MH on the site of application. The non-aqueous EC gel would be more invaluable as a vehicle for treatment of conditions where the application site can remain undisturbed. An example of this potential use lies in the treatment of periodontitis where the gel is introduced into the periodontal pocket. An important criterion for such formulations is their ability to sustain drug release over a long period of time of 2 weeks or more (Elkayam *et al.,* 1988; Kalachandra *et al.,* 2002; Markman *et al.,* 1995) and this could be met by the non-aqueous EC gel.

VI. CONCLUSIONS

Two types of non-aqueous gels, one of hydrophilic nature and the other of lipophilic nature had been formulated and evaluated for their ability to form a structured gel and to stabilize a model moisture-sensitive drug, MH for topical drug delivery.

In the stability studies, the non-aqueous solvents and the formulated gels demonstrated different extent of MH stabilization as compared to the pure water system, indicating that a non-aqueous system would form a more appropriate gel vehicle than an aqueous system in providing stability to moisture-sensitive drugs. The type of solvents and cations additive used in the non-aqueous hydrophilic solvent systems was shown to have an influence on MH stability. The solvent system consisting of propylene glycol, glycerin and the stabilizing agent, magnesium chloride was found to offer relatively better stability profile for MH. Thus, this solvent system was employed in the formulation of the hydrophilic gel using PNVA, Gantrez S-97 or Plasdone S-630 as gelling agent. The non-aqueous lipophilic gel system was successfully formulated using the lipophilic solvent propylene glycol dicaprylate/dicaprate and three fine particle grades of ethylcellulose as gelling agents. This gel possessed the advantage of lower gelling temperature than a previously reported EC gel system. The non-aqueous lipophilic gel system was found to be superior to its hydrophilic counterparts in term of ability to stabilize moisture-sensitive drugs.

The physical properties of the non-aqueous gel matrices such as rheological and mechanical properties, wettability and spreadability were found to be affected by formulation variables such as the types of polymer, polymer concentration and polymeric chain length. Since these physical properties were concentration dependent, they could be

optimized by varying the polymer-solvent ratio in the gel matrix. The dynamic rheological properties of the hydrophilic gel matrices were dependent on the type and concentration of polymer as well as the propylene glycol-glycerin ratio. For the non-aqueous EC gels, EC chain length and concentration influenced the continuous shear properties, viscoelasticity and mechanical properties of the gels. The EC gels exhibited rheological profiles typical of physically crosslinked three dimensional gel network, as reflected by their predominant elastic behavior, presence of yield stress and thixotropy. The existence and stability of the three-dimensional solid-like gel structure were dependent on the balance between intermolecular hydrogen bonding between EC polymer chains, and dipole-dipole interactions between EC and solvent molecules. Molecular conformation of the solvent was shown to play a crucial role in determining the strength of such interactions. The hydrophilic gelling agents exhibited a narrow working range for gel formation. Besides, hydrophilic solvent systems were less effective in stabilizing MH as compared to the lipophilic solvent. Hence, hydrophilic gel system was not employed for subsequent evaluations.

The feasibility of employing dynamic contact angle combined with axisymmetric drop shape analysis-profile as an alternative method to investigate wettability and spreadability of non-aqueous gel matrices had been demonstrated. This method was deemed to be relevant for wettability measurement of topical gels as the gel substrate was used in its original semisolid forms and the small volume of liquid involved mimicked the relatively “dry” surfaces where the gel was applied such as skin and buccal mucosa. Gel spreading parameters obtained using this method were relevant to topical application as the effect of interaction between the sample and a substrate mimicking human skin, a

silicone elastomer was incorporated. The similarity of the silicone elastomer to human skin in term of hydrophilic/lipophilic property had been demonstrated in this study. EC gel matrices possessed both hydrophilic and lipophilic properties as shown by their water and IPM wettability. The lipophilic property was found to predominate in the EC gels. The applicability of equilibrium contact angle to quantify gel spreadability was verified through a linear correlation between θ_e:S ratio and EC gel compressibility, a parameter routinely used to characterize gel spreadability. EC gel wettability and spreadability were governed by a balance between gel chemical characteristics (hydrophilic/lipophilic properties) and physical characteristics (rheological and mechanical properties).

Performance characteristics of the EC gels had been evaluated in terms of MH stability, *in vitro* release and antibacterial efficacy. MH was shown to be chemically stable in EC gels over three months. The *in vitro* release of MH from EC gel matrices was diffusion-controlled and was modeled by the Higuchi kinetics. The amounts and rates of MH release were dependent on EC chain length and concentration. MH release was postulated to occur firstly by hydration followed by dissolution of the dispersed MH particles and then MH diffusion for its release. MH release was affected by the interplay among several mechanisms, namely gel matrix hydration, drug-polymer interaction and polymeric chain coiling. EC gels incorporated with MH exhibited potent antibacterial activities against *S. aureus* and *P. acnes*. Antibacterial activities were independent of EC concentration but dependent on EC chain length. Gel hydration via water absorption from the agar medium formed the prerequisite for MH release and the resulting antibacterial activities. Thus, antibacterial activities were influenced by factors governing *in vitro* MH release. Besides, the inherent sensitivity of the bacteria to MH was also a highly

influential factor on antibacterial activities. In contrast to the common conjecture for drug release phenomena from many gel systems, rheological properties was shown to be a poor predictor for MH release and antibacterial activities of EC gels. Thus, our hypothesis stating the dependence of gel performance characteristics on gel rheological and mechanical properties was disproved. However, the significant influence of gel rheology on gel wettability and spreadability served an important aspect in the clinical efficacy of the gel formulation as the ease of gel application, bioadhesion and gel retention at the site of action would be affected.

As alluded from the dynamic contact angle measurement, the ability of the non-aqueous EC gel matrices to adapt its surface configuration in response to the surrounding environment allowed the gels to serve as effective moisture barrier to ensure stability of moisture-sensitive drugs during storage and as easily wettable gel matrices upon application. The water and IPM wettability in turn served as a favorable property facilitating bioadhesion and drug release for topical drug delivery. The possibility of EC gels to spread on the skin ensured the ease of gel application and an efficient measurement of spreadability would serve the formulator well when designing topical drug delivery systems. The prominent sustained release behavior of the EC gel and its high antibacterial efficacy indicated a potential application in topical antibacterial therapy that required long term and sustained drug delivery.

VII. FUTURE STUDIES

Future studies relating to this project will aim at developing more in-depth understanding of the formulated EC gel matrices in the attempt to extend the applicability of the gel matrices as topical delivery systems for different types of drug. To achieve this aim, further investigations on the gel physical properties, drug release characteristics and *in vivo* drug delivery and efficacy of the gel as a topical drug delivery system need to be carried out.

1. Gel physical properties

Moisture has been found to have an influential role in EC gel rheological properties and MH release characteristics. Thus, information on the different types of water such as the unbound freezing water (Type I) and bound non-freezing water (Type III) present in the gel matrices would contribute interesting insights into the understanding of gel-moisture interactions occurring within the gel network. For this purpose, thermal analysis of the non-hydrated gel matrices and gel matrices of different levels hydration could be performed using thermal gravimetric analysis (TGA) and differential scanning colorimetry (DSC).

In the oscillatory rheometry of the gel matrices, a temperature sweep can be performed to determine important gel properties such as the gel-sol transition temperature, gel melting temperature, melting rate, gelation time and gelation rate. Such information enables better understanding of gelation process and the response of gel to temperature changes (heating or cooling). The latter is important as the gel could be subjected to temperature variation during processing, storage and use.

The physically crosslinked three dimensional gel network of the EC gel matrices was postulated to originate from intermolecular hydrogen bonding between EC polymer chains and dipole-dipole interaction between polymer and solvent molecules. To verify this postulation, the existence of these interaction forces can be determined by the fourier transformed infrared (FTIR) technique. A temperature-controlled FTIR would be useful to correlate the changes in the molecular interactions within the gel network to the corresponding gel structural changes in response to the change in temperature.

2. Drug release characteristics

The release characteristics and mechanism of the model drug MH, a predominantly hydrophilic compound has been elucidated in this study. As the gel matrix was only evaluated using MH, the validity of the results can only be applied to this particular drug, hence imposing a limitation to the usefulness of the formulated EC gel matrices. In order to obtain a comprehensive understanding on the value of EC gel matrices as a topical drug delivery system, the release characteristics should be investigated using drugs of different properties. The selection criteria for the drug candidates include molecular weight and partition coefficient. Drug possessing molecular weight around 500 kDa or less should be employed as this is the commonly adopted molecular weight cut-off for drug delivery through skin. Based on the partition coefficient values, a range of drugs possessing hydrophilic, amphiphilic and hydrophobic properties should be selected. Incorporation of drugs of different nature into the gel matrices would be expected to result in different drug release characteristics and mechanisms in view of the different extent of drug solubility in the gel matrices. There is

a possibility of drug-gel matrix interactions affecting drug release. Such interactions could be elucidated using the FTIR and DSC techniques. The data obtained from this study would be useful to provide predictive information on drug release characteristics of drugs possessing different properties from the EC gel matrices, thus allowing greater extent of generalization on applicability of the gel as a topical drug delivery system.

3. *In vivo* drug delivery and efficacy

Determination of the *in vivo* drug delivery and efficacy of the MH topical gel formulation should be performed as a direct extension of the present study. As gel hydration was found to be a prerequisite for drug release and antibacterial activities of MH gel, the ability of the gel matrices to absorb sufficient moisture to facilitate gel hydration would be an issue of concern. The moisture needed for gel hydration could come from two sources, that are the skin and/or the environment. Dependence of gel hydration on ambient moisture is undesirable as such gel system would be subjected to huge variation of ambient humidity at different places. As EC gel is lipophilic, it is expected to impart physical occlusion to the skin and consequently promote skin hydration. Thus, the gel could possibly obtain the required moisture from the hydrated skin. The issue on drug release and antibacterial activities upon gel application to the skin could be addressed by establishing the presence of *in vivo* drug delivery and efficacy of the gel formulations. This study could be performed using a suitable acne-induced animal model. *In vivo* drug delivery could be established by visualizing drug localization within the skin layers of the excised skins using the confocal microscopy technique. This is important to ensure delivery of MH from the gel formulations to its target site, the

pilosebaceous units. *In vivo* efficacy could be by the presence of treatment effect in the animal model. This *in vivo* study would provide direct evidence to the clinical potential of the topical MH gel.

VIII. REFERENCES

Agrawal A.M., Manek R.V., Kolling W.M., and Neau S.H., 2003b. Studies on the interaction of water with ethylcellulose: effect of polymer particle size. *AAPS PharmSciTech.* **4 (4)**: Article 60.

Agrawal A.M., Neau S.H., and Bonate P.L., 2003a. Wet granulation fine particle ethylcellulose tablets: effect of production variables and mathematical modeling of drug release. *AAPS PharmSci.* **5 (2)**: Article 13.

Alvarez-Lorenzo C., and Concheiro A., 2001. Effects of surfactants on gel behavior. Design implications for drug delivery systems. *Am. J. Drug Deliv.* **1 (2)**: 77-101.

McEvoy K.G., 2006. Tetracyclines. In: *AHFS Drug Information*. American Society of Health-System Pharmacist, Maryland, pp. 440-467.

Anderson F.A., 2001. Amended final report on the safety assessment of PPG-40 butyl ether with an addendum to include PPG-2, -4, -5, -9, -12, -14, -15, -16, -17, -18, -20, -22, -24, -26, -30, -33, -52, and -53 butyl ethers. *Int. J. Toxicol.* **20 (Suppl. 4)**: 39-52.

Arora P., and Mukherjee B., 2002. Design, development, physicochemical, and *in vitro* and in vivo evaluation of transdermal patches containing diclofenac diethylammonium salt. *J. Pharm. Sci.* **91 (9)**: 2076-2089.

Bajdik J., Regdon Jr. G., Marek T., Erős I., Süvegh K., and Pintye-Hódi K., 2005. The effect of solvent on the film-forming parameters of hydroxypropyl-cellulose. *Int. J. Pharm.* **301**: 192-198.

Baker N.D., Griffin R.J., and Irwin W.J., 1990. The percutaneous absorption of *m*-azidopyrimethamine: a soft antifolate for topical use. *Int. J. Pharm.* **65**: 115-125.

Bamba F.L., and Wepiere J., 1993. Role of appendageal pathway in percutaneous absorption of pyridostigmine bromide in various vehicles. *Eur. J. Drug Metab. Pharmacokinet.* **18**: 339-348.

Barry B.W. and Meyer M.C., 1979a. The rheological properties of carbopol gels II. Oscillatory properties of carbopol gels. *Int. J. Pharm.* **2**: 27-40.

Barry B.W. and Meyer M.C., 1979b. The rheological properties of Carbopol gels I. Continuous shear and creep properties of Carbopol gels. *Int. J. Pharm.* **2**: 1-25.

Barry B.W., 1983. In: *Dermatological formulations. Percutaneous absorption.* Marcel Dekker, New York.

Baumgartner S., Kristl J., and Peppas N.A., 2002. Network structure of cellulose ethers used in pharmaceutical applications during swelling and at equilibrium. *Pharm. Res.* **19 (8)**: 1084-1090.

Behl C.R., Char H, Patel S.B., Mehta D.B., Piemontese D., and Malick A.W., 1993. *In vivo* and *in vitro* skin uptake and permeation studies: critical considerations and factors which affect them. In: Shah V.P., and Maibach H.I. (eds.), *Topical drug bioavailability, bioequivalence, and penetration.* Plenum Press, New York, pp. 225-259.

Bergfeld W.F., Belsito D.V., Carlton W.W., Klaassen C.D., Schroeter A.L., Shank R.C., and Slaga T.J., 1999. Final report on the safety assessment of propylene glycol (PG) dicaprylate, PG dicaprylate/dicaprate, PG dicocoate, PG dipelargonate, PG isostearate, PG laurate, PG myristate, PG oleate, PG oleate SE, PG dioleate, PC dicaprate, PG diisostearate, and PG dilaurate. *Int. J. Toxicol.* **18 (Suppl. 2)**: 35-52.

Berthon G., Brion M., and Lambs L., 1983. Metal ion-tetracycline interactions in biological fluids. 2. Potentiometric study of magnesium complexes with tetracycline,

oxytetracycline, doxycycline, minocycline, and discussion of their possible influence on the bioavailability of these antibiotics in blood plasma. *J. Inorg. Chem.* **19**: 1-18.

Bertolami C.N., Shetty V., Milavec J.E., Ellis D.G., and Cherrick H.M., 1991. Preparation and evaluation of a nonproprietary bilayer skin substitute. *Plast. Reconstr. Surg.* **87 (6)**: 1089-1098.

Bhola R., and Chandra S., 1999. Parameters controlling solidification of molten wax droplets falling on a solid surface. *J. Mat. Sci.* **34**: 4883-4894.

Böcker R.H., Peter R., Machbert G., Bauer W., 1991. Identification and determination of the two principal metabolites of minocycline in humans. *J. Chromatogr. B-Biomed.* **568 (2)**: 363-374.

Bodmeier R., and Paeratakul O., 1991. Process and formulation variables affecting the drug release from chlorpheniramine maleate-loaded beads coated with commercial and self-prepared aqueous ethyl cellulose pseudolatexes. *Int. J. Pharm.* **70**: 59-68.

Bouchillon S.K., Hoban D.J., Johnson B.M., Johnson J.L., Hsiung A., and Dowzicky M.J., 2005. *In vitro* activity of tigecycline against 3989 gram-negative and gram-positive clinical isolates from the United States Tigecycline Evaluation and Surveillance Trial (TEST Program; 2004). *Diagn. Micr. Infec. Dis.* **52**: 173-179.

Bromberg L., Temchenko M., Alakhov V., and Hatton T.A., 2004. Bioadhesive properties and rheology of polyether-modified poly(acrylic acid) hydrogels. *Int. J. Pharm.* **282**: 45-60.

Brook I., Frazier E.H., Cox M.E., and Yeager J.K., 1995. The aerobic and anaerobic microbiology of pustular acne lesions. *Anaerobe.* **1**: 305-307.

Brummer R., and Godersky S., 1999. Rheological studies to objectify sensations occurring when cosmetic emulsions are applied to the skin. *Colloid. Surface. A.* **152**: 89–94.

Buckton G., 1990. The role of compensation analysis in the study of wettability, solubility, disintegration and dissolution. *Int. J. Pharm.* **66**: 175-182.

Buckton G., Efentakis M., Al-Hmoud H., and Rajan Z., 1991. The influence of surfactants on drug release from acrylic matrices. *Int. J. Pharm.* **74**: 169-174.

Budden M.G., 1988. Topical and oral tetracycline in the treatment of acne vulgaris. *Practitioner*. **232 (6)**: 669-674.

Burkhart C.G., Burkhart C.N., and Lehmann P.F., 1999. Acne: a review of immunologic and microbiologic factors. *Postgrad. Med. J.* **75 (884)**: 328-331.

Carstensen J.T., 2000. Solution kinetics. In: *Drug stability: principles and practices.* Marcel Dekker, New York, pp. 25-30.

Chambin O., Champion D., Debray C., Ronchat-Gonthier M.H., Le Meste M., and Pourcelot Y., 2004. Effects of different cellulose derivatives on drug release mechanism studied at a preformulation stage. *J. Controlled Release.* **95**: 101-108.

Chang J.Y., Oh Y., Choi H., Kim Y.B., and Kim C., 2002. Rheological evaluation of thermosensitive and mucoadhesive vaginal gels in physiological conditions. *Int. J. Pharm.* **241**:155-163.

Charnock C., Brudeli B., and Klaveness J., 2004. Evaluation of the antibacterial efficacy of diesters of azelaic acid. *Eur. J. Pharm. Sci.* **21**: 589-596.

Chartone-Souza E., Loyola T.H., Bucciarelli-Rodriguez M., Menezes M.Ã.B.C., Rey N.A., and Pereira-Maia E.C., 2005. Synthesis and characterization of tetracycline-

platinum(II) complex active against resistant bacteria. *J. Inorg. Biochem.* **99**: 1001-1008 .

Chen J.D., 1988. Experiments on a spreading drop and its contact angle on a solid. *J. Colloid Interface Sci.* **122**: 60-72.

Chen Y.-C., and Lin C.-E., 1998. Migration behavior and separation of tetracycline antibiotics by micellar electrokinetic chromatography. *J. Chromatogr. A.* **802**: 95-105.

Chiu H.T., and Wang J.H., 1998. Characterization of the rheological behaviour of UHMWPE gels using parallel plate rheometry. *J. Appl. Pol. Sci.* **70**: 1009-1016.

Chopra I., 1995. Tetracycline Uptake and Efflux in Bacteria. In: Georgopapadakou, N.H. (eds.), In: *Drug Transport in Antimicrobial and Anticancer Cancer Chemotherapy*. Marcel Dekker, New York, pp. 221-224.

Chopra I., and Roberts M., 2001. Tetracycline antibiotics: mode of action, applications, molecular biology, and epidemiology of bacterial resistance. *Microbiol. Mol. Biol. R.* 65 (2): 232-260.

Cohen D.E., and Rice R.H., 2001. Toxic responses of the skin. In: Klaassen C.D. (ed.), *Casarett and Doull's toxicology: the basic science of poisons*, 6th Ed. McGraw-Hill, New York, pp. 653-671.

Contreras M.D., and Sánchez R., 2002a. Application of factorial design to the study of the flow behavior, spreadability and transparency of a Carbopol ETD 2020 gel. Part II. *Int. J. Pharm.* **234**: 149-157.

Contreras M.D. and Sánchez R., 2002b. Application of factorial design to the study of specific parameters of a Carbopol ETD 2020 gel. Part I. Viscoelastic parameters. *Int. J. Pharm.* **234**: 139-147.

Contreras M.D., Vialard A.P., and Vilchez F.G., 1993. *In vitro* percutaneous absorption of naproxen from gels using a double-layer artificial membrane. *Int. J. Pharm.* **98**: 37-43.

Costa P., and Lobo J.M.S., 2001. Modeling and comparison of dissolution profiles. *Eur. J. Pharm. Sci.* **13**: 123-133.

Craig D.Q.M., Tamburic S., Buckton G., and Newton J.M., 1994. An investigation into the structure and properties of Carbopol 934 gels using dielectric spectroscopy and oscillatory rheometry. *J. Controlled Release.* **30**: 213-223.

Davis S.S., 1969. Viscoelastic properties of pharmaceutical semisolids I: Ointment bases. *J. Pharm. Sci.* **58 (4)**: 412-418.

De Almeida W.B., Dos Santos H.F., and Zerner M.C., 1998. A theoretical studies of the interaction of anhydrotetracycline with Al(III). *J. Pharm. Sci.* **87 (9)**: 1101-1108.

Dean J.A., 1999. Lange's handbook of chemistry, 15th Ed. McGraw-Hill, New York, p. 5.87.

Dietz D., 1989. Toxicology and carcinogenesis studies of tetracycline hydrochloride (cas no. 64-75-5) in F44/N rats and B6C3F1 mice (feed studies). In: *National Toxicology Program Technical Report Series*, no. 344, NIH publication no. 89-2600.

Duarte H.A., Carvalho S., Paniago E.B., and Simas A.M., 1999. Importance of tautomers in the chemical behaviour of tetracyclines. *J. Pharm. Sci.* **88 (1)**: 111-120.

Eady E.A., Cove J.H., Holland K.T., and Cunliffe W.J., 1990. Superior antibacterial action and reduced incidence of bacterial resistance in minocycline compared to tetracycline-treated acne patients. *Brit. J. Dermatol.* **122 (2)**: 233-244.

Eady E.A., Jones C.E., Gardner K.J., Taylor J.P., Cove J.H., and Cunliffe W.J., 1993. Tetracycline-resistant propionibacteria from acne patients are cross-resistant to doxycycline, but sensitive to minocycline. *Br. J. Dermatol.* **128**: 556-560.

Eccleston G.M., Barry B.W., and Davis S.S., 1973. Correlation of viscoelastic functions for pharmaceutical semisolids: comparison of creep and oscillatory tests for oil-in-water creams stabilized by mixed emulsifiers. *J. Pharm. Sci.* **62**: 1954-1961.

Edlund C., and Nord C.E., 1996. Microbiological aspects and development of drug resistance related to systemic and topical administration of antimicrobial agents. In: *Workshop. Treatment of Acne.* The Norwegian Medicines Control Authority, Norway, [and] Medical Products Agency, Sweden, pp. 63-71.

Efentakis M., Al-Hmoud, Buckton G., and Rajan Z., 1991. The influence of surfactants on drug release from a hydrophobic matrix. *Int. J. Pharm.,* **70**: 153-158.

El-Faham T.H., 1994. Transdermal delivery of bromhexidine hydrochloride from various formulations through excised hairless mouse skin. *S.T.P. Pharma Sci.* **4 (3)**: 240-244.

El-Faham T.H. and Massoud A.A., 1994. Assessment of bromhexidine hydrochloride formulations in human dry eye patients. *J. Controlled Release.* **32 (3)**: 279-283.

Elkayam R., Friedman M., Stabholz A., Soskolne A.W., Sela M.N., and Golub L., 1988. Sustained release device containing minocycline for local treatment of periodontal disease. *J. Controlled Release.* **7**: 231-236.

Esposito P., Colombo I., and Lovrecich M., 1994. Investigation of surface properties of some polymers by a thermodynamic and mechanical approach: Possibility of predicting mucoadhesion and biocompatibility. *Biomaterials.* **15 (3)**: 177-182.

Ferguson G.S., and Whitesides J.M., 1992. Thermal reconstruction of the functionalized interface of polyethylene carboxylic acid and its derivatives. In: M.E. Schrader, and G.I. Loeb (eds.), *Modern approaches to wettability. Theory and applications,* Plenum, New York, pp. 143-177.

Ferrari F., Bertoni M., Caramella C., and La Manna A., 1994. Description and validation of an apparatus for gel strength measurements. *Int. J. Pharm.* **109**: 115-124.

Ferrero C., Bravo I., and Jiménez-Castellanos M.R., 2003. Drug release kinetics and fronts movement studies from methyl methacrylate (MMA) copolymer matrix tablets: effect of copolymer type and matrix porosity. *J. Controlled Release.* **92**: 69-82.

Flynn G.L., Linn E.E., Kurihara-Bergstrom T., Govil S.K., and Hou S.Y.E., 1987. Parameters of skin condition and function. In: Kydonieus A.F., and Berner B. (eds.), *Transdermal delivery of drugs. Volume II.* CRC Press, Boca Raton, FL, pp. 3-17.

Ford J.L., and Mitchell K., 1995. Thermal analysis of gels and matrix tablets containing cellulose ethers. *Thermochim. Acta.* **248**: 329-345.

Gardner K.J., Eady E.A., Cove J.H., Taylor J.P., and Cunliffe W.J., 1997. Comparison of serum antibiotic levels in acne patients receiving the standard or modified release formulation of minocycline hydrochloride. *Clin. Exp. Dermatol.* **22**: 72-76.

Garnier G., Bertin M., and Smrckova M., 1999. Wetting dynamics of alkyl ketene dimer on cellulosic model surfaces. *Langmuir.* **15**: 7863-7869.

Garnier G., Wright J., Godbout L., and Yu L., 1998. Wetting mechanism of alkyl ketene dimers on cellulose films. *Colloid Surface A.* **145**: 153-165.

Gemeinhart R.A., and Guo C., 2004. Fast swelling hydrogel systems. In: N. Yui, R.J. Mrsny, and K. Park (eds.), *Reflexive polymers and hydrogels: Understanding and designing fast-responsive polymeric systems,* CRC Press, Boca Raton, FL, pp. 245-257.

Gérentes P., Vachoud L., Doury J., and Domard A., 2002. Study of a chitin-based gel as injectable material in periodontal surgery. *Biomaterials*. **23**: 1295-1302.

Gosselet N.M., Beucler F., Renard E., Amiel C., and Sebille B., 1999. Association of hydrophobically modified poly (*N,N*-dimethylacrylamide hydroxyethylmethacrylate) with water soluble β-cyclodextrin polymers. *Colloid Surface A.* **155**: 177-188.

Goulden V., Glass D., and Cunliffe W.J., 1996. Safety of long-term high-dose minocycline in the treatment of acne. *Brit. J. Dermatol.* **134**: 693-695.

Greenstein G., and Polson A., 1998. The role of local drug delivery in the management of periodontal diseases: a comprehensive review. *J. Periodontol.* **69**: 507-520.

Greenwood R., Luckham P.F., and Gregory T., 1997. The effect of diameter ratio and volume ratio on the viscosity of bimodal suspensions of polymer latices. *J. Colloid Interface Sci.* **191**: 11-21.

Gribbon E.M., Shoesmith J.G., Cunliffe W.J., and Holland K.T., 1994. The microaerophily and photosensitivity of *Propionibacterium acnes. J. Appl. Bacteriol.* **77**: 583-590.

Grundke K., Pospiech D., Kollig W., Simon F., and Janke A., 2001. Wetting of heterogenous surfaces of block copolymers containing fluorinated segments. *Colloid Polym. Sci.* **279**: 727-735.

Gupta R.K., 2000. Dynamic mechanical properties. In: *Polymer and Composite Rheology.* Marcel Dekker, New York, p.133.

Hadgraft J., Walters K.A., and Wotton P.K., 1986. Facilitated percutaneous absorption: a comparison and evaluation of two *in vitro* models. *Int. J. Pharm.* **32**: 257-263.

Hall G.S., Pratt-Rippin K., Meisler D.M., Washington J.A., Roussel T.J., and Miller D., 1994. Growth curve for *Propionibacterium acnes. Curr. Eye Res.* **13 (6)**: 465-466.

Hasegawa K., Nakashima K., Eguchi T., and Ota M., 1987. US Patent. US 4701320.

Heng P.W.S., Chan L.W., and Ong K.T., 2003. Influence of storage conditions and type of plasticizers on ethylcellulose and acrylate films formed from aqueous dispersions. *J. Pharm. Pharmaceut. Sci.* **6 (3)**: 334-344.

Heng P.W.S., Chan L.W., Easterbrook M.G., and Li X., 2001. Investigation of the influence of mean HPMC particle size and number of polymer particles on the release of aspirin from swellable hydrophilic matrix tablets. *J. Controlled. Release* **76**: 39-49.

Higuchi T., 1961. Rate of release of medicaments from ointment bases containing drugs in suspension. *J. Pharm. Sci.* **50**: 874-875.

Hogt A.H., Gregonis D.E., Andrade J.D., Kim S.W., Dankert J., and Feijen J., 1985. Wettability and ζ potentials of a series of methacrylate polymers and copolymers. *J. Colloid Interface Sci.* **106 (2)**: 289-298.

Holman R.K., Cima M.J., Uhland S.A., and Sachs E., 2002. Spreading and infiltration of inkjet-printed polymer solution droplets on a porous substrate. *J. Colloid Interface Sci.* **249**: 432-440.

Hughes L.J., Stezowski J.J., and Hughes R.E., 1979. Chemical-structural properties of tetracycline deriatives. 7. Evidence for the coexistence of the zwitterionic and nonionized form of the free base in solution. *J. Am. Chem. Soc.* **101**: 7655-7657.

Hussar D.A., Niebergall P.J., Sugita E.T., and Doluisio J.T., 1968. Aspects of epimerization of certain tetracycline derivatives. *J. Pharm. Pharmac.* **20**: 539-546.

Islam M.T., Rodríguez-Hornedo N., Ciotti S., and Ackermann C., 2004. Rheological characterization of topical carbomer gels neutralized to different pH. *Pharm. Res.* **21 (7)**: 1192-1199.

Itagaki H., Tokai M., and Kondo T., 1997. Physical gelation process for cellulose whose hydroxyl groups are regioselectively substituted by fluorescent groups. *Polymer.* **38 (16)**: 4201-4205.

Ito Y., Nakayama S., Son M., Kume H., and Yamaki K., 2001. Protection by tetracyclines against ion transport disruption caused by nystatin in human airway epithelial cells. *Toxicol. Appl. Pharmacol.* **177**: 232-237.

Jaiswal J., Poduri R., and Panchagnula R., 1999. Transdermal delivery of naloxone: Ex vivo permeation studies. *Int. J. Pharm.* **179**: 129-134.

Jappe U., 2003. Pathological mechanisms of acne with special emphasis on *Propionibacterium acnes* and related therapy. *Acta. Derm. Venereol.* **83**: 241–248.

Jezowska-Bojczuk M., Lambs L., Kozlowski H., and Berthon G., 1993. Metal ion-tetracycline interactions in biological fluids. 10. Structural investigations on copper(II) complexes of tetracycline, oxytetracycline, chlortetracycline, 4-(dedimethylamino)tetracycline, and 6-desoxy-6-demethyltetracycline and discussion of their binding modes. *Inorg. Chem.*. **32**: 428-437.

Joanny J.F., Johner A., and Vilgris T.A., 2001. Gels at interfaces. *Eur. Phys. J. E.* **6**: 201-209.

Johnsson M., 1996. Treatment with oral antibiotics. In: *Workshop. Treatment of Acne.* The Norwegian Medicines Control Authority, Norway, [and] Medical Products Agency, Sweden, pp. 55-62.

Jones D., and Collins M.D., 1986. Irregular, nonsporing gram-positive rods. In: Sneath P.H.A., Mair N.S., Sharpe M.E., and Holt J.G. (eds.), *Bergey's manual of systematic bacteriology, volume 2*. Williams and Wilkins, Maryland, pp. 1261-1434.

Jones D.S., Lawlor M.S., and Woolfson A.D., 2002. Examination of the flow rheological and textural properties of polymer gels composed of poly(methylvinylether-*co*-maleic anhydride) and poly(vinylpyrrolidone): Rheological and mathematical interpretation of textural parameters. *J. Pharm. Sci.* **91**: 2090-2101.

Jones D.S., Woolfson A.D., and Brown A.F., 1997a. Textural analysis and flow rheometry of novel, bioadhesive antimicrobial oral gels. *Pharm. Res.* **14 (4)**: 450-457.

Jones D.S., Woolfson A.D., and Brown A.F., 1997b. Textural, viscoelastic and mucoadhesive properties of pharmaceutical gels composed of cellulose polymers. *Int. J. Pharm.* **151**: 223-233.

Jones D.S., Woolfson A.D., and Djokic J., 1996b. Texture profile analysis of bioadhesive polymeric semisolids: Mechanical characterization and investigation of interactions between formulation components. *J. Appl. Pol. Sci.* **61**: 2229-2234.

Jones D.S., Woolfson A.D., Brown A.F., Coulter W.A., McClelland C., and Irwin C.R., 2000. Design, characterisation and preliminary clinical evaluation of a novel mucoadhesive topical formulation containing tetracycline for the treatment of periodontal disease. *J. Controlled. Release.* **67**: 357-368.

Jones D.S., Woolfson A.D., Djokic J., and Coulter W.A., 1996a. Development and mechanical characterization of bioadhesive semi-solid, polymeric systems containing tetracycline for the treatment of periodontal diseases. *Pharm. Res.* **13 (11)**: 1734-1738.

Joshi H.N., and Wilson T.D., 1993. Calorimetric studies of dissolution of hydroxypropyl methylcellulose E5 (HPMC E5) in water. *J. Pharm. Sci.* **82 (10)**: 1033-1038.

Kajiwara K., 2001. Structure of gels. In: Osada Y., and Kajiwara K. (eds.), *Gel handbook. Volume 1. The fundamentals.* Academic Press, San Diego, pp. 123-171.

Kalachandra S., Lin D., and Offenbacher S., 2002. Controlled drug release for oral condition by a novel device based on ethylene vinyl acetate (EVA) copolymer. *J. Mater. Sci. Mater. Med.* **13**: 53-58.

Kalia Y.N., and Guy R.H., 2001. Modeling transdermal drug release. *Adv. Drug Deliv. Rev.* **48**: 159-172.

Kalyon D.M., Birinci E., Yazici R., Karuv B., and Walsh S., 2002. Electrical properties of composites as affected by the degree of mixedness of conductive filler in the polymer matrix. *Polym. Eng. Sci.* **42 (7)**: 1609-1617.

Kaneko D., Gong J.P., Zrínyi M., and Osada Y., 2005. Kinetics of fluid spreading on viscoelastic substrates. *J. Polym. Sci. B Polym. Phys.* **43**: 562-572.

Kavanagh G.M., and Ross-Murphy S.B., 1998. Rheological characterisation of polymer gels. *Prog. Polym. Sci.* **23**: 533-562.

Kim C., 2004. Ionic equilibrium. *Advanced pharmaceutics. Physicochemical principles.* CRC Press, Boca Raton, FL, pp. 45-112.

Klech C.M., 1992. Gels and jellies. In: Swarbrick J., and Boylan J.C. (eds.), *Encyclopedia of Pharmaceutical Technology. Volume 6.* Marcel Dekker, New York, pp. 415-439.

Kohyama K., and Nishinari K., 1993. Rheological studies on the gelation process of soybean 7S and 11S proteins in the presence of glucono-δ-lactone. *J. Agric. Food Chem.* **41**: 8-14.

Kondo T., and Miyamoto T., 1998. The influence of intramolecular hydrogen bonds on handedness in ethylcellulose/CH_2Cl_2 liquid crystalline mesophases. *Polymer.* **39 (5)**: 1123-1127.

Kurokawa I., Nishijima S., and Kawabata S., 1999. Antimicrobial susceptibility of *Propionibacterium acnes* isolated from acne vulgaris. *Eur. J. Dermatol.* **9**: 25-28.

Kwok D.Y., Gietzelt T., Grundke K., Jacobasch H.J., and Neumann A.W., 1997. Contact angle measurements and contact angle interpretation. 1. Contact angle measurements by axisymmetric drop shape analysis and a goniometer sessile drop technique. *Langmuir.* **13**: 2880-2894.

Kwok D.Y., Lam C.N.C., Li A., Leung A., Wu R., Mok E., and Neumann A.W., 1998. Measuring and interpreting contact angles: a complex issue. *Colloid Surface A.* **142**: 219-235.

Kydonieus A.F., 1987. Fundamentals of transdermal drug delivery. In: Kydonieus A.F., and Berner B. (eds.), *Transdermal delivery of drugs. Volume I.* CRC Press, Boca Raton, FL, pp. 3-16.

Lahooti S., Del Rio O.I., Neumann A.W., and Cheng P., 1996. Axisymmetric drop shape analysis (ADSA). In: Neumann A.W., and Spelt J.K. (eds.), *Applied surface thermodynamics.* Marcel Dekker, New York, pp. 441-507.

Lambs L., and Berthon G., 1988. Metal ion-tetracycline interactions in biological fluids. Part 7. Quantitative investigation of methacycline complexes with Ca(II), Mg(II), Cu(II) and Zn(II) ions and assessment of their biological significance. *Inorg. Chim. Acta.* **151**: 33-43.

Larson R.G., 1999. *The structure and rheology of complex fluids.* Oxford University Press, New York.

Lazghab M., Saleh K., Pezron I., Guigon P., and Komunjer L., 2005. Wettability assessment of finely divided solids. *Powder Technol*. **157**: 79-91.

Lee C.K., Kitagawa K., Uchida T., Kim N.S., and Goto S., 1995. Transdermal delivery of theophylline using an ethanol panasate 800-ethylcellulose gel preparation. *Biol. Pharm. Bull.* **18 (1)**: 176-180.

Lee T.-W., Kim J.-C., and Hwang S.-J., 2003. Hydrogel patches containing triclosan for acne treatment. *Eur. J. Pharm. Biopharm.* **56**: 407-412.

Lehr C., Boddé H.E., Bouwstra J.A., and Junginger H.E., 1993. A surface energy analysis of mucoadhesion II. Prediction of mucoadhesive performance by spreading coefficients. *Eur. J. Pharm. Sci.* **1**: 19-30.

Lehr C., Bouwstra J.A., Boddé H.E., and Junginger H.E., 1992. A surface energy analysis of mucoadhesion: Contact angle measurements on polycarbophil and pig intestinal mucosa in physiologically relevant fluids. *Pharm. Res.* **9 (1)**: 70-75.

Lippold B.H., Sutter B.K., and Lippold B.C., 1989. Parameters controlling drug release from pellets coated with ethyl cellulose aqueous dispersion. *Int. J. Pharm.* **54**: 15-25.

Liu W., Zhang B., Lu W.W., Li X., Zhu D., Yao K.D., Wang Q., Zhao C., and Wang C., 2004. A rapid temperature-responsive sol–gel reversible poly(*N*-isopropylacrylamide)-*g*-methylcellulose copolymer hydrogel. *Biomaterials.* **25**: 3005-3012.

Lizaso E., Muñoz M.E., Santamaría A., 1999a. Formation of gels in ethylcellulose solutions. An interpretation from dynamic viscoelastic results. *Macromolecules.* **32**: 1883-1889.

Lizaso I., Muñoz M.E., and Santamaría A., 1999b. Transient rheological behaviour of lyotropic solutions of ethyl cellulose in *m*-cresol. *Rheol. Acta.* **38**: 108-116.

Loth H., 1991. Vehicular influence on transdermal drug penetration. *Int. J. Pharm.* **68**: 1-10.

Loukas Y.L., Vraka V., and Gregoriadis G., 1998. Drugs, in cyclodextrins, in liposomes: A novel approach to the chemical stability of drugs sensitive to hydrolysis. *Int. J. Pharm.* **162 (1-2)**: 137-142.

Lowman A.M., and Peppas N.A., 2000. Hydrogels. In: E. Mathiowitz (ed.), *Encyclopedia of controlled drug delivery,* Wiley, New York, pp. 397-417.

Luckham P.F., and Ukeje M.A., 1999. Effect of particle size distribution on the rheology of dispersed systems. *J. Colloid Interface Sci.* **220**: 347-356.

Luner P.E., and Oh E., 2001. Characterization of the surface free energy of cellulose ether films. *Colloid Surface A.* **181**: 31-48.

Luner P.E., Babu S.R., and Mehta S.C., 1996. Wettability of a hydrophobic drug by surfactant solutions. *Int. J. Pharm.,* **128**: 29-44.

Machiste E.O., and Buckton G., 1996. Dynamic surface tension studies of hydroxypropylmethylcellulose film-coating solution. *Int. J. Pharm.* **145**: 197-201.

Macosko C.W., 1994. Viscous liquid. In: *Rheology: principles, measurement and applications.* VCH, Inc., New York, pp. 65-108.

Madkour T.M., 2001. A combined statistical mechanics and molecular dynamics approach for the evaluation of the miscibility of polymers in good, poor and non-solvents. *Chem. Phys.* **274**: 187-198.

Maisch T., Szeimies R., Jori G., and Abels C., 2004. Antibacterial photodynamic therapy in dermatology. *Photochem. Photobiol. Sci.* **3**: 907-917.

Malmsten M., and Lindman B., 1990. Ellipsometry studies of the adsorption of cellulose ethers. *Langmuir.* **6**: 357-364.

Mani N., Park M.O., and Jun H.W., 2005. Effects of formulation variables and characterization of guaifenesin wax microspheres for controlled release. *Pharm. Dev. Technol.* **1**: 71-83.

Markman C., Fracalanzza S.E.L., Novaes Jr.A.B., and Novaes A.B., 1995. Slow release of tetracycline hydrochloride from a cellulose membrane used in guided tissue regeneration. *J. Periodontol.* **66 (11)**: 978-983.

McCrystal C.B., Ford J.L., and Rajabi-Siahboomi A.R., 1999. Water distribution studies within cellulose ethers using differential scanning calorimetry. 1. Effect of polymer molecular weight and drug addition. *J. Pharm. Sci.* **88 (8):** 792-796.

McTaggart L.E., and Halbert G.W., 1993. Assessment of polysaccharide gels as drug delivery vehicles. *Int. J. Pharm.* **100**: 199-206.

Melzer E., Kreuter J., and Daniels R., 2003. Ethylcellulose: A new type of emulsion stabilizer. *Eur. J. Pharm. Biopharm.* **56**: 23-27.

Menon G.K., 2002. New insights into skin structure: scratching the surface. *Adv. Drug. Deliv. Rev.* **54 (Suppl. 1)**: S3-S17.

Meyer G.A., Lostritto R.T., and Johnson J.F., 1991. Characterization of hydroxypropylcellulose-indomethacin grafts as a function of molecular weight. *J. Appl. Pol. Sci.* **42**: 2247-2253.

MICROMEDEX Healthcare Series. *Minocycline hydrochloride*. http://www.thomsonhc.com.libproxy1.nus.edu.sg/hcs/librarian/ND_PR/Main/SBK/2/PFPUI/A94m3Me1kU4PEb/ND_PG/PRIH/CS/91D540/ND_T/HCS/ND_P/Main/DUPLICATIONSHIELDSYNC/7B9A78/ND_B/HCS/PFActionId/hcs.common.RetrieveDocumentCommon/DocId/2359/ContentSetId/31#secN69446 (accessed 29 May 2006).

Mitchell K., Ford J.L., Armstrong D.J., Elliott P.N.C., Rostron C., and Hogan J.E., 1993. The influence of concentration on the release of drugs from gels and matrices containing Methocel. *Int. J. Pharm.* **100**: 155-163.

Mitscher L.A., 1978. Degradation and structure proofs. In: *The Chemistry of Tetracycline Antibiotics, Medicinal Research Series, Vol 9.* Marcel Dekker, New York, pp. 122-164.

Miyajima M., Koshika A., Okada J., Ikeda M., and Nishimura K., 1997. Effect of polymer crystallinity on papaverine release from poly (L-lactic acid) matrix. *J. Controlled. Release.* **49**: 207-215.

Miyazaki S., Kawasaki N., Nakamura T., Iwatsu M., Hayashi T., Hou W.-M., and Attwood D., 2000. Oral mucosal bioadhesive tablets of pectin and HPMC: *in vitro* and *in vivo* evaluation. *Int. J. Pharm.* **204**: 127-132.

Mohan Y.M., Murthy P.S.K., Rao K.M., Sreeramulu J., and Raju K.M., 2005. Swelling behavior and diffusion studies of high-water-retaining acrylamide/potassium methacrylate hydrogels. *J. Appl. Polym. Sci.* **96**: 1153-1164.

Moreno-Cerezo J.M., Córdoba-Díaz M., Córdoba-Díaz D., and Córdoba-Borrego M., 2001. A stability study of tetracycline and tetracycline cyclodextrins in tablets using a new HPLC method. *J. Pharmaceut. Biomed.* **26**: 417-426.

Myers D., 1999. Wetting and spreading. *Surfaces, interfaces and colloids. Principles and applications.* John Wiley & Sons, New York, pp. 415-447.

Nahringbauer I., 1995. Dynamic surface tension of aqueous polymer solutions, I: Ethyl (hydroxyethyl) cellulose (BERMOCOLL cst-103). *J. Colloid Interface Sci.* **176**: 318-328.

Needleman I.G., Martin G.P., and Smales F.C., 1998. Characterisation of bioadhesives for periodontal and oral mucosal drug delivery. *J. Clin. Periodontol.* **25**: 74-82.

Nelis H.J.C.F., and De Leenheer A.P., 1982. Metabolism of minocycline in humans. *Drug Metab. Dispos.* **10 (2)**:142-146.

Nieh S.Y., Ybarra R.M., and Neogi P., 1996. Wetting kinetics of polymer solutions. Experimental observations. *Macromolecules.* **29**: 320-325.

Nilges M.J., Enochs W.S., and Swartz H.M., 1991. Identification and characterization of a tetracycline semiquinone formed during the oxidation of minocycline. *J. Org. Chem.* **56**: 5623-5630.

Novák-Pékli M., Mesbah M.E., Pethő G., 1996. Equilibrium studies on tetracyline-metal ion systems. *J. Pharm. Biomed. Anal.* **14**: 1025-1029.

Oh E., and Luner P.E., 1999. Surface free energy of ethylcellulose films and the influence of plasticizers. *Int. J. Pharm.* **188**: 203-219.

Ohyama T., and Cowan J.A., 1995. Calorimetric studies of metal binding to tetracycline. Role of solvent structure in defining the selectivity of metal ion-drug interactions. *Inorg. Chem.* **34**: 3083-3086.

Osada Y., 2001. Polymer gels: crosslink formations. In: Osada Y., and Kajiwara K. (eds.), *Gel handbook. Volume 1. The fundamentals.* Academic Press, San Diego, pp. 13-25.

Panchagnula R., 1996. Transdermal drug delivery of tricyclic antidepressants: feasibility study. *STP Pharma Sci.* **6 (6)**: 441-444.

Parfitt G.D. (ed.), 1981. Fundamental aspects of dispersion. In: *Dispersion of powders in liquids*. John Wiley & Sons, New York, pp. 1-50.

Park D., Keszler B., Galiatsatos V., and Kennedy J.P., 1995. Amphiphilic networks. 9. Surface characterization. *Macromolecules.* **28 (8)**: 2595-2601.

Pasandideh-Fard M., Qiao Y.M., Chandra S., and Mostaghimi J., 1996. Capillary effects during drop impact on a solid surface. *Phys. Fluids.* **8 (3)**: 650-659.

Paula I.C.D., Ortega G.G., Bassani V.L., and Petrovick P.R., 1998. Development of ointment formulations prepared with *Achyrocline satureioides* spray-dried extracts. *Drug Dev. Ind. Pharm.* **24 (3)**: 235-241.

Pena L.E., Lee B.L., and Stearns J.F., 1994. Structural rheology of a model ointment. *Pharm. Res.* **11 (6)**: 875-881.

Peppas N.A., 1987. Diffusion through polymers. In: Kydonieus A.F., and Berner B. (eds.), *Transdermal delivery of drugs. Volume I.* CRC Press, Boca Raton, FL, pp. 17-28.

Peppas N.A., and Buri P.A., 1985. Surface, interfacial and molecular aspects of polymer bioadhesion on soft tissues. *J. Controlled Release.* **2**: 257-275.

Peppas N.A., and Mongia N.K., 1997. Ultrapure poly(vinyl alcohol) hydrogels with mucoadhesive drug delivery characteristics. *Eur. J. Pharm. Biopharm.* **43**: 51-58.

Peppas N.A., and Sahlin J.J., 1989. A simple equation for the description of solute release. III. Coupling of diffusion and relaxation. *Int. J. Pharm.* **57**: 169-172.

Perkins N.C., and Heard C.M., 1999. *In vitro* dermal and transdermal delivery of doxycycline from ethanol/migliol 840 vehicles. *Int. J. Pharm.* **190**: 155-164.

Persson B., Nilsson S., and Bergman R., 1999. Dynamic surface tension of dilute aqueous solutions of nonionic cellulose derivatives in relation to other macromolecular characterization parameters. *J. Colloid Interface Sci.* **218**: 433-441.

Pinsuwan S., Alvarez-Núñez F.A., Tabibi S.E., and Yalkowsky S.H., 1999. Spectrophotometric determination of acidity constants of 4-dedimethylamino sancycline (Col-3), a new antitumor drug. *J. Pharm. Sci.* **88 (5)**: 535-537.

Plewig G., and Kligman A.M., 1993. Microorganisms. In: *Acne and rosacea.* Springer-Verlag, New York, pp. 59-63.

Poulsen B.J., Young E., Coquilla V., and Katz M., 1968. Effect of topical vehicle composition on the *in vitro* release of fluocinolone acetonide and its acetate ester. *J. Pharm. Sci.* **57**: 928-933.

Rampon V., Brossard C., Mouhous-Riou N., Bousseau B., Llamas G., and Genot C., 2004. The nature of the apolar phase influences the structure of the protein emulsifier in oil-in-water emulsions stabilized by bovine serum albumin. A front-surface fluorescence study. *Adv. Colloid Interfac.* **108-109**: 87-94.

Ranade V.V., and Hollinger M.A., 2004. Transdermal drug delivery. In: *Drug delivery systems.* CRC Press, Boca Raton, FL, pp. 207-248.

Rangwalla H., Schwab A.D., Yurdumakan B., Yablon D.G., Yeganeh M.S., and Dhinojwala A., 2004. Molecular structure of an alkyl-side-chain polymer-water interface: Origins of contact angle hysteresis. *Langmuir.* **20**: 8625-8633.

Rapedius M., and Blanchard J., 2001. Comparison of the Hanson Microette and the Van Kel apparatus for *in vitro* release testing of topical semisolid formulations. *Pharm. Res.* **18 (10)**: 1440-1447.

Remmers E.G., Sieger G.M., Doerschuk A.P., 1963. Some observations on the kinetics of the C·4 epimerization of tetracycline. *J. Pharm. Sci.* **52**: 752-756.

Remuñán-López C., Portero A., Vila-Jato J.L., and Alonso M.J., 1998. Design and evaluation of chitosan/ethylcellulose mucoadhesive bilayered devices for buccal drug delivery. *J. Controlled Release.* **55**: 143-152.

Ritger P.L., and Peppas N.A., 1987. A simple equation for description of solute release. I. Fickian and non-fickian release from non-swellable devices in the form of slabs, spheres, cylinders or discs. *J. Controlled Release.* **5**: 23-36.

Ritter L., 1992. Stable, cosmetically acceptable topical gel formulation and method of treatment for acne. US Patent. US 5122519.

Rodriguez R., Alvarez-Lorenzo C., and Concheiro A., 2001. Rheological evaluation of the interactions between cationic celluloses and Carbopol 947P in water. *Biomacromolecules.* **2**: 886-893.

Romero A.P., Caramella C., Ronchi M., Ferrari F., and Chulia D., 1991. Water uptake and force development in an optimized prolonged release formulation. *Int. J. Pharm.* **73**: 239-248.

Romeu N.V., Miñones J., Iribarnegaray E., Conde O., and Casas M., 1997. Influence of the solvent on the spreading of poly[(D,L-lactic acid)-*co*-(glycolic acid)] monolayers. *Colloid Polym. Sci.* **275**: 580-586.

Rosa M.J., and Pinho M.N., 1997. Membrane surface characterization by contact angle measurements using the immersed method. *J. Membrane Sci.* **131**: 167-180.

Rosen M.J., 1989. Wetting and its modification by surfactants. In: *Surfactants and interfacial phenomena*. John Wiley & Sons, New York, pp. 240-275.

Rosilio V., Costa M.L., and Baszkin A., 1998. Wettability of drug loaded polymer matrices. *J. Disper. Sci. Technol.* **19 (6-7)**: 821-841.

Ross J.I., Snelling A.M., Eady E.A., Cove J.H., Cunliffe W.J., Leyden J.J., Collignon P., Dréno B., Reynaud A., Fluhr J., and Oshima S., 2001. Phenotypic and genotypic characterization of antibiotic-resistant *Propionibacterium acnes* isolated from acne patients attending dermatology clinics in Europe, the U.S.A., Japan and Australia. *Br. J. Dermatol.* **144**: 339-346.

Santamaría A., Lizaso M.I., and Muñoz M.E., 1997. Rheology of ethyl cellulose solutions. *Macromol. Symp.* **114**: 109-119.

Sarkar D., and Somasundaran P., 2004. Conformational dynamics of poly(acrylic acid). A study using surface plasmon resonance spectroscopy. *Langmuir*. **20**: 4657-4664.

Sasaki T., Kano R., Sato H., Nakamura Y., Watanabe S., and Hasegawa A., 2003. Effects of staphylococci on cytokine production from human keratinocytes. *Br. J. Dermatol.* **148**: 46–50.

Schmitt M.O., and Schneider S., 2000. Spectroscopic investigation of complexation between various tetracyclines and Mg^{2+} or Ca^{2+}. *Phys. Chem. Comm.* **1-14**: Article 9.

Seaman H.E., Lawrenson R.A., Williams T.J., MacRae K.D., and Farmer R.D.T., 2001. The risk of liver damage associated with minocycline: a comparative study. *J. Clin. Pharmacol.* **41**: 852-860.

Sekiguchi Y., Sawatari C., and Kondo T., 2003. A gelation mechanism depending on hydrogen bond formation in regioselectively substituted *O*-methylcelluloses. *Carbohyd. Polym.* **53**: 145-153.

Shah V.P., 2003. Transdermal drug delivery system regulatory issues. In: Guy R.H., and Hadgraft J. (eds.), *Transdermal drug delivery.* Marcel Dekker, New York, pp. 361-367.

Shah V.P., 2005. IV-IVC for topically applied preparations-a critical evaluation. *Eur. J. Pharm. Biopharm.* **60**: 309-314.

Shah V.P., Elkins J., Shaw S., and Hanson R., 2003. *In vitro* release: comparative evaluation of vertical diffusion cell system and automated procedure. *Pharm. Dev. Technol.* **8 (1)**: 97-102.

Shani S., Friedman M., and Steinberg D., 1998. *In vitro* assessment of the antimicrobial activity of a local sustained release device containing amine fluoride for the treatment of oral infectious diseases. *Diagn. Microbiol. Infect. Dis.* **30**: 93-97.

Shavit U., Reiss M., and Shaviv A., 2003. Wetting mechanisms of gel-based controlled-release fertilizers. *J. Controlled Release.* **88**: 71-83.

Shigeyama M., Ohgaya T., Kawashima Y., Takeuchi H., and Hino T., 1999. Mixed base of hydrophilic ointment and purified lanolin to improve the drug release rate and absorption of water of minocycline hydrochloride ointment for treatment of bedsores. *Chem. Pharm. Bull.* **47 (6)**: 744-748.

Shigeyama M., Ohgaya T., Kawashima Y., Takeuchi H., and Hino T., 2000. Modification of the physicochemical properties of minocycline hydrochloride ointment with cyclodextrins for optimum treatment of bedsore. *Chem. Pharm. Bull.* **48 (5)**: 617-622.

Smith E.W., Surber C., and Maibach H.I., 1999. Topical dermatological vehicles: a holistic approach. In: Bronaugh R.L., and Maibach H.I. (eds.), In: *Percutaneous absorption: drugs-cosmetics-mechanisms-methodology.* Marcel Dekker, New York, pp. 779-787.

Spireas S., and Sadu S., 1998. Enhancement of prednisolone dissolution properties using liquisolid compacts. *Int. J. Pharm.* **166**: 177-188.

Spireas S., Sadu S., and Grover R., 1998. *In vitro* release evaluation of hydrocortisone liquisolid tablets. *J. Pharm. Sci.* **87 (7)**: 867-872.

Stading M., Langton M., and Hermansson A., 1995. Small and large deformation studies of protein gels. *J. Rheol.* **39 (6)**: 1445-1450.

Starov V.M., Kostvintsev S.R., Sobolev V.D., Velarde M.G., and Zhdanov S.A., 2002. Spreading of liquid drops over dry porous layers: Complete wetting case. *J. Colloid Interface Sci.* **252**: 397-408.

Summ B.D., and Samsonov V.M., 1999. Concepts of Rehbinder's school and modern theories of spreading. *Colloid. Surface. A*. **160**: 63-77.

Suzuki A., and Kobiki Y., 1999. Static contact angle of sessile air bubbles on polymer gel surfaces in water. *Jpn. J. Appl. Phys*. **38**: 2910-2916.

Szczesniak A.R., Brandt M.A., and Friedman H.H., 1963. Development of standard rating scales for mechanical parameters of texture and correlation between the objective and the sensory methods of texture evaluation. *J. Food Sci.* **28**: 397-403.

Takayama K., Okabe H., Obata Y., and Nagai T., 1990. Formulation design of indomethacin gel ointment containing *d*-limonene using computer optimization methodology. *Int. J. Pharm.* **61**: 225-234.

Talukdar M.M., Vinckier I., Moldenaers P., and Kinget R., 1996. Rheological characterization of xanthan gum and hydroxypropylmethylcellulose with respect to controlled-release drug delivery. *J. Pharm. Sci.* **85 (5)**: 537-540.

Tamburic S., and Craig D.Q.M., 1995. An investigation into the rheological, dielectric and mucoadhesive properties of poly (acrylic acid) gel systems. *J. Controlled Release.* **37**: 59-68.

Tamburic S., and Craig D.Q.M., 1997. A comparison of different *in vitro* methods for measuring mucoadhesive performance. *Eur. J. Pharm. Biopharm*. **44**: 159-167.

Tamura T., Takayama K., Satoh H., Tanno K., and Nagai T., 1997. Evaluation of oil/water- type cyclosporine gel ointment with commercially available oral solution. *Drug Dev. Ind. Pharm.* **23 (3)**: 285-291.

Tan H., Xie X., Li J., Zhong Y., and Fu Q., 2004. Synthesis and surface mobility of segmented polyurethanes with fluorinated side chains attached to hard blocks. *Polymer.* **45**: 1495-1502.

Tavares M.F.M., and McGuffin V.L., 1994. Separation and characterization of tetracycline antibiotics by capillary electrophoresis. *J. Chromatogr. A*. **686**: 129-142.

Telis V.R.N., Telis-Romero J., and Gabas A.L., 2005. Solids rheology for dehydrated food and biological materials. *Dry. Technol.* **23**: 759–780.

Tesch R., Ramon O., Ladyzhinski I., Cohen Y., and Mizrahi S., 1999. Water sorption isotherm of solution containing hydrogels at high water activity. *Int. J. Food Sci. Tech.* **34**: 235-243.

Thiboutot D.M., 2000. Acne and rosacea. New and emerging therapies. *Dermatol. Clin.* **18 (1)**: 63-71.

Toledano M., Osorio R., Perdigao J., Rosales J.I., Thompson J.Y., and Cabrerizo-Vilchez M.A., 1999. Effect of acid etching and collagen removal on dentin wettability and roughness. *J. Biomed. Mater. Res.* **47 (2)**: 198-203.

Tretinnikov O.N., and Ikada Y., 1994. Dynamic wetting and contact angle hysteresis of polymer surfaces studied with the modified Wilhelmy balance method. *Langmuir.* **10**: 1606-1614.

Twitchell A.M., Hogan J.E., and Aulton M.E., 1995. The behaviour of film coating droplets on their impingement onto uncoated and coated tablets. *STP Pharma. Sci.* **5 (3)**: 190-195.

Um S., Poptoshev E., and Pugh R.J., 1997. Aqueous solutions of ethyl (hydroxyethyl) cellulose and hydrophobic modified ethyl (hydroxyethyl) cellulose polymer: Dynamic surface tension measurements. *J. Colloid Interface Sci.* **193**: 41-49.

Uno K., Sakaguchi H., and Hayakawa I., 2002. Minocycline-containing compositions. US Patent. US 2002002151 A1.

Vachoud L., Zydowicz N., and Domard A., 2000. Physicochemical behaviour of chitin gels. *Carbohyd. Res.* **326**: 295-304.

Vandenbossche G.M.R., Vanhaecke E., Muynck C.D., and Remon J.P., 1991. Stability of erythromycin formulations. *Int. J. Pharm.* **67**: 195-199.

Wan L.S.C., Heng P.W.S., and Wong L.F., 1991. The effect of hydroxypropylmethylcellulose on water penetration into a matrix system. *Int. J. Pharm.,* **73**: 111-116.

WebElements. http://www.webelements.com/webelements/elements/text/Al/radii.html (accessed 22 December 2006).

Wessels J.M., Ford W.E., Szymczak W., and Schneider S., 1998. The Complexation of tetracycline and anhydrotetracycline with Mg^{2+} and Ca^{2+}: A Spectroscopic Study. *J. Phys. Chem. B.* **102**: 9323-9331.

Wikipedia, the free encyclopedia. http://en.wikipedia.org/wiki/Ionic_radius (accessed 22 December 2006).

Wilkinson M.C., and Elliott T.A., 1974. Dynamic contact angle in mercury/carbon tetrachloride/solution systems III. The mechanism and kinetics of spreading. *J. Colloid Interface Sci.* **48 (2)**: 225-241.

Wolf R., Wolf D., Tüzün B., and Tüzün Y., 2001. Contact dermatitis to cosmetics. *Clin. Dermatol.* **19**: 502-515.

Wu P., Huang Y., Chang J., Tsai M., and Tsai Y., 2003. Preparation and evaluation of sustained release microspheres of potassium chloride prepared with ethylcellulose. *Int. J. Pharm.* **260**: 115-121.

Wu S., 1982. *Polymer interface and adhesion.* Marcel Dekker, New York.

Wu Y., and Fassihi R., 2005. Stability of metronidazole, tetracycline HCl and famotidine alone or in combination. *Int. J. Pharm.* **290**: 1-13.

Xu M.X., Liu W.G., Wang J., Gao W., and Yao K.D., 1997. Surface rearrangement of vinyl acetate and acrylate terpolymer adhesives investigated by dynamic contact angles. *Polym. Int.* **44**: 421-427.

Yamada K., Minoda M., Fukuda T., and Miyamoto T., 2001. Amphiphilic block and statistical copolymers with pendant glucose residues: Controlled synthesis by living cationic polymerization and the effect of copolymer architecture on their properties. *J. Polym. Sci. Pol. Chem.* **39**: 459-467.

Yamauchi A., 2001. Gels: introduction. In: Osada Y., and Kajiwara K. (eds.), *Gel handbook. Volume 1. The fundamentals.* Academic Press, San Diego, pp. 4-25.

Yasuda T., and Okuno T., 1994. Contact angle of water on polymer surfaces. *Langmuir.* **10**: 2435-2439.

Yoshioka S., Aso Y., and Terao T., 1992. Effect of water mobility on drug hydrolysis rates in gelatin gels. *Pharm. Res.* **9 (5)**: 607-612.

Zografi G., and Kontny M.J., 1986. The interactions of water with cellulose- and starch-derived pharmaceutical excipients. *Pharm. Res.* **3 (4)**: 187-194.

IX. LIST OF PUBLICATIONS

International Refereed Journal

1. P.W.S. Heng, L.W. Chan and K.T. Chow, 2005. Development of Novel Non-aqueous Ethylcellulose Gel Matrices: Rheological and Mechanical Characterization. *Pharm. Res.* **22 (4)**: 676-684.
2. L.W. Chan, K.T. Chow, and P.W.S. Heng, 2006. Investigation of wetting behavior of non-aqueous ethylcellulose gel matrices using dynamic contact angle. *Pharm. Res.* **23 (2)**: 408-421.
3. K.T. Chow, L.W. Chan, P.W.S. Heng. Characterization of spreadability of non-aqueous ethylcellulose gel matrices using dynamic contact angle. *J. Pharm. Sci.* (Submitted for publication).

Conference Presentations

1. K.T. Chow, L.W. Chan and P.W.S. Heng. Evaluation of antimicrobial activity of non-aqueous ethylcellulose gel loaded with minocycline hydrochloride. *Proceedings of 2006 AAPS Annual Meeting and Exposition,* October 29 - November 2, San Antonio, Texas, USA.
2. K.T. Chow, L.W. Chan and P.W.S. Heng. Evaluation of sustained release characteristics of non-aqueous ethylcellulose gel. *Proceedings of 33rd Annual Meeting and Exposition of the Controlled Release Society,* July 22-26, 2006, Vienna, Austria.
3. K.T. Chow, L.W. Chan and P.W.S. Heng. Mechanical characterization of non-aqueous gel matrices. *Proceedings of 2004 AAPS Annual Meeting and Exposition,* November 7-11, Baltimore, Maryland, USA.

4. K.T. Chow, L.W. Chan, J.S. Hao and P.W.S. Heng. Prediction of hydrophilic/hydrophobic gel properties of non-aqueous gel matrices using dynamic contact angles. *Proceedings of Inaugural AASP Conference*, June 4-6, 2004, Beijing, China, p.58.
5. K.T. Chow, L.W. Chan and P.W.S. Heng. Viscoelastic characterization of non-aqueous gel matrices. *Proceedings of 2003 AAPS Annual Meeting and Exposition*, October 26-30, Salt Palace Convention Center, Salt Lake City, Utah, USA.
6. K.T. Chow, P.W.S. Heng and L.W. Chan. Stability study of minocycline hydrochloride in various solvents. *Proceedings of 2002 AAPS Annual Meeting and Exposition*, November 10-14, Toronto, Ontario, Canada.